SORPTION OF CARBON COMPOUND VAPOURS ON POROUS SOLIDS

By

Owen Edwin Facey, B.Sc.

A Thesis submitted for the Degree of Doctor of Philosophy in the University of London.

ROYAL HOLLOWAY COLLEGE
(University of London)
Englefield Green, Surrey

1964

ABSTRACT

The isotherms of a series of hydrocarbon compounds containing various functional groups and their fluorinated analogues have been examined, with silica gel and ferric oxide as adsorbents. The isotherms are compared and contrasted to find any variations due to substituting fluorine in place of hydrogen.

In addition low pressure isotherms (at 20°C, 25°C and 30°C) were obtained for the systems ethyl alcohol/ferric oxide and trifluoroethanol/ferric oxide. The validity of these results are discussed and, assuming their correctness, various factors which might give rise to them are suggested.

ACKNOWLEDGEMENTS

The author would like to thank the late Dr. A.G. Foster for his early encouragement and advice which provided the incentive to continue after Dr. Foster's untimely death in 1962.

In addition the author sincerely thanks Dr. K. Singer for his interest and advice during the remainder of this work and to Professor Bourne and the other members of the Chemistry Department of Royal Holloway College who were always ready to offer their assistance.

Grateful acknowledgement is also made to the U.S. Department of the Army who financed this work from 1961 to 1964.

CONTENTS

INTRODUCTION

> "A slow sort of country!" said the Queen. "Now, here, you see, it takes all the running you can do, to keep in the same place. If you want to get somewhere else, you must run at least twice as fast as that!"
>
> Lewis Carroll

As is often the case the phenomenon of sorption has been used, if not actually recognised, for many years; for example the cleaning of wool with fullers earth and in the dyeing industry. The first recorded accounts of any scientific study on sorption are usually accredited to Scheele, who described some experiments with gases exposed to charcoal in 1773 and, independently, to the Abbè Fontana for similar experiments in 1777. However little work of importance could be done on vapour/solid sorption until suitable vacuum apparatus became available, and the major work began about the end of the nineteenth century.

It was also at about the beginning of the twentieth century that the nomenclature became reasonably standardised, the uptake of a gas or vapour by a solid being termed 'sorption'. This was further defined as absorption

or adsorption depending on whether the gas or vapour diffuses from the surface into the lattice of the solid or not. Further the gas or vapour attached to the surface is known as the adsorbate and the solid to which it is adsorbed the adsorbent.

The forces holding the adsorbate to the surface can be thought of in terms of two extreme cases, one where there is an actual chemical bond formed, when it is said to be chemisorbed, and the other where the forces are the same as in condensation when it is said to be physically adsorbed. These two forms grade imperceptibly into each other so that is is often difficult, if not in certain cases pointless, to try to separate them.

The variables normally measured in physical adsorption are the concentration of the adsorbate on the adsorbent q measured in suitable units, e.g. mg/gm., c.c. at STP/gm, moles/unit area etc., the vapour pressure over the adsorbent, p, and the temperature, T, i.e.

$$q = f(p, T) \qquad (1)$$

This is usually simplified by keeping the temperature constant, the resulting graph

$$q = f(p)_T \qquad (2)$$

being known as an isotherm.

Fig 1

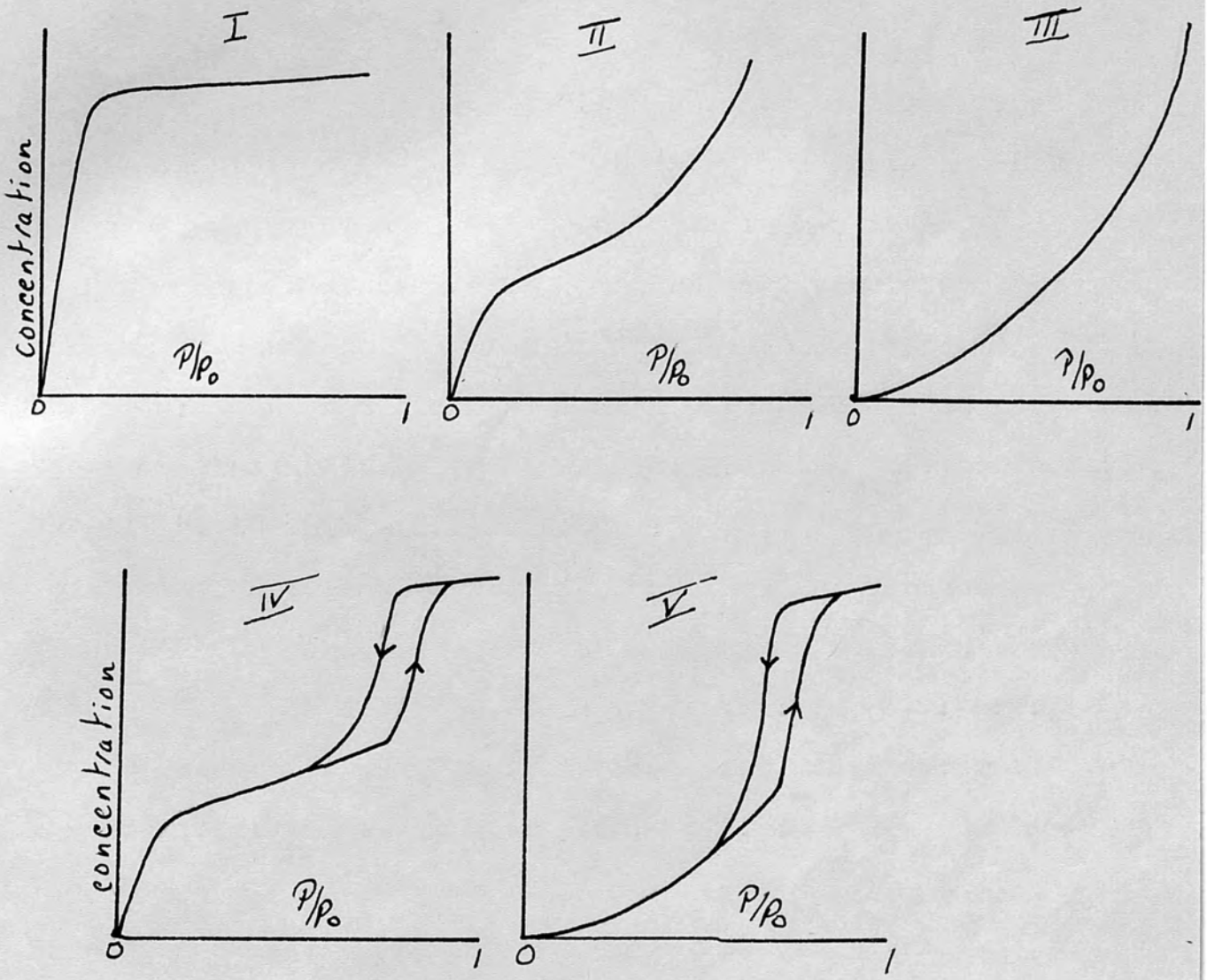

Types of physical adsorption isotherm according to Brunauer

As p $\propto$ activity, varies with $\frac{\partial G}{\partial N}$ thus the isotherm shows how the free energy of the system changes as the concentration changes. Isotherms can have widely differing shapes but generally fall into one of five types as classified by Brunauer et al (1). These are shown in Fig. 1 and will be referred to in future by number.

Type 1 is associated with limited adsorption, conventionally adsorption to form a monolayer. The remaining four are all associated with multilayer adsorption. Isotherms showing a sigmoid shape, types IV and V, are associated with porous adsorbents. In addition types IV and V may show hystersis loops, that is, the course taken by desorption lies at a lower pressure than that taken on adsorption in the upper part of the graph. Another point of interest is the close similarity of the lower parts of types II and IV to type I, lending support to the original suggestion that type I is associated with adsorption limited to a monolayer. In passing, types III and V are quite rare compared to the other three. As this work is with porous adsorbents most interest will be centred on type IV isotherms.

The development of a molecular theory, which allows mathematical treatment to give an equation that fits these graphs, has not yet been successful.

Equations which fit a part of the graph, or even a part of several graphs, and have theoretical backing have been developed and it would be useful to consider some of these.

The first was derived by Langmuir (2) using a kinetic picture of the adsorbed layer in dynamic equilibrium with the gas or vapour phase. In the derivation the following assumptions (quoting Fowler (3)) are made "that the atoms (or molecules) of the gas are adsorbed as wholes onto definite points of attachment on the surface of the adsorber, that each point of attachment can accommodate one and only one adsorbed atom, and that the energies of the states of any adsorbed atom are independent of the presence or absence of other adsorbed atoms on neighbouring points of attachment". With these assumptions one can arrive by a number of different arguments, e.g. kinetic, thermodynamic, statistical, at an equation of the form

$$\theta = \frac{bp}{1 + bp} \qquad (3)$$

where θ is the fraction of the surface covered

b is a constant

and p is the partial pressure.

It is important to realise at this point that although an isotherm may conform to this equation it does not necessarily mean that the Langmuir model applies. This is even more true for other equations where there are more

than two variable parameters, here b and θ, so that instead of testing a basic equation it becomes an exercise in curve fitting.

Thus equation 3 can be taken to represent the form of isotherm for an ideal monolayer, the molecules of which are on fixed positions on the surface, and corresponds to a type I isotherm.

A logical extension is to consider the effects of adsorbate/adsorbate interactions, this however introduces many mathematical difficulties. One may either use a crude approximation, say the distribution of molecules over the surface is random to allow calculation of nearest neighbour interactions (cf Ref. 4) or, assume some type of non-random distribution (cf Ref. 5) and find that the mathematical difficulties are enormous and the equation complex.

Another possibility that has been examined is that the adsorbate is not localised, but free to move across the surface. By assuming that the molecules obey some form of 'gas' law one can derive a number of equations. One of the best known is Volmer's equation (6).

$$\ln \frac{P}{\phi} = \frac{\beta\phi}{kT} + c \qquad (4)$$

where c is a constant, ϕ is the spreading or two dimensional "pressure", and β a correction factor analogous to the volume correction factor in the Van der Waals equation.

The "gas law" corresponding to this equation is

$$\phi(A - N\beta) = NkT \qquad (5)$$

where A = area of the film

N = number of molecules in the film

A neat way of including adsorbate/adsorbate interactions would be to use a two dimensional analogue of the Van der Waals equation instead of equation 5. If it is written in the form

$$\left(\phi + \alpha \frac{N^2}{A^2}\right)(A - N\beta) = NkT \qquad (6)$$

where α is the analogue of the 'a' constant in the Van der Waal's equation

Hill (7) has shown by statistical mechanical reasoning that this gives rise to an isotherm of the form

$$p = \frac{(2\pi m)^{\frac{1}{2}} (kT)^{3/2}}{h\beta} \frac{1}{j_n} e^{-\epsilon/kT} \frac{\theta}{1 - \theta} \exp\left(\frac{\theta}{1 - \theta} - \frac{2\alpha\theta}{\beta kT}\right) \qquad (7)$$

where j_n is the partition function for the vibration of an adsorbed molecule perpendicular to the surface and $-\epsilon$ is the energy of adsorption at absolute zero, other constants have their previous meaning. Another assumption in the Langmuir isotherm that could be examined is that the adsorption sites are all energetically equal. This is unlikely for most adsorbents, and it is well known that in a heat of adsorption versus quantity adsorbed plot there is usually a very steep drop initially. This heterogenaity of the surface can easily be determined from the isotherm

where $\theta<1$, by differentiating quantity adsorbed versus lnp graph (cf Ref. 8). However using this distribution when found, or even a simpler idealised distribution, gives awkward complex equations which are of little practical use (9). This is in fact quite a normal situation, a model is proposed and assumptions are made so that the result can be easily handled. Further refinement or alterations generally result in unusable equations. Thus four alterations to Langmuir's original assumptions have been mentioned, i.e. adsorption with lateral interactions, a mobile adsorbed layer, with and without adsorbate/adsorbate interactions and a heterogeneous surface, none of which give equations that are of practical use, except perhaps for Volmer's equation. For this reason only certain of the theories that are relevant to the subject in hand will be mentioned ; for a fuller treatment see reviews such as (1, 10).

The next major advance was the extension of Langmuir's theory by Bruneaur, Emmett and Teller (11), in future referred to as B.E.T., to include adsorption of more than one layer of molecules. Their success lies in the simplifying assumption that after the first layer the heat of adsorption is the same as the heat of liquifaction for the bulk liquid. This, coupled with the assumption that there can be an infinite number of layers adsorbed on a free surface, allows summation of the separate equations

for each layer giving

$$\theta = \frac{cx}{(1 - x)(1 - x + cx)} \qquad (8)$$

where c is a constant, and equal to $ke^{(E_1 - E_L)/RT}$ from the theory, k being a constant usually assumed to be one, and E_1 is the heat of adsorption of the first layer and E_L the heat of liquifaction. $x = P/P_o$, is the relative pressure. Putting $\theta = \frac{V}{V_m}$ where V is the quantity adsorbed and V_m the quantity adsorbed in the monolayer, and rearranging the equation one obtains

$$\frac{P}{V(P_o - P)} = \frac{1}{V_m c} + \frac{c - 1}{V_m c} \cdot \frac{P}{P_o} \qquad (9)$$

Thus a plot of $\frac{P}{V(P_o - P)}$ against $\frac{P}{P_o}$ should give a straight line and allow the evaluation of the constants V_m and c.

If the adsorption is limited to n layers then on performing the summations one obtains

$$\frac{V}{V_m} = \frac{cx\ 1 - (n + 1)x^n + nx^{n + 1}}{(1 - x)\ 1 + (c - 1)x - cx^{n + 1}} \qquad (10)$$

This equation is of interest as it reduces to Langmuir's equation when n = 1 for all values of c, and can be made to take on the form of all five types of isotherm for certain ranges of n and c (12).

In practice it is found that equation 8 is capable of describing most isotherms in the regions $\cdot 05 < \frac{P}{P_o} > \cdot 35$ and that the surface areas determined by using V_m are in reasonable agreement with those determined by independent

Fig 2

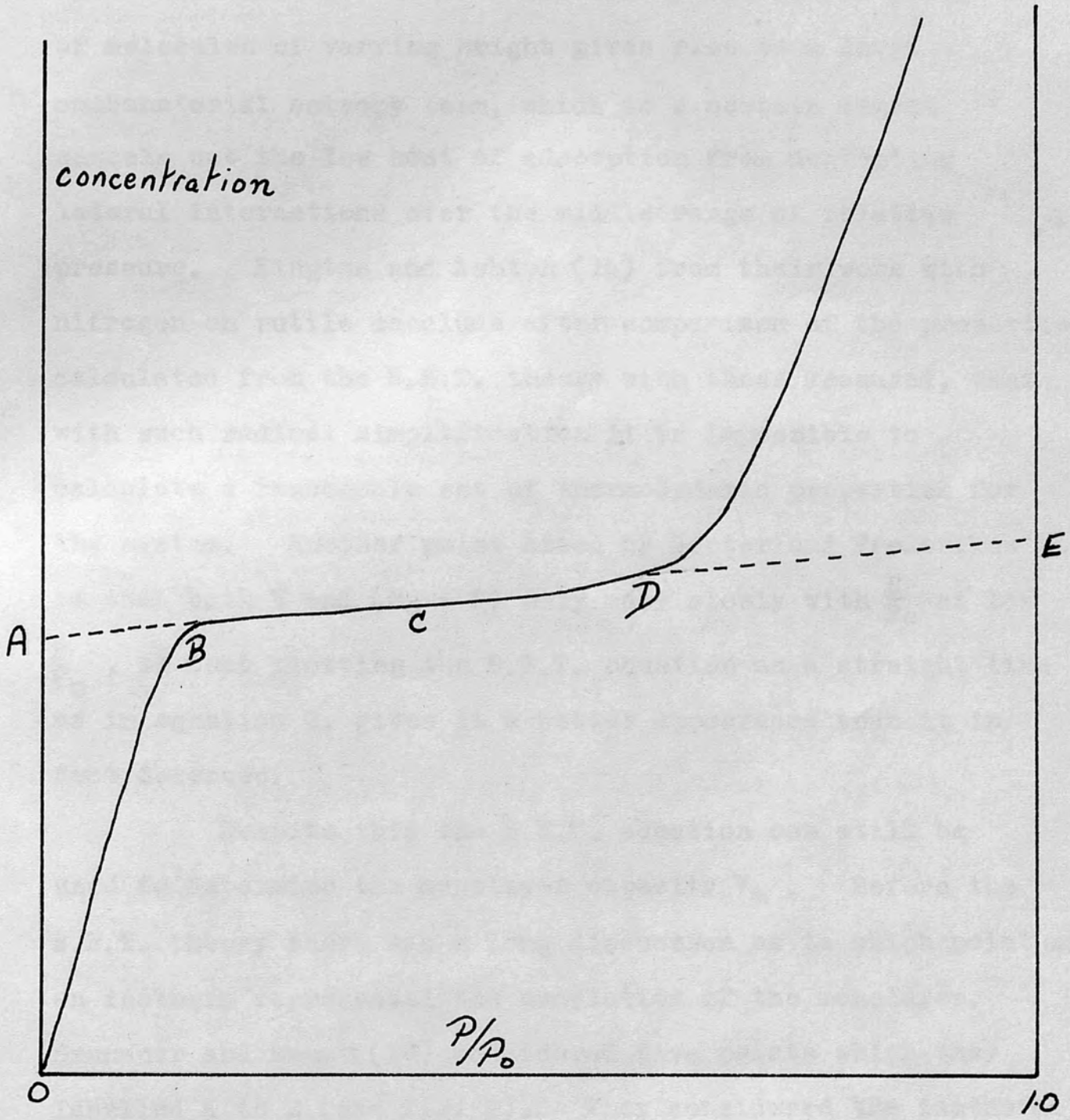

methods (cf 13, 1, 10).

However this apparent agreement is to a large extent fortuitous. The B.E.T. concept of random piles of molecules of varying height gives rise to a large combanatorial entropy term, which to a certain degree cancels out the low heat of adsorption from neglecting lateral interactions over the middle range of relative pressure. Kington and Ashton (14) from their work with nitrogen on rutile conclude after comparison of the properties calculated from the B.E.T. theory with those measured, that with such radical simplification it is impossible to calculate a reasonable set of thermodynamic properties for the system. Another point noted by Gorter and Frederikse (15) is that both V and $(P_o - P)$ only vary slowly with $\frac{P}{P_o}$ at low $\frac{P}{P_o}$, so that plotting the B.E.T. equation as a straight line as in equation 9, gives it a better appearance than it in fact deserves.

Despite this the B.E.T. equation can still be used to determine the monolayer capacity V_m. Before the B.E.T. theory there was a long discussion as to which point on an isotherm represented the completion of the monolayer. Brunauer and Emmett (16) considered five points which they labelled A to E (see Fig. 2). They considered the isotherms of a number of simple molecules that were roughly the same size on a single adsorbent, and calculated the surface area assuming liquid and solid packing. They found point 'B'

results gave the most consistent results, and suggested that this be taken as a measure of the monolayer. This suggestion has received backing from heats of adsorption measurements (cf 17), independent determinations of surface areas (10), and a mathematical analysis of Halsey (18). This indicates that point 'B' can with reasonable certainty be taken to represent the filling of the statistical monolayer, and explains the success of the B.E.T. method in determining surface areas, as now their equation represents an analytical method for finding point 'B'.

Another point that showed internal consistency was 'A', this giving a 7 - 28% spread of results, point 'B' giving 3 - 12%. This is due to the fact that most isotherms show a high value of 'c' in the B.E.T. equation. This gives a flat "plateau" region of small slope in the isotherm. This when extrapolated back will give an answer little different from point 'B', and has been used when the B.E.T. equation is not followed, or point 'B' lies at too low a relative pressure to be accurately located.

There is another factor to be considered when discussing surface areas; this is the value that the effective cross-sectional area of the molecule should be given. The normal method is to calculate the area from the constants of state of the bulk phase at the temperature of adsorption. One such equation is due to Livingstone (19)

$$\sigma = F\left(\frac{M}{N\rho}\right)^{2/3} \qquad (11)$$

where M = molecular weight of the molecule

N = Avagardro's number

ρ = density of adsorbate at the temperature of the isotherm

and F is a packing factor which depends on an assumed structure for the bulk phase and the adsorbed phase, and varies between ·866 and 1·260. Normally nitrogen is assumed to have an effective cross-sectional area of 16·2Å at -195°C, which corresponds to a factor of 1·091. This is derived from the assumption of a face centred cubic packing in the bulk phase and hexagonal close packing in the adsorbed phase. One also notes that face centred cubic and hexagonal close packing give the largest free volumes and therefore the lowest free energies for a fixed volume of liquid.

The other assumption implicit in this and similar formulae is that the molecules are spherical. This is approximately true for simple molecules like nitrogen and carbon dioxide and even water and ethanol, but not butane or n-hexane; for example see the work of Brown and Foster (20) on the sorption of amines.

One is now in the same position with the B.E.T. as with the Langmuir equation, i.e. there are some obvious lines for improvement, but, as in that case, the theoretical improvements lose the practical simplicity (cf 10).

A different way of approaching multilayer isotherms is to consider the adsorbate as essentially a liquid in the potential energy field of the adsorbent. This model, first discussed by Frenkel (21), then by Halsey (22), and in a series of papers by Hill (7, 23), can only apply for two or more statistical layers. Using this idea, and assuming the normal 6 - 12 Lennard-Jones potential which is "smeared" out by replacing the summation by an integration over the surface, results in an equation of the form

$$\ln \frac{P}{P_o} = -\frac{a}{r^3} \qquad (12)$$

where a is a constant depending on temperature and r the surface concentration.

This equation has most success with types I and II isotherms, but does fit the other types over varying ranges of $\frac{P}{P_o}$. The equation was further refined by Barrer and Robins (24), and again by Hill (25), but these only give rise to complex equations.

None of the equations so far discussed predict the phenomena of hysteresis which can be shown by types IV and V. It was initially thought that this was an artifact due to the methods used, as in some cases the hysteresis loop could be eliminated after a number of adsorptions and desorptions. However a number of careful investigations (26, 27) established the reality and repeatability of this effect. As noted before hysteresis

is normally associated with adsorbents that are microporous, such as silica gel, charcoal etc. and Zsigmondy (28), who had shown using an ultiamicroscope that silica gel was indeed microporous, proposed that this could explain the hysteresis.

W. Thompson (29) had shown that the vapour pressure over a curved surface was different to that over a plain surface; the equation is now written for greater generality as

$$\ln \frac{P}{P_o} = - \frac{V \gamma \cos \theta}{RT} \left(\frac{1}{r_1} + \frac{1}{r_2} \right) \qquad (13)$$

where V is the molar volume, γ the surface tension, θ the angle of contact between the liquid and container and r_1, r_2 the radii of curvature. This equation has been experimentally verified by Thomä (30) and La Mer and Gruen (31).

Originally Zsigmondy suggested that the hysteresis was due to the change in contact angle on advancing over the bare surface in adsorption compared to that when moving over the wetted surface in desorption. This is unlikely as there are already several layers of adsorbate held on the surface over the pressures that hysteresis normally occur.

In a cylindrical open ended capillary which has liquid condensed in it the liquid having zero angle of contact the vapour pressure is

Fig 3

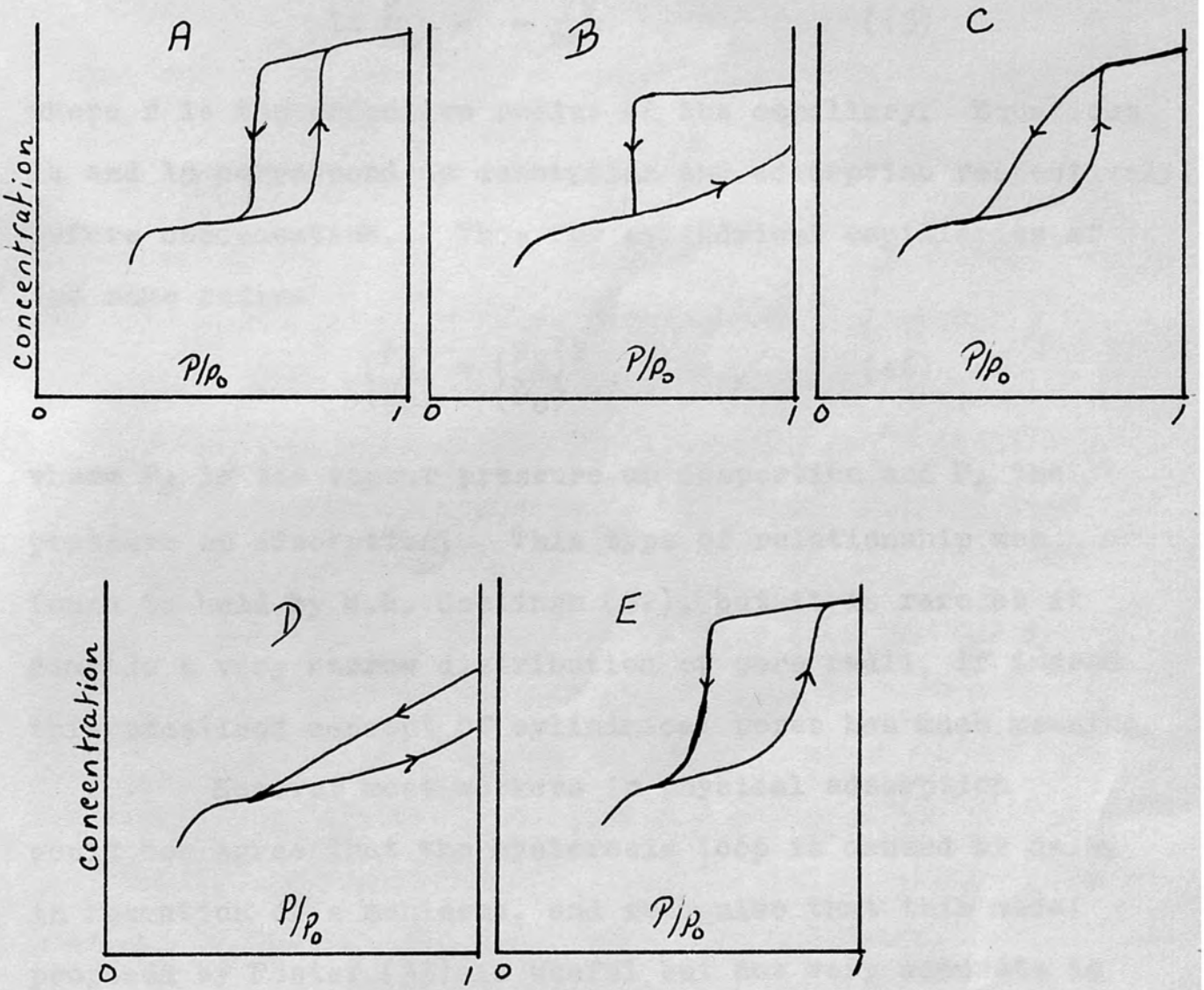

Types of hysteresis loops
according to de Boer

$$\ln \frac{P}{P_o} = - \frac{2V\gamma}{rRT} \qquad (14)$$

where r is the radius of curvature of the meniscus, but when the capillary has a number of layers condensed on the walls the equation is

$$\ln \frac{P}{P_o} = - \frac{V\gamma}{rRT} \qquad (15)$$

where r is the effective radius of the capillary. Equations 14 and 15 correspond to desorption and adsorption respectively, before condensation. Thus for cylindrical capillaries of the same radius

$$\left(\frac{P_d}{P_o}\right) = \left(\frac{P_a}{P_o}\right)^2 \qquad (16)$$

where P_d is the vapour pressure on desportion and P_a the pressure on adsorption. This type of relationship was found to hold by M.B. Coelingh (32), but it is rare as it demands a very narrow distribution of pore radii, if indeed this idealised concept of cylindrical pores has much meaning.

However most workers in physical adsorption would now agree that the hysteresis loop is caused by delay in formation of a meniscus, and recognise that this model proposed by Foster (33) is useful but not very accurate in detail. de Boer has examined this problem of the structure of the adsorbent (34) and its effect on the shape of the isotherm using the Kelvin equation. He classifies the isotherms with hysteresis loops into five shapes (Fig. 3) and discusses the structures that might give rise to them.

The isotherms obtained in this work resemble types A, C or E. Type C could be caused by tapered or doubly tapered capillaries or by wedge shaped capillaries. Types A and E can be caused by tubular capillaries of varying types of cross-section, capillaries with slightly widened parts, trough shaped capillaries and capillaries with one narrow part.

This is of interest as much work has been done on the structure of porous solids by means of electron microscopy. This shows that ferric oxide gel probably has a plate like structure (35) (the transformation $FeOOH \rightarrow Fe_2O_3$ is a topotatic reaction (36)) and that silica gel has a globular type structure (37) which fit the type of structures predicted above.

Two further things follow from this concept of "pores". One is that the adsorbent ought to have a "pore volume" which can be measured by the saturation volume i.e. the quantity of adsorbent held by the gel when the vapour pressure of the adsorbent first reaches the saturated vapour pressure of the liquid. This was first noted empirically by Gurvich (38) and also tested by Bachmann (39). Thus a plot of the saturation volume expressing as milligrammes of adsorbate per gramme of adsorbent against density should give a straight line.

Another relationship that is derivable from this model gives an estimate of the capillary radius from the pore volume. If it is assumed that all the pores are cylindrical with a narrow distribution of pore radii and lengths, then one obtains

$$r_w = \frac{2V}{\Sigma} \qquad (17)$$

where V is the pore volume = saturation volume
and Σ is the surface area of the adsorbent.

Until now one has tried a theoretical approach, and this is to a large extent inadequate, there being no comprehensive theory of adsorption which allows calculation of the isotherm and other properties of the system from first principles. Perhaps more information could be obtained from a more empirical approach using thermodynamics? The answer is yes and no. One is able to compute the various thermodynamic properties and to draw broad generalities from them, but to obtain any detailed information the results have to be compared with those obtained, usually by statistical thermodynamics, from a theoretical model.

There was one major trouble with this approach, this being the correlation of the term measured with its correct thermodynamic relationship. This was due in part to difficulty in defining the system under consideration. The aspects of this have been reviewed by Hill (7), Everett (40), Drain (41), and Young and Crowell (10).

The simplest choice is to regard the adsorbate/adsorbent as a two component phase in equilibrium with the unadsorbed vapour. If the adsorbent is inert this simplifies to an adsorbed phase in equilibrium with unadsorbed vapour. Hill has shown that both models can be treated in a manner analogous to that used in solution thermodynamics (cf 42,7,43) In the following the treatment used by Hill (43) will be used.

If the thermodynamic system is taken as the adsorbent plus adsorbed vapour which are in equilibrium with unadsorbed vapour, then applying the methods of solution thermodynamics to the n_A moles of adsorbent, n_S moles of adsorbed vapour at temperature T and pressure P, enclosed in volume V - (N.B. in this method one implies a boundary surface, but in fact never actually have to define the boundary) - allows one to write for the change in internal energy E

$$dE = Tds - PdV + \mu_A dn_A + \mu_S dn_S \qquad (18)$$

where S is the entropy of the system, μ_A the chemical potential of the adsorbent, μ_S that of the adsorbed vapour, defined as $\left(\frac{\partial E}{\partial n_A}\right)_{SVn_S}$ and $\left(\frac{\partial E}{\partial n_S}\right)_{SVn_A}$ respectively.

However for most cases the adsorbent can be considered as inert, so that it may be factored out of equation 18, i.e. in the absence of any adsorbate equation 18 becomes

$$dE_{oA} = TdS_{oA} - PdV_{oA} + \mu_{oA}dn_A \qquad (19)$$

We can now define the thermodynamic functions associated with the formation of an adsorbed layer as

$$\left.\begin{aligned} E_S &= E - E_{oA} \\ S_S &= S - S_{oA} \\ V_S &= V - V_{oA} \end{aligned}\right\} \qquad (20)$$

Using these and subtracting 19 from 18 one obtains

$$dE_S = TdS_S - PdV_S + (\mu_A - \mu_{oA})\, dn_A + \mu_S dn_S \qquad (21)$$

This equation is thermodynamically valid whether the adsorbent is inert or not but if these quantities are taken as applying to the adsorbed layer, when comparing them with the corresponding statistically derived quantities there is the possibility that any difference found is due to variation of the adsorbent. However the approximation seems generally valid (7), and so the surface area Σ' of the adsorbent can be taken as proportional to n_A, provided the adsorbent is always added or removed in exactly the same form. Thus one can write

$$dE_S = TdS_S - PdV_S - \phi d\Sigma + \mu dn_S \qquad (22)$$

where ϕ is defined as $-\left(\frac{\partial E}{\partial \Sigma'}\right)_{S_S V_S n_S}$

A free energy now must be defined and as Everett showed (59) the choice of Gibbs free energy determines which quantities can be easily found.

Defining G_S as $G_S = E_S + PV_S - TS_S$ (23)

then $dG_S = -SdT_S + V_S dP - \phi d\Sigma + \mu_S dn_S$ (24)

Defining $\bar{S}_S = \left(\frac{\partial S_S}{\partial n_S}\right)_{PT\Sigma}$, $\bar{V}_S = \left(\frac{\partial V_S}{\partial n_S}\right)_{PT\Sigma}$

one obtains

$$d\mu_S = -\bar{S}_S dT + \bar{V}_S dP - \left(\frac{\partial \phi}{\partial n_S}\right)_{PT\Sigma} d\Sigma + \left(\frac{\partial \mu_S}{\partial n_S}\right)_{PT\Sigma} dn_S \quad (25)$$

Considering a change in P and T, at constant amount adsorbed and with a constant surface, then 25 gives

$$d\mu_S = -\bar{S}_S dT_{n_S\Sigma} + \bar{V}\, dP_{n_S\Sigma} \quad (26)$$

If the adsorbed vapour is in equilibrium with the unadsorbed vapour then $d\mu_S = d\mu_G$ or

$$-\bar{S}_S dT_{nS\Sigma} + \bar{V} dP_{nS\Sigma} = -S_G dT_{nS\Sigma} + V_G\, dp_{nS\Sigma} \quad (27)$$

where S_G and V_G are the molar entropy and volume, respectively, of the unadsorbed vapour. In the absence of an inert gas $p = P$ and

$$dp_{n_S\Sigma} = \frac{S_G - \bar{S}_S}{V_G - \bar{V}_S}\, dT_{n_S\Sigma} \quad (28)$$

Making the normal approximations of $V_G \gg \bar{V}_S$ and that the unadsorbed vapour behaves as an ideal gas

$$\left(\frac{\partial \ln p}{\partial T}\right)_{n_S\Sigma} = \frac{S_G - \bar{S}_S}{RT} \quad (29)$$

thus the heat of adsorption obtained from isosteres

$$\left(\frac{d \ln p}{d\left(\frac{1}{T}\right)}\right)_{\Gamma} = -\frac{q}{R} \quad (30)$$

can be used to find the differential entropy and hence the other differential functions.

Similarly by defining a free energy $F_S = G_S + \Sigma$ and using a similar method one obtains

$$\left(\frac{\partial \ln p}{\partial T}\right)_{\varphi} = \frac{S_G - S_S}{RT} \qquad (31)$$

This however requires knowledge of the spreading pressure φ which can be obtained from either

$$\varphi = RT \int_0^p \Gamma \, d(\ln p) \quad (T \text{ constant}) \qquad (32)$$

or

$$d\varphi_T = \Gamma (V_G - V_S) \, dp_T \qquad (33)$$

both of which involve extrapolation of the isotherms back to zero pressure.

Allowing that this can be done with reasonable accuracy then one is able to use equation 31 and other similar equations where φ is to be kept constant. This is important as it is the integral molar entropy that is needed for a statistical treatment and in more qualitative treatments, e.g. randomness of motion, phase changes etc. Also as Hill points out (60) it ought to be easier to understand curves of S_S varying with surface coverage or relative pressure than those of $\bar{S}_S$.

Graham (44) has devised a useful method, partly based on thermodynamics for analysing adsorbate/adsorbent adsorbate/adsorbate interactions. He defines a quantity K, which he calls the equilibrium function, as

Fig 4

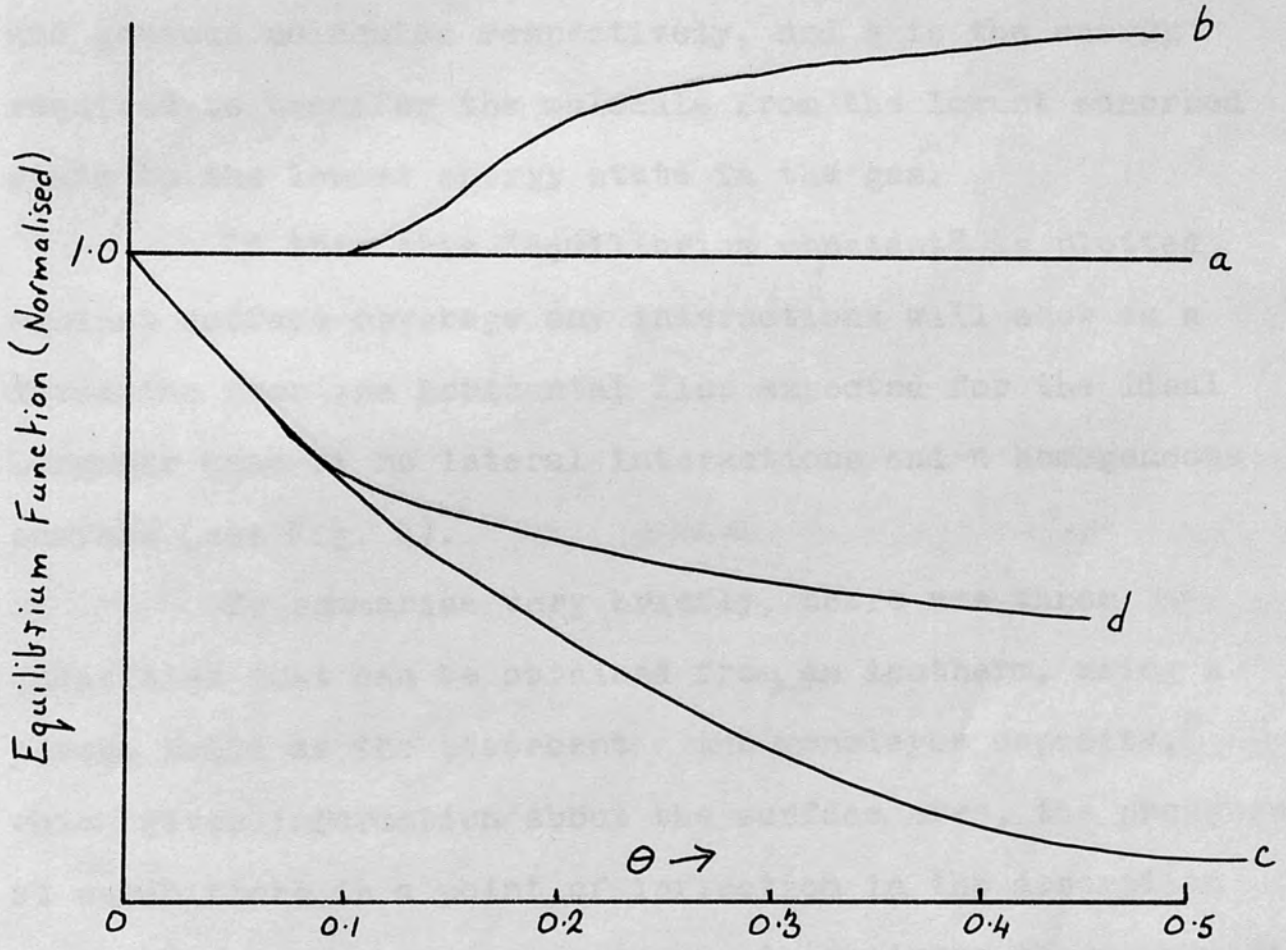

Variation of "equilibrium function" with surface coverage for localised monolayers. a) ideal b) uniform surface - interacting c) non-uniform surface - non-interacting d) non-uniform - interacting

$$K = \left(\frac{\theta}{(1 - \theta)}\right) \frac{1}{p} \qquad (34)$$

Thus K is in fact the constant b in Langmuir's equation and can be shown to be (45)

$$b = (\text{const.}) \frac{fa}{fg} e^{q/kT} \quad (T \text{ const.}) \qquad (35)$$

where fa, fg are the partition functions of the adsorbed and gaseous molecules respectively, and q is the energy required to transfer the molecule from the lowest adsorbed state to the lowest energy state in the gas.

If then this "equilibrium constant" is plotted against surface coverage any interactions will show as a deviation from the horizontal line expected for the ideal Langmuir case of no lateral interactions and a homogeneous surface (see Fig. 4).

To summarise very briefly, there are three quantities that can be obtained from an isotherm, using a porous solid as the adsorbent: the monolayer capacity, which gives information about the surface area, the pressure at which there is a point of inflection in the desorption hysteresis branch of the isotherm, this giving the most probable radius of the pores as calculated by the Kelvin equation, and the saturation volume which gives information about the pore volume and hence the average pore radius. In addition, if sufficient low pressure data are available a plot of the "equilibrium constant" against surface coverage gives information about the various adsorbate/ adsorbent interactions. If isotherms at other temperatures are also available then

it is possible to obtain the isosteric heat of adsorption from a Clausius-Clapyron type equation.

Using these it was hoped that one could gain some insight into the physical adsorption of fluorocarbons. Fluorocarbons were chosen as fluorine is less polarisable than hydrogen, thus in general fluorocarbons have lower boiling points than their corresponding hydrocarbon analogues. As the forces of physical adsorption are influenced to a large degree by the polarisability of the molecule, one would expect significant differences in the behaviour of hydrocarbons and fluorocarbons on adsorption, and so a general comparison of as many types of fluorocarbon as possible with their analogous hydrocarbons has been attempted.

However, fluorine in a carbon chain molecule can also affect its chemical properties as compared to a similar hydrocarbon. In general it renders it more resistant to oxidation in the chain and due to its large electronegitivity exerts a large inductive effect on any active groups in the molecule. Thus fluoro acids are of comparable strength to weak mineral acids, fluoroamines, are far weaker bases than their hydrocarbon analogues and fluoroalcohols are weak acids of comparable strength to phenol.

This being the case it would be instructive to use two types of adsorbent, one of a "basic" nature, e.g. ferric oxide, and one of an "acidic" nature, e.g. silica gel.

The choice of these could also be of interest from the point of view of their different microstructure; ferric oxide comprising of long rectangular rods, whilst silica gel is made up of spherical particles. Perhaps from the point of view of a straight comparison it would have been better to use adsorbents of the same structure, but any effects due to structure alone should be detectable from comparisons of the same adsorbate on a different adsorbent, and that any effect ought to be of the same order and direction for each adsorbate on the various adsorbents.

EXPERIMENTAL

"I see you're admiring my little box," the Knight said in a friendly tone. "It's my own invention - to keep clothes and sandwiches in. You see I carry it upside-down, so that the rain can't get in."

Lewis Carroll

1. Adsorbents

Ferric Oxide

Three batches of ferric oxide have been used in this work. The first, ferric oxide I was prepared by Dr. Hendra (unpublished work) according to the method of Lambert and Clark (47), and closely resembled it. A second batch was also prepared, using the same method. This was called ferric oxide II and showed a low saturation volume and narrow capillaries. This was suitable for most purposes but a gel with larger saturation volume and larger capillaries was wanted for work with the alcohols. This was made using the same method and called ferric oxide III.

These gels after air-drying over night were placed in an oven at 60°C for about four hours and then further dried in an oven at 110°C for four hours. They were then allowed to cool in a desiccator and then kept in a screw top jar until used.

Silica Gel

All the samples of silica gel available were considered unsuitable for the present work, and a new batch was made according to the method of Thorpe (46) for silica gel SW2. After air-drying the gel was dried in an oven at at 60°C for twenty-four hours and then heated at 110°C for a further six hours. The gel was allowed to cool in a desiccator and then kept in a screw cap jar until used. This gave a clear hard gel with suitable properties. This batch has been used throughout this work.

2. Adsorbates

The hydrocarbons used in this work were all available commercially in analytical or better grades. Further purification was therefore limited to standard methods recommended for these compounds (cf "Techniques of Organic Chemistry" Ed. Weisberger Vol. VII) and the purity of the product checked by gas chromatography (G.L.C.). Only samples having a purity of 99% or better were used and all underwent a high vacuum distilation in the vacuum line.

β-trifluoroethanol

β-trifluoroethanol (from L. Lights) was fractionally distilled through a semi-microcolumn, the middle fraction boiling at 74°C and constituting about 95% of the total. The purity was better than 99% by G.L.C.

2:2:3:3 tetrafluoropropan-1-ol

This was a research sample (donated by I.E. du Pont de Nemours) and was dried over magnesium sulphate and then distilled from a small volume of concentrated sulphuric acid, the middle fraction, boiling point 106°C, being collected. Purity better than 99% by G.L.C.

Perfluorobenzene

This was donated(by The Imperial Smelting Corporation) as a research sample. A check of the purity showed it to be better than 99·9%.

1:1:1 trifluoroacetone

1:1:1 trifluoroacetone (from Hopkins & Williams) consisted mainly of the hydrate. This was broken down by distilling from an equal volume of concentrated sulphuric acid, the fraction boiling 22 - 23°C, being collected. This was found to be better than 99% pure by G.L.C. and put into the vacuum line.

Trifluoroacetic Acid

Trifluoroacetic acid (from Eastman Kodak) had some water in it. This was removed by standing over phosphorous pentoxide for a day and then, after filtering, distilling the fraction boiling 72 - 73°C, being collected.

β monofluoroethanol

β monofluoroethanol was made following the method of Hoffmann (49). 100 gm. (1·7 moles) of powdered anhydrous potassium fluoride was dissolved in a mixture of 92 gm.ethylene

glycol and 37 gm. of diethylene glycol, in a three necked one litre flask which is equipped with a stirrer and is being heated by an oil bath at 170°C. A short (approximately 1 ft.) Vigreux column with a Liebig condenser is added to one neck and 97 gm. (1.2 moles) of anhydrous 2 chloroethanol is slowly added over three hours down the other neck. The flask is kept at 170°C during this period and the crude product distils over but the temperature in the column head is never allowed to go above 110°C. After all the 2 chloroethanol has been added a stream of dry air is drawn through the apparatus to remove the last traces of 2 fluoroethanol.

The crude product is then kept over anhydrous sodium fluoride for two days and then distilled through a franctionating column (approximately twenty theoretical plates). The middle fraction boiling 102 - 103°C and a higher fraction 103 - 115°C are collected; Hoffmann only collected the middle fraction. The middle fraction was further dried over phosphorous pentoxide and then redistilled to give 22 gm. (i.e. 30% theoretical yield) of β monofluoroethanol, purity 99% estimated by G.L.C.

The higher boiling fraction smelled strongly of the fluorinated alcohol, and in an endeavour to break the azeotrope, benzene was added in the ratio of 1:2 by volume. The mixture was then distilled and the middle fraction boiling 100 - 106°C was collected. After drying over

phosphorous pentoxide and distilling 10 gm. of 96% pure (G.L.C.) β monofluoroethanol boiling at 103 - 104°C were collected.

n Pentafluoropropan-1-ol

Pentafluoropropan-1-ol was prepared by a similar method to that of Hazeldine and Leedham (48). 70 gms. (.43 moles) of anhydrous pentafluoropropionic acid dissolved in 440 mls. of absolute ether was slowly added over 3½ hours to 20 gms. (·53 moles) of lithium aluminium hydride in 660 mls. of absolute ether, the reaction vessel being cooled in an ice bath.

The mixture was stirred for a further two hours and then 20 mls. of concentrated sulphuric acid in 70 mls. of water were added. The liquid was distilled off of the resulting solids and dried over phosphorous pentoxide. The ether was distilled out, using a fractionating column, and two fractions collected, one boiling at 75 - 85°C and the other at 92 - 96°C. The latter consisted mainly of pentafluoropropional hydrate, and was not worked up.

The other fraction contained both the alcohol and aldehyde hydrate. To further dry the alcohol the mixture was distilled from concentrated sulphuric acid and a fraction boiling 78 - 81°C was collected. This was carefully redistilled through a micro column, packed with single turn helices, and a fraction 80 - 81°C (764 mm. Hg.) was collected.

The infra red spectrum taken on a Perkin Elmer SP 137 "Infracord", corresponded to that reported by Husted and Ahlbrecht, and G.L.C. showed one large peak corresponding to 99% purity. Yield 20% theoretical.

n Heptafluorobutanol

As the yield in Hazeldine and Leedhams method for preparing the alcohol from the acid was low, it was decided to try to reduce the ester instead (cf 50).

The ester was prepared by a similar method to that of Husted and Ahlbrecht (51), the main difference being that less concentrated sulphuric acid was used, this improved the yield. Heptafluorobutyric acid, ethanol and sulphuric acid were mixed in a molar ratio of 9:4:2 (i.e. 95 gm. : 11·8 mls: 5·5 mls.). This was refluxed for 8 hours, then fractions b.p.'s 69 - 70°C and approximately 86°C were distilled out. This was rapidly washed twice with distilled water and dried over magnesium sulphate. It was then distilled, the fraction boiling 95·0 - 95·5°C at 760 mm., being collected. Yield 86·6 gms.

The ester was then dissolved in 400 mls. of absolute ether and slowly added to a well stirred slurry of 20 gms. (·53 moles) of lithium aluminium hydride in 500 mls. of absolute ether, the whole being kept under reflux, and cooled in an ice/salt bath. The addition of the ester took 3½ hours and the mixture was stirred for a further 8 hours, while the reaction flask was slowly warmed up to room temperature.

The flask was again cooled in an ice/salt bath and flushed out with nitrogen, then 65 mils. of water were carefully added. The liquids were then distilled from the resulting solids using an oil bath heated to 150°C. The liquids were then fractionally distilled, the fraction boiling at 84 - 85°C being collected. This was washed with a small quantity of water to remove any ether, and then dried over phosphorous pentoxide, before being distilled, the fraction boiling 96 - 97°C at 758 mm., being collected. Yield 20·9 gms. (51% theoretical if calculated on the ester, 40% when calculated on the acid).

Ethyl trifluoroacetate and Ethyl pentafluoropropionate

Both of these esters were prepared as decribed in the previous section, (see heptafluorobutanol). Originally Husted and Ahlbrect's (51) method was used, but it was found that using such large quantities of concentrated sulphuric acid resulted in the formation of ether which leads to the formation of azeotropes, and the charring of organic material. Thus one can compare a yield of 60% when making ethyl pentafluoropropionate by Husted and Ahlbrect's method to those of 80% and 90% when making ethyl pentafluorobutyrate and ethyl trifluoroacetate where the quantity of sulphuric acid is reduced.

n pentafluoropropylamine and n heptafluorobutylamine

As the esters of the perfluoro-acids were available -

see above - the easiest route to the amines was via the acid amide i.e.

$$R\cdot C(=O)-OEt \xrightarrow{NH_3} R-C(=O)-NH_2 \xrightarrow{LiAlH_4} R\cdot CH_2\cdot NH_2$$

The acid amide was made following the method of Husted and Ahlbrect (51). The ester was dissolved in the smallest possible quantity of absolute ether and dry ammonia was passed through, the flask being initially cooled in an ice bath. When no more ammonia was being adsorbed, the flask was removed and stoppered and left over-night.

The bulk of the ether-alcohol mixture was then distilled out and the amide crystalised in large white platelets. These were filtered off and a second crop obtained from the mother liquors, the amide being extremely soluble in ether. The yields were uniformly high, at approximately 85%.

The acid amide was then dissolved in absolute ether to give a 1.5 molar solution. This was then added to a 2 molar slurry of lithium aluminium hydride in absolute ether, so that there is roughly an eightfold excess of lithium aluminium hydride, the reaction flask being cooled and having an efficient reflux condenser. The apparatus was left over-night, then a small excess of water was added, the reaction flask being cooled and having been flushed out with nitrogen.

The liquids were then distilled from the solid residue using an oil bath kept at 150°C. Concentrated sulphuric acid was then added to the liquid until it was acid and the amine sulphate filtered off. It was then made into a slurry in a round bottomed flask with a small quantity of water and a large excess of 10 N caustic soda was added carefully down a reflux condenser, the flask being cooled in an ice bath.

The liberated amine was distilled out, a fraction boiling over a 10°C range being collected. This was dried over potassium hydroxide pellets and redistilled through a semi-micro column.

n pentafluoropropylamine - boiling point 49 - 50°C at 740 mm., purity 99%, yield 45% calculated on the ester, 50% calculated on the amide.

n heptafluorobutylamine - boiling point 68 - 69°C at 759 mm., purity 99%, yield 54% calculated on the ester, 60% calculated on the amide.

3. Vacuum System

The pumping arrangement consisted of a two stage Edwards "Speedivac" pump which, by means of a by-pass, could be used as a course pump to obtain a vacuum of 10^{-3} mm. in the line beyond the traps, or as a backing pump to an Edwards silicone oil diffusion pump. With this system a vacuum of 10^{-6} mm. could be obtained, according to the McLeod gauge,

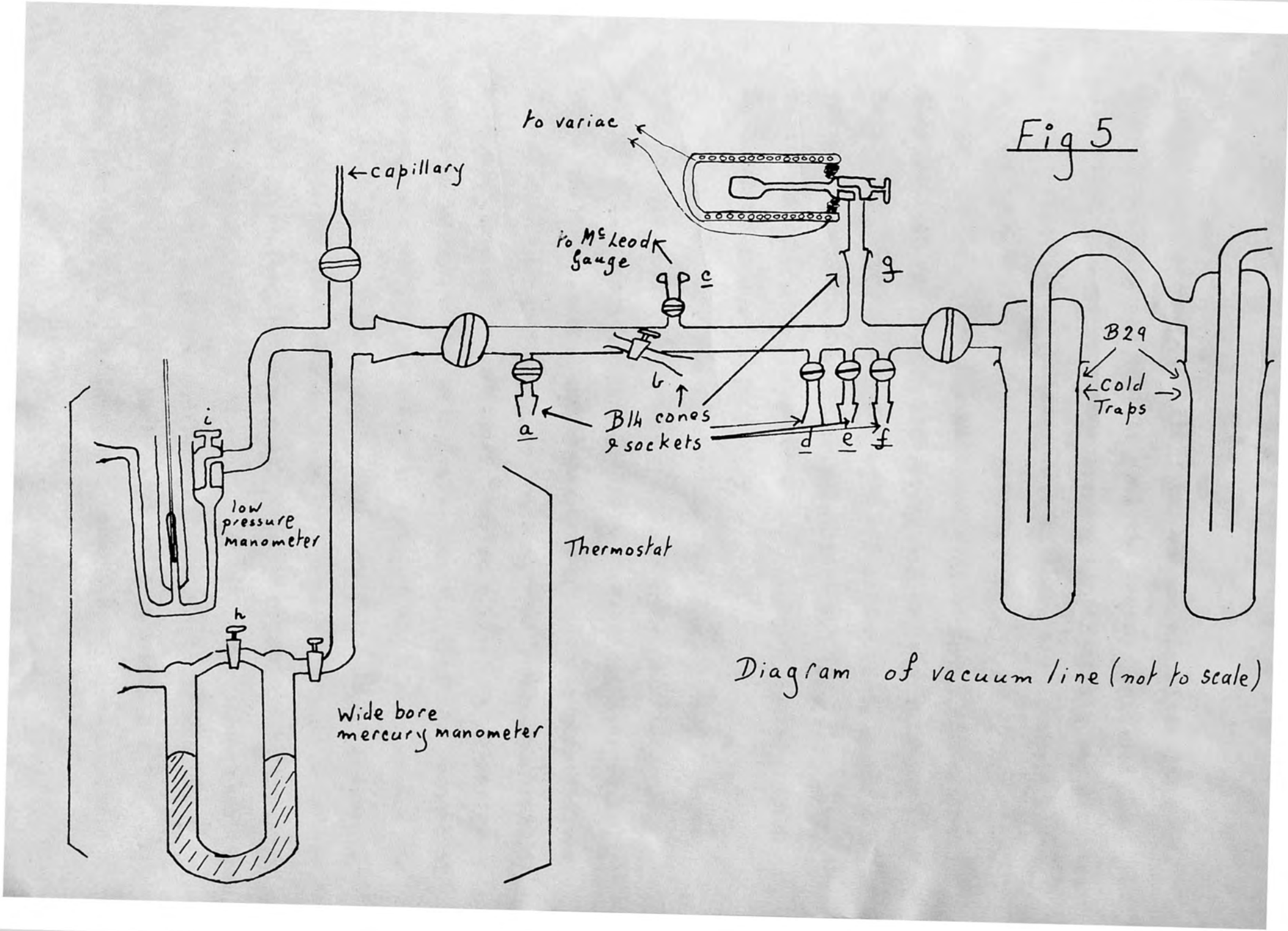
Fig 5
to variac
capillary
to McLeod Gauge
c
g
B29
Cold Traps
b
a
B14 cones & sockets
d
e
f
i
low pressure manometer
Thermostat
h
Wide bore mercury manometer
Diagram of vacuum line (not to scale)

and no work at less than 10^{-5} mm. vacuum was attempted. Liquid nitrogen was used to cool the traps; this had the disadvantage that if ever a large quantity of air was admitted liquid oxygen would condense out in them, and it would take a long time to reach a good vacuum.

The system was made entirely of pyrex glass, the main part of the vacuum line being 1.5 cm. pyrex tubing (see Fig. 5). There were seven take off points a, d, e and f being for general use, b for use when distilling adsorbate on to the gel, g for activating the gel and c connecting up to a McLeod gauge.

The taps and joints were all greased with Edwards high vacuum silicone grease. This was chosen after using a number of commercial greases such as Apiezon, Fluorolube, Kel F etc., and some "home made" greases such as polyethylene glycol/celulose acetate grease made by Polley and Cabot (52); a "sugar" grease consisting of manitol/dextrin and glycerol was also tested. The main difficulty was that the commercial greases are rapidly dissolved by most of the fluorocarbons and some of the hydrocarbons, while the "home made" greases usually broke down quickly (i.e. in under a week) or were too stiff at room temperatures. The silicone grease normally would remain usable for about a fortnight under these conditions.

The line was periodically cleaned initially, by filling with chloroform over-night and then washing with more chloroform and acetone, but later R.S.B. cleaning fluid

was used over-night, the system then being washed with water and organic solvents.

The furnace h, was made of nicrome wire wound on a glass former and insulated with a number of layers of asbestos paper. The current could be varied by means of a Variac transformer, but due to fluctuations in the mains voltage the temperature control was only ± 5°C at 150°C. When in use the furnace was moved up to the tap of the sample tube and the mouth was packed with asbestos wool.

4. Pressure Gauges

Four types of pressure gauge were used, a McLeod, an Ionisation gauge, a wide bore mercury U tube manometer and a Pirani guage based on a thermistor. The McLeod and ionisation guages were used as checks on the pressure in the line, the ionisation gauge showing the absolute pressure and the McLeod the partial pressure due to the permanent gases.

The pressure measurements for the isotherms were in the main taken from the U tube manometer, the difference in height between the mercury columns being measured by means of a cathetometer accurate to ±·01 mm. By using a plate, the top of which was painted black to cut off reflections from the mercury surface with the lower half white (53), it was possible to get readings with a consistency of ±· 03 mm. In actual fact the readings were only of an accuracy of ±.05 mm. on accout of aberration resulting from viewing the

Fig 6

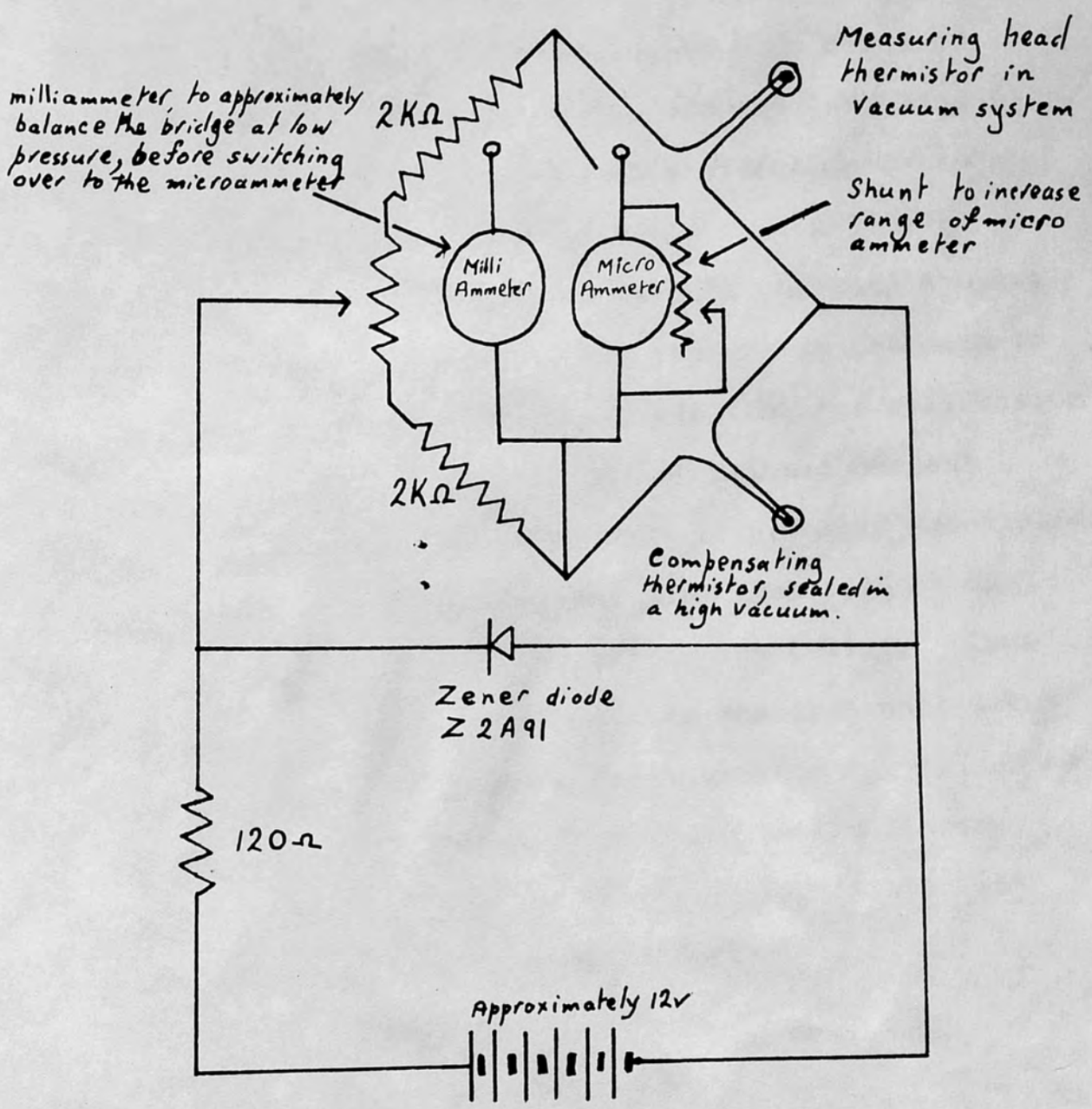

Circuit for low pressure gauge

mercury meniscus through a plate of glass, two inches of water, and a glass tube.

For low pressure work, i.e. 10^{-3} - 10 mm. a Pirani gauge using thermistors - pairs of matched thermistors suitable for low pressure manometers are available from Standard Telephones & Cables - was used. The circuit (see Fig. 6) was based on a Wheatstone bridge with a microammeter as a detector. It was hoped that this would give a linear response for a plot of log (out of balance current) against log (pressure) (54). Unfortunately vapours do not seem to give linear graphs as do gases. In addition the calibration curve of vapour pressure against out of balance current resembles a hyperbola; the steep rise is probably associated with the geometry of the gauge, the mean free path of the molecules approaching the dimensions of the tubing. Thus the lower pressures could be accurately measured whilst the transition region Pirani gauge - mercury manometer is not so accurate. As these pressures correspond to the linear portion (i.e. B to D in Fig.2)of the isotherm, it was felt that this loss of accuracy was not significant.

5. Density Measurements

Where sufficient material was available e.g.(12 ml.) a normal specific gravity bottle (10 ml. capacity) that had been standardised with water, was used. Where only a small amount was available a half ml. bottle with a ground glass

Fig 1 a

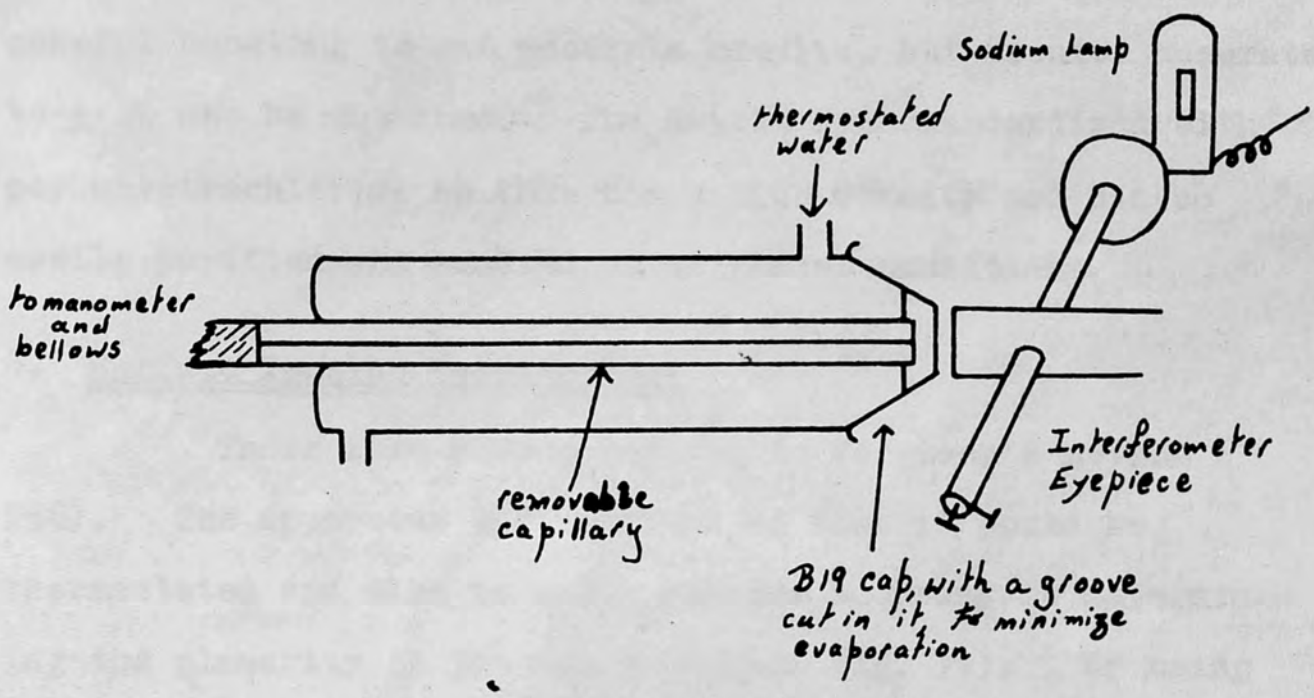

Diagram of Ferguson's apparatus for surface tensions (not to scale)

b

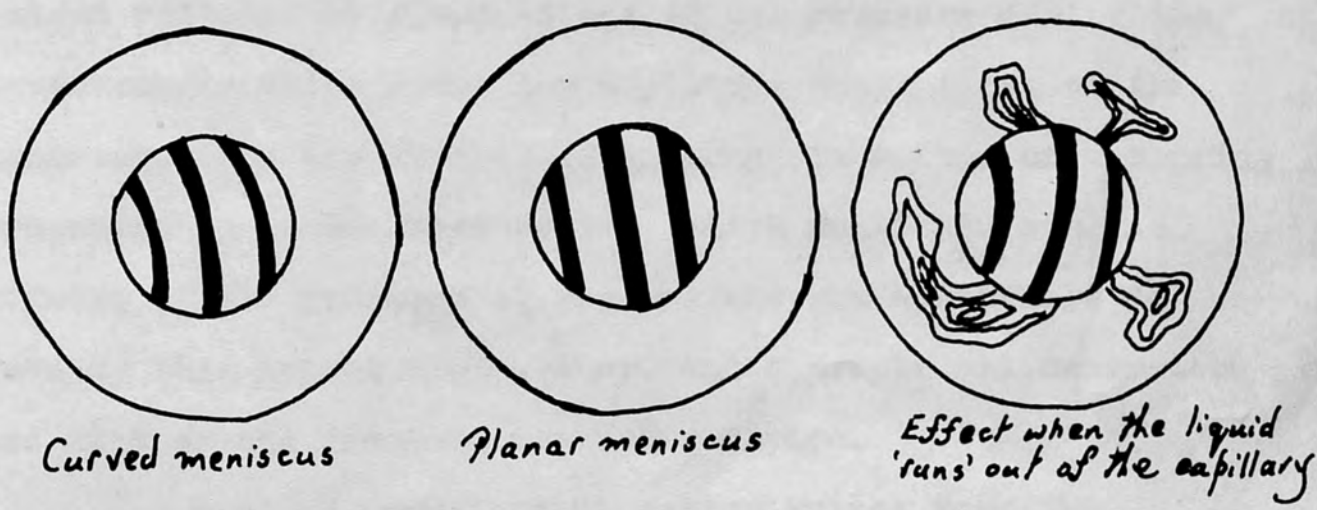

Field of view in the interferometer eye-piece

cap, similar to that used by Fontana and Calvin (55), was used. This had to be filled using a vacuum, and needed careful handling to get accurate results, but results accurate to ±.1% can be obtained. The bottle was standardised with carbontetrachloride as this has a high density and can be easily purified and handled under vacuum conditions.

6. Surface Tension Measurements

These were made according to Ferguson's method (56). The apparatus was modified so that it could be thermostated and also to allow greater accuracy in determining the planarity of the meniscus (see Fig. 7a). By using an interferometer eye piece, adjusted so that three or four lines cross the meniscus, it is possible to judge by when the lines are straight and parallel when the meniscus is flat (see Fig. 7b). This greater accuracy was to a large extent vitiated by fluctuations of air pressure during the measurements which cause low amplitude occilations of the meniscus. In the absence of an accurate method of measuring pressures in an enclosed system which would obviate the effects of air pressure it was not thought worthwhile to develop this method any further, and a simple oil manometer was used as the pressure measuring device.

Another complicating factor arises from the assumption that the angle of contact is 90° and that the surface is wetted. It was noticed for a number of samples

that there was great difficulty in keeping them in the tube when the meniscus was about to become planar despite the fact that the ends had been carefully ground and polished and had been examined with a microscope to detect any imperfections. This is probably due to the surface of the tube not being wetted by the liquid, so that the meniscus moves forwards in little jumps and thus over shooting the edge of the capillary. Using the interferometer method this effect becomes very obvious, whereas it would have little effect on the normal method of observing the specular reflection.

7. Experimental Techniques

(a) Activation of the gels

The gels were heated for between 15 and 18 hours at $150^{\circ} \pm 5^{\circ}C$ in a good vacuum i.e. 10^{-5} mm. Under these conditions silica gel attained a constant weight but ferric oxide continued to lose weight slowly even after two days. It was decided that the best course was to standardise the conditions of preparation as far as possible, thus the ferric oxide gel was also heated for 15 hours, this being a convenient period and one after which it was losing weight slowly.

The sequence of weighings to find the weight of the activated gel was:-

(a) weigh clean empty sample tube

(b) weigh sample tube plus the unactivated gel

Fig 8

Sample tube (not to scale)

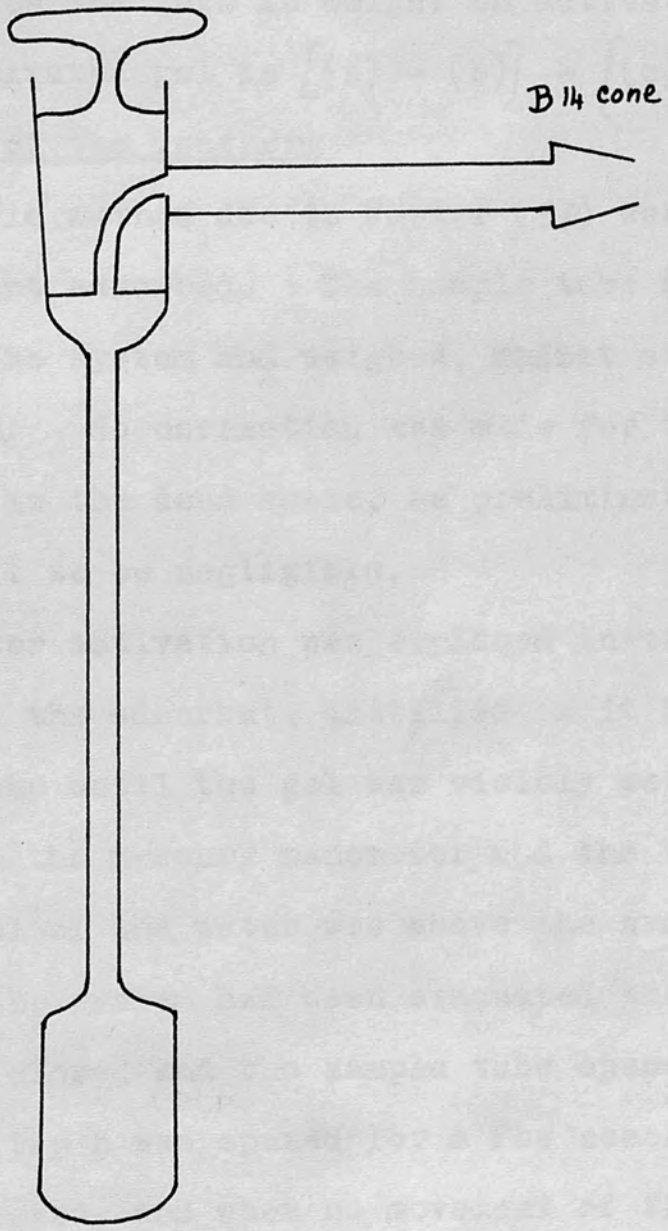

(c) weigh the sample tube with stopcock greased plus the unactivated gel

(d) weigh the sample tube and grease with the activated gel

Thus (a) - (b) gives the weight of the unactivated gel and (c) - (d) gives the loss in weight on activation, hence the weight of the activated gel is $\left[(a) - (b)\right] - \left[(c) - (d)\right]$.

(b) Determination of the isotherm

A gravimetric method due to Foster (57) was used to determine the amount adsorbed. The sample tube (Fig. 8) can be removed from the system and weighed, whilst still holding a good vacuum. No correction was made for the weight of unadsorbed vapour in the dead space, as preliminary calculations showed it to be negligible.

The gel after activation was replaced in the vacuum line at b, and the adsorbate distilled on it by cooling the sample tube until the gel was visibly wet. It was then connected to the mercury manometer and the thermostat filled until the level of the water was above the arm of the sample tube. When the system had been evacuated the tap h on the manometer was closed and the sample tube opened to the manometer. The tap h was opened for a few seconds to the pumps and then closed, and when no movement of the meniscus could be detected a reading taken. It was necessary to pump off part of the vapour over the gel as the adsorbate tends to displace any remaining vapours or gases on the gel, so the first reading, which should merely be the saturated

vapour pressure of the adsorbate, was often found to be high unless this was done.

After this first reading the water in the thermostat was lowered, air admitted to the manometer system and the sample tube removed. The grease was wiped off with a duster and the sample tube dried. It was found to be quite sufficient to wipe the joint; weighings within $\pm \cdot 4$ mg. were quite easily attainable. The sample tube was then left in the balance room to come to equilibrium with its surroundings, and then weighed. This is particularly important when isotherms at $0^{\circ}C$ are being determined. This sequence was then repeated until sufficient points on the desorption isotherm were obtained.

In addition, for the first few readings a technique known as the "pressure drop" method was used. If the ideal gas laws hold to a sufficient degree of accuracy then

$$pv = nRT$$

Now provided that the pressure changes were not too great the volume of the dead space including one limb of the manometer stays constant, that is

$$p = n \times \text{constant}, \quad V, T \text{ constant}$$

or the mass of vapour in the dead space, i.e. that which has been removed is proportional to the pressure. If the pressures corresponding to the removal of vapour from the dead space are known together with the initial and final

weights of the sample tube, then the intervening weights can be calculated. This method is not very accurate and usually one point in that region is determined by direct observation.

The lower points on the adsorption isotherm can be obtained simply by opening the gel to the vapour and after closing tap h and waiting for equilibrium to be attained, measuring the pressure and increased weight. In the hysteresis region this method does not work very well as the gel takes a long time to adsorb more adsorbate, so the process is speeded by cooling the sample tube. However one must be careful not to cool the sample tube too vigorously because it is possible to distil off vapour from the adsorbent to the walls of the sample tube; an ice bath or cooling the sample with ether was found satisfactory. Fewer readings were taken for the adsorption isotherm as the system takes longer - about three hours - to come to equilibrium than for the desporption isotherm - which takes about half an hour.

The points on the desorption and adsorption isotherm were then checked. Fewer readings being taken if the graph appeared to be reproducible.

Exactly the same procedure was followed when the low pressure manometer was used, except that both adsorption and desorption points take a long time to reach equilibrium.

(c) Low Pressure Manometer

The low pressure manometer and the compensating

head are both held in the thermostat. The sample tube is fitted into the system and water run into the thermostat until it is above the side arm of the sample tube. The system is then evacuated and when the McLeod gauge shows a vacuum of less than 10^{-5} mm. Hg., the bridge circuit is balanced, using the milli-ammeter to obtain a rough balance, then the micro-ammeter to obtain an accurate balance. It was found that the microammeter (full scale deflection 10 micro amps.) was too sensitive to cover the full range, and so it was shunted with a decade resistance box so that values 2, 3,4 and 5 times the scale deflection could be obtained - these were checked and found to be internally consistent.

After balancing the gauge was switched off if vapour was to be admitted to the sample, otherwise it was left and vapour pumped off of the gel. Tap i was then closed and the system was allowed to come to equilibrium.

The major disadvantage with this system was that the gauge must be calibrated for each vapour. The method employed was to use slush baths of compounds which melt at known temperatures round the liquid adsorbate to give the low vapour pressures necessary and measure the corresponding out of balance current.

No pressure temperature relationships for the fluorinated alcohols have been published. These were measured for the range where the mercury manometer could be used to measure the vapour pressures, and then extrapolated to low

pressures by means of the Clausius - Clapyron equation.

There are two possible errors in this method of calibration - firstly the Clausius -Clapyron equation does not give a linear plot over such a large range of temperature and pressure. This is quite possible, there are many recorded cases of a slight curvature in the graph. Secondly the pressure in the manometer, thermostated at 20°, 25° or 30°C may not be the same as the pressure over the adsorbate cooled to low temperatures in a slush bath, due to thermal transpiration effects (58).

The error due to this can not be evaluated except for the case where the mean free path is very much longer than the diameter of the connecting tubing; and so no correction was made.

RESULTS

"I know what you're thinking about," said Tweedledum: "but it isn't so, nohow." "Contrariwise," continued Tweedledee, "if it was so, it might be; and if it were so, it would be: but as it isn't, it ain't. That's logic."

Lewis Carroll

The individual experiments are described in the following pages. The experiments are not necessarily in the order in which they were performed, but are grouped together according to which adsorbate was used to facilitate comparison.

For the isotherms the relative pressure as abcissae are plotted against the quantity adsorbed, in milligrammes per gramme, as ordinates. All the experimental points are shown on the associated graphs, and an abbreviated table is also given in the script for each system. Where the numbers are divided by a double line there is a change from adsorption to desorption or vice-versa. In the following tables the concentration in units of milligrammes of adsorbate per gramme of adsorbent will be abbreviated to mg/gm., and the relative pressure to p/p_o.

Each run was carried out at least twice to check the reproducibility of the results. The points obtained in different runs, and in adsorption and desorption are distinguished from each other.

Fig 9

Ethyl alcohol on Silica gel

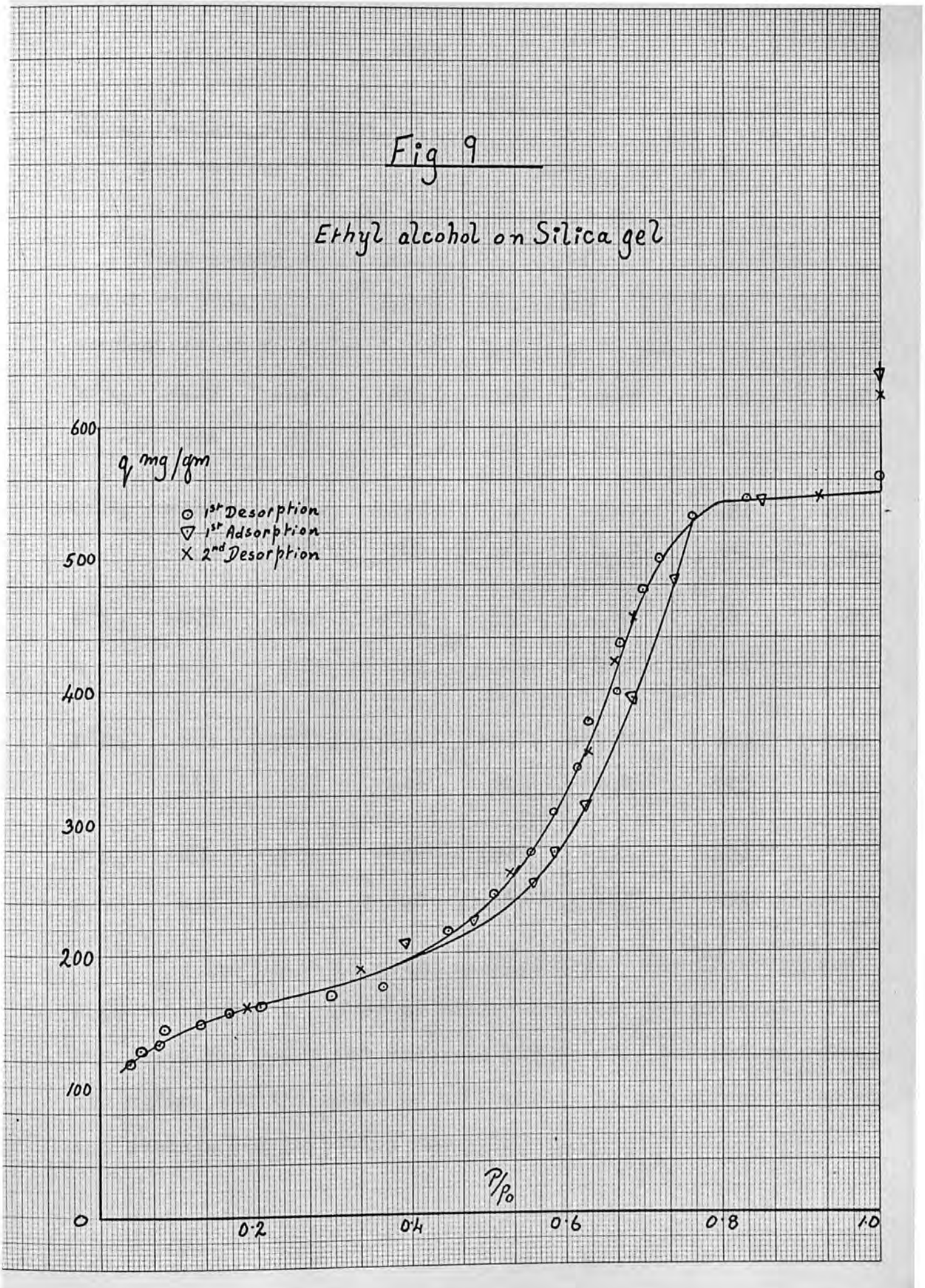

Ethyl alcohol on silica gel

Activation: 16 hrs. at 150°C

Weight of activated gel: ·7638 gm.

Temperature of isotherm: 25·0°C

relative pressure	1·000	·890	·761	·717	·695	·667	
concentration in mg/gm.	562	546	531	500	475	437	
p/p_o	·648	·627	·614	·583	·553	·507	·448
q	398	374	340	307	275	243	216
p/p_o	·364	·295	·239	·203	·160	·128	·081
q	194	181	169	162	155	148	144
p/p_o	·073	·050	·037 //	·393	·479	·556	·584
q	135	129	122 //	209	223	251	274
p/p_o	·623	·683	·737	·851	1·000 //	1·000	·923
q	313	392	485	545	640 //	625	549
p/p_o	·684	·659	·628	·528	·333	·186	
q	466	422	352	260	187	159	

The graph is shown in figure 9. The isotherm was repeatable over a number of adsorptions and desorptions. From the graph the point 'A' value is 125 mg/gm., saturation value 550 mg/gm. and the point of inflection, p_i/p_o corresponding to the average Kelvin radius was ·635.

Fig 10

Ethyl alcohol on ferric oxide I

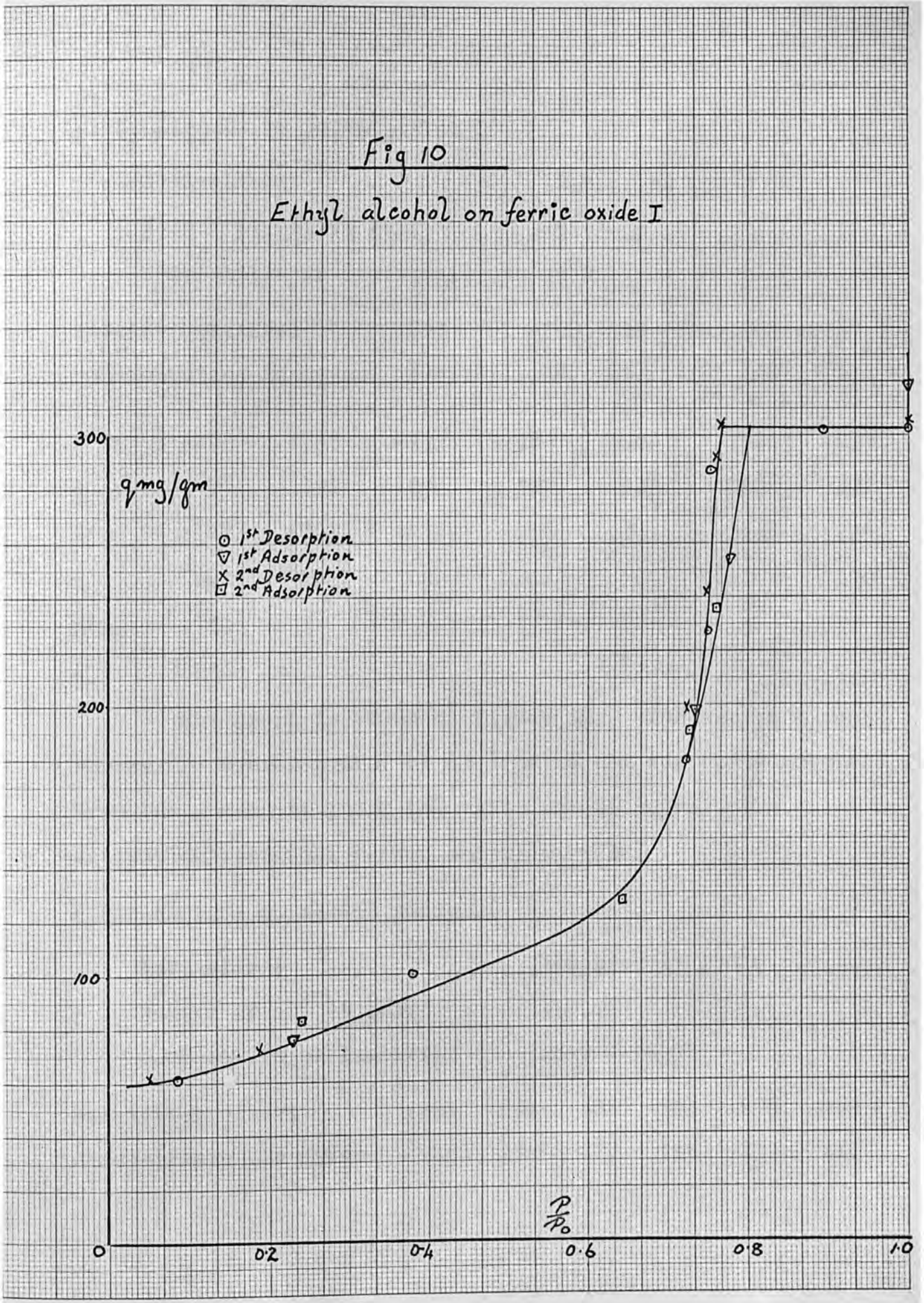

Ethyl alcohol on ferric oxide I

Activation: 18 hrs. at 150°C

Weight of active gel: ·9153 gm.

Temperature of isotherm: 25°C

relative pressure	·893	·761	·745	·726	·722	·382	·083 //
concentration in mg/gm.	302	287	227	227	179	100	61

p/p_o	·163	·735	·777	1·000 //	1·000	·780	·757
q	76	198	274	329	305	304	292
p/p_o	·747	·723	·178	·056	·241	·645	·726
q	241	195	72	62	83	127	190
p/p_o	·759						
q	236						

The graph is shown as figure 10. The isotherm was repeatable over a number of adsorption and desorption cycles. From the graph the point 'A' value was 51 mg/gm., the saturation value 304 mg/gm. and p_i/p_o ·732.

Ethyl alcohol on ferric oxide II

Activation: 16½ hrs. at 150°C

Weight of active gel: 1·0308

Temperature of isotherm: 25·0°C

relative pressure	·981	·974	·821	·503	·495	·469
concentration in mg/gm.	248	234	173	156	139	113

Fig II

Ethyl alcohol on Ferric oxide II

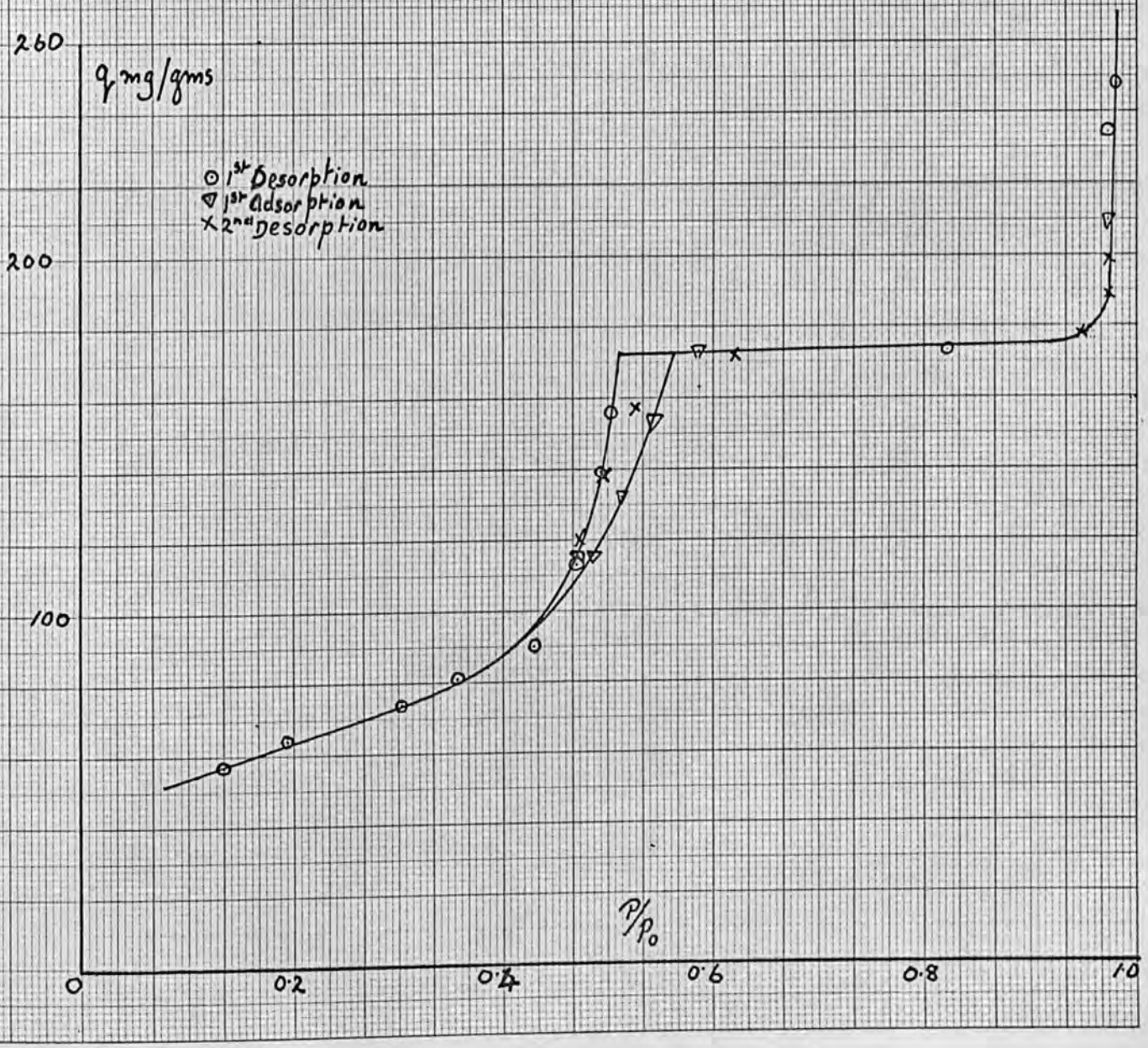

Fig 13

Ethyl alcohol on Ferric oxide III

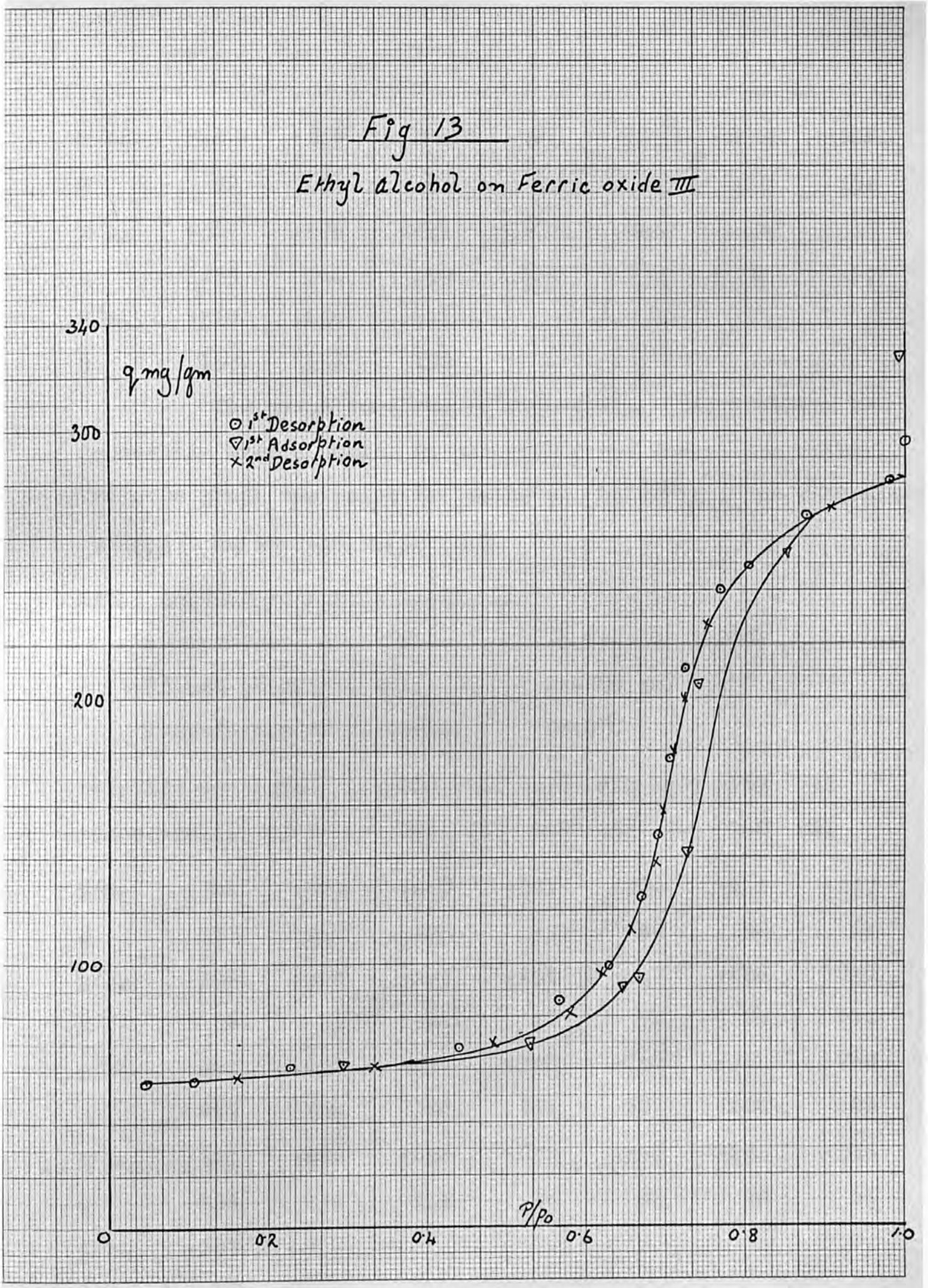

p/p$_o$	·430	·356	·304	·193	·135	·470	·514
q	90	81	74	64	57	115	152
p/p$_o$	·587	·974	·974	·972	·948	·620	·527
q	173	210	199	189	178	172	167
p/p$_o$	·512	·497	·473				
q	157	138	120				

The graph is shown in figure 11. The isotherm was repeatable over a number of adsorption and desorption points. From the graph the point 'A' value was 42 mg/gm., the saturation value 175 mg/gm. and p$_i$/p$_o$ ·513.

Ethyl alcohol on ferric oxide III

Activation: 15 hrs. at 150°C

Weight of active gel: 1·0758 gm.

Temperature of isotherm: 25·0°C

relative pressure	1·000	·981	·876	·832	·805	·769	·722
concentration mg/gm.	296	281	268	258	249	240	211
p/p$_o$	·704	·689	·669	·631	·568	·442	·227
q	177	149	125	99	86	68	61
p/p$_o$	·108	·048	·293	·531	·647	·666	·726
q	56	55	62	70	91	94	142
p/p$_o$	·740	·852	·994	·908	·750	·724	·710
q	205	254	328	271	227	200	180
p/p$_o$	·698	·686	·656	·621	·580	·483	·335
q	158	138	113	96	81	70	61
p/p$_o$	·155						
q	57						

Fig 14

Low pressure isotherms of ethyl alcohol on Ferric oxide III

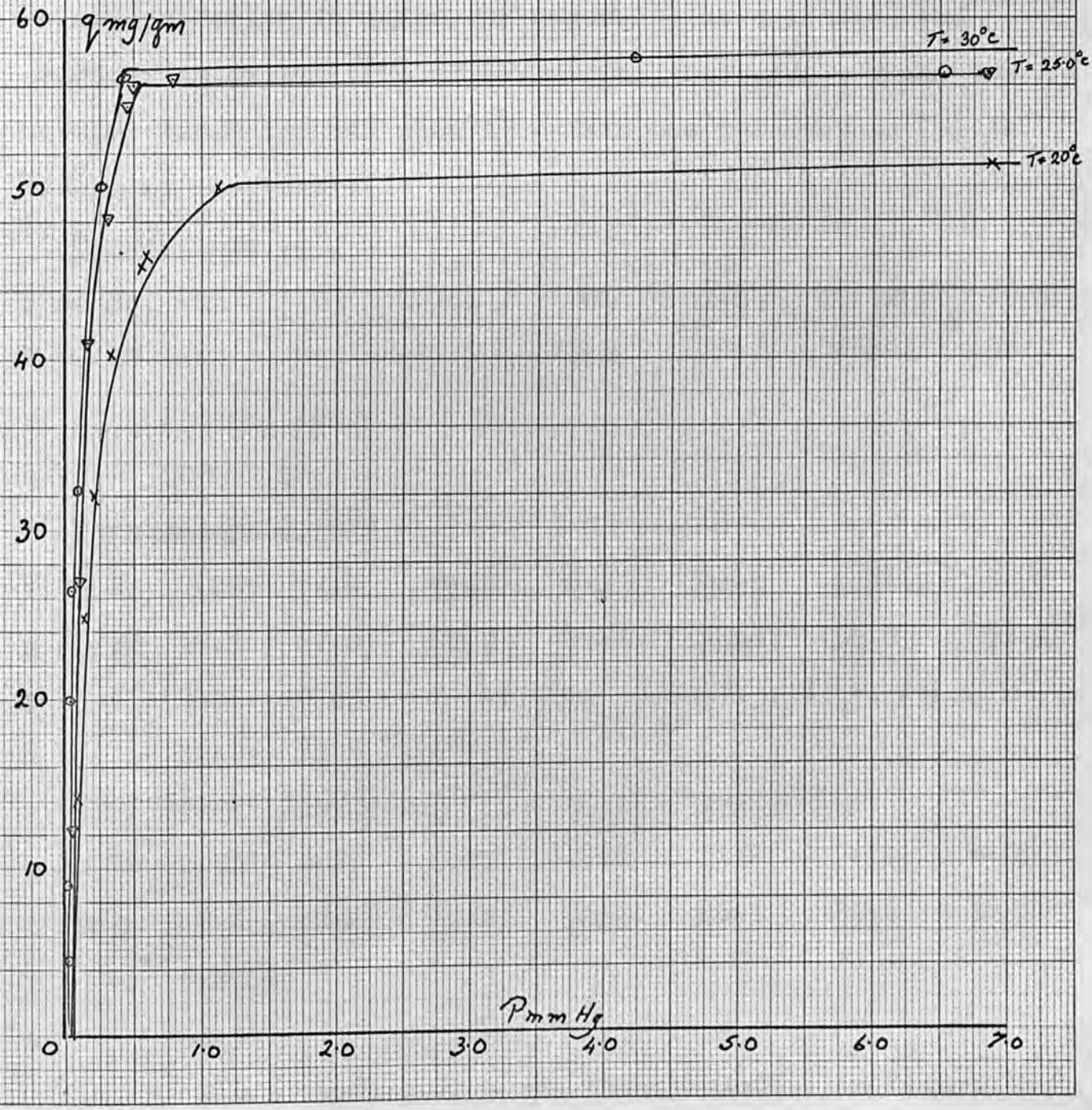

The graph is shown in figure 13. The isotherm was repeatable over a number of adsorption and desorption points. From the graph the point 'A' value was 54 mg/gm., the saturation value 283 mg/gm. and p_i/p_o ·715.

Low pressure data

The same sample of gel was used as for the high pressure regions of the isotherm. The data will be given as concentration in mg/gm. of adsorbent as ordinates and pressure in millimeters of mercury as abcissae. Where the mercury manometer was used to obtain the pressure an (m) is placed by the result.

Temperature 20°C

p mm Hg	·03	·03	·04	·04	1·89	10·12(m) //	6·54(m)
q mg/gm	4·5	8·9	19·9	25·5	50·1	58·39	56·2
p	1·32(m)	·42					
q	50·4	46·3					

Temperature 25·0°C

p mm Hg	0.05	0.10	0.15	0.31	0.45	6.85(m)	0.78
q mg/gm	12.3	27.0	40.9	48.3	54.6	56.8	56.4
p	0.50	0.22					
q	56.0	53.0					

Temperature 30.0°C

p mm Hg	0·33	0·55	0·13	1·11	0·58(m)	0·20	0·09
q mg/gm	40·3	45·4	24·8	50·0	46·1	32·4	14·2
p	6·88(m)						
q	51·3						

These three graphs are shown together in figure 14.

Fig 15

β trifluoroethanol on Silica gel

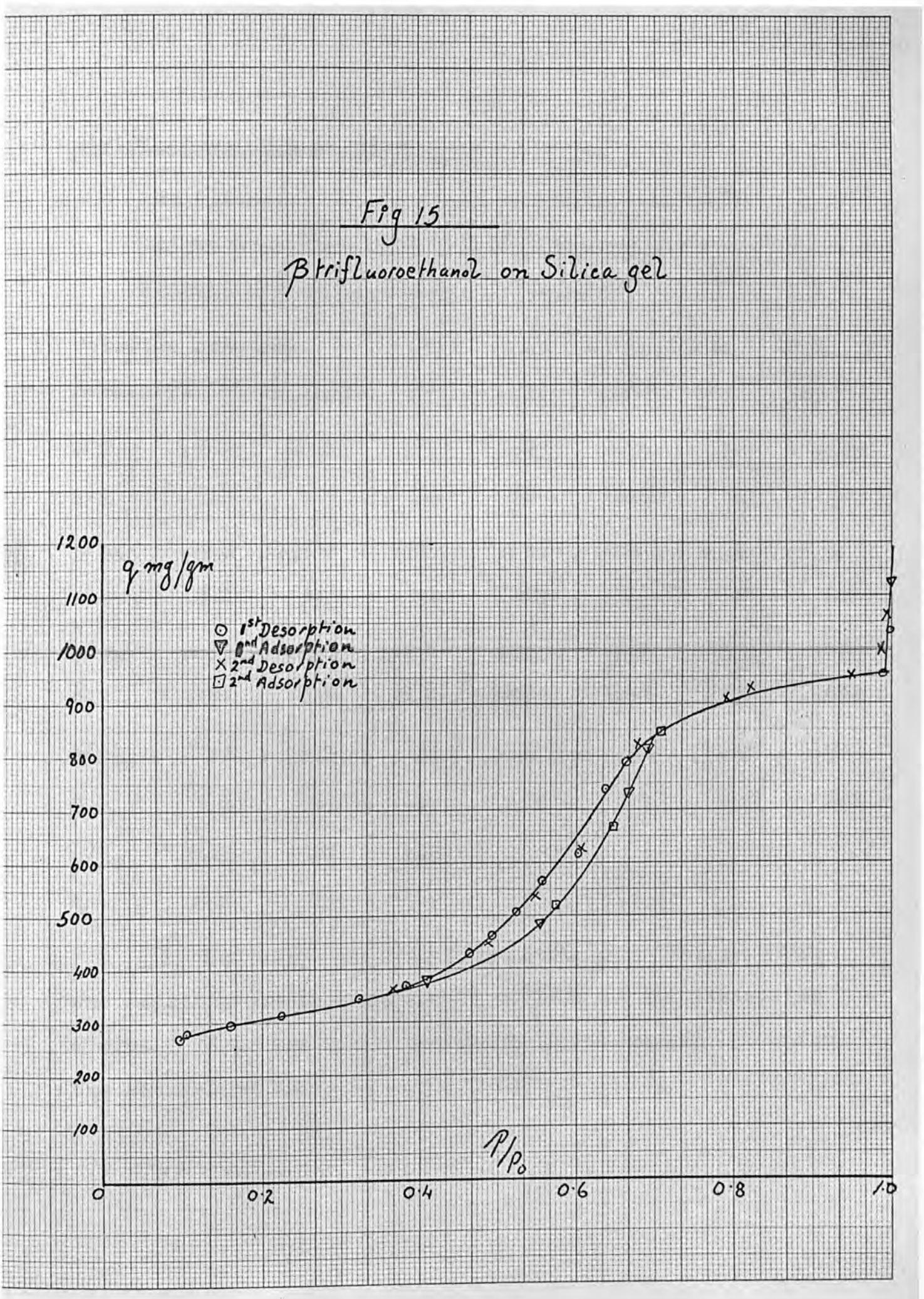

β-trifluoroethanol on silica gel

Activation: 16 hrs. at 150°C

Weight of active gel: ·8251 gm.

Temperature of isotherm: 25·0°C

relative pressure			·999	·990	·691	·680	·654
concentration in mg/gm.			1033	957	866	842	789
p/p_o	·637	·601	·558	·523	·494	·465	·383
q	739	617	564	507	460	428	369
p/p_o	·322	·225	·163	·112	·095 //	·410	·556
q	342	313	294	280	270 //	379	486
p/p_o	·667	·691	1·000 //	·992	·985	·951	·753
q	731	816	1124 //	1065	1007	952	930
p/p_o	·722	·677	·640	·608	·549	·486	·370 //
q	910	821	718	629	536	447	362 //
p/p_o	·706	·572	·648				
q	849	520	669				

The graph is shown in figure 15. The isotherm was repeatable over a number of adsorption and desorption cycles. From the graph the point 'A' value was 237 mg/gm., the saturation value 955 mg/gm. and p_i/p_o ·639.

Fig 16

β trifluoroethanol on Ferric oxide I

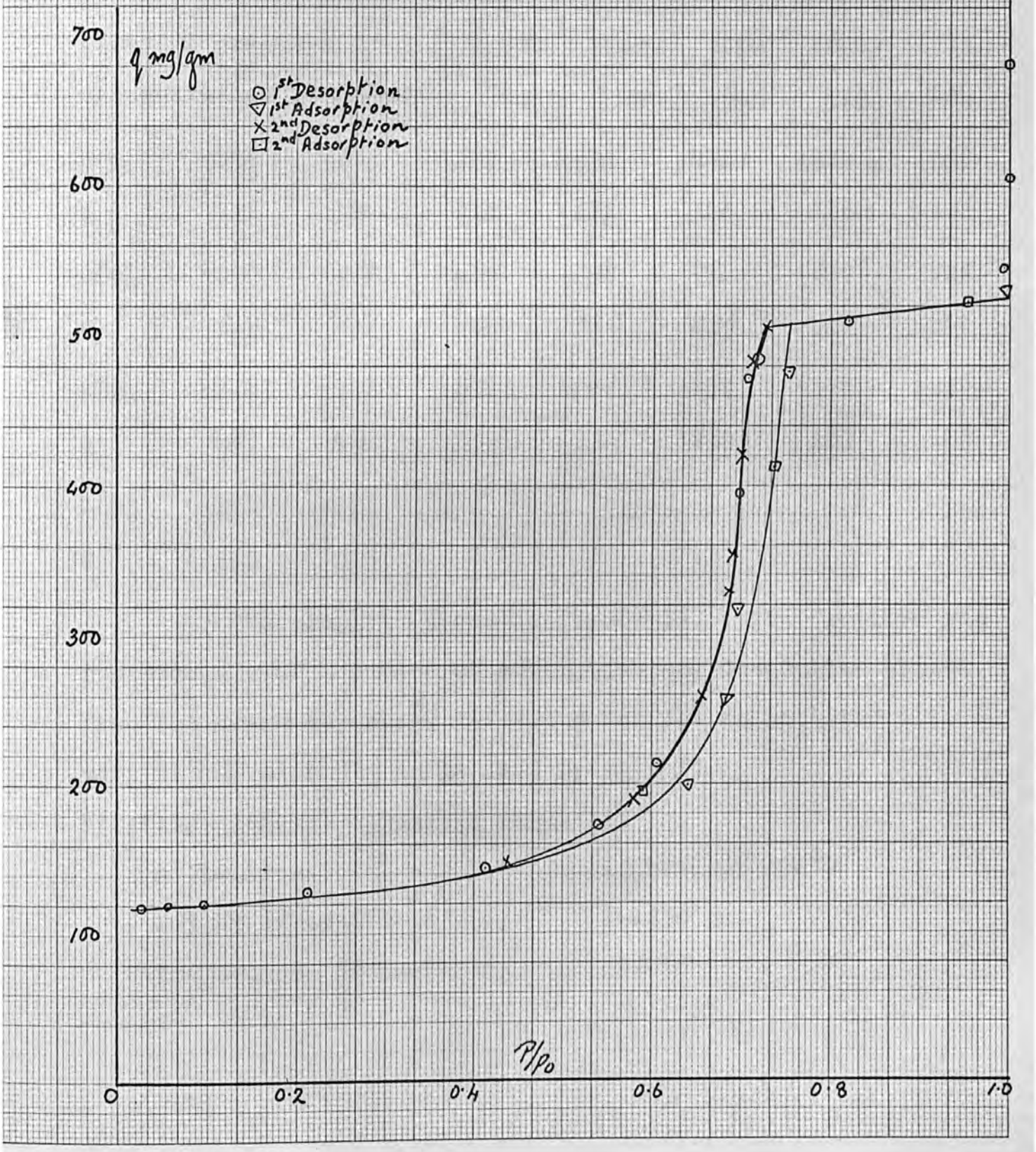

βtrifluoroethanol on ferric oxide I

Activation: 16 hrs. at 150°C

Weight of activated gel: ·8985 gm.

Temperature of isotherm: 25·0°C

relative pressure			1·000	1·000	·994	·821	·715
concentration in mg/gm.			682	605	545	510	484
p/p_o	·708	·698	·607	·538	·414	·213	·098
q	472	394	213	172	144	128	121
p/p_o	·056	·030 //	·639	·698	·754	·997 //	·726
q	119	117	199	317	476	529	506
p/p_o	·712	·701	·691	·688	·656	·578	·436 //
q	483	421	354	331	259	190	148
p/p_o	·591	·953					
q	195	523					

The graph is shown in figure 16. The isotherm was repeatable over a number of adsorption and desorption cycles. From the graph the point 'A' value was 116 mg/gm., the saturation value 520 mg/gm. and p_i/p_o ·833.

βtrifluoroethanol on ferric oxide III

Activation: 15 hrs. at 150°C

Weight of activated gel: 1·1250 gm.

Temperature of isotherm: 25·0°C

Fig 17

β trifluoroethanol on Ferric oxide III

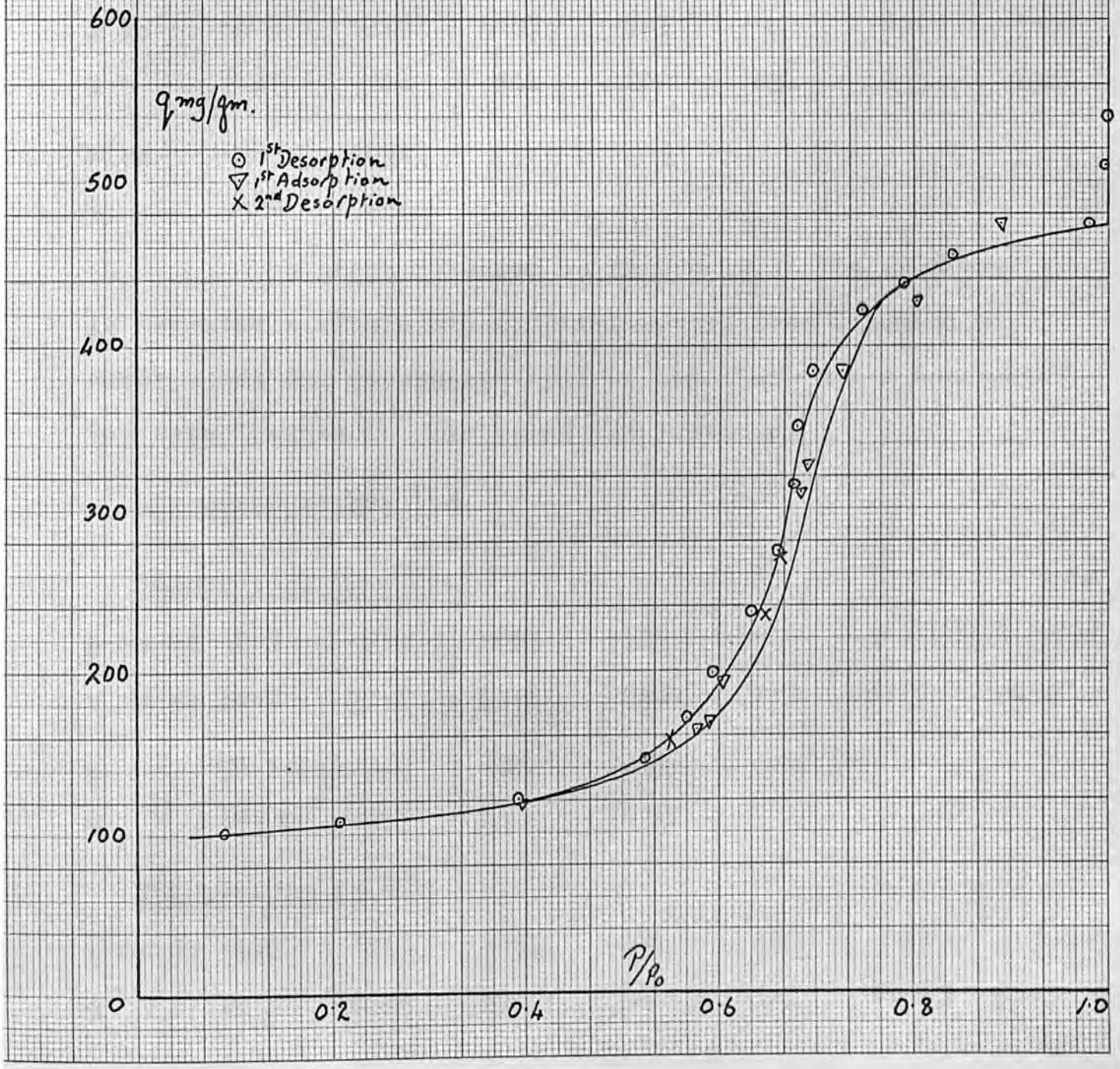

relative pressure			1·000	·997	·982	·840	·790	·747
concentration in mg/gm.			540	511	474	455	438	422
p/p_o	·696	·681	·677	·662	·634	·593	·565	
q	384	350	315	274	236	198	169	
p/p_o	·525	·396	·208	·091	·397	·576	·891	
q	145	121	108	101	118	164	474	
p/p_o	·802	·726	·683	·663	·647	·602	·550	
q	427	384	311	271	231	193	158	
p/p_o	·589	·691						
q	168	327						

The graph is shown in figure 17. The isotherm is repeatable within experimental error, over a number of adsorptions and desorption cycles, but there was a tendency for later points to lie below the isotherm.

Low pressure results

Temperature 20·0°C

p mm Hg	·065	·099	·293	·520	1·16	3·61(m)	8·65(m)
q mg/gm	38·2	47·8	63·4	68.1	77·5	87·4	94·3
p	16·65(m)	·072	·041	·028			
q	102·4	40·7	25·1	14·0			

Temperature 25·0°C

p mm Hg	·010	·013	·024	·069	·52	·53	1·39(m)
q	13·9	28·8	40·1	53·6	65·7	74·8	86·3

Fig 18

Low pressure isotherms of β trifluoroethanol on Ferric oxide III

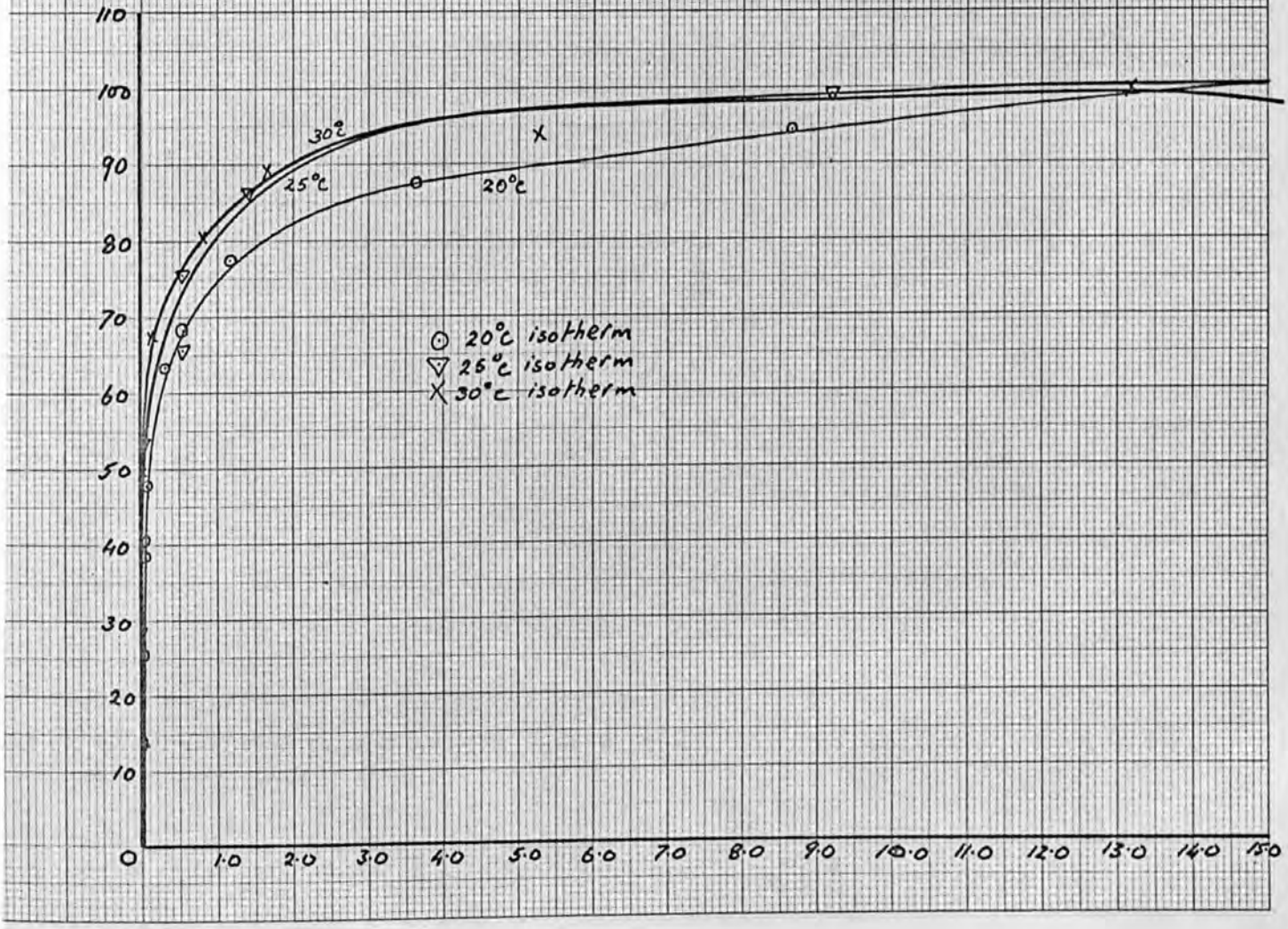

Fig 19

Bmonofluoroethanol on Silica gel

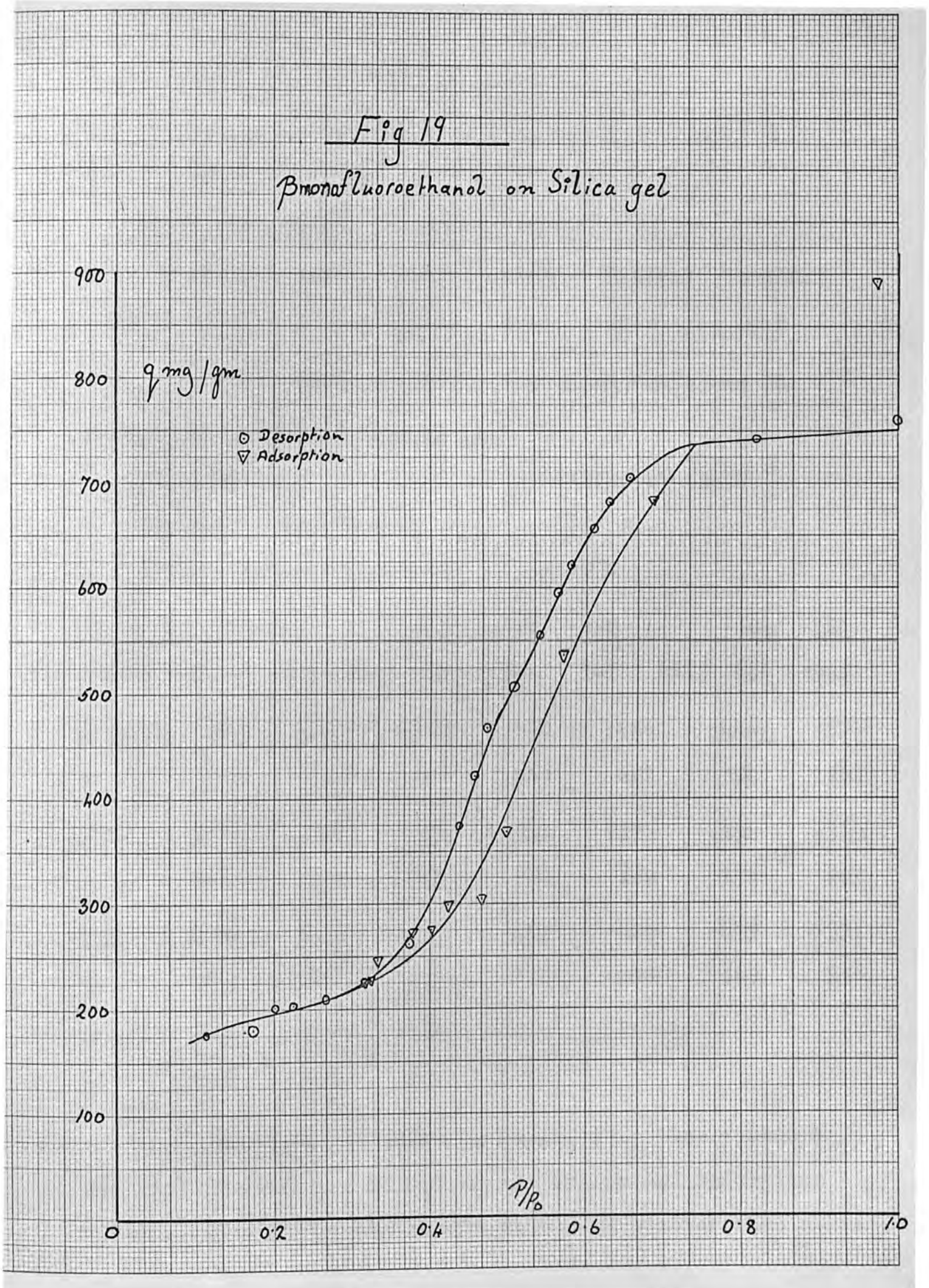

p	9·19(m)	17·75
q	99·2	105·5

Temperature 30·0°C

p mm Hg	·020	·121	·805	1·65	5·26(m)	13·18(m)
q mg/gm	49·07	67·4	80·5	89·2	93·8	99·8

These three isotherms are shown in figure 18.

βmonofluoroethanol on silica gel

Activation: 16 hrs. at 150°C

Weight of active gel: ·7895 gm.

Temperature of isotherm: 25·0°C

relative pressure		1·000	·802	·656	·629	·604	·581
concentration in mg/gm		810	741	705	681	656	622
p/p_o	·564	·540	·517	·478	·456	·446	·374
q	595	555	507	467	421	374	261
p/p_o	·268	·262	·224	·201	·172	·114 //	·315
q	208	232	200	201	180	176	225
p/p_o	·323	·333	·378	·402	·423	·499	·571
q	228	246	273	275	299	369	536
p/p_o	·688	·973 //	·465				
q	684	892	305				

The graph is shown in figure 19. The isotherm was repeatable over a number of adsorption and desorption cycles, but although the points show more scatter than normal,

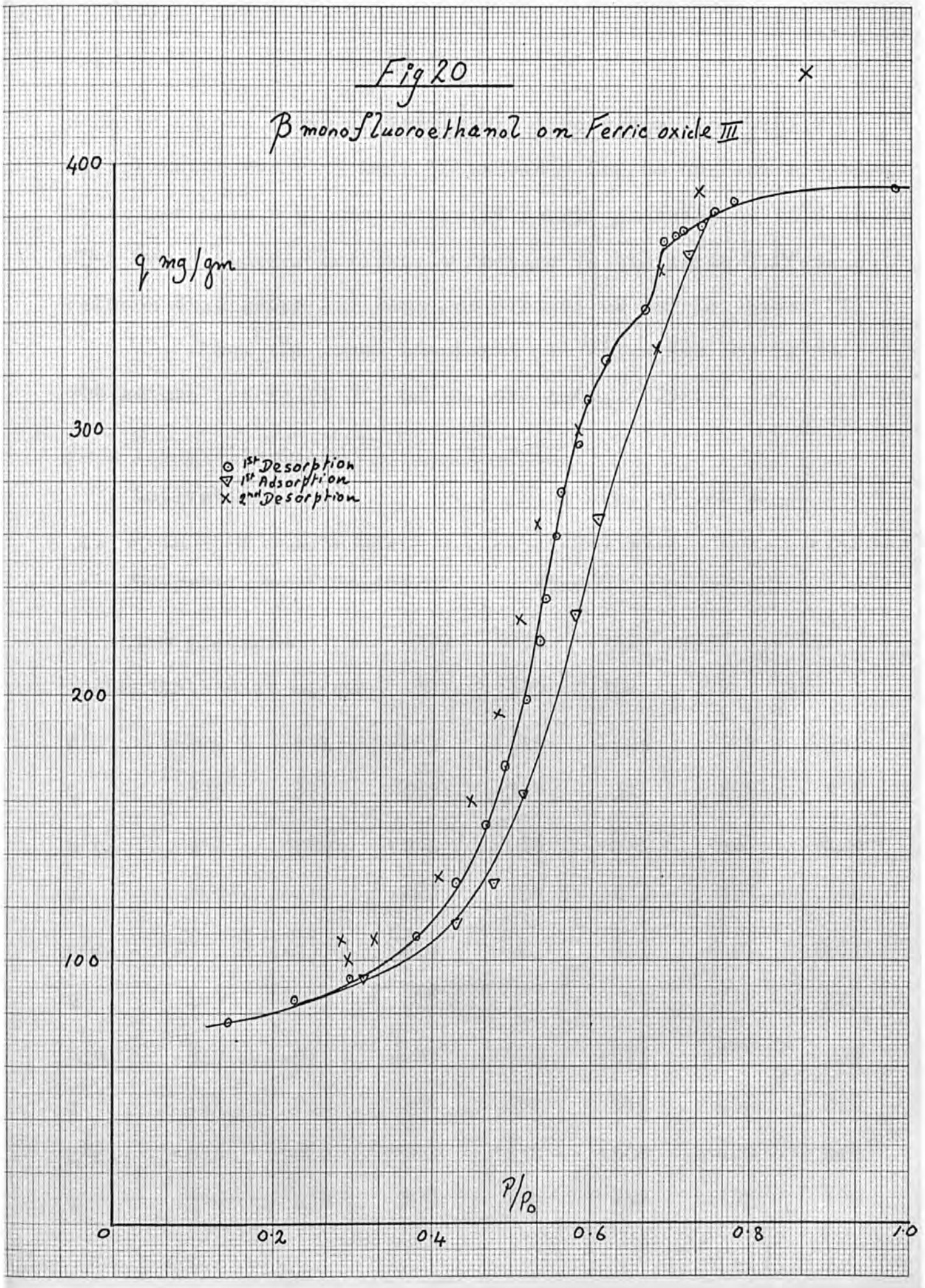
Fig 20
β monofluoroethanol on Ferric oxide III
400
300
200
100
q mg/gm
1st Desorption
1st Adsorption
2nd Desorption
P/Po
0
0·2
0·4
0·6
0·8
1·0

a curve can be drawn so that their divergence lies within experimental error. This is probably due to the low pressures to be measured e.g. the saturated vapour pressure at 25°C is 25.6 mm. Another noticeable feature is the large difference between this graph and that for ethanol on ferric oxide III.

From the graph the point 'A' value was 183 mg/gm. the saturation value 755 mg/gm. and p_i/p_o $\cdot 519_5$.

βmonofluoroethanol on ferric oxide III

Activation: $15\frac{1}{2}$ hrs. at 150°C

Weight of active gel: 1·2616 gm.

Temperature of isotherm: 25·0°C

relative pressure			·979	·770	·752	·737	·714
concentration in mg/gm			391	386	382	377	375
p/p_o	·704	·691	·663	·616	·593	·583	·560
q	373	371	345	326	311	294	276
p/p_o	·552	·539	·532	·516	·491	·467	·429
q	259	236	220	198	173	151	129
p/p_o	·378	·297	·228	·143	·313	·431	·474
q	109	93	85	77	93	114	129
p/p_o	·517	·577	·606	·719	·883	·867	·799
q	163	230	266	366	449	435	390
p/p_o	·686	·610	·581	·530	·508	·480	·445
q	360	330	300	264	228	193	160

Fig 21

n propanol on Silica gel

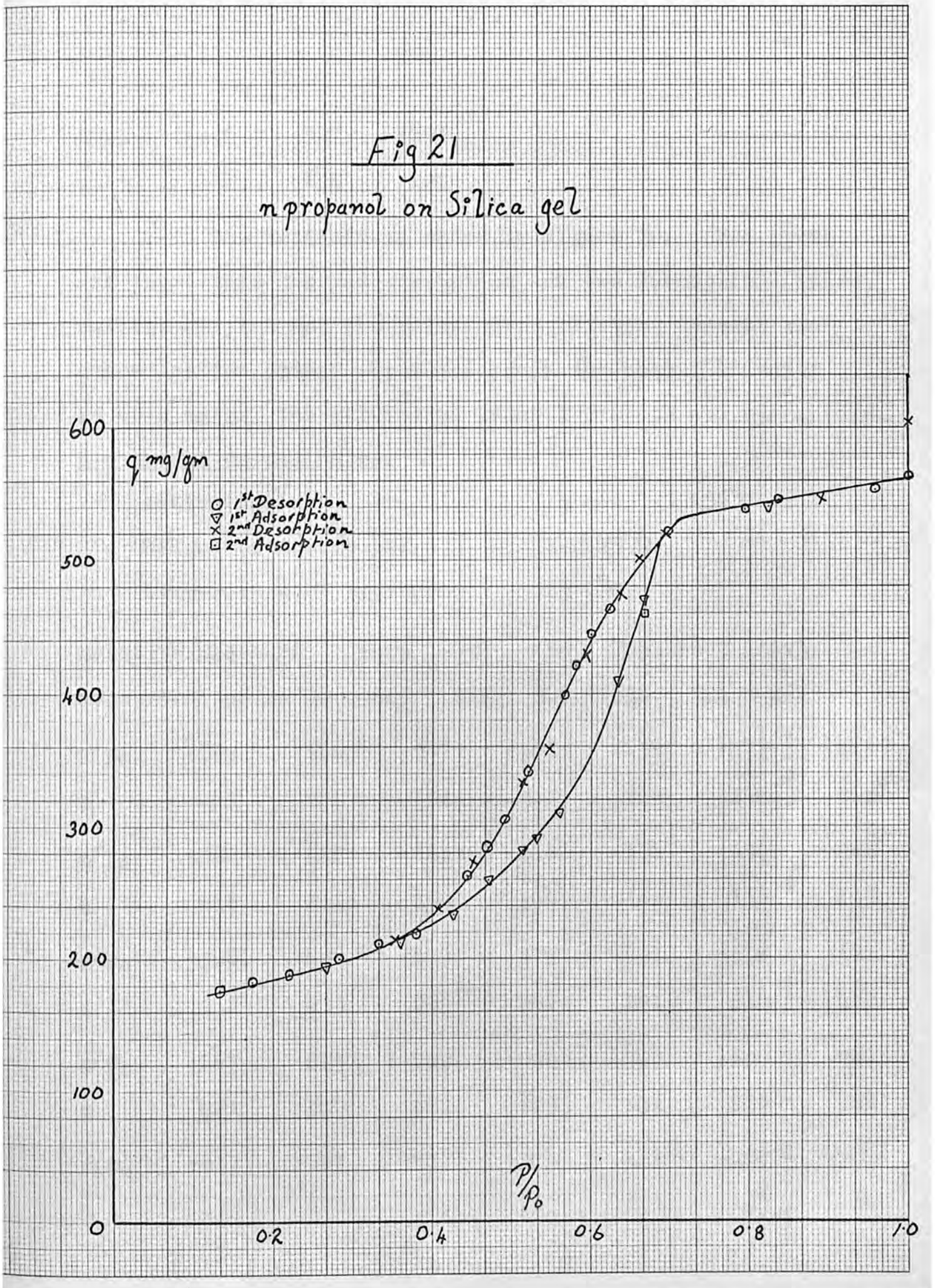

p/p_o	·406	·327	·293
q	131	108	100

The isotherm is shown in figure 20. The graph was repeatable over an adsorption and two desorption cycles, but towards the end the points were drifting towards the concentration axis. From the graph the point 'A' value is 60·4 mg/gm, the saturation value 392 mg/gm and p_i/p_o ·570.

n-propanol on silica gel

Activation: 15 hrs. at 150°C

Weight of active gel: 1·0425 gm.

Temperature of isotherm: 25·0°C

relative pressure	·999	·958	·858	·795	·697	·623	
concentration mg/gm	563	553	545	538	521	462	
p/p_o	·599	·586	·567	·521	·491	·471	·443
q	443	421	392	341	305	284	264
p/p_o	·382	·332	·283	·218	·174	·134 //	·266
q	218	211	199	188	182	176	195
p/p_o	·358	·428	·470	·513	·531	·559	·634
q	212	233	259	282	291	310	410
p/p_o	·667	·823	1·000 //	1·000	·890	·694	·661
q	471	540	681	605	546	519	501
p/p_o	·637	·592	·547	·515	·451	·407	·354 //
q	475	428	357	333	271	238	214

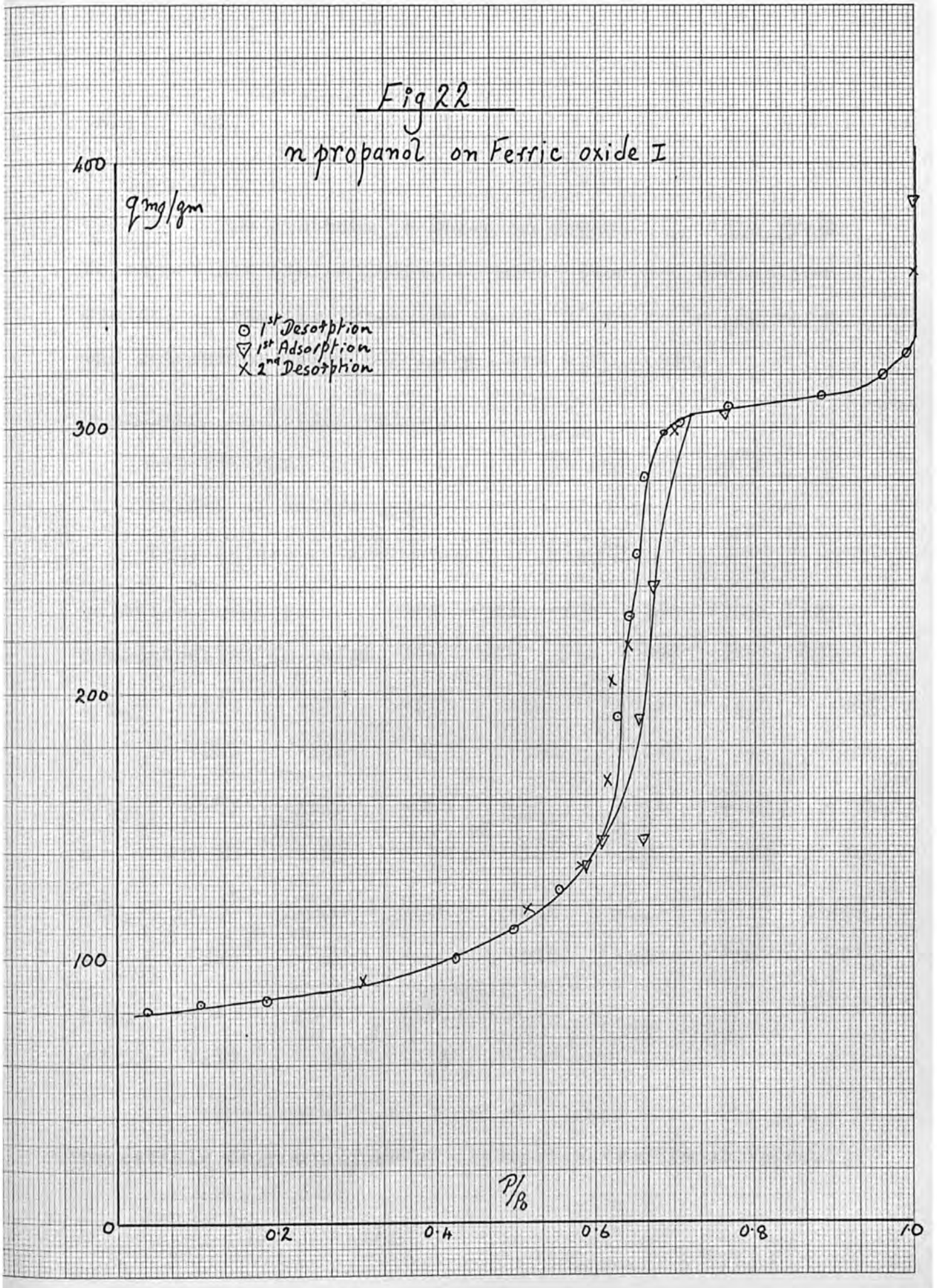
Fig 22
n propanol on Ferric oxide I
400
q mg/gm
300
200
100
0
0·2
0·4
0·6
0·8
1·0
P/P0
○ 1st Desorption
▽ 1st Adsorption
× 2nd Desorption

p/p_o	·667
q	459

The isotherm is shown in figure 21. The graph is repeatable over a number of adsorption and desorption cycles. From the graph the point 'A' value is 152 mg/gm., the saturation value 563 mg/gm. and p_i/p_o ·536.

n-propanol on ferric oxide I

Activation:	16 hrs. at 150°C
Weight of active gel:	·7881 gm.
Temperature of isotherm:	25·0°C

relative pressure		·989	·961	·884	·769	·708	·685
concentration in mg/gm.		328	320	312	308	302	298
p/p_o	·660	·650	·639	·626	·552	·497	·423
q	281	252	229	191	126	111	100
p/p_o	·187	·110	·044	·606	·653	·669	·764
q	84	83	80	145	190	260	305
p/p_o	1·000	1·000	·699	·638	·617	·615	·579
q	386	359	299	218	205	167	135
p/p_o	·513	·304	·587				
q	119	92	135				

The isotherm is shown in figure 22. The graph is repeatable over a number of adsorptions and desorptions.

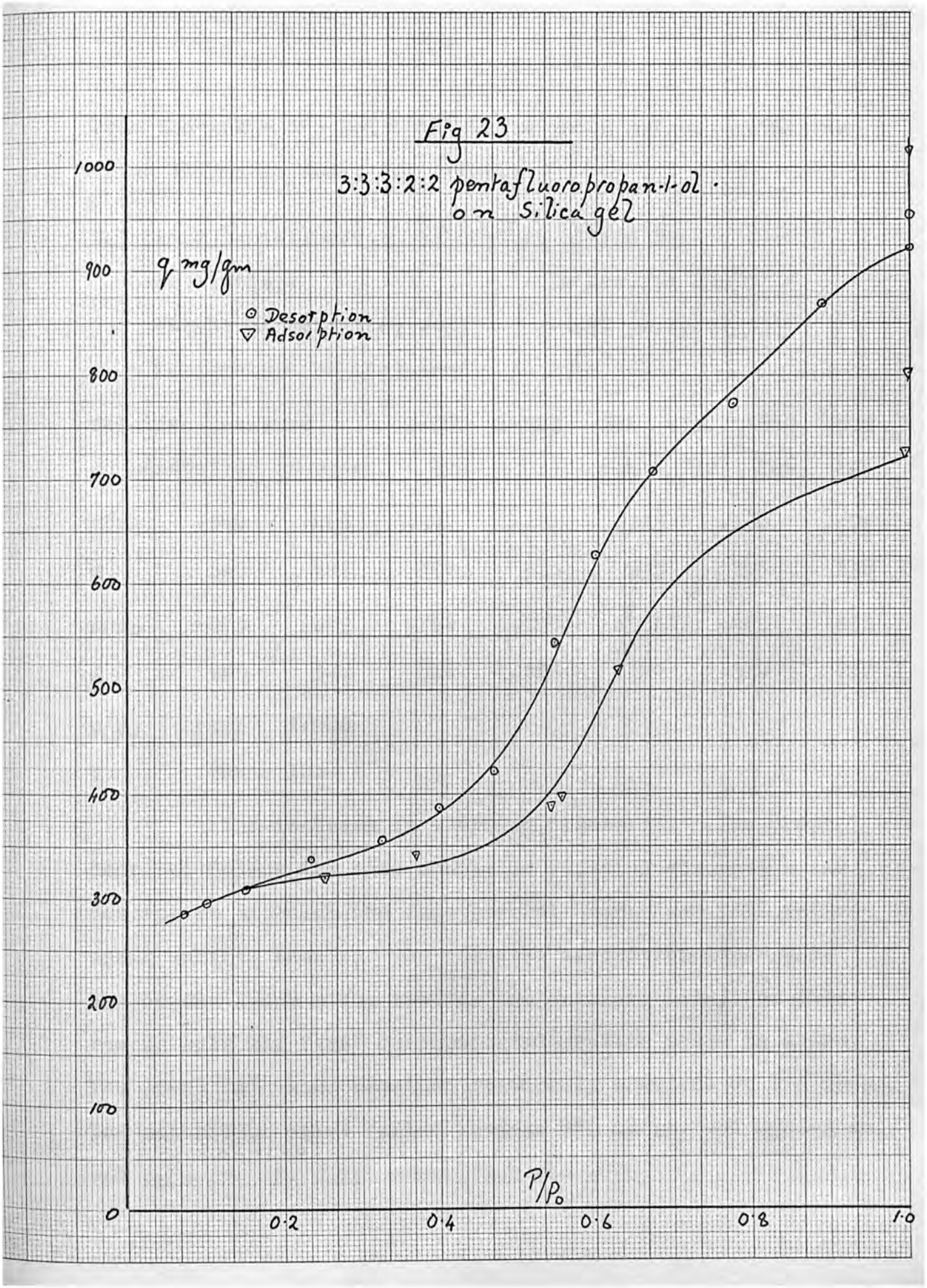
Fig 23
3:3:3:2:2 pentafluoropropan-1-ol · on silica gel
q mg/gm
⊙ Desorption
▽ Adsorption
1000
900
800
700
600
500
400
300
200
100
0
P/P₀
0·2
0·4
0·6
0·8
1·0

From the graph the point 'A' value is 78 mg/gm., saturation value 317 mg/gm and p_i/p_o ·625.

3:3:3:2:2 pentafluoropropan-1-ol on silica gel

Activation: 16 hrs. at 150°C

Weight of activated gel: ·9477 gm.

Temperature of isotherm: 25°C

relative pressure			1·000	1·000	·886	·758	·669	·596
concentration in mg/gm.			955	923	864	772	706	626
p/p_o	·544	·468	·397	·324	·233	·150	·100	
q	560	421	386	355	337	309	296	
p/p_o	·073	·249	·366	·539	·553	·625	·993	
q	285	320	341	388	397	519	727	
p/p_o	·995	1·000						
q	802	1016						

The isotherm is shown in figure 23. The graph does not follow the same course on repeated adsorption and desorption although the same general course was followed on using another sample. On repeated adsorption/desorption cycles the graph moves towards the pressure axis, for this reason only the first desorption/adsorption cycle is shown. The point 'A' value remained reasonably constant at 270 mg/gm. The saturation value varied between 880 mg/gm. and 850 mg/gm., and p_i/p_o for the first desorption was ·678.

Fig 24

2:2:3:3:3 pentafluoropropan-1-ol on Ferric oxide I

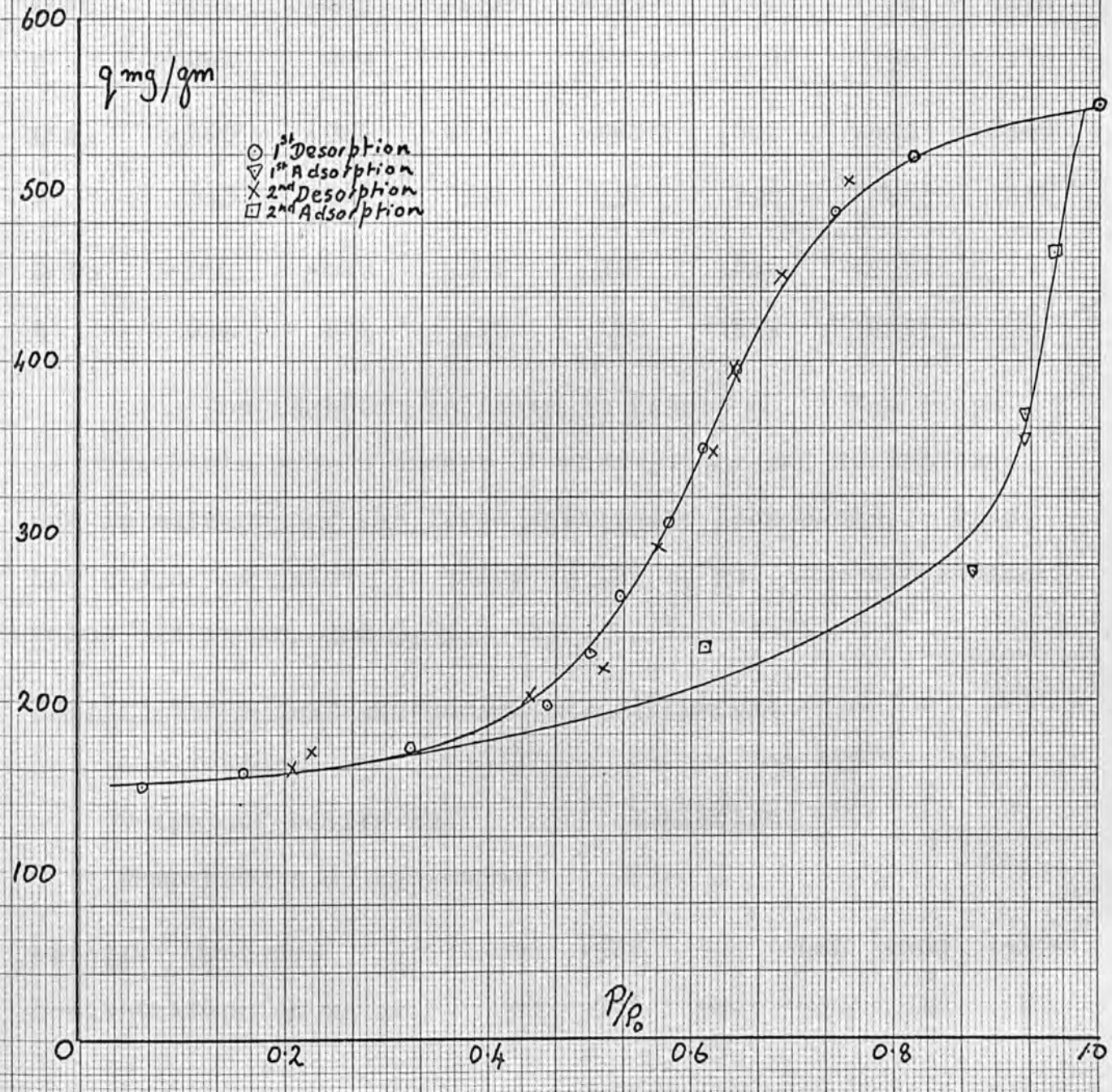

2:2:3:3:3 pentafluoropropan-1-ol on ferric oxide I

Activation: 15½ hrs. at 150°C

Weight of active gel: ·7934 gm.

Temperature of isotherm: 25·0°C

relative pressure	1·000	·818	·739	·644	·611	·576
concentration in mg/gm.	550	519	487	394	348	305

p/p_o	·531	·499	·458	·322	·161	·060	·878 //
q	261	229	197	172	158	150	276
p/p_o	·925	·926 //	·753	·888	·641	·622	·566
q	355	368	505	450	396	346	291
p/p_o	·514	·440	·293	·207	·614 //	·956	
q	218	202	170	160	232	463	

The isotherm is shown in figure 24. The graph is repeatable over a number of adsorptions and desorptions but is notable for the large hysteresis loop shown. From the graph the point 'A' value is 142 mg/gm., the saturation value 525 mg/gm. and p_j/p_o ·651.

2:2:3:3 tetrafluoropropan-1-ol on silica gel

Activation: 16 hrs. at 150°C

Weight of active gel: 1·1128 gm.

Temperature of isotherm: 25·0°C

relative pressure	1·000	·985	·794	·646	·609	·587
concentration in mg/gm.	998	966	946	930	918	902

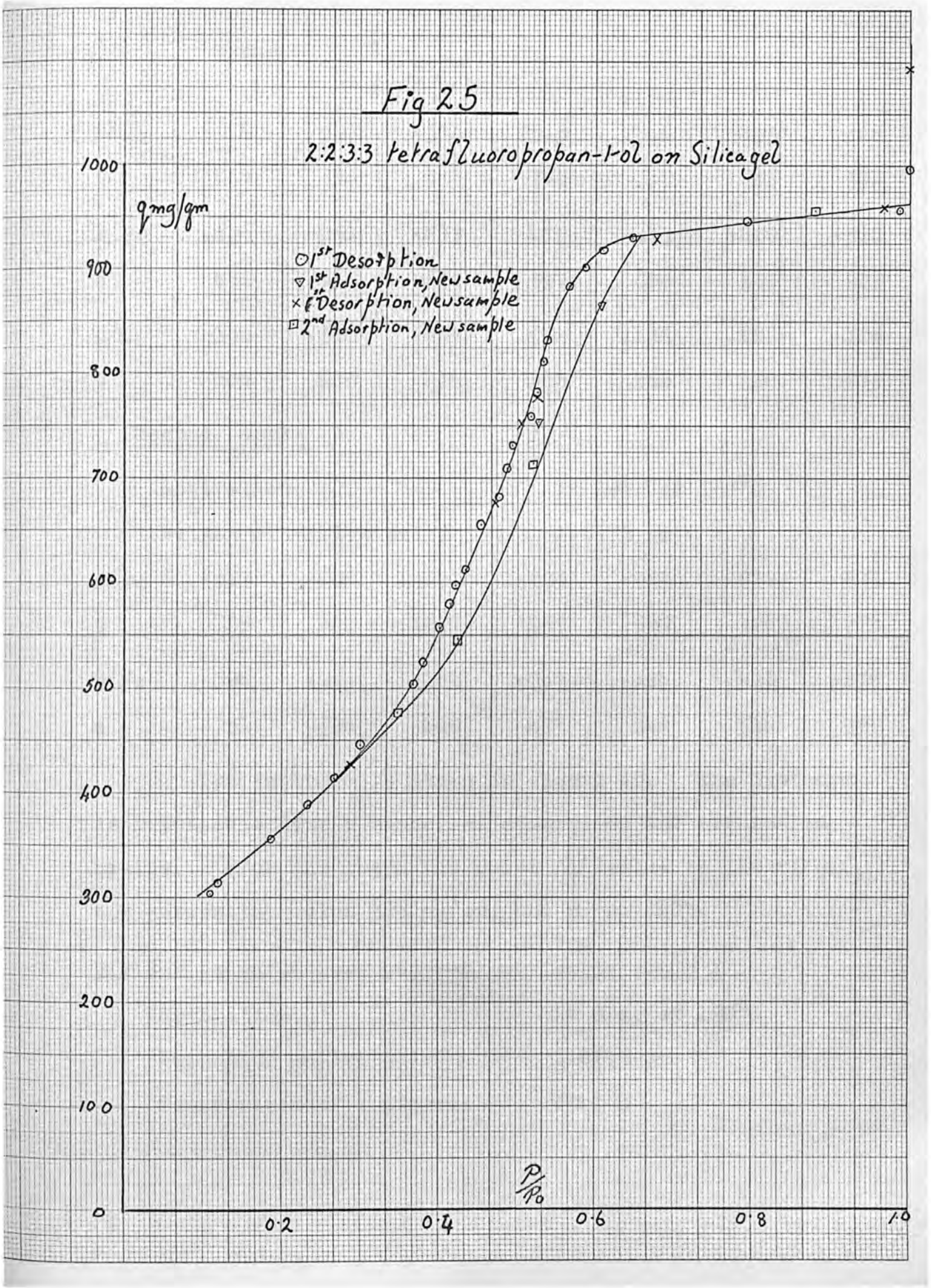
Fig 2.5
2:2:3:3 Tetrafluoropropan-1-ol on Silicagel
q mg/gm
1000
900
800
700
600
500
400
300
200
100
0
1st Desorption
1st Adsorption, New sample
1st Desorption, New sample
2nd Adsorption, New sample
P/P0
0·2
0·4
0·6
0·8
1·0

p/p_o	•568	•538	•536	•525	•516	•495	•486
q	884	831	812	782	759	731	708
p/p_o	•476	•454	•433	•419	•413	•400	•382
q	681	655	612	597	580	557	525
p/p_o	•366	•310	•267	•234	•188	•128	•116
q	504	445	414	388	356	314	303

Second sample

Activation: 16 hrs. at 150°C

Weight of active gel: 1•0775 gm.

p/p_o	•527	•608	1•000 //	1•000	•965	•678	•523
q	759	865	1207 //	1093	960	928	776
p/p_o	•504	•471	•288 //	•347	•424	•521	•878
q	751	676	428 //	476	546	714	957

The isotherm is shown in figure 25. The isotherm is repeatable over a number of adsorption and desorption cycles. From the graph the point 'A' value is 220 mg/gm., the saturation value 966 mg/gm. and p_i/p_o •473.

2:2:3:3 tetrafluoropropan-1-ol on ferric oxide I

Activation: 16 hrs. at 150°C

Weight of active gel: 1•0145 gm.

Temperature of isotherm: 25•0°C

Fig 26

2:2:3:3 tetrafluoropropan-1-ol on Ferric oxide I

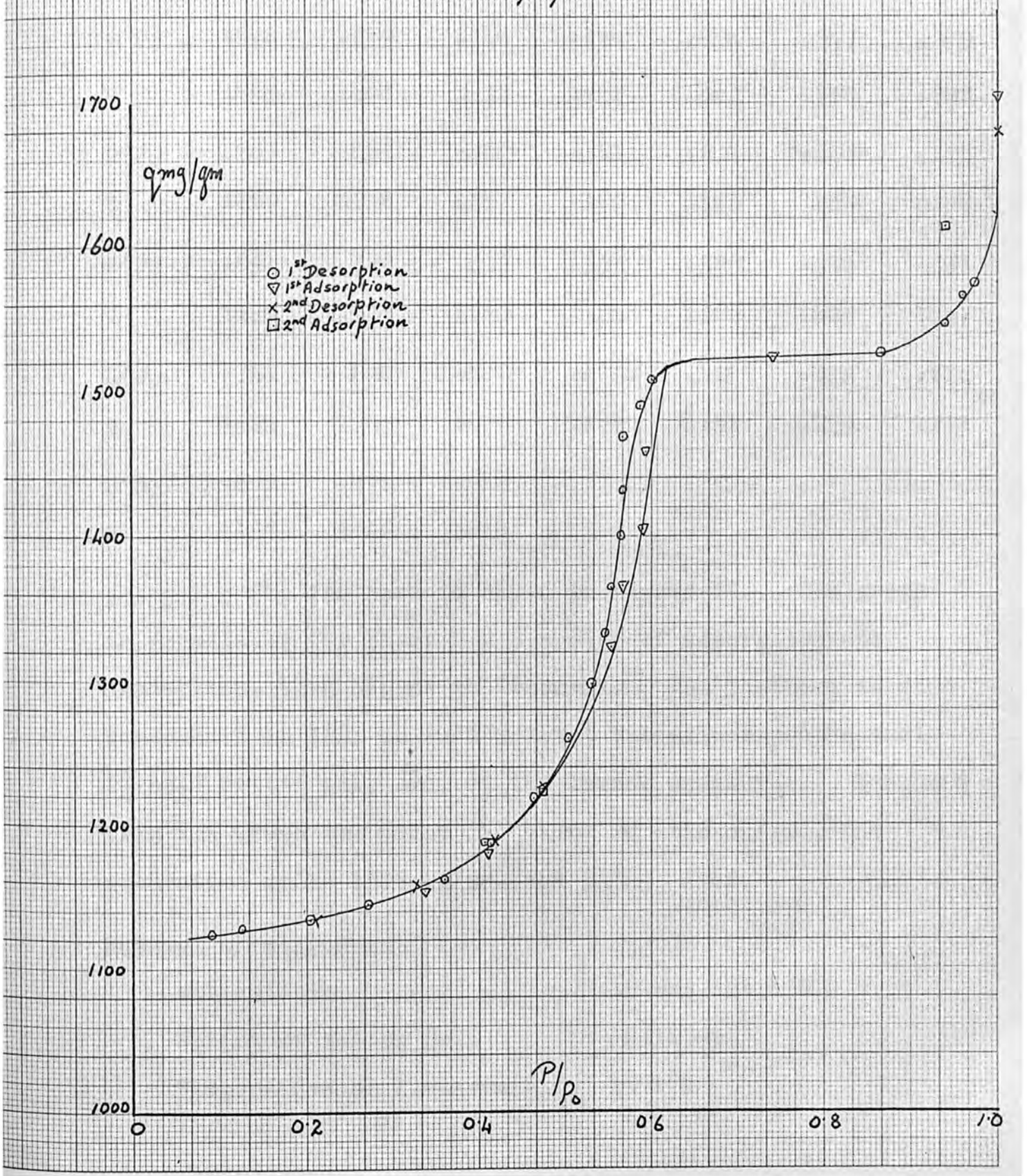

relative pressure			.973	.960	.941	.865	.598
concentration in mg/gm.			1575	1566	1557	1526	1508
p/p_o	.586	.569	.568	.564	.554	.547	.529
q	1489	1468	1432	1400	1365	1334	1298
p/p_o	.505	.463	.412	.361	.271	.203	.125
q	1260	1218	1187	1162	1145	1134	1128
p/p_o	.091	.326	.409	.553	.568	.590	.593
q	1124	1155	1180	1324	1366	1405	1457
p/p_o	.741	1.000	1.000	.472	.418	.325	.210
q	1524	1704	1679	1228	1191	1159	1134
p/p_o	.408	.474	.942				
q	1188	1226	1614				

The isotherm is shown in figure 26. The graph is repeatable for about 2 - 3 cycles of adsorption and desorption, then begins to "wander". The isotherm is also remarkable in that so much 2:2:3:3 tetrafluoropropan-1-ol is held by the gel, even at the lowest pressures. Measured from the graph the point 'A' value is 1116 mg/gm., the saturation value 1526 mg/gm. and p_i/p_o .548.

Butanol on silica gel

Activation:	15 hrs. at 150°C
Weight of active gel:	.8534 gm.
Temperature of isotherm:	25.0°C

Fig 27

n butanol on Silica gel

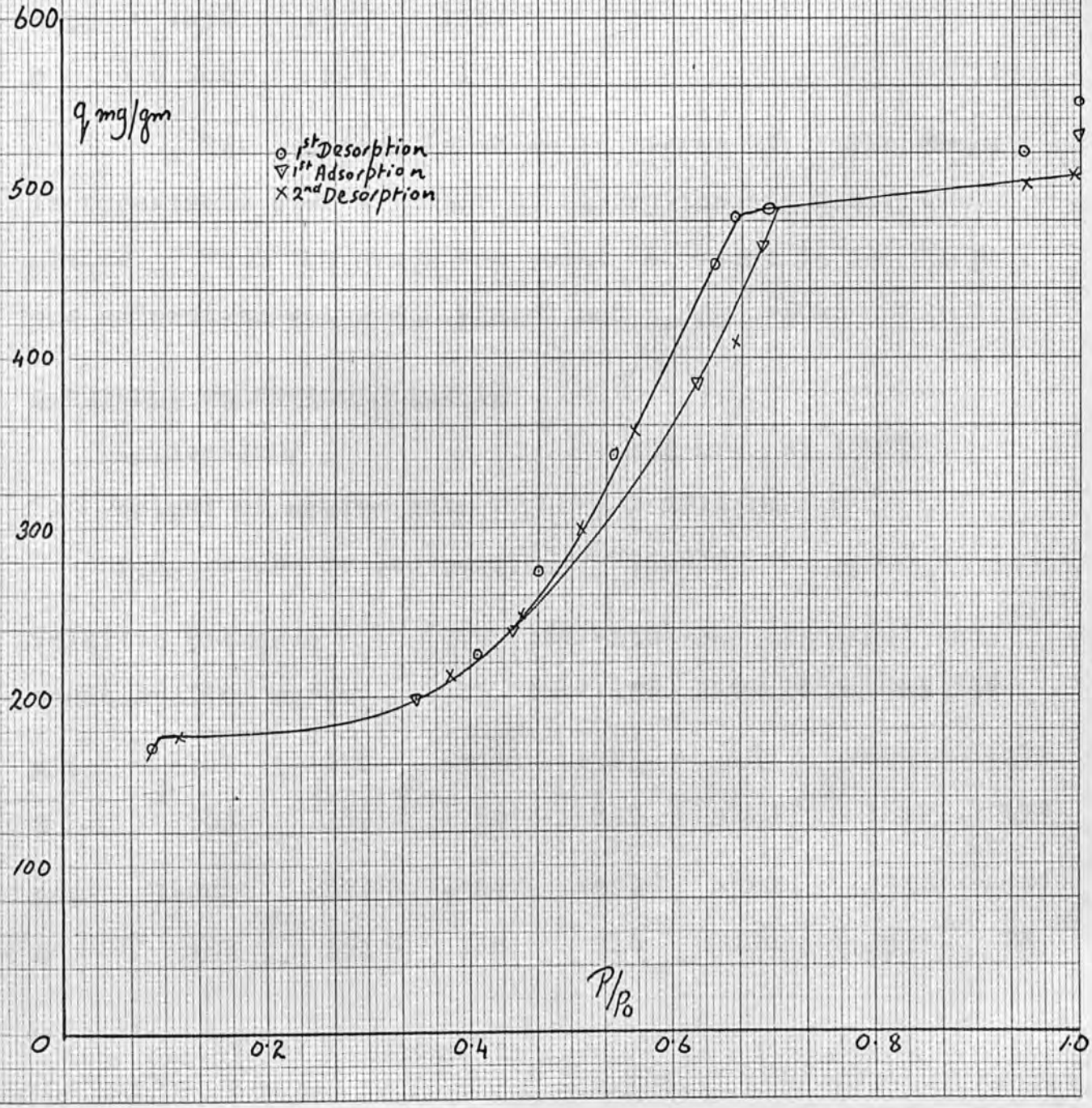

relative pressure			1.000	.845	.692	.659	.651	.639
concentration in mg/gm.			551	520	487	482	458	455
p/p_o	.542	.467	.408	.088	.345	.442	.631
q	342	274	225	170	199	239	385
p/p_o	.686	.990	.961	.945	.606	.559	.508
q	466	531	527	523	409	358	300
p/p_o	.450	.379	.114				
q	248	213	177				

The isotherm is shown in figure 27. The graph is repeatable over a number of adsorption and desorption cycles. From the graph the point 'A' value is 166 mg/gm., the saturation value 530 mg/gm. and p_i/p_o .594.

n butanol on ferric oxide II

Activation: $15\frac{1}{2}$ hrs. at 150°C

Weight of active gel: 1.2711 gm.

Temperature of isotherm: 25.0°C

relative pressure			.375	.368	.356	.347	.295	.261	.203
concentration mg/gm.			145	144	130	116	106	94	88
p/p_o	.144	.098	.319	.383	.467	.654	.932
q	83	82	89	118	140	168	175
p/p_o	1.000	.581	.369	.328	.290	.233	.057
q	167	167	128	116	104	94	72

Fig 28

n butanol on Ferric oxide II

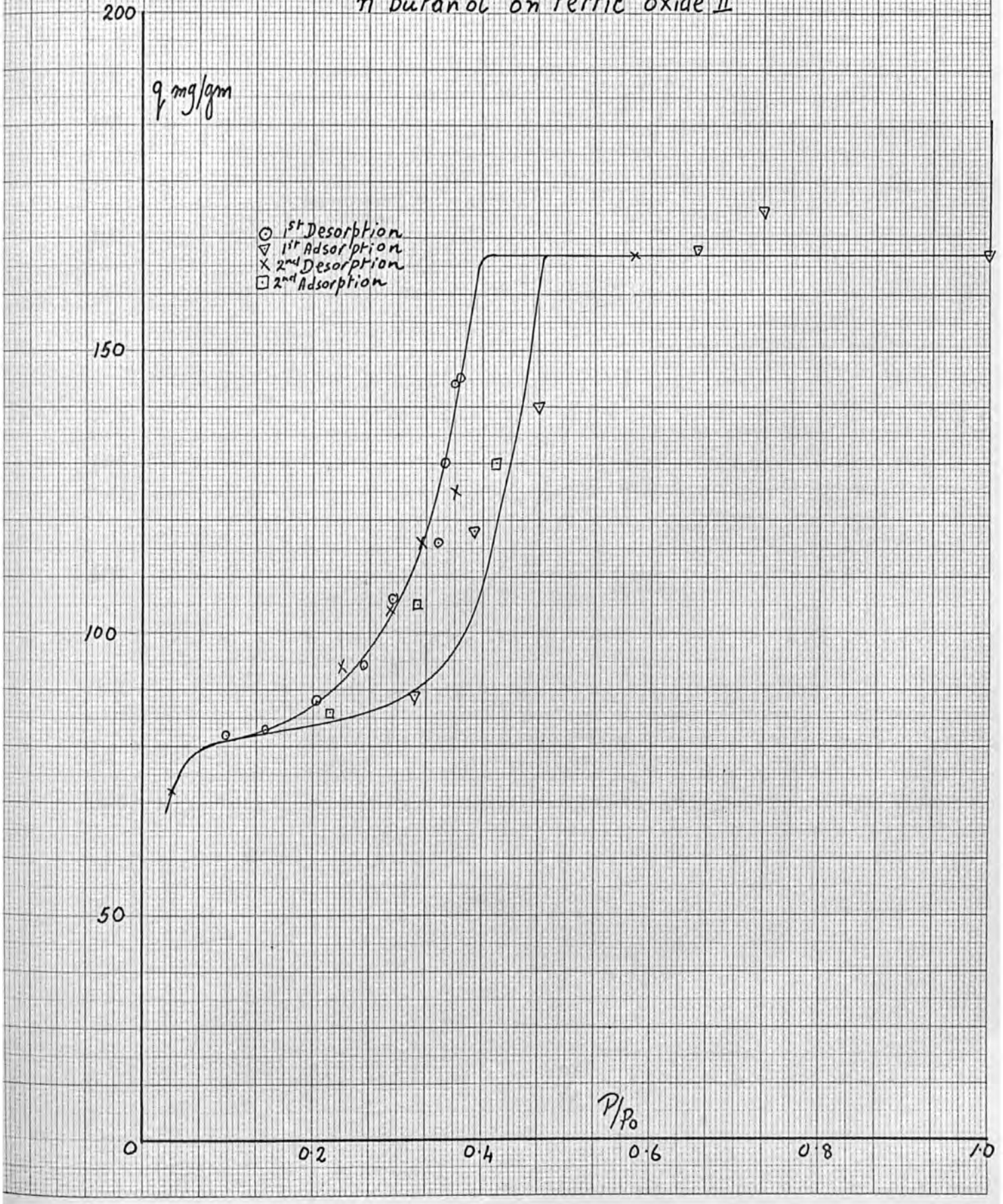

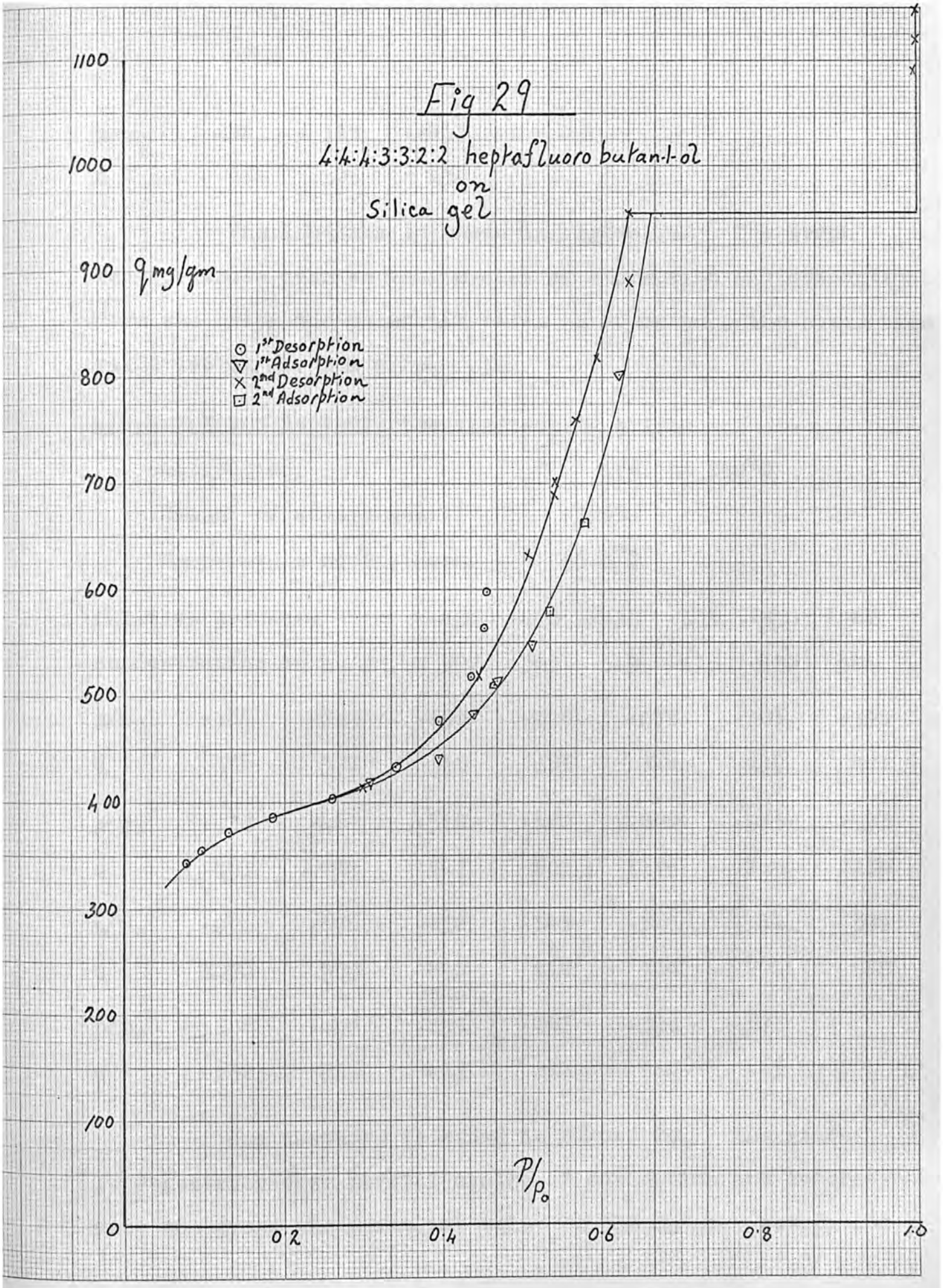
Fig 29
4:4:4:3:3:2:2 heptafluoro butan-1-ol
on
Silica gel
q mg/gm
1100
1000
900
800
700
600
500
400
300
200
100
0
1st Desorption
1st Adsorption
2nd Desorption
2nd Adsorption
0·2
0·4
0·6
0·8
1·0
P/P₀

p/p_o	·220	·325	·417
q	86	105	130

The isotherm is shown in figure 28. The graph is repeatable over several cycles of adsorption and desorption. From the graph the point 'A' value is 80 mg/gm., the saturation value 166 mg/gm. and p_i/p_o ·344.

4:4:4:3:3:2:2 heptafluorobutan-1-ol on silica gel

Activation: 16 hrs. at 150°C

Weight of active gel: ·7555

Temperature of isotherm: 25.0°C

relative pressure	·454	·450	·435	·393	·340	·262
concentration in mg/gm.	597	563	517	475	432	404

p/p_o	·184	·129	·096	·096	·078	//	·306	·394
q	386	371	355	353	344		419	441
p/p_o	·438	·467	·510	·622	1·000	//	·995	·995
q	483	514	547	802	1179		1149	1120
p/p_o	·991	·670	·632	·595	·569		·541	·539
q	1090	955	890	818	760		701	689
p/p_o	·506	·443	·299	//	·463	·535	·577	
q	632	520	413		511	580	663	

The isotherm is shown in figure 29. The graph is repeatable over several cycles of adsorption and desorption. From the graph the point 'A' value is 330 mg/gm., saturation

Fig 30

4:4:4:3:3:2:2 heptafluorobutan-1-ol
on
Ferric oxide III

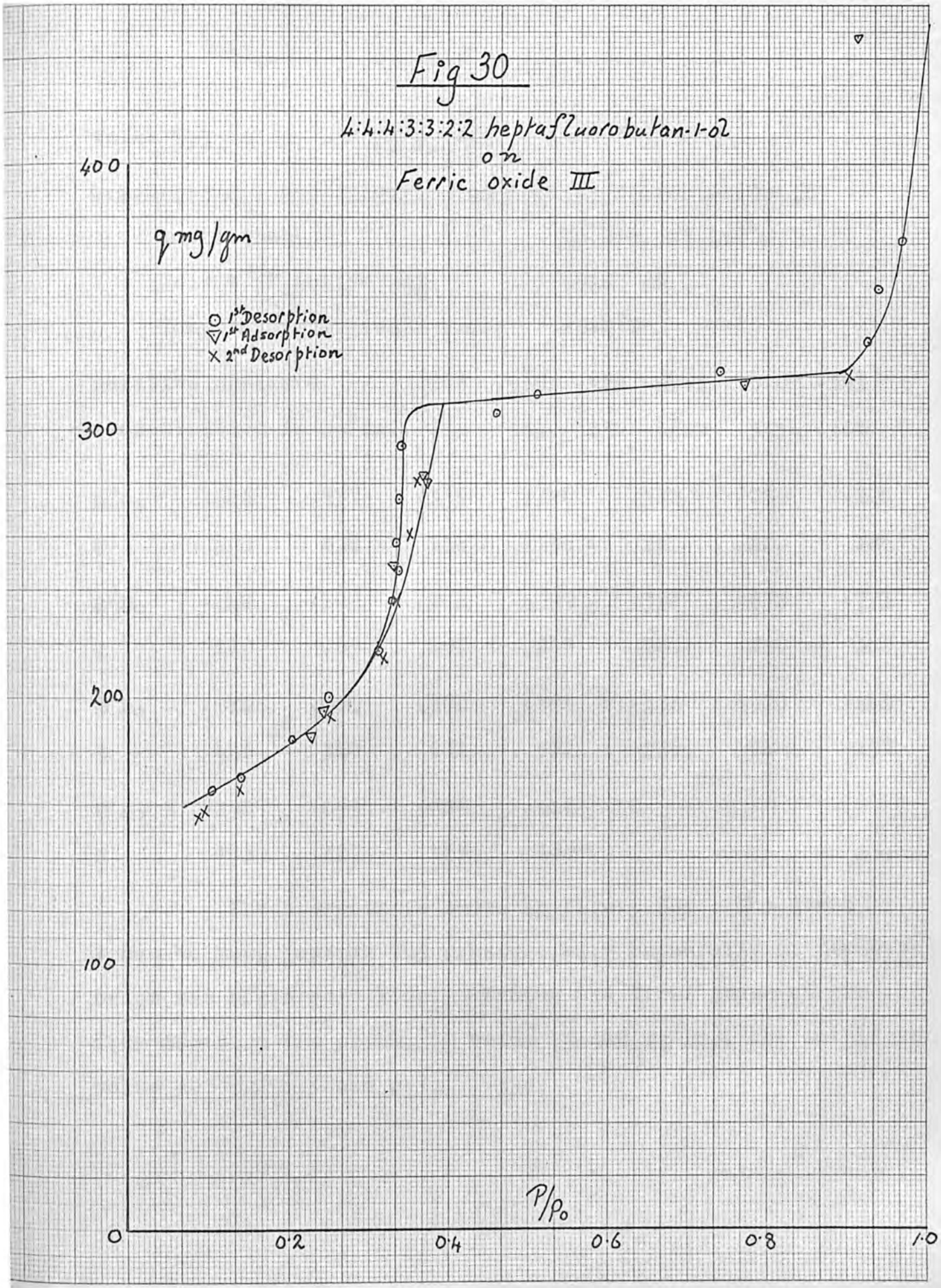

value 993 mg/gm. and p_i/p_o ·541.

<u>4:4:4:3:3:2:2 heptafluorobutan-1-ol on ferric oxide II</u>

Activation: 15 hrs. at 150°C

Weight of active gel: ·9124 gm.

Temperature of isotherm: 25.0°C

relative pressure	·969	·939	·924	·743	·510	·393
concentration in mg/gm.	371	353	334	322	313	306

p/p_o	·342	·337	·335	·326	·312	·250	·204
q	294	274	258	236	217	200	184
p/p_o	·140	·104	// ·244	·329	·368	·372	·771
q	170	165	195	249	283	280	317
p/p_o	·912	// ·901	·360	·351	·335	·316	·249
q	448	320	281	261	236	214	192
p/p_o	·138	·095	·086	// ·226			
q	165	157	155	185			

The isotherm is shown in figure 30. The graph tends to move towards the pressure axis especially at pressures below the hysteresis loop. Taking the first graph as the true isotherm the point 'A' value is 140 mg/gm., the saturation value 325 mg/gm., and p_i/p_o ·330.

Fig 31

Ethyl acetate on Silica gel

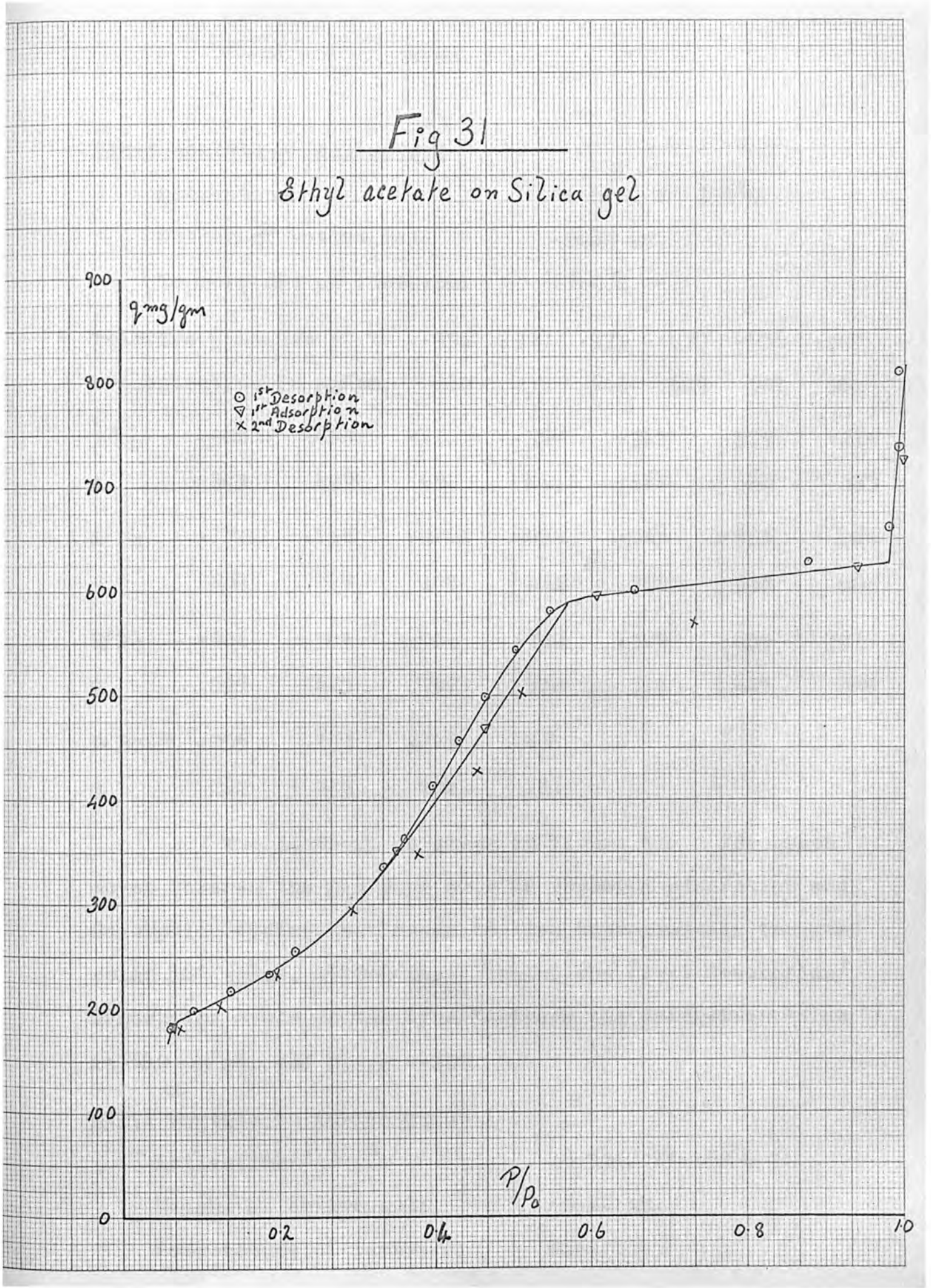

Ethyl acetate on silica gel

Activation: 16 hrs. at 150°C

Weight of active gel: ·9444 gm.

Temperature of isotherm: 25·0°C

relative pressure		·994	·994	·979	·879	·656	·545
concentration in mg/gm.		810	737	666	629	601	581
p/p_o	·502	·463	·431	·396	·362	·333	·219
q	543	499	457	414	367	336	255
p/p_o	·179	·136	·092	·059	·060	·351	·464
q	234	217	198	181	182	338	469
p/p_o	·606	·941	1·000	·730	·509	·455	·377
q	595	623	762	570	502	428	349
p/p_o	·295	·197	·123	·074			
q	282	233	202	181			

The isotherm is shown in figure 31. The graph moves towards the pressure axis on repeated adsorption and desorption cycles, but seems to give approximately the same point 'A' value, 152 mg/gm. Taking the first desorption/adsorption cycle as the true isotherm the saturation value is 640 mg/gm. and p_i/p_o ·402.

Ethyl acetate on ferric oxide I

Activation: 16 hrs. at 150°C

Weight of active gel: ·8940 gm.

Temperature of isotherm: 25·0°C

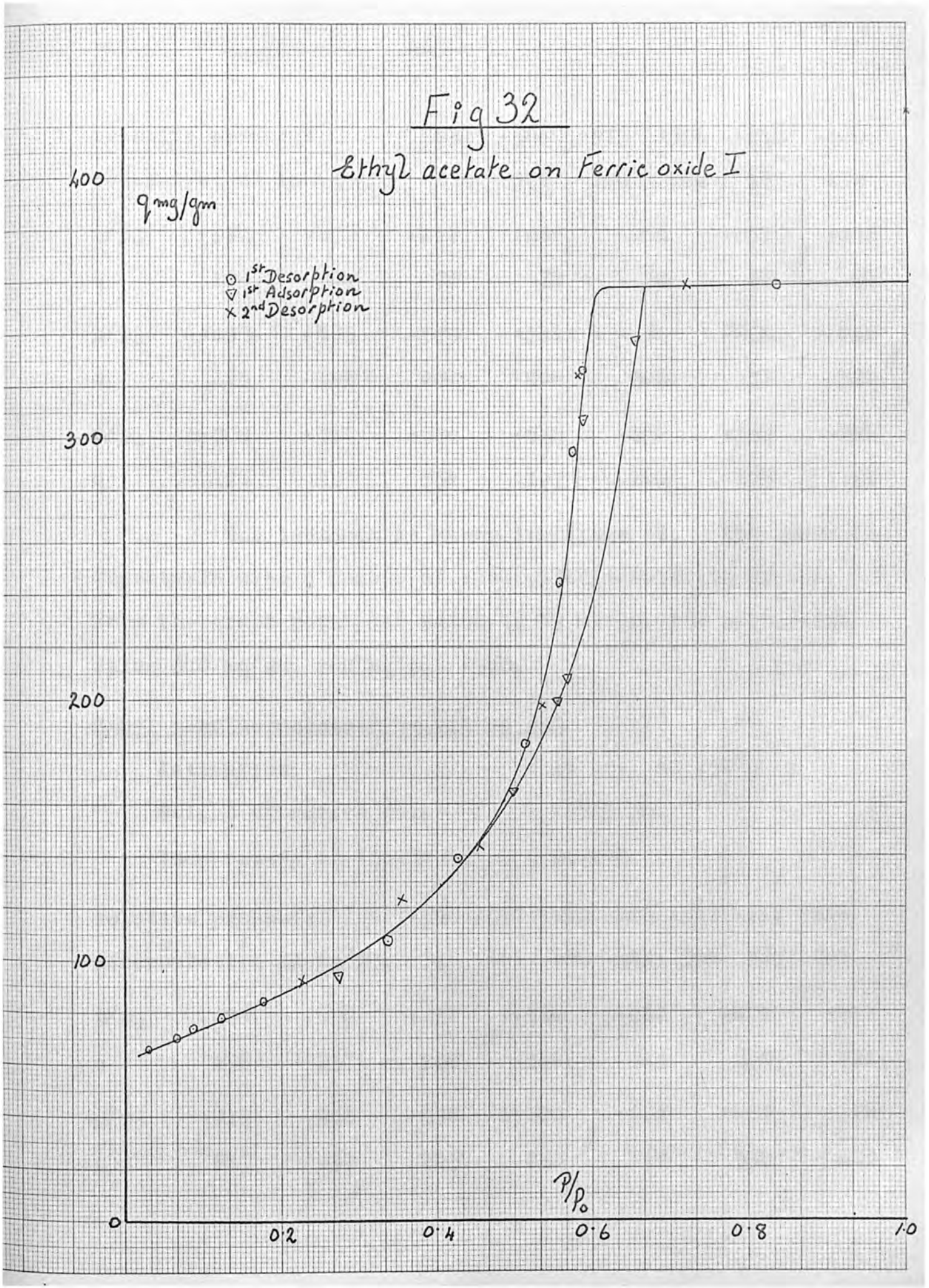
Fig 32
Ethyl acetate on Ferric oxide I
400
q mg/gm
300
200
100
0
1st Desorption
1st Adsorption
2nd Desorption
P/P₀
0·2
0·4
0·6
0·8
1·0

relative pressure			•834	•588	•573	•556	•514	•440
concentration in mg/gm.			359	326	294	244	183	139
p/p_o	•337	•177	•125	•087	•066	•031	//	•272
q	109	84	78	74	70	66		94
p/p_o	•495	•555	•559	•511	•585	•655	1•000	//
q	165	199	208	264	316	337	521	
p/p_o	1•000	•717	•579	•534	•454	•353	•226	
q	426	359	304	197	144	123	92	

The isotherm is shown in figure 32. The graph is repeatable over a number of adsorption/desorption cycles. From the graph point 'A' value is 69 mg/gm. the saturation value 340 mg/gm. and p_i/p_o •560.

Ethyl perfluoroacetate on silica gel

Activation: 16 hrs. at 150°C

Weight of active gel: •9529 gm.

Temperature of isotherm: 25.0°C

relative pressure			•590	•532	•496	•423	•343	•218	•126
concentration in mg/gm.			746	681	624	488	396	325	281
p/p_o	•086	•059	•031	//	•304	•462	•477	•571
q	258	237	208		368	523	550	721
p/p_o	•915	•988	•998	1•000	//	•622	•457	•376
q	811	837	825	850		768	530	415

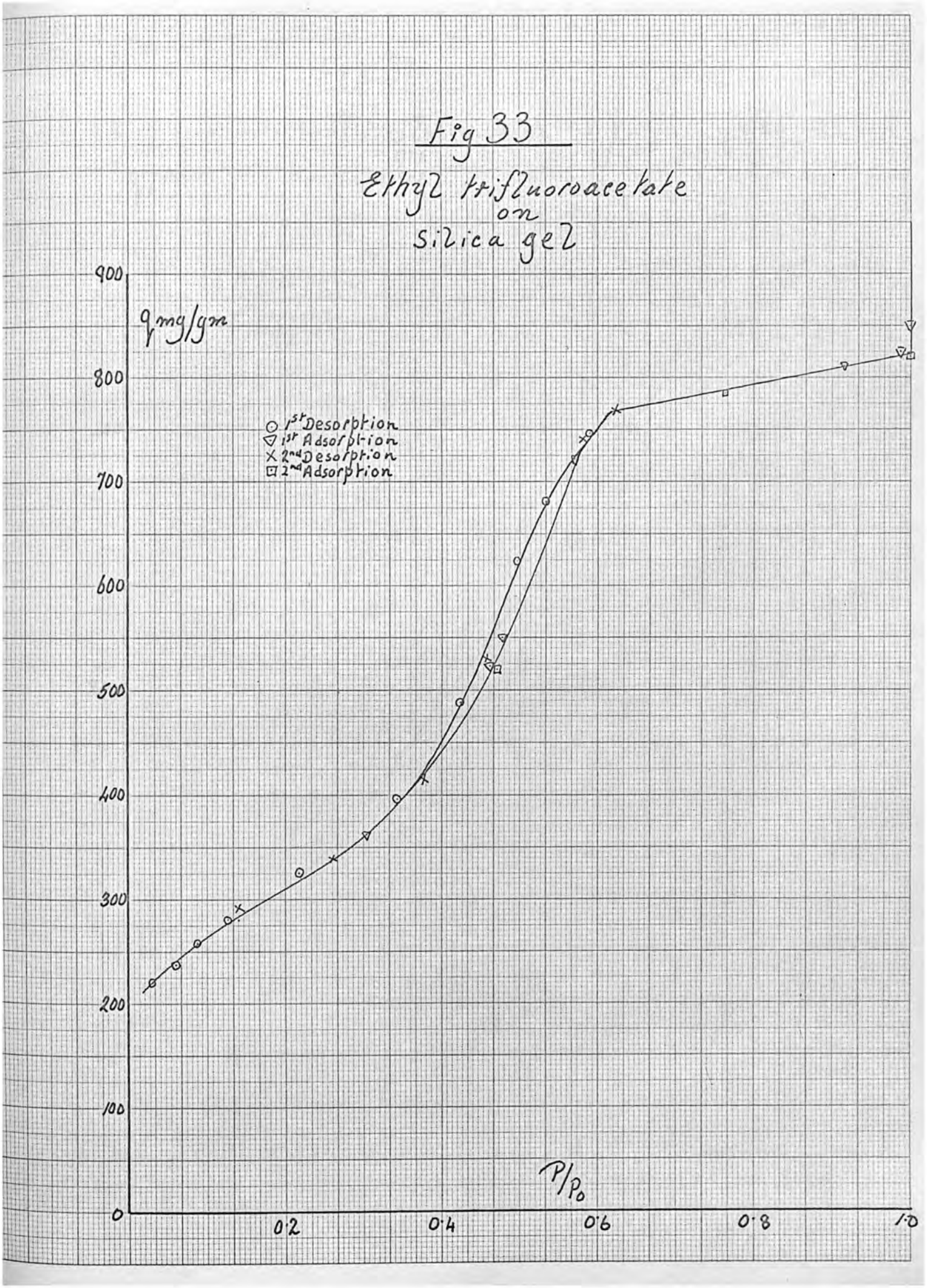
Fig 33
Ethyl trifluoroacetate
on
silica gel
900
800
700
600
500
400
300
200
100
0
q mg/gm
1st Desorption
1st Adsorption
2nd Desorption
2nd Adsorption
P/P0
0·2
0·4
0·6
0·8
1·0

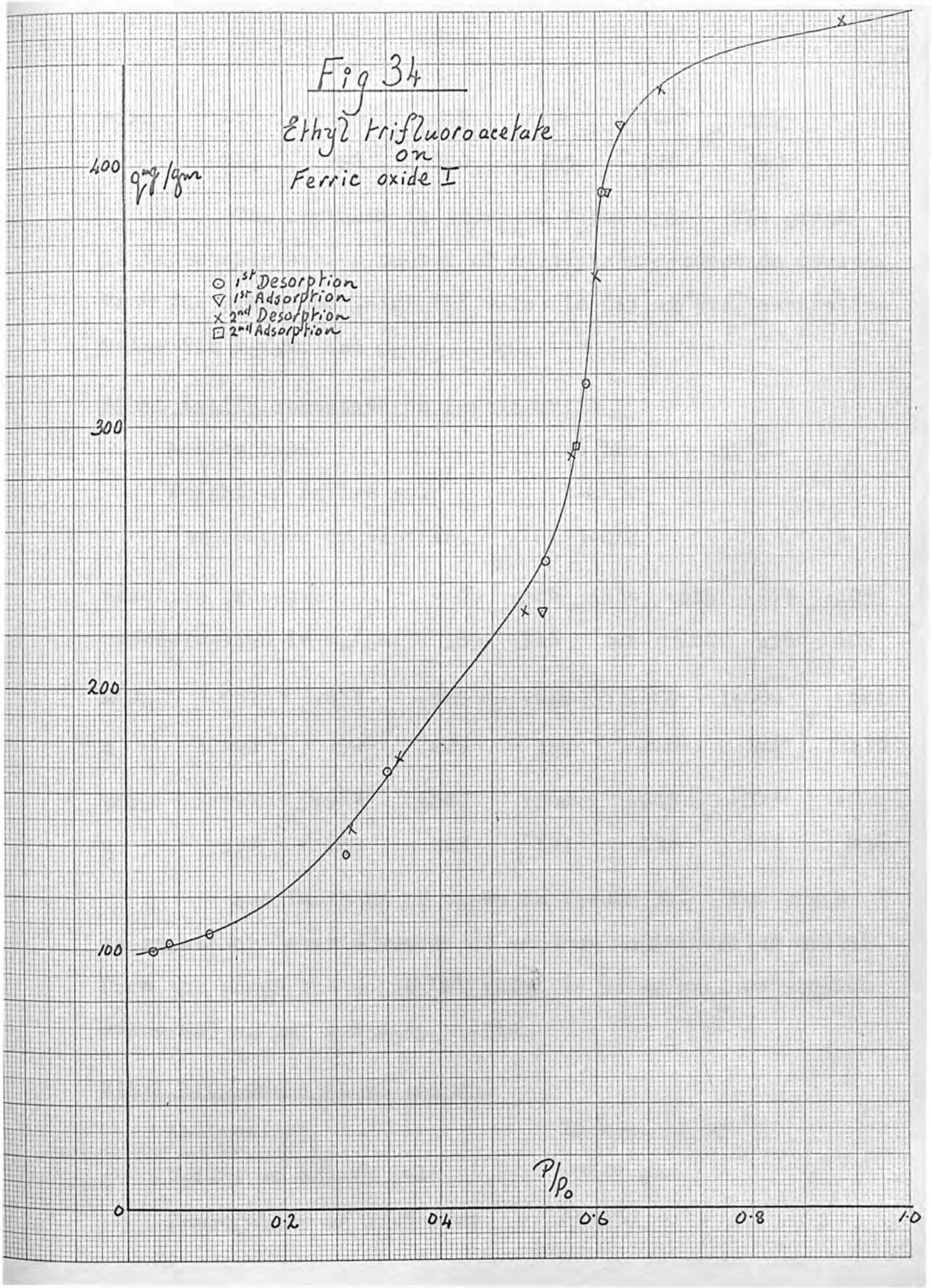
Fig 34
Ethyl trifluoroacetate
on
Ferric oxide I
400
300
200
100
0
cm³/gm
1st Desorption
1st Adsorption
2nd Desorption
2nd Adsorption
P/P₀
0·2
0·4
0·6
0·8
1·0

p/p_o	·259	·139	//	·469	·764	1·000	//	·587
q	339	292	//	520	785	820	//	740

The isotherm is shown in figure 33. The graph is repeatable over a number of adsorption/desorption cycles. From the graph the point 'A' value is 213 mg/gm., saturation value 818 mg/gm. and p_i/p_o ·507.

Ethyl trifluoroacetate on ferric oxide I

Activation: 16 hrs. at 150°C

Weight of active gel: 1·0212

Temperature of isotherm: 25·0°C

relative pressure	·608	·586	·536	·335	·279	·105
concentration in mg/gm.	389	316	248	168	138	106

p/p_o	·057	·033	//	·529	·614	·629	1·000	//	·682
q	102	99	//	229	390	416	741	//	430

p/p_o	·597	·567	·507	·349	·285	//	·573	·914
q	357	289	229	173	156	//	292	456

The isotherm is shown in figure 34. The graph is repeatable over a number of adsorption/desorption cycles. From the graph the point 'A' value is 95 mg/gm., saturation value 465 mg/gm. and p_i/p_o ·569.

Ethyl propionate on silica gel

Activation: 16 hrs. at 150°C

Weight of active gel: ·9638 gm.

Temperature of isotherm: 25·0°C

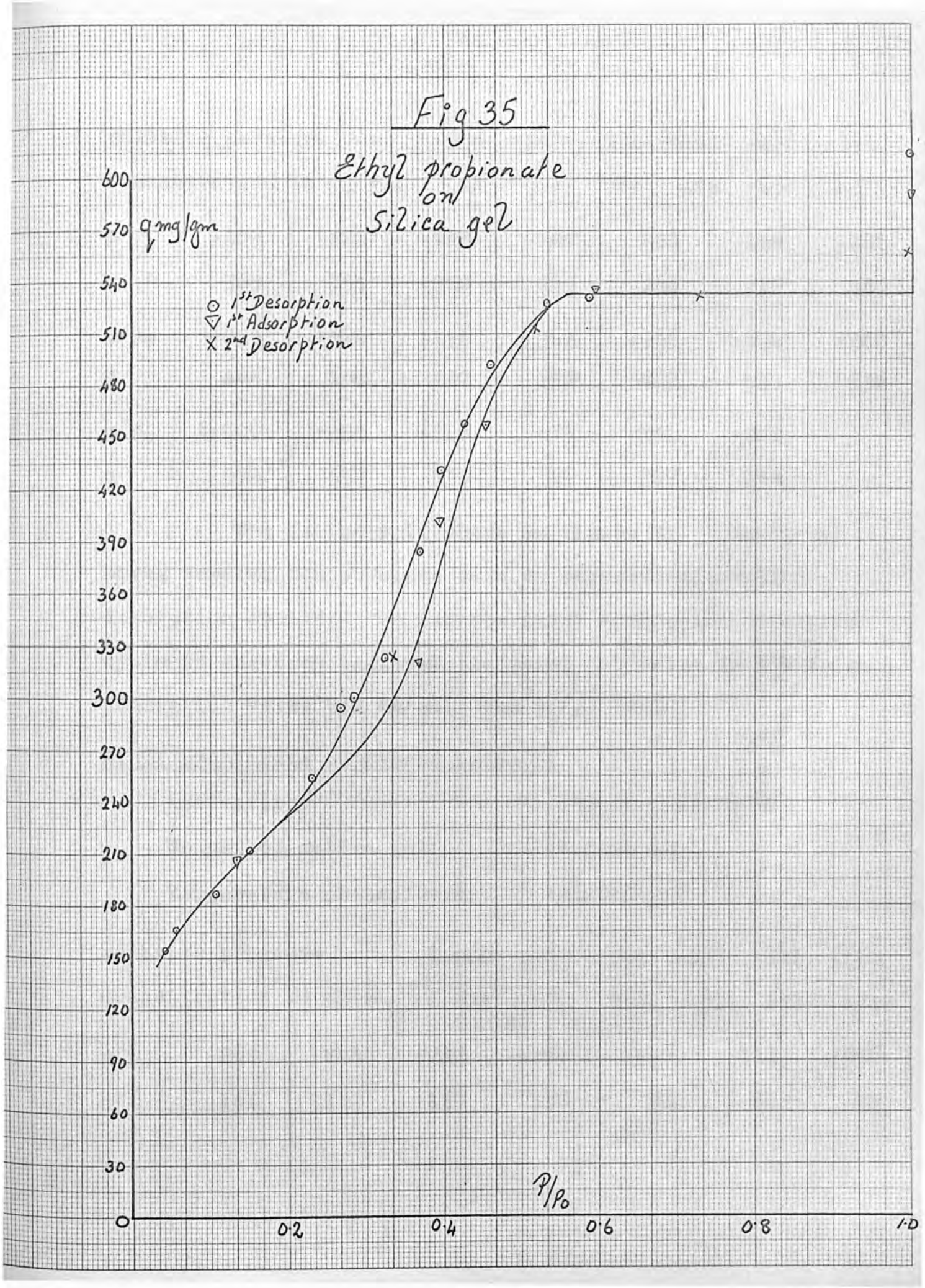
Fig 35
Ethyl propionate
on
Silica gel
600
570
q mg/gm
540
510
480
450
420
390
360
330
300
270
240
210
180
150
120
90
60
30
0
○ 1st Desorption
▽ 1st Adsorption
× 2nd Desorption
P/Po
0·2
0·4
0·6
0·8
1·0

relative pressure			·998	·587	·532	·460	·428	·395
concentration in mg/gm.			614	532	527	492	458	431
p/p_o	·369	·323	·283	·268	·230	·150	·105
q	385	353	300	295	254	212	187
p/p_o	·055	·042	//	·132	·367	·395	·454	·660
q	166	154	//	207	320	402	457	536
p/p_o	1·000	//	·995	·726	·573	·334	·026	
q	579	//	557	533	513	324	263	

The isotherm is shown in figure 35. The graph moves towards the pressure axis on repeated adsorption/desorption cycles. Taking the first desorption/adsorption cycle as the true isotherm the point 'A' value is 138 mg/gm., saturation value 536 mg/gm., and p_i/p_o ·412.

<u>Ethyl propionate on ferric oxide II</u>

Activation: $16\frac{1}{2}$ hrs. at 150°C

Weight of active gel: 1·5535 gm.

Temperature of isotherm: 25·0°C

relative pressure			1.000	.981	.940	.530	.321	.300
concentration in mg/gm.			293	252	212	181	177	171
p/p_o	·260	·243	·229	·204	·149	·111	·075
q	161	153	139	116	96	84	75

Fig 36

Ethyl propionate on Ferric oxide II

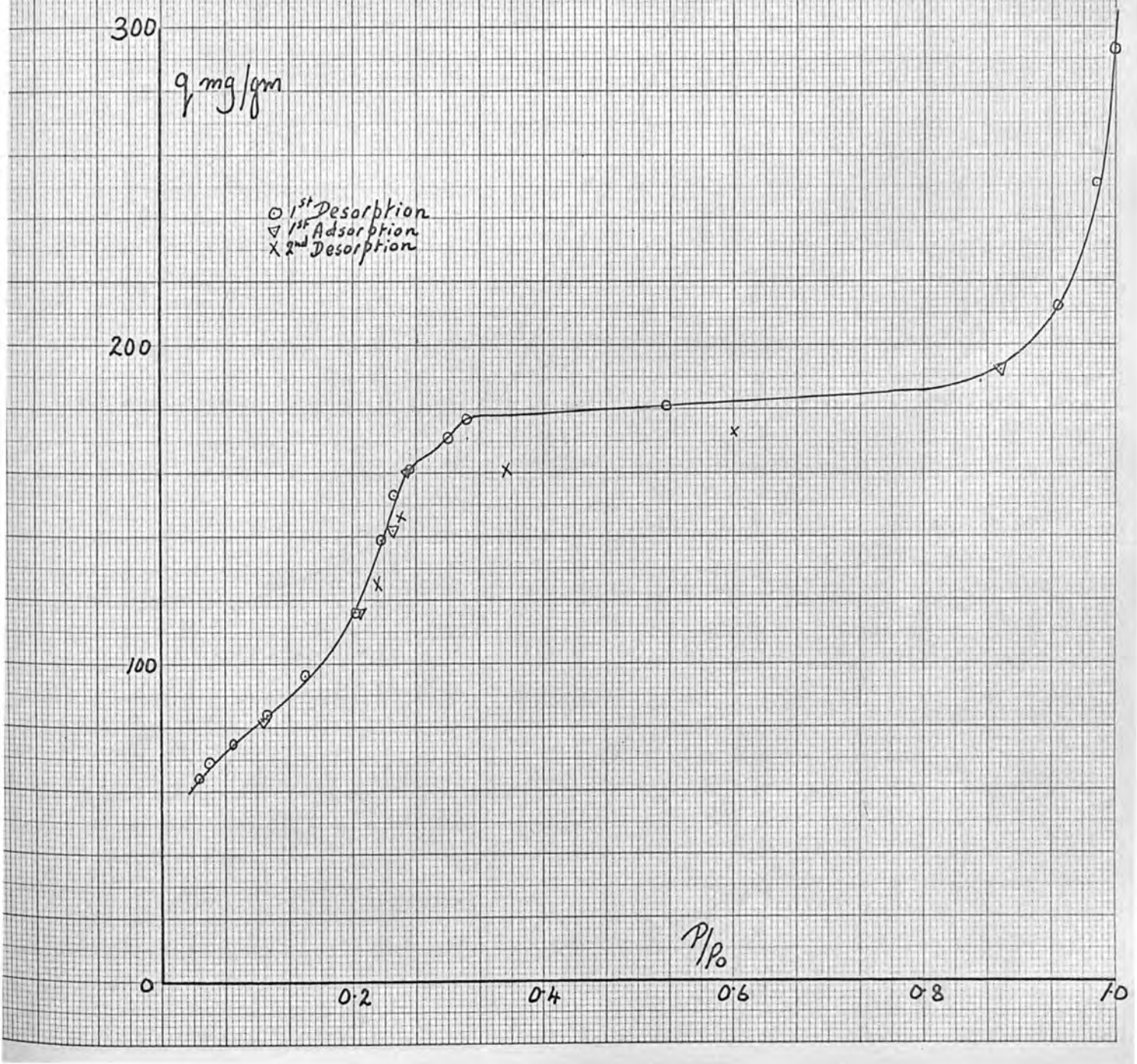

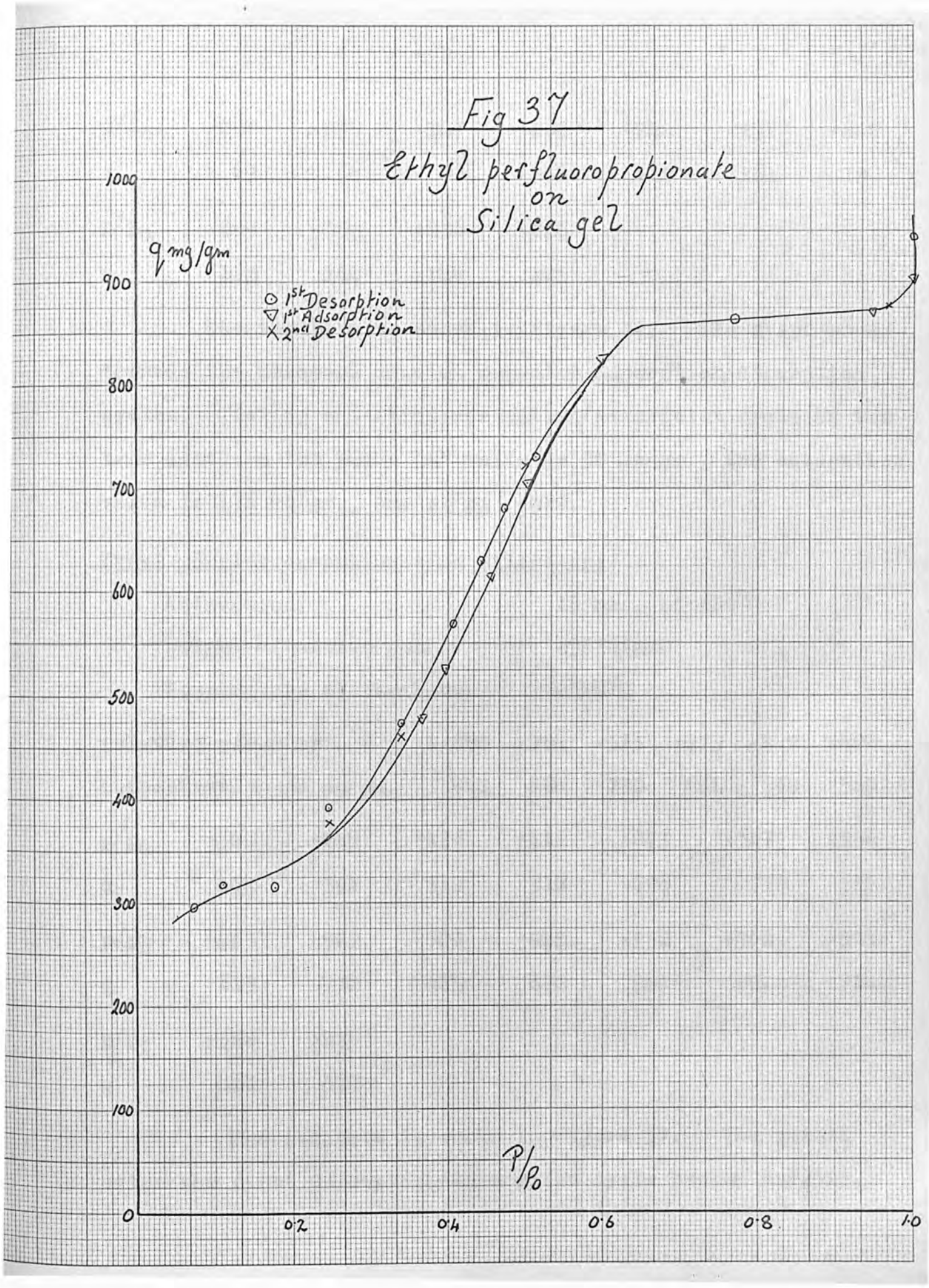
Fig 37
Ethyl perfluoropropionate
on
Silica gel
q mg/gm
1000
900
800
700
600
500
400
300
200
100
0
⊙ 1st Desorption
▽ 1st Adsorption
× 2nd Desorption
0·2
0·4
0·6
0·8
1·0
P/P0

p/p_o	•057	•038	//	•107	•208	•242	•257	•880	//
q	69	64		82	118	142	161	192	
p/p_o	•599	•359		•250	•225				
q	173	161		146	125				

The isotherm is shown in figure 36. The graph moves towards the pressure axis on repeated adsorption/desorption cycles. Taking the first desorption/adsorption cycle as the true isotherm the point 'A' value is 50 mg/gm., the saturation value is 176 mg/gm., and p_i/p_o •229.

Ethyl perfluoropropionate on silica gel

Activation: 16 hrs. at 150°C

Weight of active gel: •9578 gm.

Temperature of isotherm: 25•0°C

relative pressure	1•000	•704	•513	•473	•442	•408	
concentration in mg/gm.	944	864	730	681	630	569	
p/p_o	•340	•246	•176	•111	•073	//	•367	•396
q	474	392	315	318	295		477	527
p/p_o	•455	•502	•600	•945	•990	//	•966	•501
q	615	702	825	872	901		891	724
p/p_o	•342	•246						
q	461	377						

The isotherm is shown in figure 37. The points after the first desorption/adsorption cycle become erratic,

Fig 38

Ethyl perfluoropropionate
on
Ferric oxide II

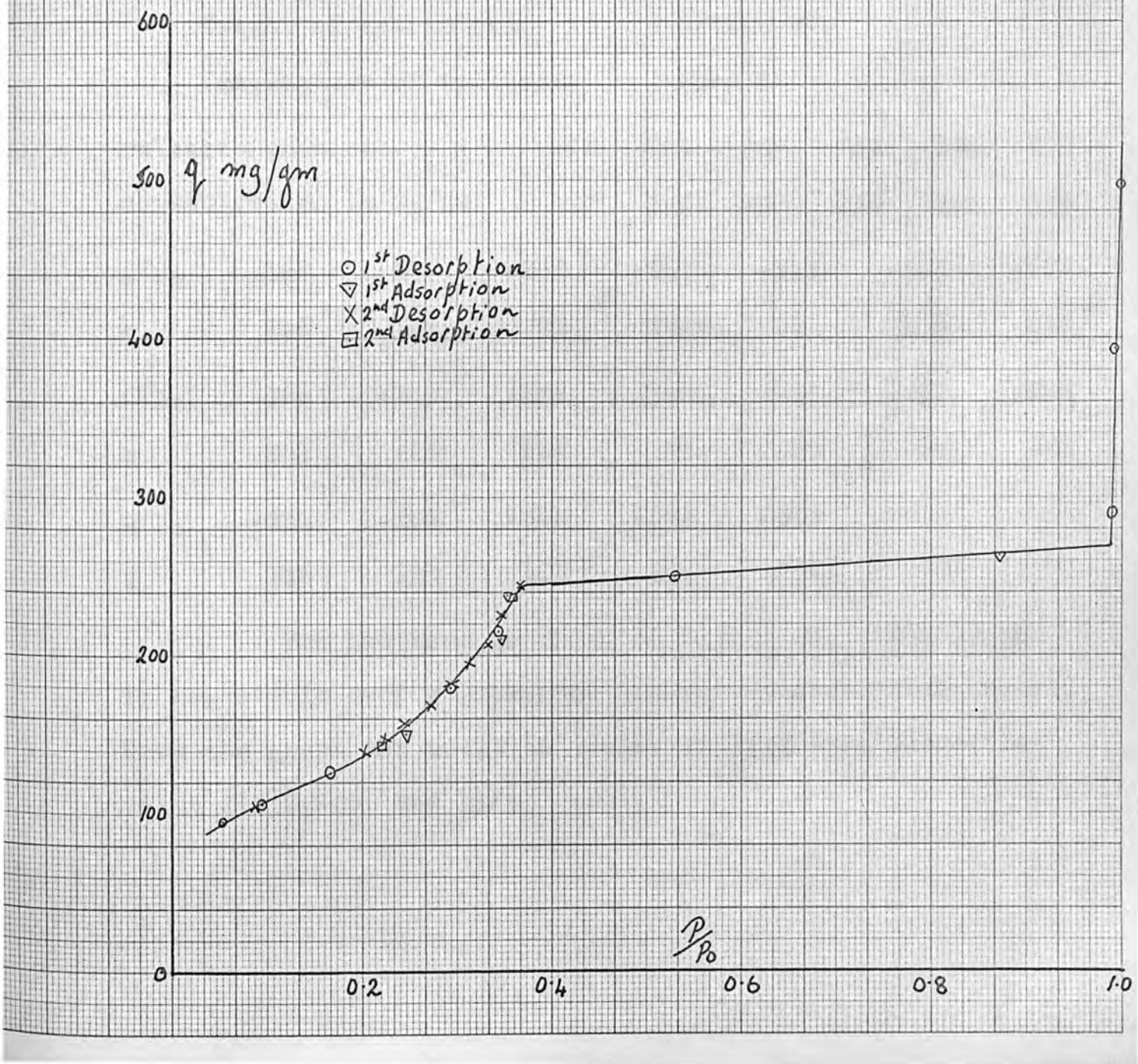

no trend being obvious; only a few are reported. Taking the first cycle, which gives a smooth curve, as the true isotherm the point 'A' value is 261 mg/gm., saturation value 868 mg/gm., and p_i/p_o .466.

Ethyl perfluoropropionate on ferric oxide II

Activation: 14½ hrs. at 150°C

Weight of active gel: 1.5229 gm.

Temperature of isotherm: 25.0°C

relative pressure			1.000	.995	.990	.531	.344	.293
concentration in mg/gm.			497	393	290	250	215	179
p/p_o	.166	.095	.053	.247	.347	.353	.872	
q	126	106	95	151	211	238	263	
p/p_o	.368	.345	.332	.312	.292	.273	.244	
q	244	226	209	195	182	169	158	
p/p_o	.224	.202	.088	.219	.359			
q	148	139	105	144	237			

The isotherm is shown in figure 38. The graph is repeatable over a number of adsorption/desorption cycles. From the graph the point 'A' value is 79 mg/gm., saturation value 268 mg/gm. and p_i/p_o .284.

Fig 39

n-propylamine on Silica gel

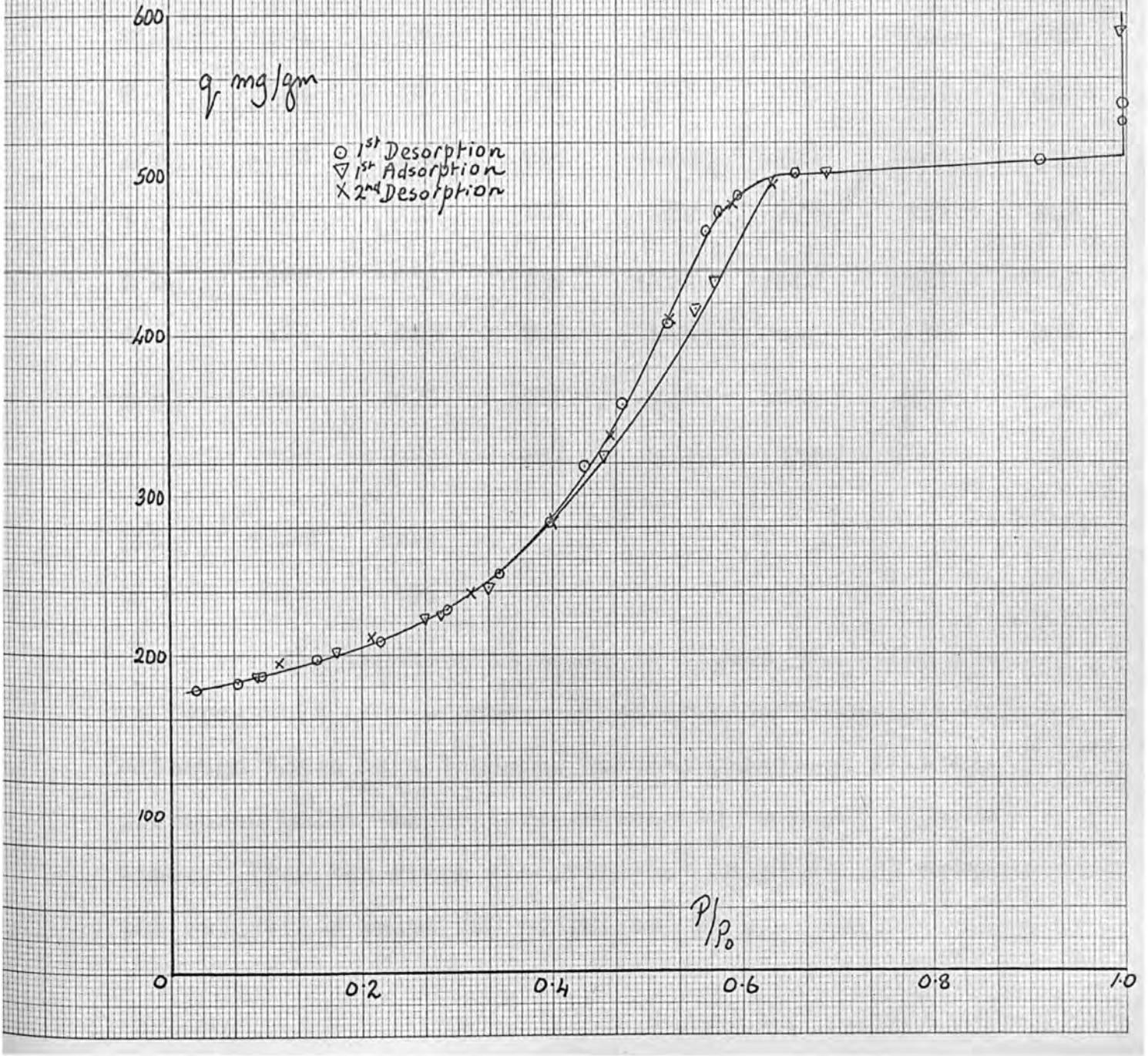

n propylamine on silica gel

Activation: 15 hrs. at 150°C

Weight of active gel: 1·0405 gm.

Temperature of isotherm: 0·0°C

relative pressure			·996	·996	·911	·656	·595	·573
concentration in mg/gm.			554	533	514	500	487	476
p/p_o	·561	·520	·473	·433	·397	·344	·290	
q	464	407	358	318	283	251	228	
p/p_o	·220	·154	·095	·070	·026	·090	·172	
q	209	197	187	182	178	187	202	
p/p_o	·268	·283	·334	·452	·550	·571	·687	
q	223	225	242	325	417	434	502	
p/p_o	·995	·629	·588	·522	·459	·399	·314	
q	589	495	481	410	338	283	239	
p/p_o	·210	·112						
q	211	195						

The isotherm is shown in figure 39. The graph is repeatable over a number of adsorption/desorption cycles, although there is a tendency for the points at relative pressures below the hysteresis loop to "wander" after a time. From the graph the point 'A' value is 173 mg/gm., the saturation value 520 mg/gm. and p_i/p_o ·501.

Fig 40

n-propylamine on Ferric oxide II

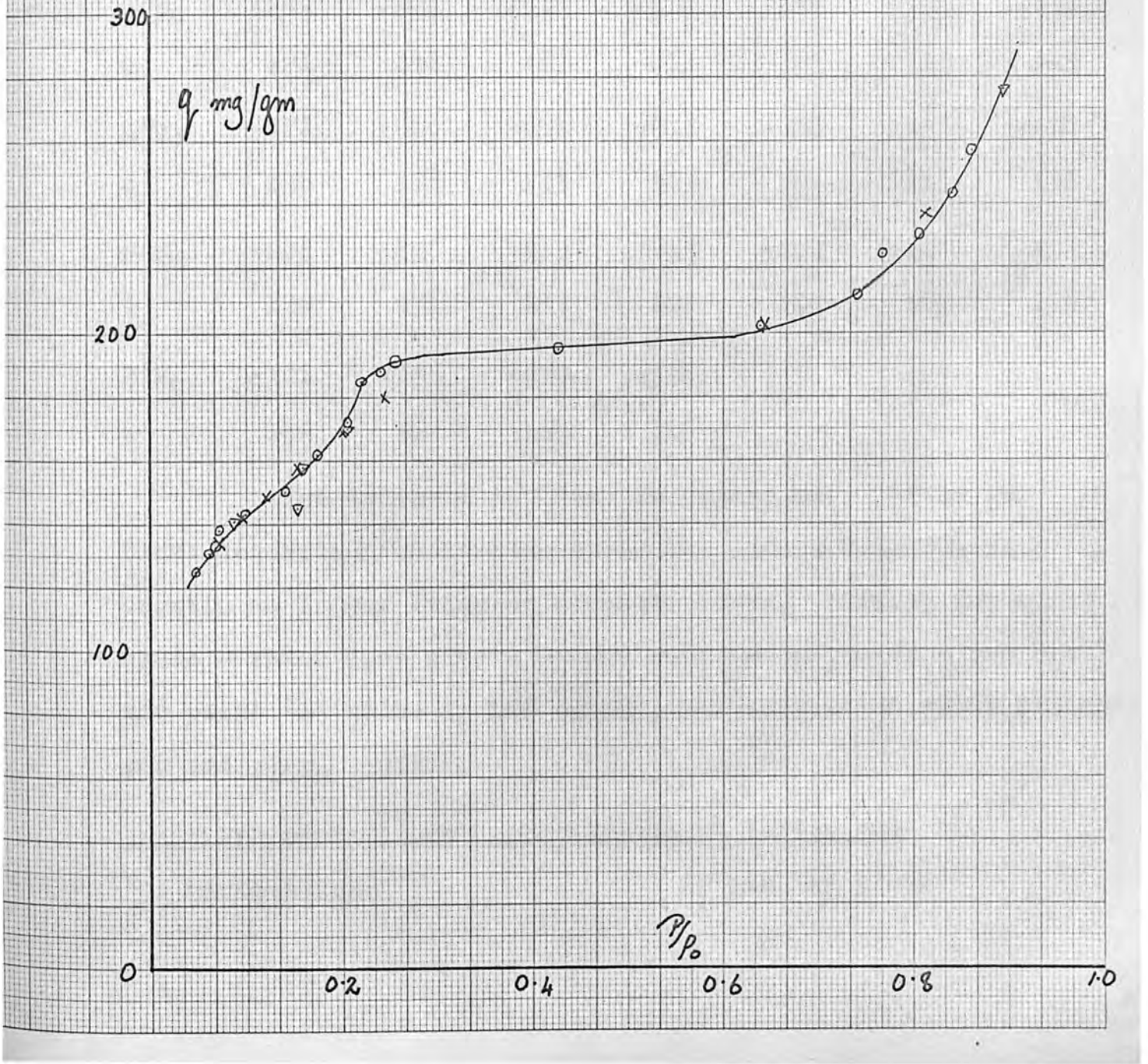

n propylamine on ferric oxide II

Activation: 15 hrs. at 150°C

Weight of active gel: 1·4844 gm.

Temperature of isotherm: 0.0°C

relative pressure	·864	·840	·806	·766	·738	·638	·427
concentration in mg/gm.	257	243	230	224	212	202	195
p/p_o	·284	·240	·219	·205	·172	·139	·098
q	191	188	185	172	162	150	143
p/p_o	·071	·068	·059	·045	·088	·155	·158
q	138	133	131	125	141	145	158
p/p_o	·205	·893	·810	·645	·243	·201	·153
q	170	276	237	202	180	169	158
p/p_o	·121	·095	·070	·314			
q	149	142	134	186			

The isotherm is shown in figure 40. After the first desorption/adsorption cycle the points become highly erratic no longer lying on a smooth curve. Taking the first cycle - which does give a smooth curve - as the true isotherm the point 'A' value is 129 mg/gm., the saturation value 213 mg/gm. and p_i/p_o ·225.

3:3:3:2:2 pentafluoro n-propylamine on silica gel

Activation: 15 hrs. at 150°C

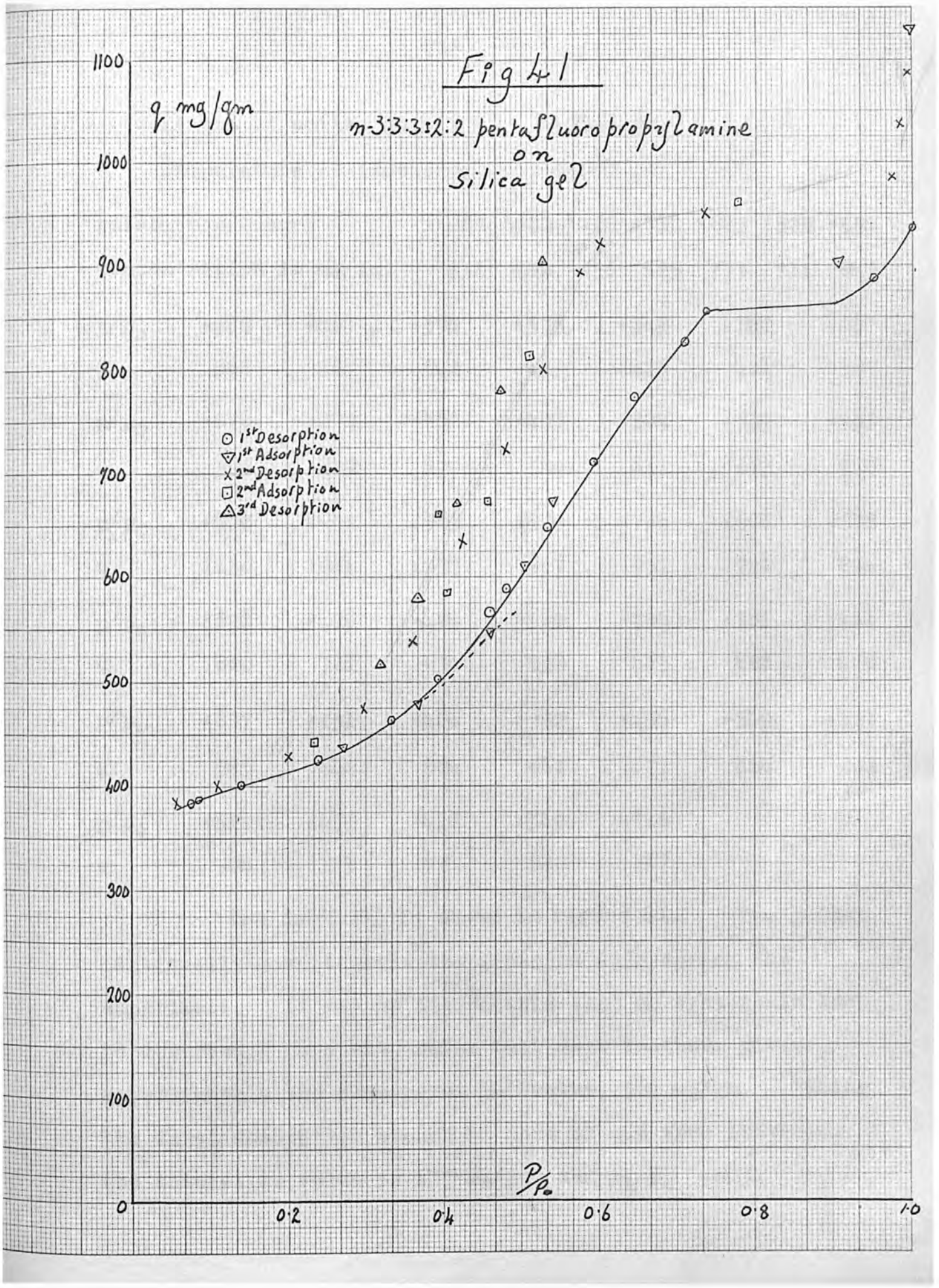
Fig 4.1
n-3:3:3:2:2 pentafluoropropylamine on silica gel
q mg/gm
1100
1000
900
800
700
600
500
400
300
200
100
0
0·2
0·4
0·6
0·8
1·0
P/P₀
⊙ 1st Desorption
▽ 1st Adsorption
× 2nd Desorption
□ 2nd Adsorption
△ 3rd Desorption

Weight of active gel: •9246 gm.

Temperature of isotherm: 0.0°C

relative pressure	1.000	•950	•736	•710	•645	•595	•534
concentration in mg/gm.	936	888	856	825	773	711	647
p/p_o	•480	•461	•394	•335	•240	•142	•087
q	588	567	502	463	425	401	387
p/p_o	•076 //	•271	•369	•459	•504	•539	•903
q	384	437	479	549	611	673	948
p/p_o	1.000 //	•992	•983	•974	•734	•601	•575
q	1130	1088	1037	987	951	922	894
p/p_o	•528	•479	•424	•362	•296	•200	•111
q	800	722	634	538	475	428	400
p/p_o	•057 //	•232	•404	•392	•456	•509	•777 //
q	385	442	584	662	672	814	981
p/p_o	•528	•473	•418	•369	•318		
q	904	779	671	580	517		

The isotherm is shown in figure 41. The points continually move towards the pressure axis during the experiment. It may be due to this that no hysteresis loop is observed. One also notes that each isotherm gives approximately the same point 'A' value, 364 mg/gm. Taking the first desorption branch as part of the true isotherm, the saturation value is 835 mg/gm. and p_i/p_o •487.

Fig 4.2

m-3:3:3:2:2 pentafluoro propyl amine
on
Ferric oxide II

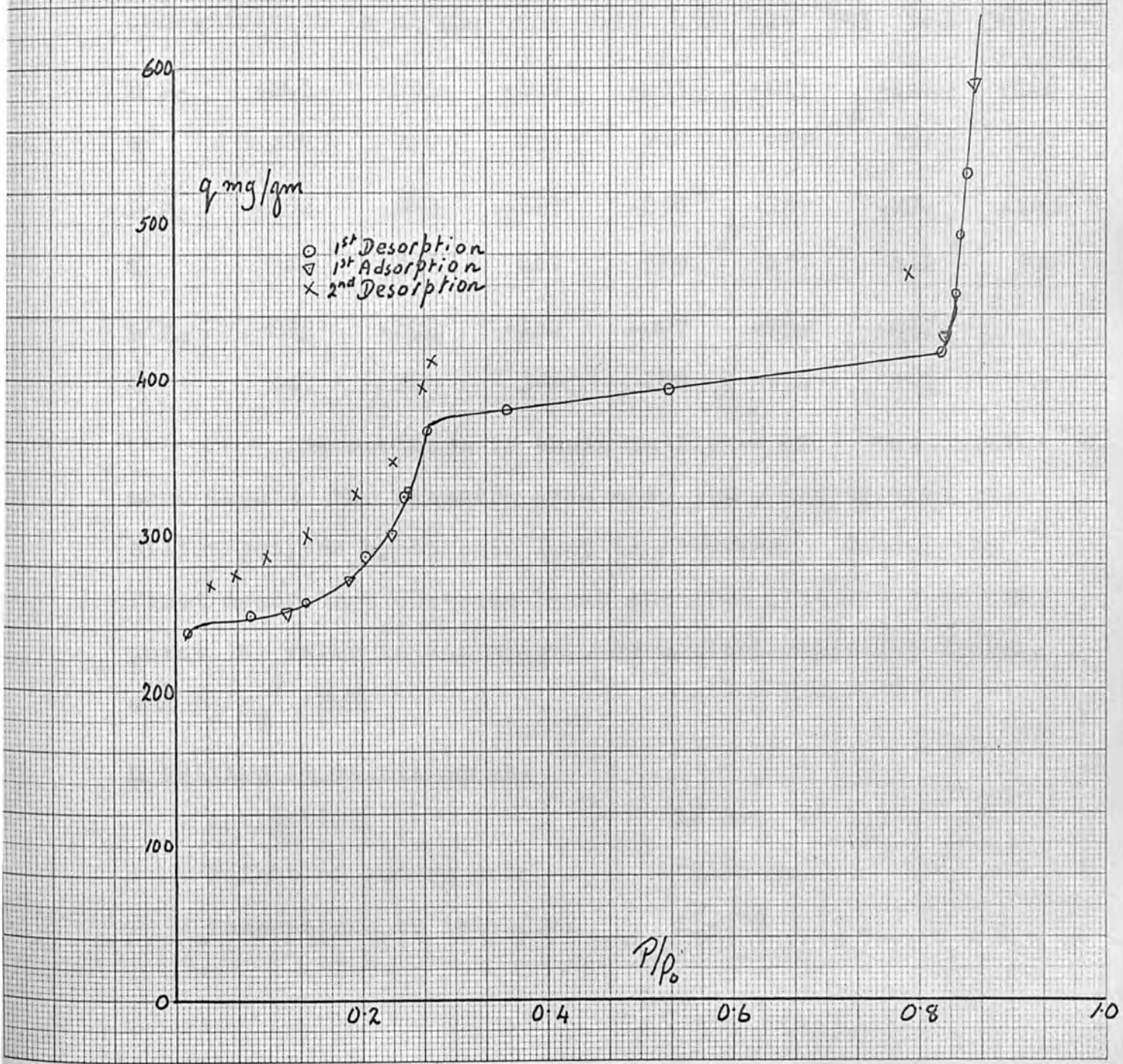

3:3:3:2:2 pentafluoro n-propylamine on ferric oxide II

Activation: 17 hrs. at 150°C

Weight of active gel: 1.0388 gm.

Temperature of isotherm: 0.0°C

relative pressure	.851	.843	.842	.823	.529	.290	.269
concentration in mg/gm.	531	492	453	416	393	380	367
p/p_o	.245	.203	.142	.083	.015	.120	.186
q	324	286	257	248	237	251	271
p/p_o	.232	.249	.827	.858	.789	.274	.263
q	301	328	467	589	477	412	394
p/p_o	.233	.193	.142	.097	.059	.037	
q	347	326	300	286	274	267	

The isotherm is shown in figure 42. The points move towards the pressure axis with time, and as with the silica gel, no hysteresis loop is observed. Taking the first desorption curve as being the true isotherm then the point 'A' value is 236 mg/gm., saturation value 415 mg/gm., and p_i/p_o .243.

n butylamine on silica gel

Activation: 16 hrs. at 150°C

Weight of active gel: .9168 gm.

Temperature of isotherm: 25.0°C

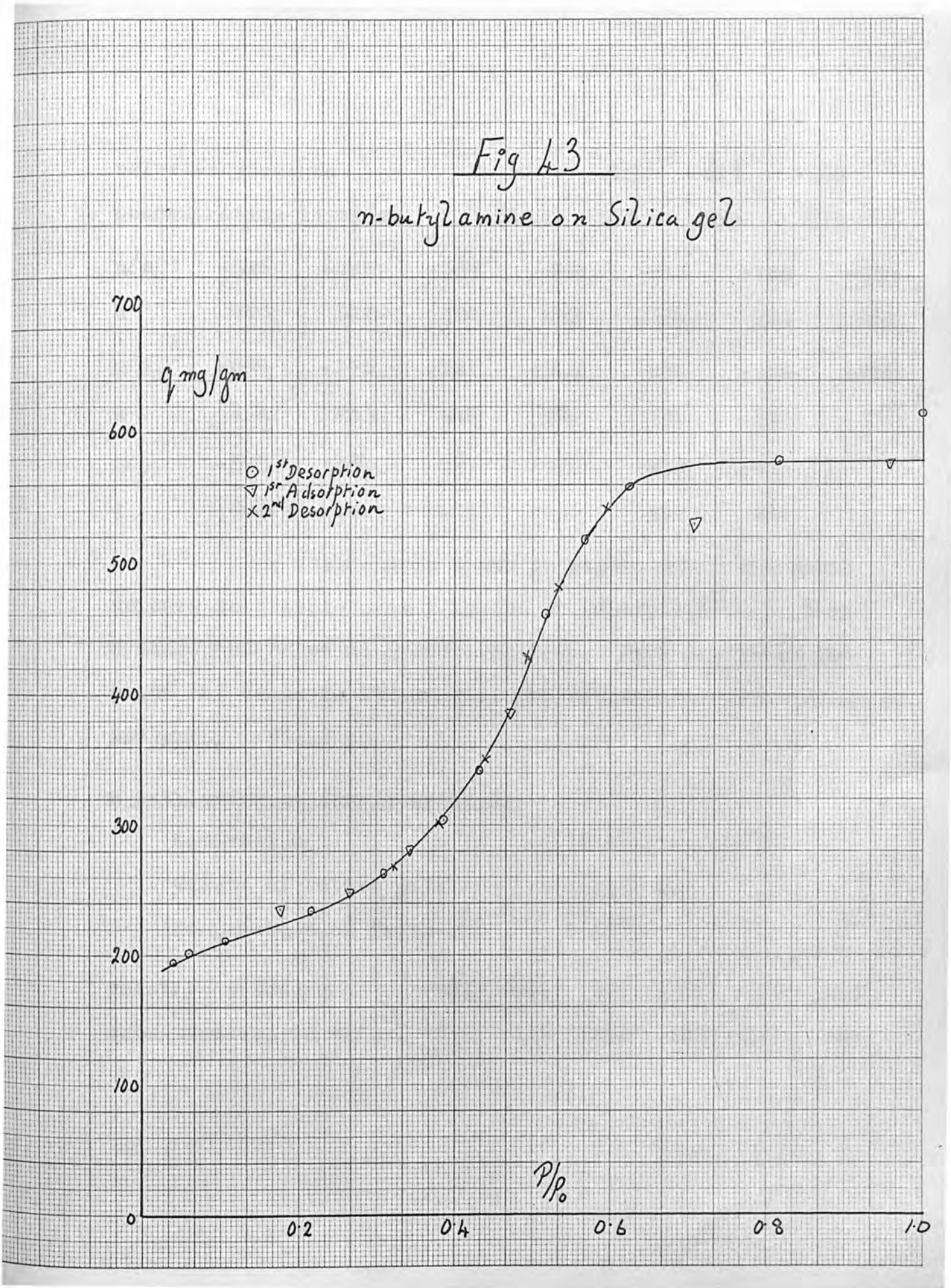
Fig 4.3
n-butylamine on Silica gel
700
600
500
400
300
200
100
0
q mg/gm
⊙ 1st Desorption
▽ 1st Adsorption
× 2nd Desorption
0·2
0·4
0·6
0·8
1·0
P/P0

relative pressure			1·000	·815	·623	·566	
concentration in mg/gm.			615	578	559	518	
p/p_o	·516	·435	·387	·309	·217	·105	·059
q	460	342	304	262	234	211	201
p/p_o	·039	·176	·265	·344	·470	·708	·956
q	194 //	235	248	281	386	530	576 //
p/p_o	·595	·534	·491	·439	·379	·322	
q	542	482	428	351	302	268	

The isotherm is shown in figure 43. The graph appears repeatable over a number of adsorption/desorption cycles, but shows no hysteresis loop. From the graph the point 'A' value is 190 mg/gm., the saturation value 575 mg/gm., and p_i/p_o ·522.

<u>n butylamine on ferric oxide II</u>

Activation: 16 hrs. at 150°C

Weight of active gel: 1·1327 gm.

Temperature of isotherm: 25·0°C

relative pressure	·683	·661	·625	·234	·176	·133
concentration in mg/gm.	233	215	198	188	173	162

Fig 44

n-butylamine on Ferric oxide II

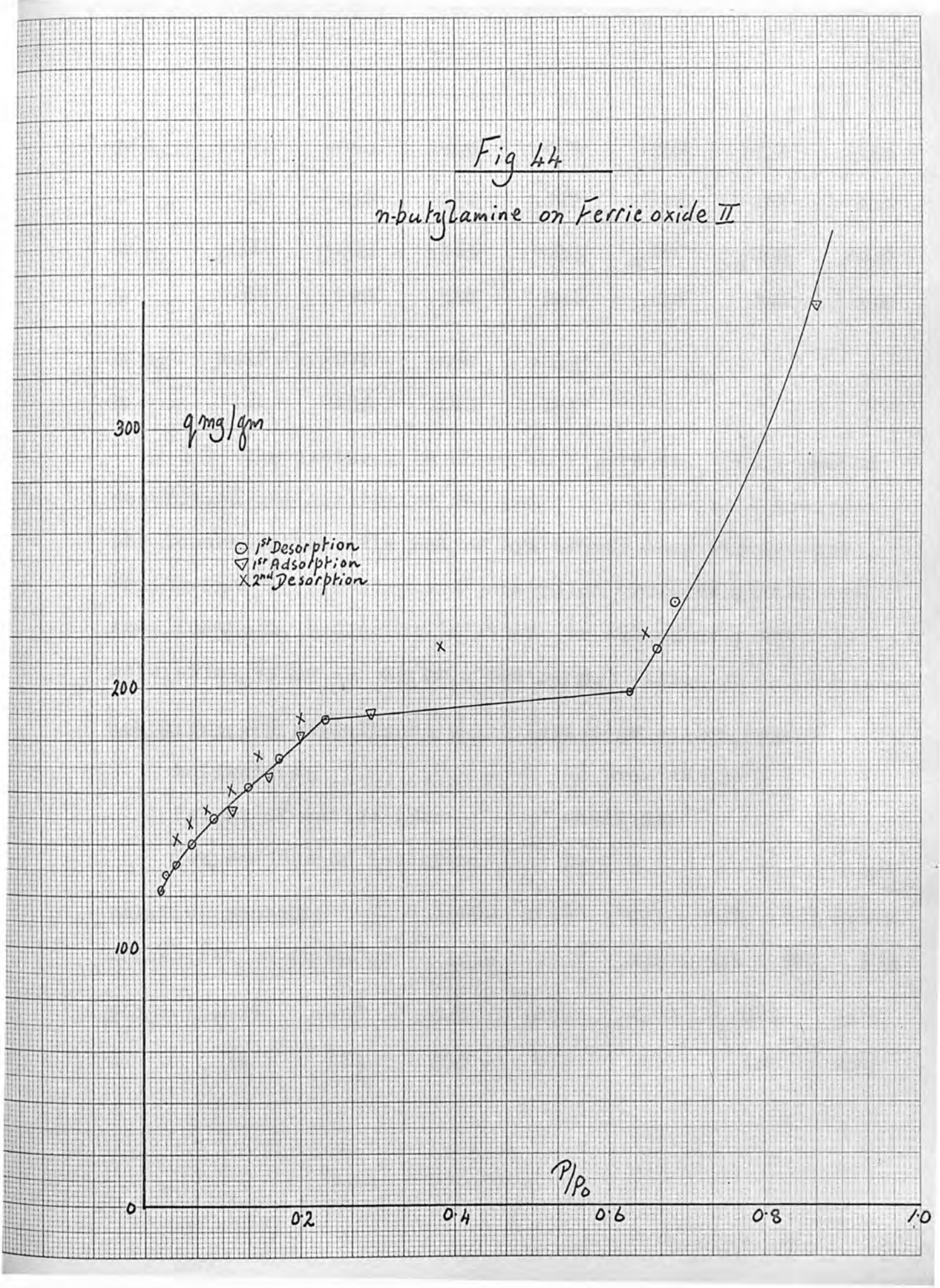

p/p_o	•091	•060	•040	•028	•022	•114 //	•158
q	150	140	132	128	122	153	166
p/p_o	•201	•289	•863 //	•643	•380	•200	•146
q	182	190	348	241	216	188	174
p/p_o	•110	•078	•056	•041			
q	161	153	148	142			

The isotherm is shown in figure 44. On repeated adsorption and desorption the points tend to shift towards the concentration axis and no hysteresis loop was observed. Taking the first desorption/adsorption cycle as giving the true isotherm, the point 'A' value is 123 mg/gm., the saturation value 195 mg/gm., and p_i/p_o •131.

4:4:4:3:3:2:2 heptafluoro n-butylamine on silica gel

Activation: 16 hrs. at 150°C

Weight of active gel: •8010 gm.

Temperature of isotherm: 25·0°C

relative pressure	1·000	1·000	•661	•588	•535	•506
concentration in mg/gm.	1236	1107	1021	945	889	835

p/p_o	•465	•403	•323	•252	•167	•041 //	•367
q	718	611	535	476	451	434	561

Fig 45

n-4:4:4:3:3:2:2 heptafluoro butylamine
on
Silica gel

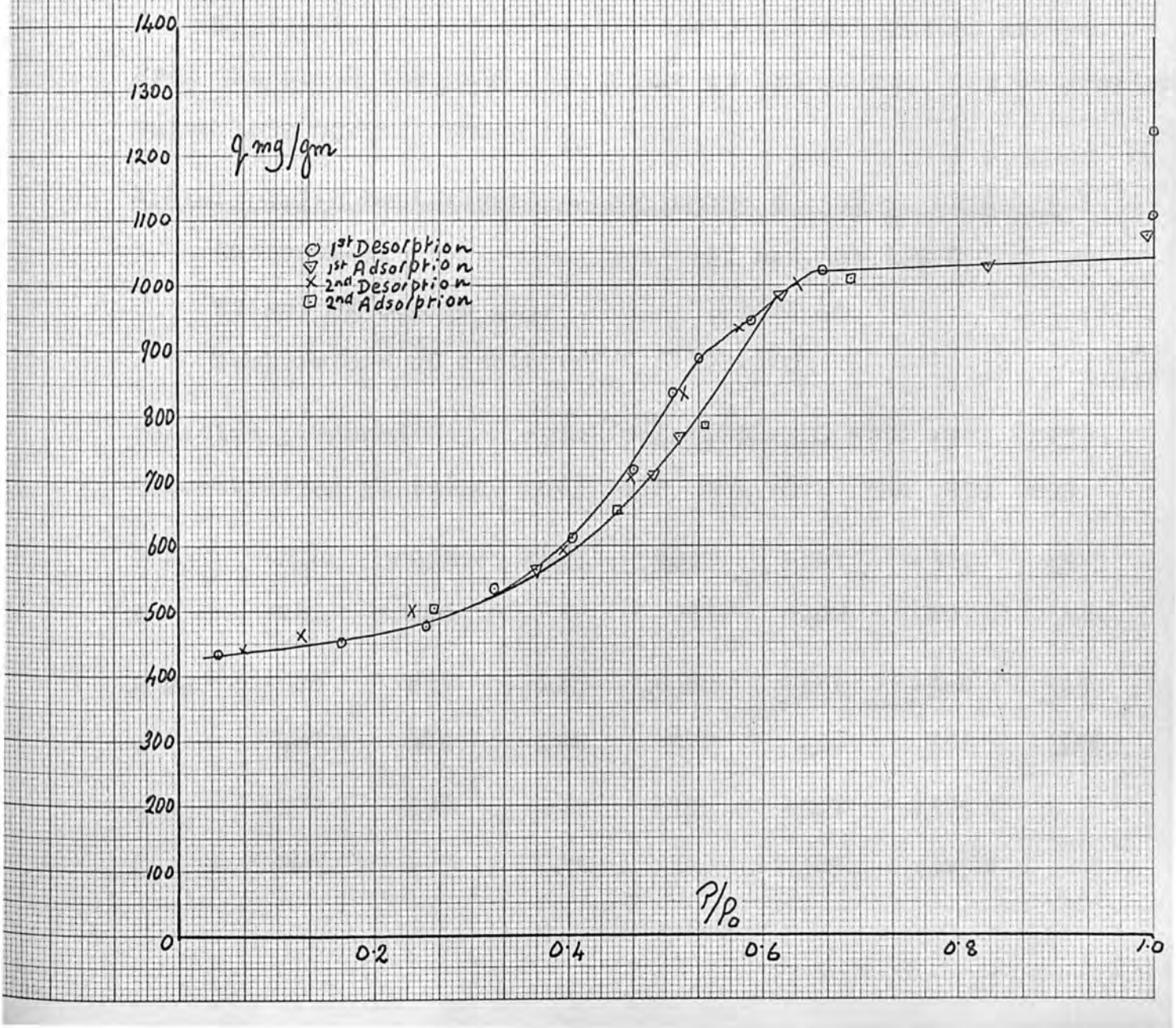

p/p_o	•487	•513	•617	•829	•995	•633	•574
q	708	769	983	1028	1075	1001	933
p/p_o	•517	•463	•393	•238	•122	•065	•262
q	833	705	591	500	462	440	505
p/p_o	•450	•538	•689				
q	655	787	1010				

The isotherm is shown in figure 45. The graph is repeatable over a number of adsorption/desorption cycles. From the graph the point 'A' value is 432 mg/gm., the saturation value 1030 mg/gm., and p_i/p_o •509.

4:4:4:3:3:2:2 heptafluoro n-butylamine on ferric oxide II

Activation: 17 hrs. at 150°C

Weight of active gel: 1•5369 gm.

Temperature of isotherm: 25.0°C

relative pressure	•984	•963	•483	•357	•358	•351	•323
concentration in mg/gm.	493	432	401	377	358	339	299

p/p_o	•218	•096	•049	•031	•291	•322	•373
q	261	240	232	227	282	297	341
p/p_o	•988	•805	•415	•360	•351	•344	•335
q	467	418	394	372	354	336	320
p/p_o	•177	•296	•301	•335	•347	•355	
q	244	277	278	300	309	349	

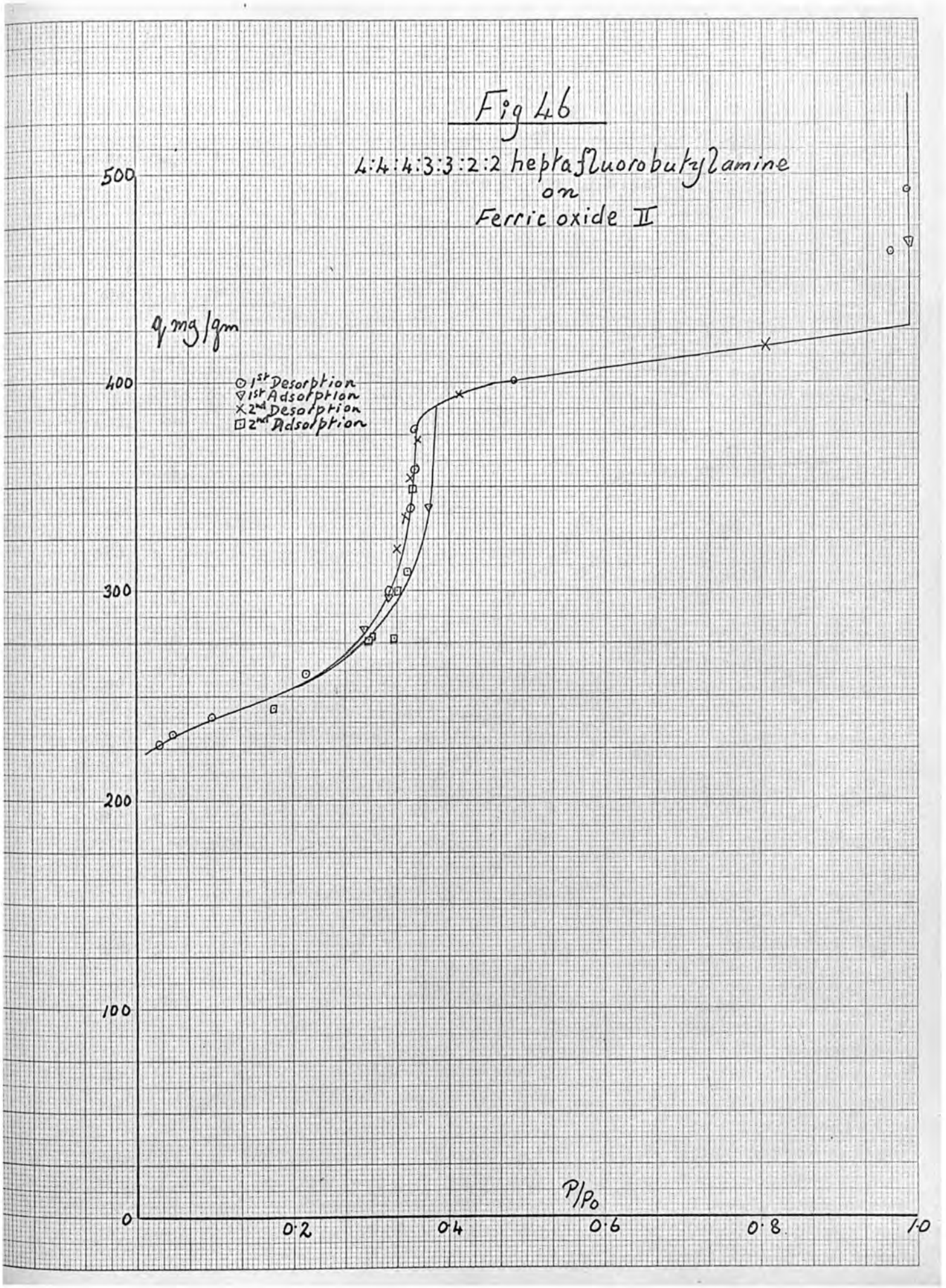
Fig 46
4:4:4:3:3:2:2 heptafluorobutylamine
on
Ferric oxide II
500
400
300
200
100
0
q mg/gm
⊙ 1st Desorption
▽ 1st Adsorption
× 2nd Desorption
□ 2nd Adsorption
P/Po
0·2
0·4
0·6
0·8
1·0

Fig 47

Benzene on Silica gel

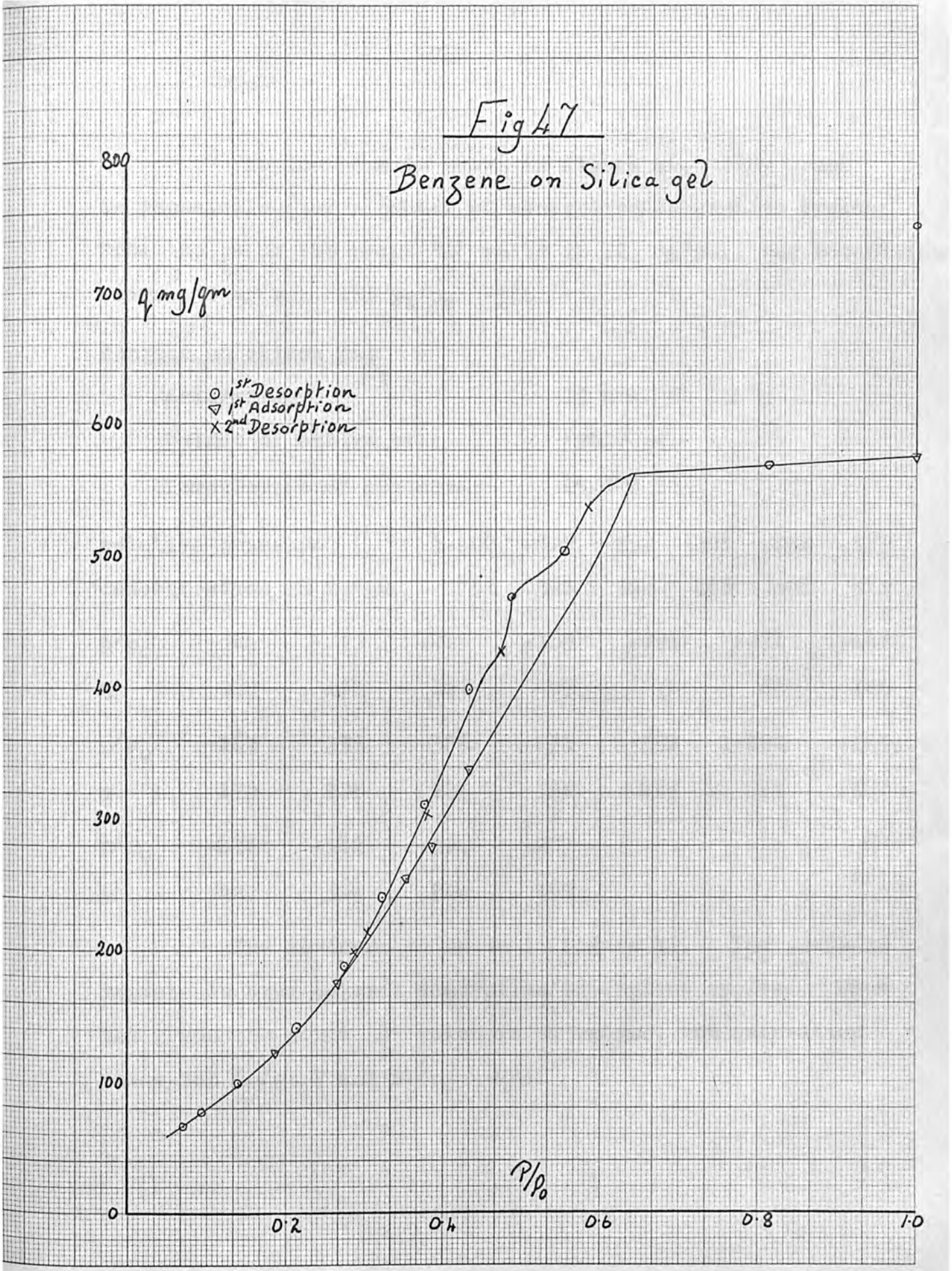

The isotherm is shown in figure 46. The graph is repeatable over a number of adsorption/desorption cycles. From the graph the point 'A' value is 123 mg/gm., the saturation value 430 mg/gm., and p_i/p_o •356.

Benzene on silica gel

Activation: 15 hrs. at 150°C

Weight of active gel: •9017 gm.

Temperature of isotherm: 25.0°C

relative pressure			1.000	•812	•552	•488	•434	•377
concentration in mg/gm.			751	568	504	468	398	311
p/p_o	•324	•275	•215	•139	•093	•071	//	•188
q	240	188	141	99	76	66	//	123
p/p_o	•267	•355	•386	•435	•357	1.000	//	•589
q	175	255	279	338	454	575	//	537
p/p_o	•472	•382	•304	•287				
q	427	304	214	199				

The isotherm is shown in figure 47. The graph is repeatable over several adsorption/desorption cycles. From the graph the point 'A' value is 34 mg/gm., the saturation value 585 mg/gm., and p_i/p_o •453.

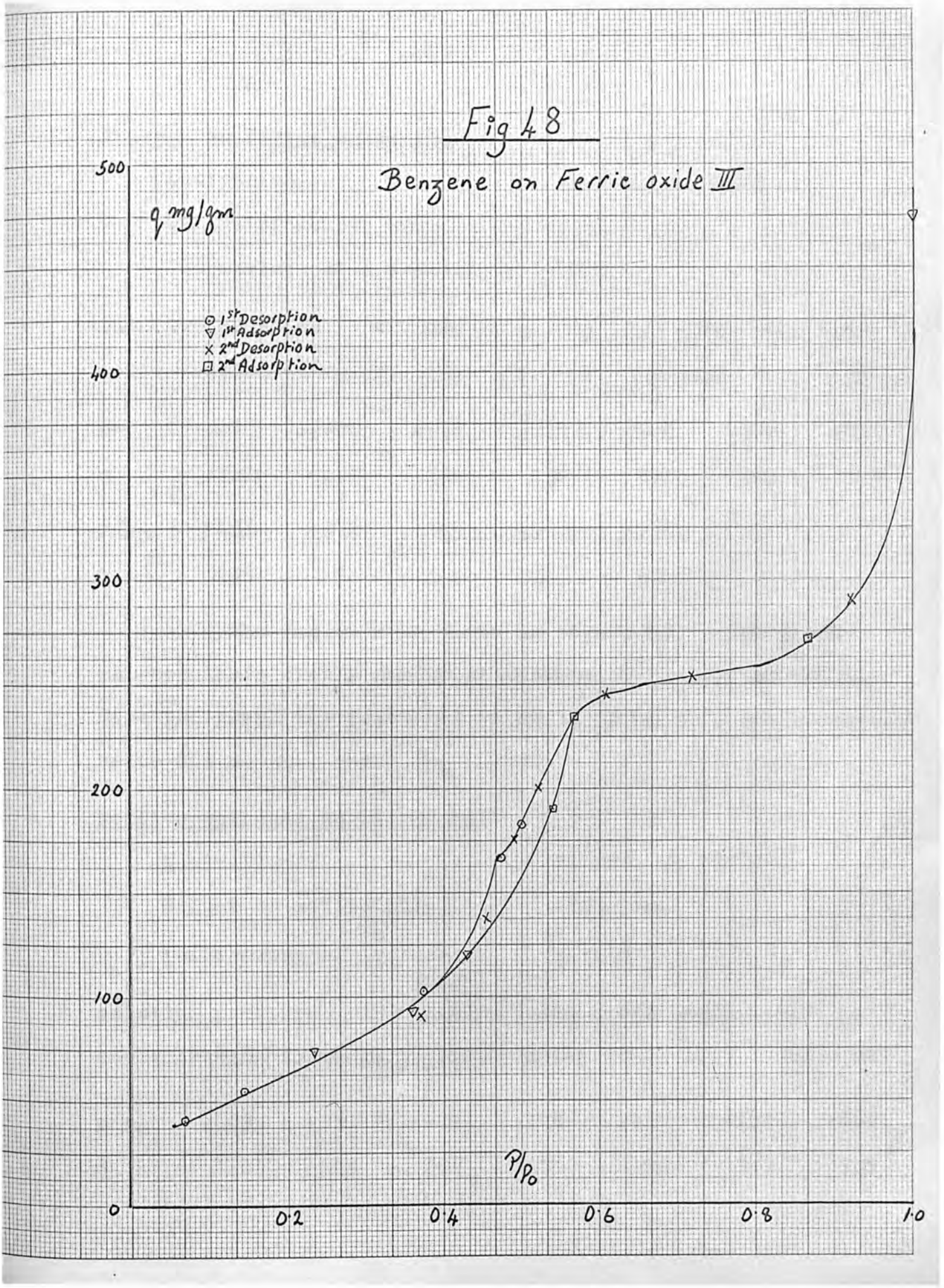
Fig 48
Benzene on Ferric oxide III
q mg/gm
⊙ 1st Desorption
▽ 1st Adsorption
× 2nd Desorption
⊡ 2nd Adsorption
500
400
300
200
100
0
0·2
0·4
0·6
0·8
1·0
P/Po

Benzene on ferric oxide III

Activation: 15 hrs. at 150°C

Weight of active gel: 1·4467 gm.

Temperature of isotherm: 25·0°C

relative pressure	·499	·474	·375	·143	·068	·234	·358
concentration in mg/gm.	183	167	102	55	41	77	93

p/p_o	·430	1·000	·922	·716	·606	·519	·491
q	121	475	290	256	242	201	178

p/p_o	·453	·371	·539	·567	·868
q	138	91	190	235	272

The isotherm is shown in figure 48. The graph is repeatable over a number of adsorption/desorption cycles. From the graph the point 'A' value is 33 mg/gm., the saturation value 283 mg/gm., and p_i/p_o ·490.

Perfluorobenzene on silica gel

Activation: 16 hrs. at 150°C

Weight of active gel: ·7251 gm.

Temperature of isotherm: 25·0°C

relative pressure	1·000	1·000	·651	·553	·517	·457
concentration in mg/gm.	1466	1309	1097	1035	981	845

p/p_o	·409	·350	·285	·211	·150	·101	·062
q	710	523	382	274	196	143	102

Fig 49

Perfluorobenzene on Silica gel

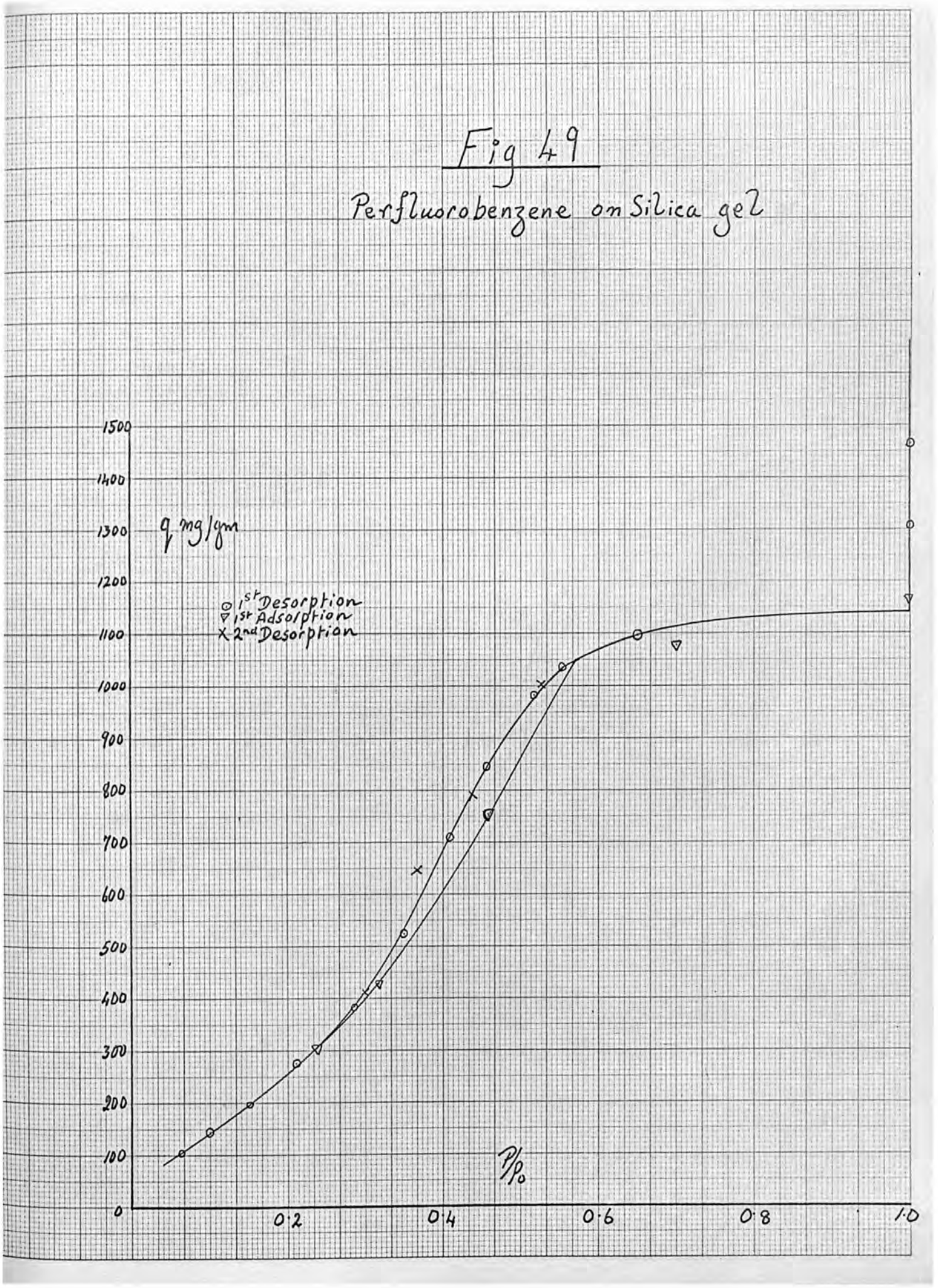

Fig 50

Perfluorobenzene on Ferric oxide III

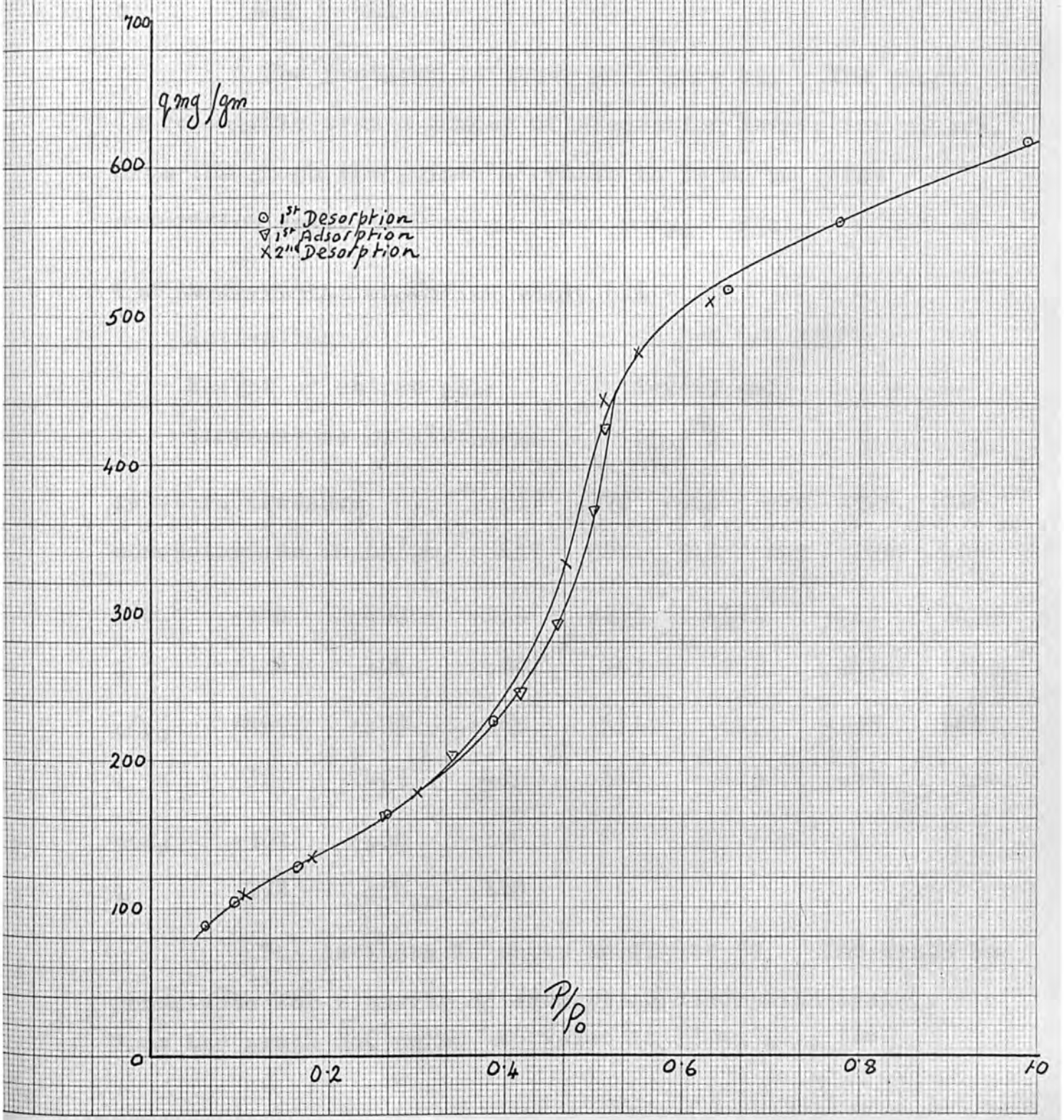

p/p_o	•236	•316	•458	•701	1•000 //	•527	•436
q	302	429	758	1078	1163 //	1002	791
p/p_o	•366	•301					
q	643	411					

The isotherm is shown in figure 49. The graph is repeatable over a number of adsorption/desorption cycles. From the graph the point 'A' value is 39 mg/gm., the saturation value 1160 mg/gm., and p_i/p_o •430.

Perfluorobenzene on ferric oxide III

Activation: 15 hrs. at 150°C

Weight of active gel: 1•2867 gm.

Temperature of isotherm: 25.0°C

relative pressure	•987	•770	•648	•576	•386	•266
concentration in mg/gm.	617	563	518	293	226	163

p/p_o	•164	•094	•059	•265 //	•341	•417	•458
q	128	104	89	163 //	203	246	293
p/p_o	•499	•509	•865	•631 //	•547	•508	•467
q	369	425	425	510 //	475	443	334
p/p_o	•302	•180	•108				
q	178	134	110				

The isotherm is shown in figure 50. The graph is repeatable for a number of adsorption/desorption cycles. From the graph the point 'A' value is 72 mg/gm., the

Fig 51

Acetone on Silica gel

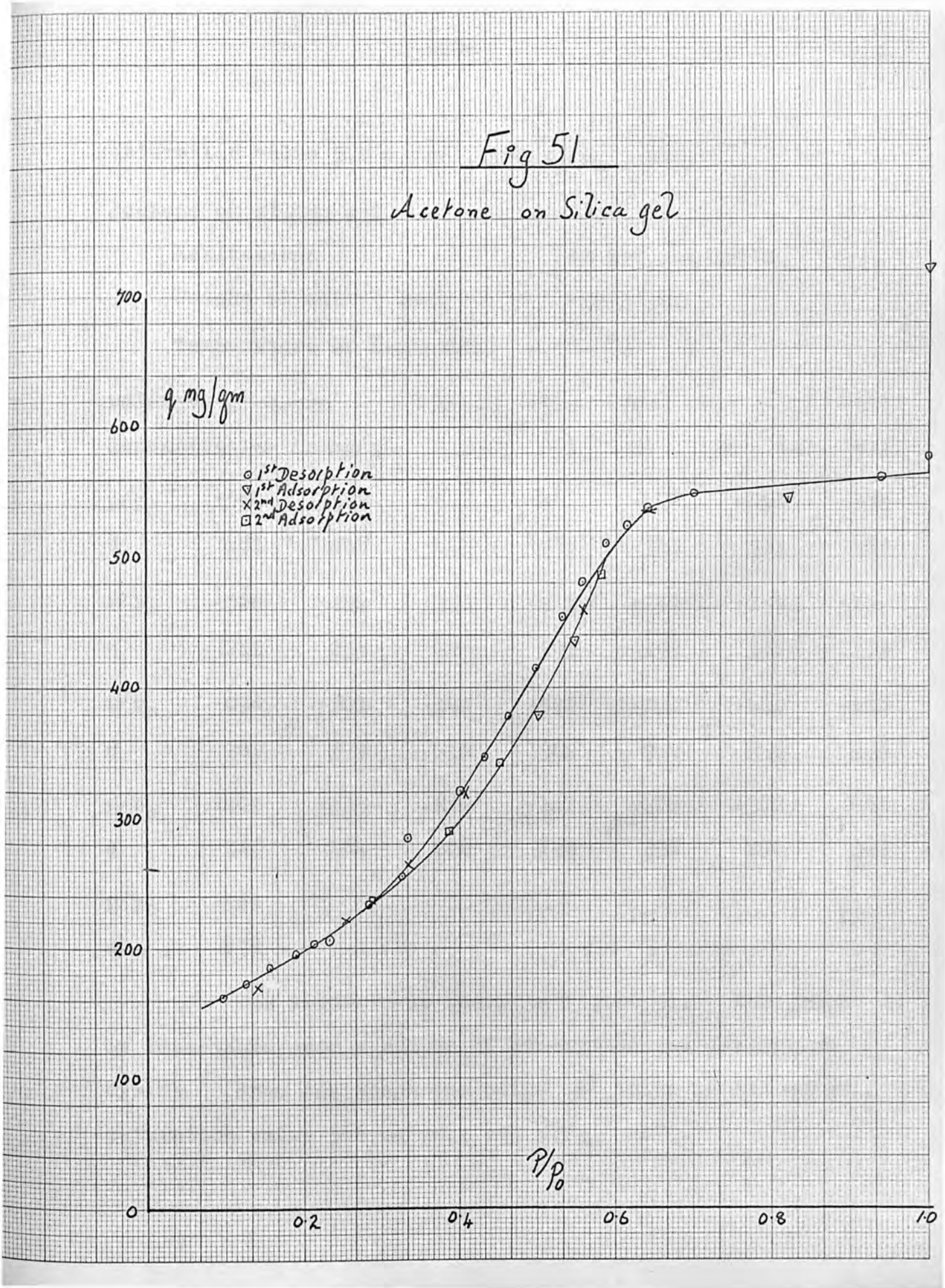

saturation value 570 mg/gm., and p_i/p_o ·448.

Acetone on silica gel

Activation: 16 hrs. at 150°C

Weight of active gel: ·8973 gm.

Temperature of isotherm: 0.0°C

relative pressure		1·000	·942	·700	·640	·612	·587
concentration in mg/gm.		577	561	549	538	524	511
p/p_o	·556	·529	·497	·462	·432	·401	·335
q	481	456	415	378	347	321	285
p/p_o	·328	·284	·233	·212	·191	·157	·127
q	255	233	206	203	195	184	173
p/p_o	·096	// ·501	·549	·820	1·000	// ·640	·556
q	162	// 379	436	546	722	// 536	459
p/p_o	·409	·335	·254	·141	// ·286	·388	·451
q	320	264	222	170	// 236	290	343
p/p_o	·582						
q	478						

The isotherm is shown in figure 51. The graph is repeatable over a number of adsorption and desorption cycles. From the graph the point 'A' value is 121 mg/gm., saturation value 566 mg/gm., and p_i/p_o ·479.

Fig 52

Acetone on Ferric oxide I

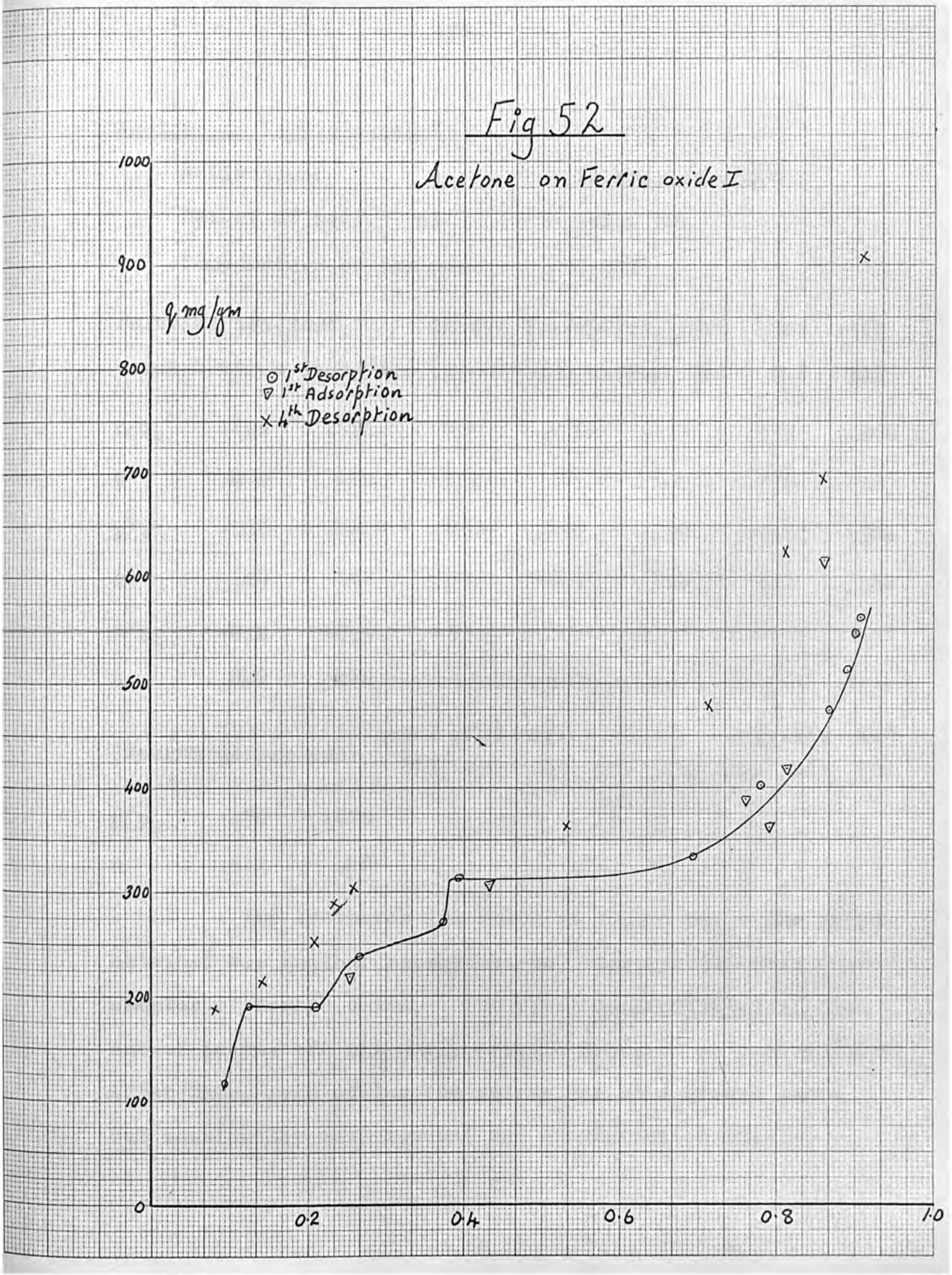

Acetone on ferric oxide I

Activation: 18 hrs. at 150°C

Weight of active gel: •9115 gm.

Temperature of isotherm: 0•0°C

relative pressure (First desorption)				•906	•902	•889	
concentration in mg/gm. (adsorption cycle)				561	547	512	
p/p_o	•866	•781	•693	•393	•375	•335	•266
q	473	402	332	313	303	271	237
p/p_o	•210	•125	•093	•254	•432	•791	•761
q	189	190	196	219	306	362	388
p/p_o	•814	•859					
q	448	616					

(Fourth desorption)	•907	•845	•810	•705	•531	•257	•234	•206
	967	695	625	479	363	304	288	251

p/p_o	•139	•078
q	214	188

The isotherms are shown in figure 52. The graph obtained was neither repeatable nor reproducible with fresh samples of ferric oxide. The first desorption/adsorption set of points are extremely erratic lying on no smooth curve. After three such cycles the points lie on a smooth curve but continually move towards the concentration axis.

Fig 53

1:1:1 trifluoroacetone on Silica gel

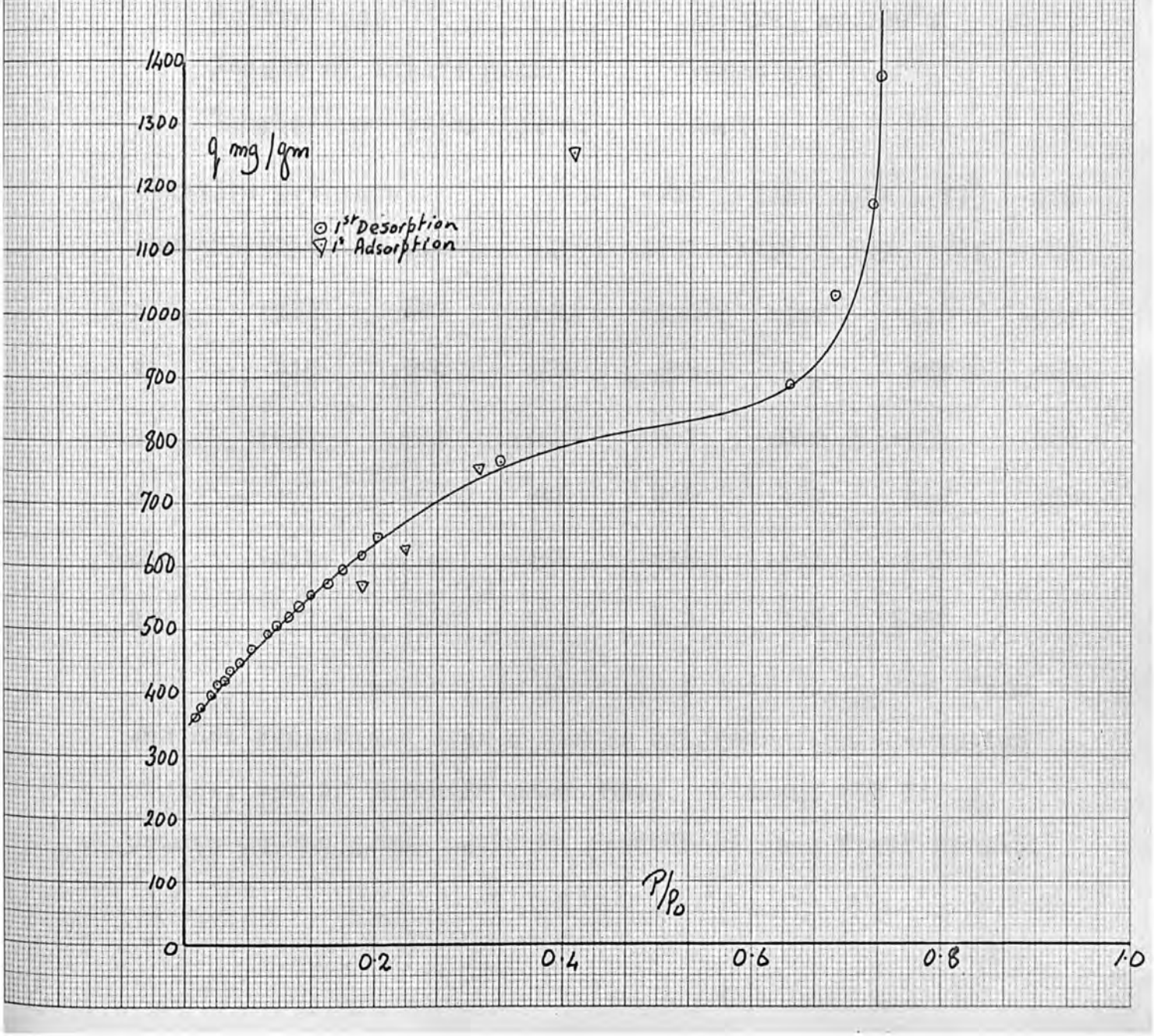

It was also found in another experiment that ferric oxide, both the sample here and non-porous commercial samples, were soluble in acetone.

Point 'A' values ranged between 125 mg/gm., and 150 mg/gm. Values for p_i and the saturation value will be discussed later.

1:1:1 trifluoroacetone on silica gel

Activation: 16 hrs. at 150°C

Weight of active gel: •9084 gm.

Temperature of isotherm: 0•0°C

relative pressure			•736	•726	•688	•639	•335	•204
concentration in mg/gm.			1377	1171	1030	899	765	646
p/p_o	•185	•167	•150	•134	•122	•110	•097	
q	619	594	572	553	535	520	507	
p/p_o	•087	•071	•056	•047	•040	•034	•026	
q	491	469	448	435	420	412	395	
p/p_o	•018	•010	•187	•235	•311	•410		
q	377	360	570	626	758	1256		

The isotherm is shown in figure 53. The graph was not repeatable over a number of desorption/adsorption cycles, one of which is shown here, although the first points on the graph could be reproduced on a fresh sample.

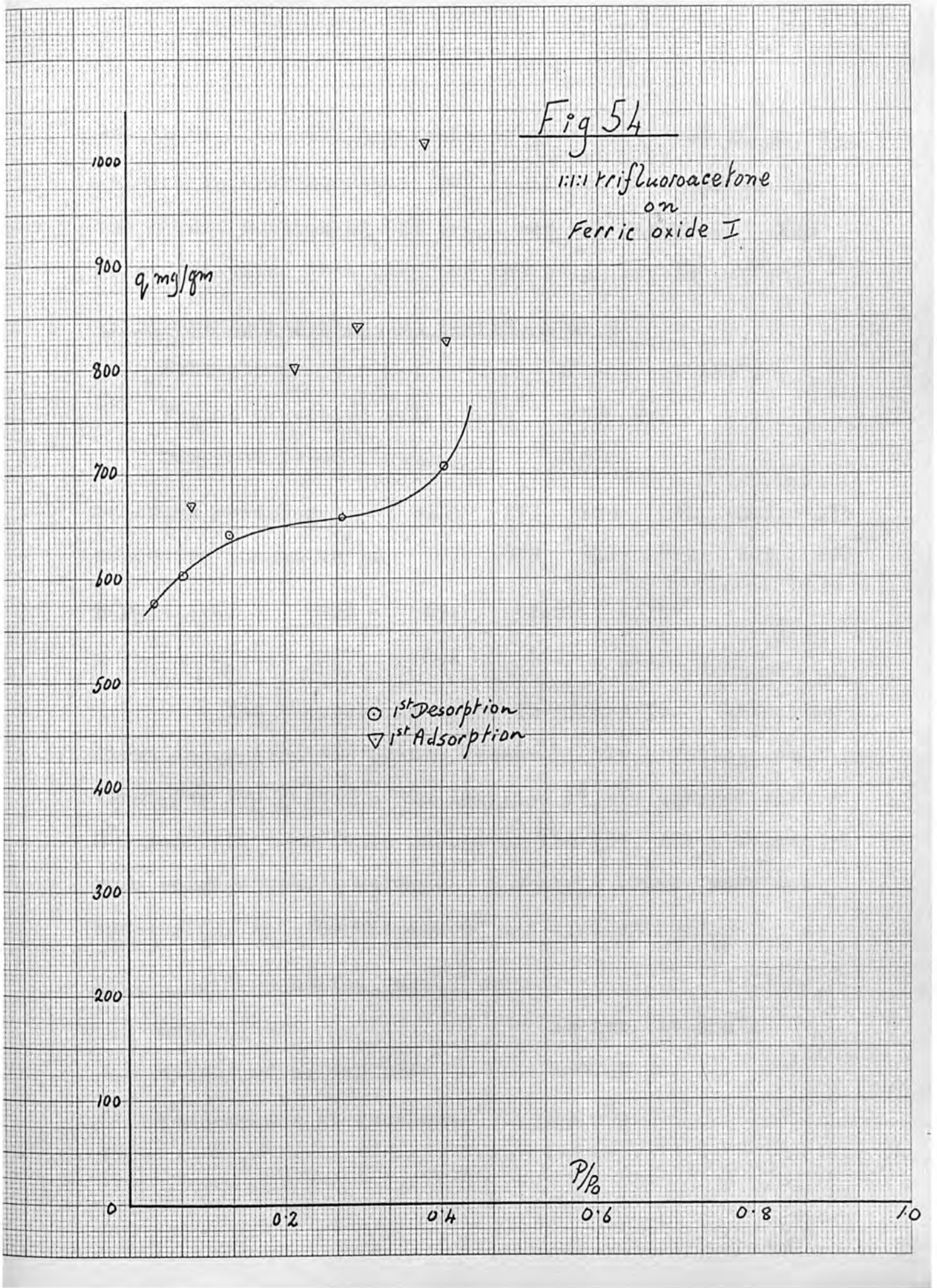
Fig 54
1:1:1 trifluoroacetone
on
Ferric oxide I
q mg/gm
1000
900
800
700
600
500
400
300
200
100
0
0·2
0·4
0·6
0·8
1·0
P/Po
⊙ 1st Desorption
▽ 1st Adsorption

Due to experimental difficulties pressures over 24 cm. Hg. (i.e. p/p_o approximately·750) could not be measured, so the higher portion of the graph was not observed. The point 'A' value obtained from the graph was 390 mg/gm.

1:1:1 trifluoroacetone on ferric oxide I

Activation:	16 hrs. at 150°C
Weight of active gel:	·9334 gm.
Temperature of isotherm:	0·0°C

relative pressure	·403	·273	·129	·071	·047	·035
concentration in mg/gm.	707	659	642	622	603	578

p/p_o	·079	·408	·292	·215	·378
q	670	827	842	802	1019

The isotherm is shown in figure 54. After the first desorption the points became highly erratic; only the first few are quoted. In addition it was noticed that at 0°C long white crystals formed on the gel, which melted at room temperature. Attempts to isolate these were not successful, and the "isotherm" was discontinued.

Acetic acid on silica gel

Activation:	16 hrs. at 150°C
Weight of active gel:	1·0093 gm.
Temperature of isotherm:	25·0°C

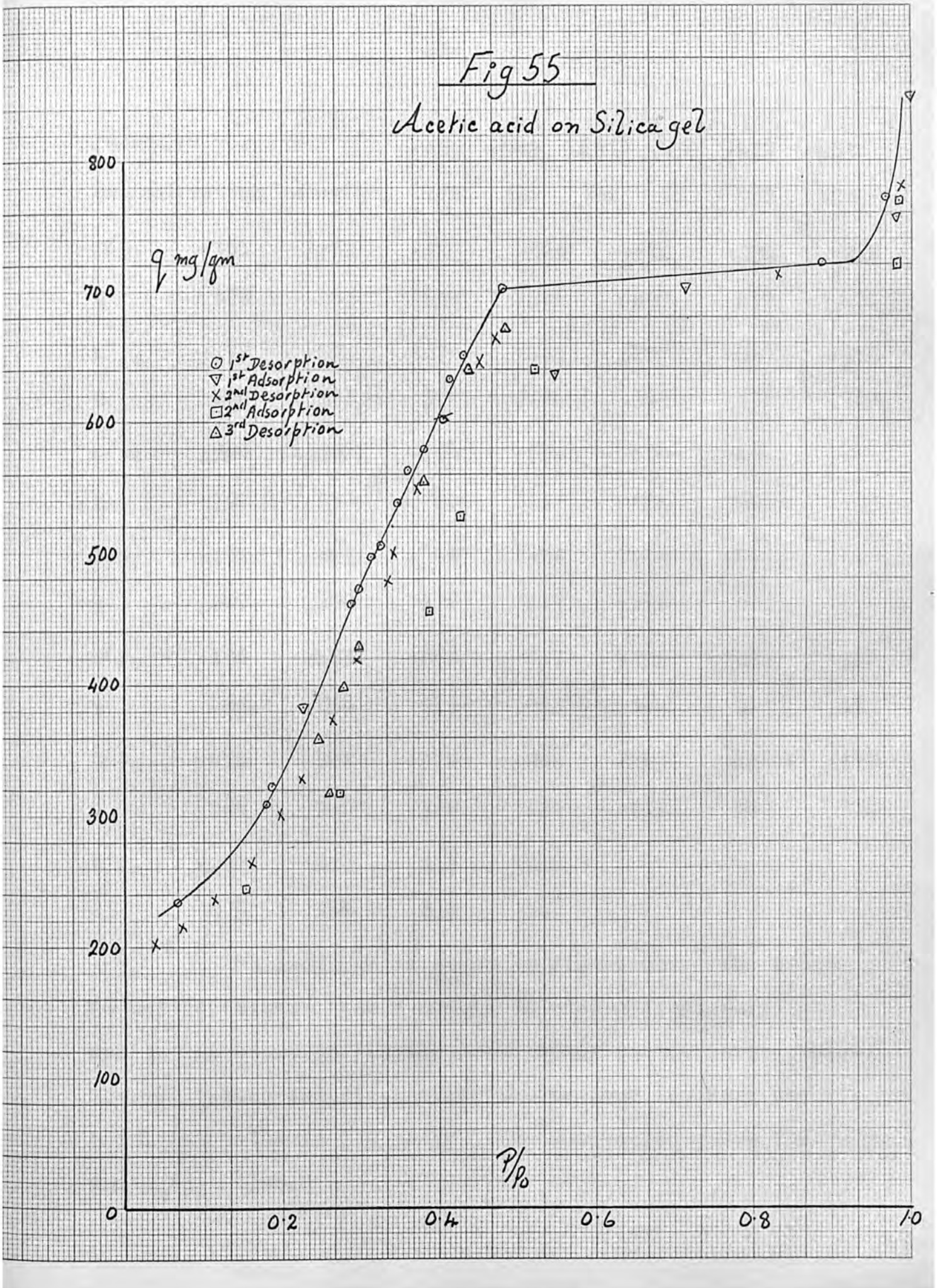
Fig 55
Acetic acid on Silica gel
800
700
600
500
400
300
200
100
0
q mg/gm
⊙ 1st Desorption
▽ 1st Adsorption
× 2nd Desorption
□ 2nd Adsorption
△ 3rd Desorption
P/Po
0·2
0·4
0·6
0·8
1·0

relative pressure			•969	•885	•481	•430	•414	•405
concentration in mg/gm.			772	721	702	651	633	602
p/p_o	•381	•361	•349	•325	•312	•298	•288
q	579	563	534	506	497	472	461
p/p_o	•472	•184	•178	•065	•227	•547	•713
q	434	321	309	234	383	636	702
p/p_o	•980	1•000	•986	•831	•469	•450	•404
q	757	850	780	712	664	646	603
p/p_o	•371	•342	•335	•293	•263	•223	•197
q	549	500	478	419	373	328	301
p/p_o	•158	•113	•069	•037	•155	•274	•386
q	264	236	215	203	244	317	455
p/p_o	•428	•524	•979	•983	•483	•438	•379
q	528	640	720	769	671	640	554
p/p_o	•297	•277	•248	•206			
q	428	398	359	317			

The isotherm is shown in figure 55. The graph is not repeatable over a number of adsorption/desorption cycles but seems to "settle down" after two to three cycles. However taking the first cycle as the true isotherm the point 'A' value is 175 mg/gm., the saturation value 720 mg/gm., and p_i/p_o •344.

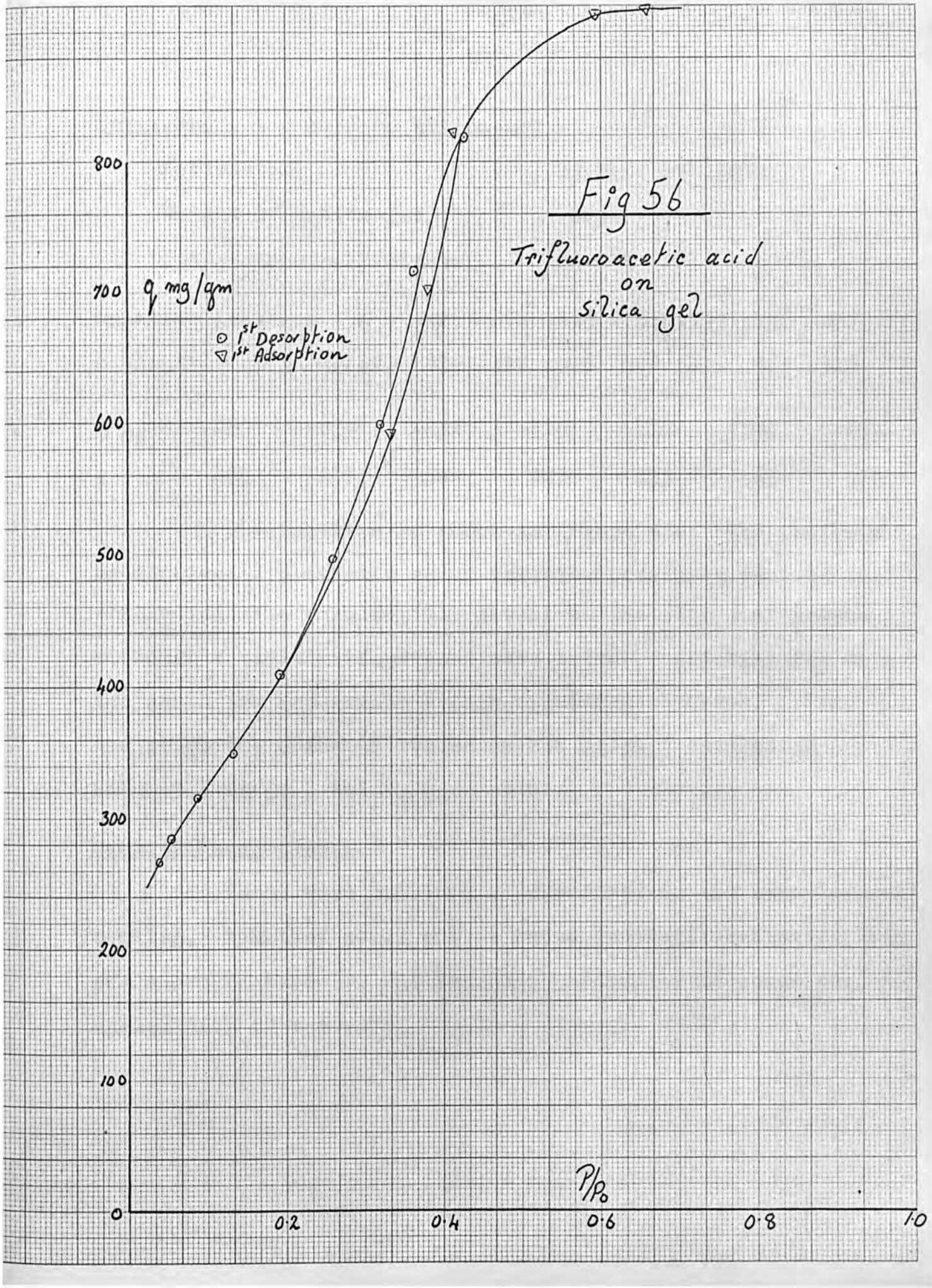

Fig 56

Trifluoroacetic acid
on
silica gel

Trifluoroacetic acid on silica gel

Activation: 17 hrs. at 150°C

Weight of active gel: •8807

Temperature of isotherm: 25•0°C

relative pressure	•426	•364	•319	•261	•193	•136	•087
concentration in mg/gm.	819	716	598	496	411	355	315

p/p_o	•053	•039	//	•332	•379	•414	•594	•649
q	284	266		592	703	823	913	918

The isotherm is shown in figure 56. The isotherm is difficult to observe as at relative pressures over •55 the trifluoroacetic acid rapidly dissolves the stop-cock grease, although a variety of greases were tried. Allowing for this the graph was repeatable within experimental error. From the graph the point 'A' value is 238 mg/gm., saturation value 918 mg/gm., and p_i/p_o •348.

Density Measurements

These were obtained as described in the experimental section, when they could not be found in the literature. They are shown in table I, and the ones personally measured are marked with an asterisk.

Surface Tension Measurements

In the cases where the surface tension was measured at 0°C, i.e. 3:3:3:2:2 pentafluoro n-propylamine, or where the liquid tended to "run" out of the tube, a number of readings at that temperature only were taken.

In the other cases a series of readings were taken at different temperatures and the value at the required temperature read from a graph of surface tension against temperature. The readings are as follows:-

2 fluoroethanol

Temperature °C	21.2	26.2	30.6	35.4	31.2	27.4	23.1
surface tension dynes/cm.	32.8	32.2	31.6	31.0	31.5	32.1	32.6

The graph is shown in figure 57.

3:3:3:2:2 pentafluoropropan-1-ol

Temperature °C	21.6	23.4	26.0	28.3	30.5	27.2	24.3	20.6
surface tension dynes/cm.	17.8	17.5	17.1	16.7	16.3	16.8	17.3	18.0

The graph is shown in figure 58.

4:4:4:3:3:2:2 heptafluorobutan-1-ol

Temperature °C	22.1	25.3	29.7	35.1	30.2	26.1	20.7
surface tension dynes/cm.	15.0	14.8	14.2	13.8	14.2	14.6	15.1

The graph is shown in figure 59.

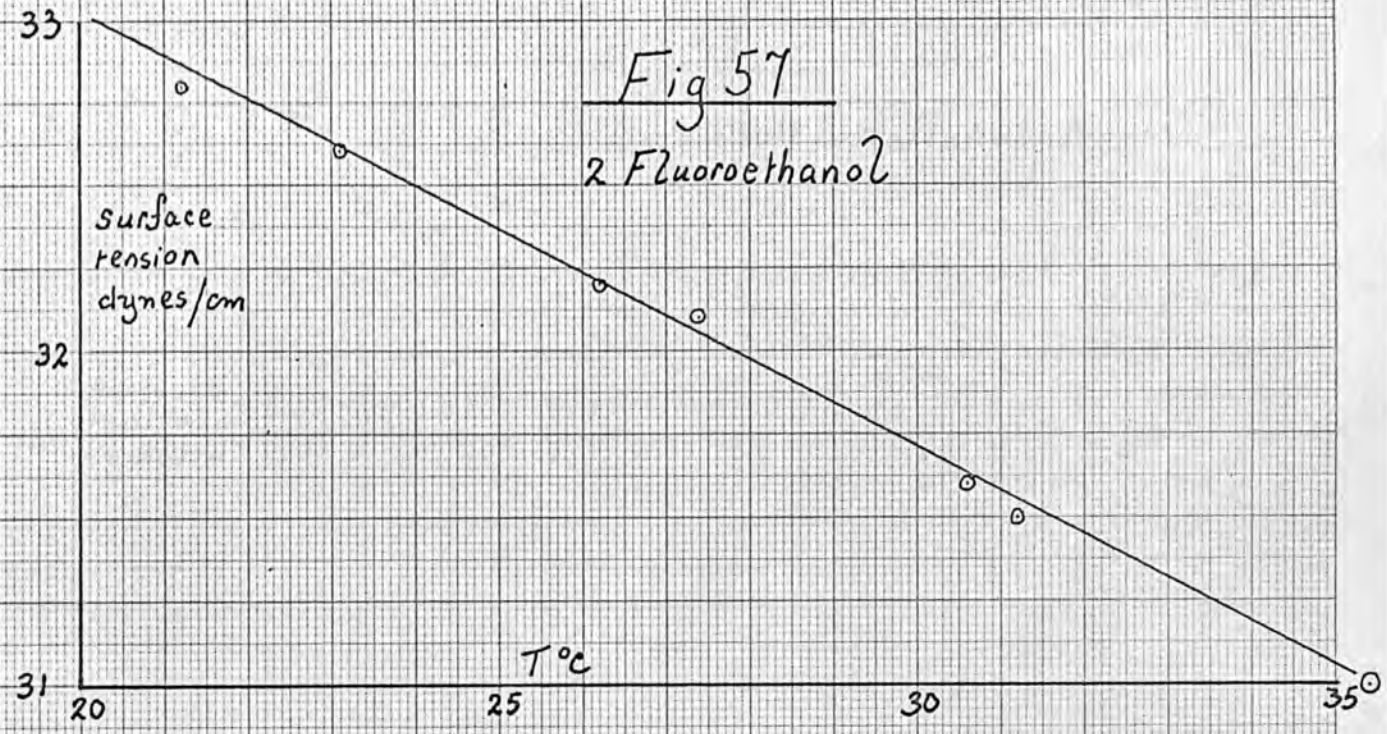

Fig 57

2 Fluoroethanol

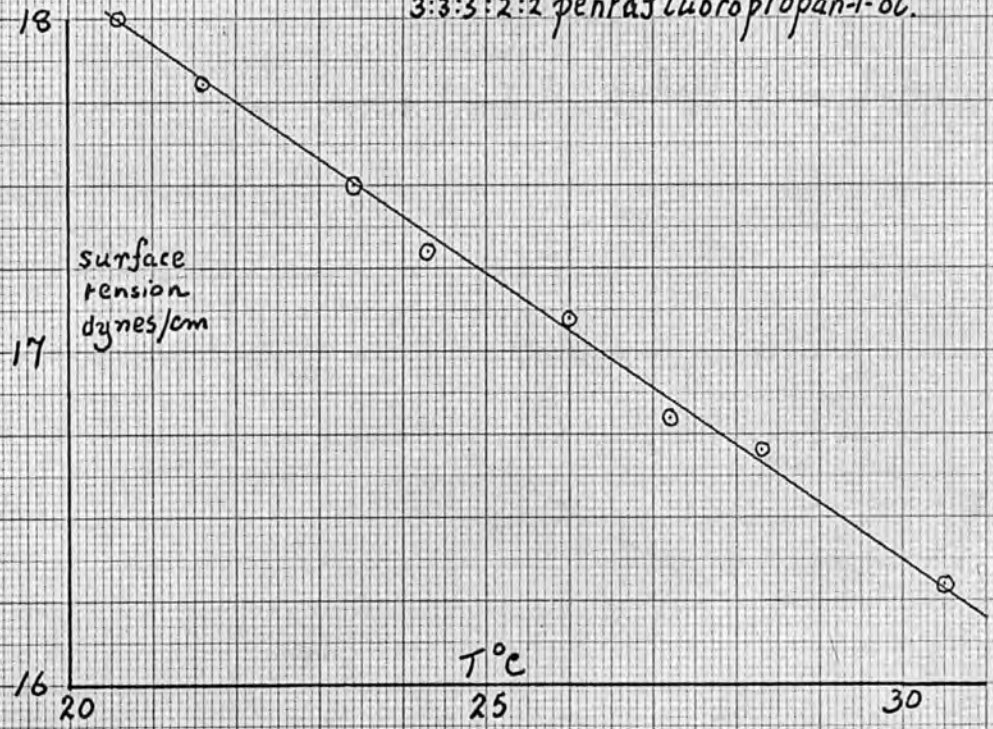

Fig 58

3:3:3:2:2 pentafluoropropan-1-ol.

Fig 59

4:4:4:3:3:2:2 heptafluorobutan-1-ol

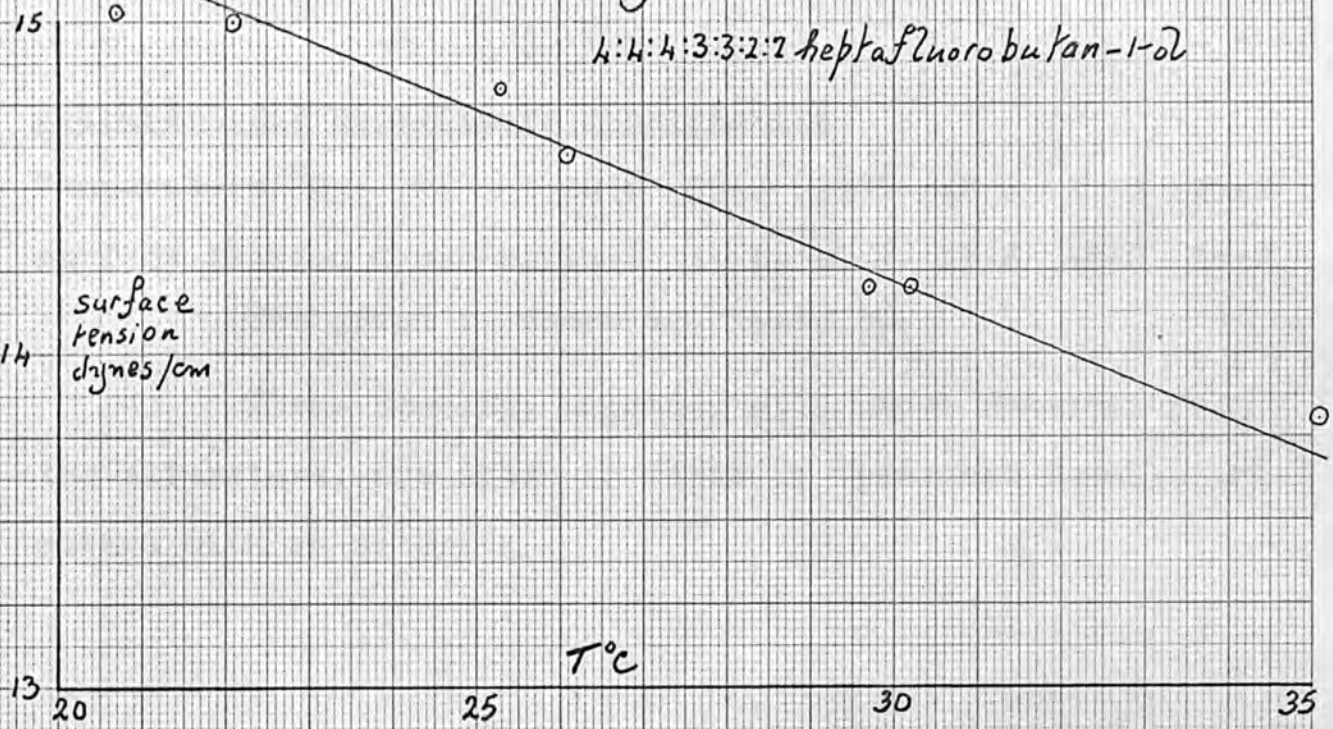

Fig 60

4:4:4:3:3:2:2 n-heptafluorobutylamine

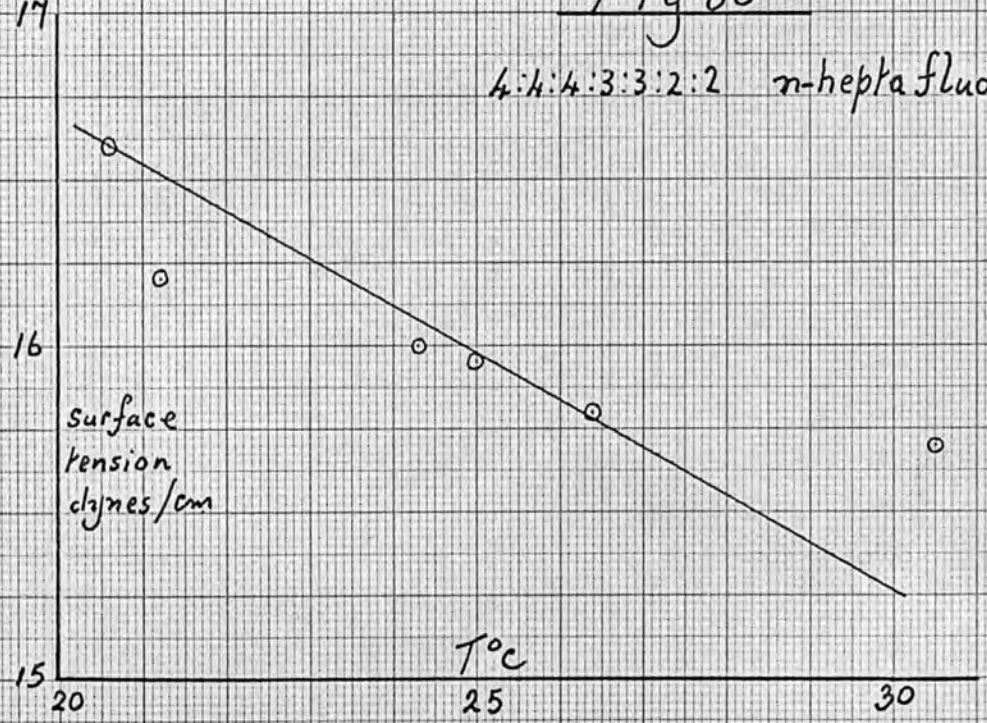

4:4:4:3:3:2:2 heptafluoro n-butylamine

Temperature °C	20·6	25·0	30·5	26·4	24·3	21·2
surface tension dynes/cm.	14·6	$15·9_5$	15·7	15·8	16·0	16·2

The graph is shown in figure 60.

These results, together with those obtained from the literature, are shown in table I; personal results are marked with an asterisk.

DISCUSSION

"The time has come," the Walrus said,
"To talk of many things:
Of shoes - and ships - and sealing wax -
Of cabbages - and kings -
And why the sea is boiling hot -
And whether pigs have wings."

Lewis Carroll

For ease of discussion the section will be divided into five sub-sections: (1) results using silica gel; (2) results using ferric oxide; (3) general comments on these results; (4) low pressure isotherms; (5) final summary.

1. Isotherms obtained on silica gel

Twenty-two isotherms were measured using silica gel as the adsorbent. A summary of the data to be discussed is shown in table 2. Consider first the values for the surface areas. These range from $.33 \times 10^6$ to 6.58×10^6 sq. cm. per gm. calculated from Livingstone's equation (cf eq. 11) and the Point 'A' value for completed monolayer. Applying simple statistics (61) one finds a variance (or root mean square deviation) (V) of 1.23×10^6 and average deviation (a) of .80, that is $\frac{a}{v} = .65$; if these results fell on a

normal Gaussian error curve then $\frac{a}{v} \doteq \cdot 79$. By casting out those values which have a deviation greater than v and recalculating v and a until $\frac{a}{v} \doteq \cdot 8$, nine results were rejected. These were:-

acetone ~~standard~~ deviation $\delta = -\cdot 61$, $\frac{\delta}{v} \sim 3$

2:2:3:3 tetrafluoropropanol $\delta = -\cdot 89$, $\frac{\delta}{v} \sim 4$

1:1:1: trifluoroacetone $\delta = +2\cdot 73$, $\frac{\delta}{v} \sim 12$

n propylamine, $\delta = +1\cdot 26$, $\frac{\delta}{v} \sim 6$

n-3:3:3:2:2 pentafluoropropylamine $\delta = +1\cdot 13$, $\frac{\delta}{v} \sim 5$

n-4:4:4:3:3:2:2 heptafluorobutylamine $\delta = +1\cdot 37$, $\frac{\delta}{v} \sim 6$

ethylpropionate $\delta = -\cdot 89$, $\frac{\delta}{v} \sim 4$

benzene $\delta = -2\cdot 79$, $\frac{\delta}{v} \sim 12\cdot_5$

perfluorobenzene $\delta = -3\cdot 52$, $\frac{\delta}{v} \sim 16$.

Except for 1:1:1 trifluoroacetone, the compounds that have δ positive are armines. This would be expected if one considers silica gel to have an "acidic" surface as chemisorption can then take place on the more reactive sites. This would not however preclude the formation of the statistical monolayer, in fact the chemisorbed amine could provide nuclei for "condensation", which would make the monolayer appear to hold even more.

n-Butylamine deserves notice as it gives a surface area which, although larger than the average is within v of it. This would appear to be a fortunate balancing out of effects, viz. butylamine is a weaker base than propylamine and so will be less extensively chemisorbed, but as before this would give a high result. In addition, no account has been taken in the calculation of the effective molecular area for n-butylamine that the molecule is more nearly linear than spherical. Such a linear molecule attached at one point to the surface of the adsorbent could lie flat or at an angle to the surface thus effectively covering a larger area than calculated on a spherical model. It would appear then that these two effects, balance for n-butylamine.

Despite this n-heptafluorobutylamine gives too large a surface area. On comparing the amount of n-butylamine and n-heptafluorobutylamine adsorbed in millimoles one finds it is 2·60 and 1·95 respectively. As there can not be much difference in size between these two molecules and less is adsorbed if considered on a molar basis the over estimation of the surface area must be due to over estimating the effective molecular area (see Table I). This is a reasonable assumption as it was noted above that this type of molecule is approximately linear rather than spherical, so that it can orientate with its long axis perpendicular to the surface.

This too is reasonable as can be seen if the forces binding the molecule are divided into two parts, one due to the amine group and the other due to the substituent carbon chain. Due to the small polarisability of the fluorine atom the van der Waals forces between the carbon chain containing fluorine at the surface, are lower than for the corresponding hydrogen-carbon chain. Thus the chain can be more easily detached from the surface leaving only the amine end group holding it, and so more closely packed.

Discussion of the other compounds that give anomalous surface areas is better left to the general section where they, and similar ones arising when ferric oxide is used, can be dealt with together. It is also advisable at this point to examine the individual isotherms more closely.

These can be broadly classified as those which are reproducible, within experimental error, over a number of adsorption-desorption cycles and those where the graph "wanders" on repeated adsorption-desorption. The isotherm of n-pentafluoropropylamine (fig. 41) is of the type that "wanders". One also notes that the other amine isotherms (figs. 39, 43, 45) show no hysteresis loops, unlike most of the other isotherms on silica gel. This, taken together with the probable chemisorption in these systems discussed

above, suggests that in the case of n-pentafluoropropylamine the observed movement is due to progressive chemisorption during the course of the experiment. On this basis the lack of hysteresis loops in the other three isotherms can be ascribed to blocking of the pores by chemisorbed material, if the rate of chemisorption is fast enough to be undetectable by the method used here to determine the isotherms. This is quite possible as an adsorption-desorption cycle takes at least four days to determine, and it is only after this that movement of the graph can be detected.

The other irreproducible system is that of acetic acid on silica gel (fig. 55). The first point to note is that whereas the amine graphs move towards the concentration axis if they show any movement, the acetic acid graph moves towards the pressure axis, i.e. less is being adsorbed at any particular pressure. However the point 'A' value remains reasonably constant despite this movement, or to go back to table 2 the surface area computed from the acetic acid point 'A' value has $\delta = -\cdot 46$ and $\frac{\delta}{v} \sim 2\cdot 0$ just within the limits.

Acetic acid is a well known solvent and in addition is often used as a peptising agent in colloid chemistry. It is natural to think that the movement of the graph is due to these effects i.e. the gross globular structure of the gel is broken down. This need not have

much effect on the surface area, nor even on the pore volume, but would show up in the hysteresis region, which is strongly dependent on pore size. In fact when one calculates the pore radius a value of 11·9 Å is found against an average value of 26·0 Å.

Having analysed the isotherm in these terms one then looks again at the apparently normal isotherm of trifluoroacetic acid when one finds that although the graph is reproducible the Kelvin radius is only 9·6 Å and even the saturation volume is lower than the average (see fig. 62). This is not surprising as trifluoroacetic acid is a far stronger acid than acetic acid and a far better solvent. Thus as with the amines the action of trifluoroacetic acid on the gel is fast compared with the time of the experiment, and this gives the isotherm the appearance of normality.

The other isotherm worthy of note, is that of pentafluoropropanol (fig. 23). Here the hysteresis loop does not close until a relative pressure of one. This type of isotherm, reasonably well known, is classified as type B by de Boer (fig. 3). Of the type of structures discussed by de Boer (34) which might give rise to this form of isotherm, the very wide body with narrow entries would fit the known silica gel structure. This however baulks the main question of why only pentafluoropropanol out of all the compounds

examined shows this type of isotherm? There does not seem to be any reasonable explanation.

Having discussed the isotherms where ~~something~~ there ~~obviously happens~~ are anomalies, one can now check back by looking at table 2. For instance one notes that ethyl trifluoroacetate gives a low Kelvin radius, while the saturation volume and surface area are quite normal. This could be due to the peptising action of a good solvent. On the other hand ethyl acetate shows no such behaviour, giving good average figures for all the constants calculated. But in general both the hydrocarbon and the fluorocarbon give comparable results for the various quantities calculated.

Isotherms on ferric oxide

From the point of view of continuity it was unfortunate that three different ferric oxides were used so that eight isotherms were run on ferric oxide I, nine on ferric oxide II, and five on ferric oxide III. With such small individual samples no detailed statistical analysis was possible as in the case of silica gel. Thus ethyl alcohol was chosen as a standard substance and values obtained from other substances compared with it. For this reason the individual isotherms will be examined rather than be dealt with ~~the isotherms~~ as a group; tables 3, 4 and 5 show the various quantities calculated from the isotherms on ferric oxides I, II and III respectively.

Consider first the isotherms run on ferric oxide I. Of these the acetone and trifluoroacetone results are best discussed in the following section together with the similar isotherms on silica gel.

Ethyl acetate (fig. 32) and ethyl trifluoroacetate (fig. 34) isotherms are of normal sigmoid shape and reproducible over a number of adsorption desorption cycles. Having noted with silica gel a low value for the pore radius, calculated from the Kelvin equation, when ethyl trifluoroacetate was used, and having attributed this to a peptising action, one would expect to find similar results with ferric oxide. This is indeed the case, the calculated Kelvin radius being 17·7 Å when ethyl trifluoroacetate is the adsorbate and 34·0 Å when ethanol is the adsorbate. Ethyl acetate, as before, gives reasonable values not only for the surface area and saturation volume but also for the pore radius, determined from Kelvin's equation, i.e. 31·9 Å.

Five isotherms with alcohols as adsorbates were run on ferric oxide I. These were ethyl alcohol, 2:2:2 trifluoroethanol, n-propanol, n-3:3:3:2:2 pentafluoropropanol, and n-3:3:2:2 tetrafluoropropanol (figs. 10, 16, 22, 24, 26 respectively). It is immediately obvious that the tetrafluoropropanol has been adsorbed to a far greater extent than can be explained on the basis of physical adsorption.

At first one might postulate very extensive chemisorption, as the fluoroalcohols are very weak acids. However trifluoroethanol has a $pK_a = 11{\cdot}4$ and for tetrafluoropropanol $pK_a = 11{\cdot}34$, so that one would expect at least as extensive chemisorption for trifluoroethanol on this basis. In addition further calculation shows that if the ethanol value of the surface area is taken as correct, six layers of tetrafluoroethanol have been adsorbed at what appears to be point 'A', or there is one tetrafluoropropanol molecule adsorbed at point 'A' for every two iron atoms in the gel. It would appear that chemisorption cannot reasonably explain this.

As further partially fluorinated propanols were not available, it was decided to examine the fluorinated ethanol series instead, as these might indicate what was happening. That they might show similar behaviour was indicated by noting that the boiling points in a series of compounds of the form $CH_3 - R$, $FCH_2 - R$, $F_2CH - R$ and $F_3C - R$, generally reach a maximum at $FCH_2 - R$ (cf table 6). Thus, as high adsorption goes with a high boiling point, one would expect that n-3:2:2 trifluoropropanol would have a high adsorption, or in the ethanol series that 2-fluoroethanol would have the highest adsorption. Unfortunately for the comparison 2:2 difluoroethanol was not so readily available as the suppliers made out and so the full comparison could not be made.

A further complication lies in the form of the isotherm of 3:3:2:2 tetrafluoropropanol - it is a typical type IV graph, with hysteresis loop, displaced along the concentration axis. If a value for the "pore radius" is calculated using the Kelvin equation one obtains a value of 28·9 Å in quite good agreement with the pore radius calculated with ethanol as adsorbate viz. 34·0 Å. On the face of it it would appear that whatever happens leaves a "pore" structure similar to the unaltered gel. Also the interval between the point 'A' value and the saturation volume is approximately 420 mg/gm., roughly what would be expected for a 'normal' isotherm.

One also notes that the hysteresis loop for pentafluoropropanol (fig. 24) does not close until the relative pressure is one, just as on silica gel. One wonders if this is a function of the adsorbate rather than the structure of the adsorbent, as, no other system in the series shows this effect, (as noted before with silica gel).

Nine isotherms were obtained on ferric oxide II, and results from these are given in table 4. The data for the surface area is however better presented as a graph (see fig. 63). The nine points appear scattered over the graph and no line can be drawn to go through them and the origin. The scatter is more than can be attributed to experimental

error (see the corresponding graph for silica fig. 61).

If the points are distinguished according to the type of molecule - only three types were run on this gel four amines, three alcohols and two esters - it then appears that the amines lie on one straight line, the alcohols and esters on another. It must be admitted that neither of the "best straight lines" obtained by a "least squares" plot fits the points particularly well, but this is due in part to lack of points.

However one can discern the trend with reasonable certainty; a greater quantity of amine is adsorbed at point 'A' than for the other types of compound. At first this seems difficult to rationalise, as, unlike silica gel, ferric oxide can be considered to have basic characteristics. However amines are good chelating compounds and a bond similar to that between nitrogen and iron in $Fe^{III}(NH_3)_6 Cl_3$ could be formed. This type of behaviour has been extensively examined by Yung-fang Yu Yao (62) by calorimetric methods on both reduced and oxidised iron surfaces, and he came to very similar conclusions.

The amine isotherms (figs. 40, 42, 44, 46) also indicate chemisorption, i.e. little or no hysteresis loop, and the graph moves towards the concentration axis, except that of n heptafluorobutylamine which although not showing a hysteresis loop moves towards the pressure axis.

This would indicate more is being adsorbed, or as at high relative pressures the isotherm is strongly influenced by the structure of the gel, the pore structure is collapsing. This would explain the more reasonable values of the surface area and pore radius calculated from the Kelvin equation as a balance between a collapsed pore structure and chemisorbed amine.

The chemisorption is large enough to affect the values of the saturation volumes. In fig. 66 it is obvious that the points for the amines lie above those of the other compounds. There are three possible explanations:-

1) The saturation volume is increased by some action of the amine with the gel.
2) The density at saturation is greater than in the bulk liquid.
3) There is sufficient chemisorption in the monolayer to make a correction necessary.

Number 1 is rather unlikely, as although peptising and chemical action may take place, they do not in general affect the value of the saturation volume - cf the results for silica gel. Number 2 is also unlikely, as calorimetric measurements show a small peak corresponding with the saturation value. This has been taken to be due to the destruction of the curved meniscii in the gel pores i.e. from

being under a tension the liquid reverts to normal bulk properties. It is therefore unlikely that the density would change from being below bulk liquid density to some 50% greater than bulk density in this short range. If 3 is the cause then by calculating from the other figures what quantity should be held by physical adsorption, it is possible to make an estimate of the amount held by chemisorption in the monolayer. Subtracting this from the found saturation volume should give a better estimate of the true saturation value - these new points are shown in fig. 66. As can be seen they lie very much nearer the best line for the other compounds. It is also noteworthy that the "worst" point is that of n-pentafluorobutylamine, which is in accord with the type of variation found in the isotherm.

The remainder of the isotherms appear to behave in a perfectly normal manner, and need no detailed comments.

Five isotherms were obtained on ferric oxide III (figs. 13, 17, 20, 48, 50) i.e. ethyl alcohol, βtrifluoroethanol, 2-fluoroethanol, benzene and perfluorobenzene respectively. These need little discussion at this point beyond noting that the 2-fluoroethanol gives a perfectly normal isotherm, and, if anything, the surface area obtained from the point 'A' value, is low.

General Comments

At this point it becomes necessary to look at some of the assumptions implicit in some of the formulae. Firstly the point 'A' method. Normally surface areas are estimated by obtaining point 'B' either by inspection or more often from a B.E.T. plot of equation 9. In the cases under discussion equation 9 either gave a curve rather than a straight line, or a small negative intercept. This method was discarded and the point 'A' method used instead as finding point 'B' by inspection was not always possible.

The use of point 'A' rests on the assumption that Langmuir's equation - i.e. equation 3 - can be applied to the low pressure part of the isotherm. If this is so then to a first order of accuracy point 'A' will represent the completion of the monolayer. Further confirmation comes from the internal consistency of the results for the surface area on silica gel, which is as good as obtained by Brunauer and Emmett (16) for point 'B'. Thus one can be reasonably confident in this assumption.

The other assumption in determining surface areas is implicit in Livingstone's equation, i.e. equation 11. The F factor is suspect, but only alters the ratio of the "true" area to the found area. The main cause of any scatter of results from using this equation lies in supposition that the molecules are spherical. This, as has already been

pointed out, is reasonable for carbon chains of two or three carbon atoms but becomes progressively less so for longer chains. This is well shown when benzene or perfluorobenzene is the adsorbate. These molecules are normally adsorbed with the ring horizontal to the plane of the adsorbent. Where this is the case it can be shown that benzene has an effective molecular area of about 40 sq. Å, where Livingstone's equation only predicts 30 sq. Å. In cases like this one can only use the values from Livingstone's equation as a first approximation, and must be doubtful of the results obtained for compounds containing chains of atoms, or other non-spherical molecules.

The results where benzene and perfluorobenzene were the adsorbates can now be discussed (see tables 2 and 5). The surface areas calculated from Livingstone's equation are far too low, although the saturation volumes are near the average values. However even after taking the improved value of 40 sq. Å for the effective molecular area of benzene; there is insufficient data for similar calculations on perfluorobenzene; the surface areas are still too low.

The reason for this appears to be in the assumption that the monolayer is close packed on the surface. With benzene it is quite possible that the ring needs to be attached to more than one active site. If this is so

then it will be impossible to close pack the surface as the molecules which were randomly packed to begin with, soon begin to interfere with each other. Calculations by Herington and Rideal (63) on the poisoning of metallic catalysts suggests that a hexagonal molecule would only be adsorbed to the extent of 35% of the true monolayer capacity. It would appear that cyclic molecules should not be used for surface area determinations.

The other group of isotherms that have not been discussed are those of acetone and 1:1:1 trifluoroacetone. Except for the case of silica gel/acetone the isotherms (see figs. 51, 52, 53, 54) are all irreproducible and 1:1:1 trifluoroacetone on silica with acetone on ferric oxide I not even repeatable. Consider first acetone on ferric oxide I. Above a relative pressure of ·75, the graph rises fairly steeply to a relative pressure of 1·00. Although other isotherms show such a curving portion, none continue for such a long interval of relative pressure. The reason for this curvature became obvious when it was shown in a separate set of experiments that ferric oxide is soluble in acetone. In addition it was observed that after a relative pressure of approximately ·8 the gel appeared 'wet' and at relative pressure of about ·9 liquid

could be seen in the sample tube. Thus the portion of the isotherm from ·75 upwards is the vapour pressure of a solution of ferric oxide in acetone.

Apart from its great solvent powers acetone is a quite reactive compound, in fact so much so that it is extremely difficult to prepare it in a pure form (64). These isotherms are probably another example of its readiness to polymerise, and the enhanced adsorption can be ascribed to this.

Trifluoroacetone will be even more reactive due to the inductive effect of the fluorine atoms and the isotherm shows wide variations when attempts are made to repeat it. On ferric oxide I after a relative pressure of ·07 had been reached white crystals were observed growing on the surface. These crystals were unstable at room temperature and could not be identified. It is however possible that they were trifluoroacetone condensation products.

Another point that needs consideration is that it has been postulated in this work that on repeated cycles of adsorption/desorption the original gel structure breaks down. It is for this reason that the normal method of flushing the gels with the adsorbate before determining the isotherm has not been used. It was felt that where

such a wide range of compounds were to be investigated, the advantage of displacing the last traces of adsorbed gases was less than obtaining an isotherm which reflected the "true" gel structure. Following from this when the isotherms were not reproducible all calculations were made using the first set of desorption-adsorption points.

Bearing this structure change in mind it is not surprising to find that the formula

$$r_w = \frac{2V}{\Sigma}$$

gives more internally consistent results than the pore radius calculated from the Kelvin equation. This is because the saturation volume is not appreciably affected unless there is a radical structure change, as for instance in sintering. In addition it only gives one value for the pore radius, which must be assumed to be an "average" value, although the actual pore distribution is not known.

Leaving aside the difficulties of whether bulk liquid values can be used for the constants in the Kelvin equation, there is also the necessity of making some correction for the molecules adsorbed on the pore walls. This is possible in a series of related compounds by adding onto the pore radius a factor of $\left(\frac{\sigma}{2\pi}\right)^{\frac{1}{2}}$, or if

an assumption about the orientation of the adsorbed molecule is made a calculated factor can be added. However where a diversity of compounds are considered then the errors inherent in such methods are not similar and the "corrected" values are just as scattered as before. The values obtained can however be used in broad comparisons, and are more informative than those obtained from equation 17.

However even when the various points dealt with above are considered no logical explanation for the large adsorption of 2:2:3:3 tetrafluoropropan-1-ol has been found, and further information was sought from low pressure isotherms. As 2:2:3:3 tetrafluoropropan-1-ol is a somewhat complicated molecule, the fluorinated ethanols were to be examined instead.

Low Pressure Isotherms

The low pressure isotherms of ethyl alcohol and β trifluoroethanol at 20°, 25° and 30°C on ferric oxide III are shown in figs. 14 and 18 respectively. The first and most remarkable observation was that the isotherms for β trifluoroethanol cross each other. This would imply that the adsorption process is endothermic over a part of the isotherm.

One is immediately suspicious as, if the heat of adsorption were endothermic, then one would expect a type III or V isotherm instead of the type IV that is found. The isotherms were all checked and the same results obtained. This leaves the experimental technique open to question.

The concentration figures are obtained by direct weighing. By using large quantities of adsorbent errors here are minimised. In addition no correction was made for unadsorbed vapour over the gel. The correction could be calculated for ethyl alcohol and was found to be of the order of 1% of the found concentration. The figure will presumably be similar for trifluoroethanol. As this is within the expected experimental error it is unlikely that this is the cause.

The pressure measurements are however suspect. Firstly there is the question of the calibration of the gauge. This includes an unestimated error due to thermal transpiration. Secondly there is no independent check on the low pressures measured only for the high pressure region where agreement is reasonable but not good. This is to be expected from the shape of the calibration

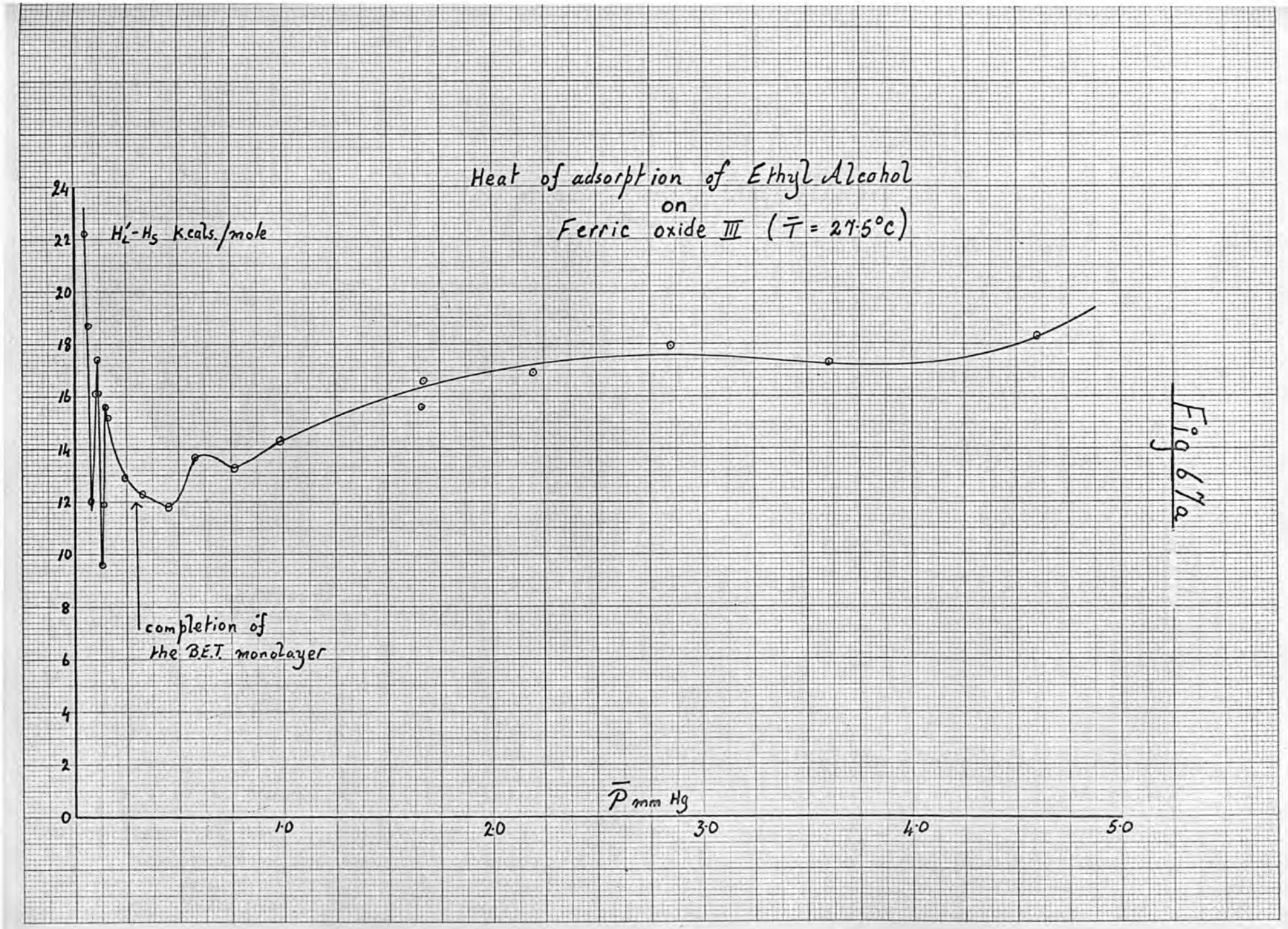
Heat of adsorption of Ethyl Alcohol
on
Ferric oxide III ($\bar{T}$ = 27·5°C)
$H'_L - H_S$ K.cals./mole
completion of the B.E.T. monolayer
$\bar{P}$ mm Hg
24
22
20
18
16
14
12
10
8
6
4
2
0
1·0
2·0
3·0
4·0
5·0

Fig 67a

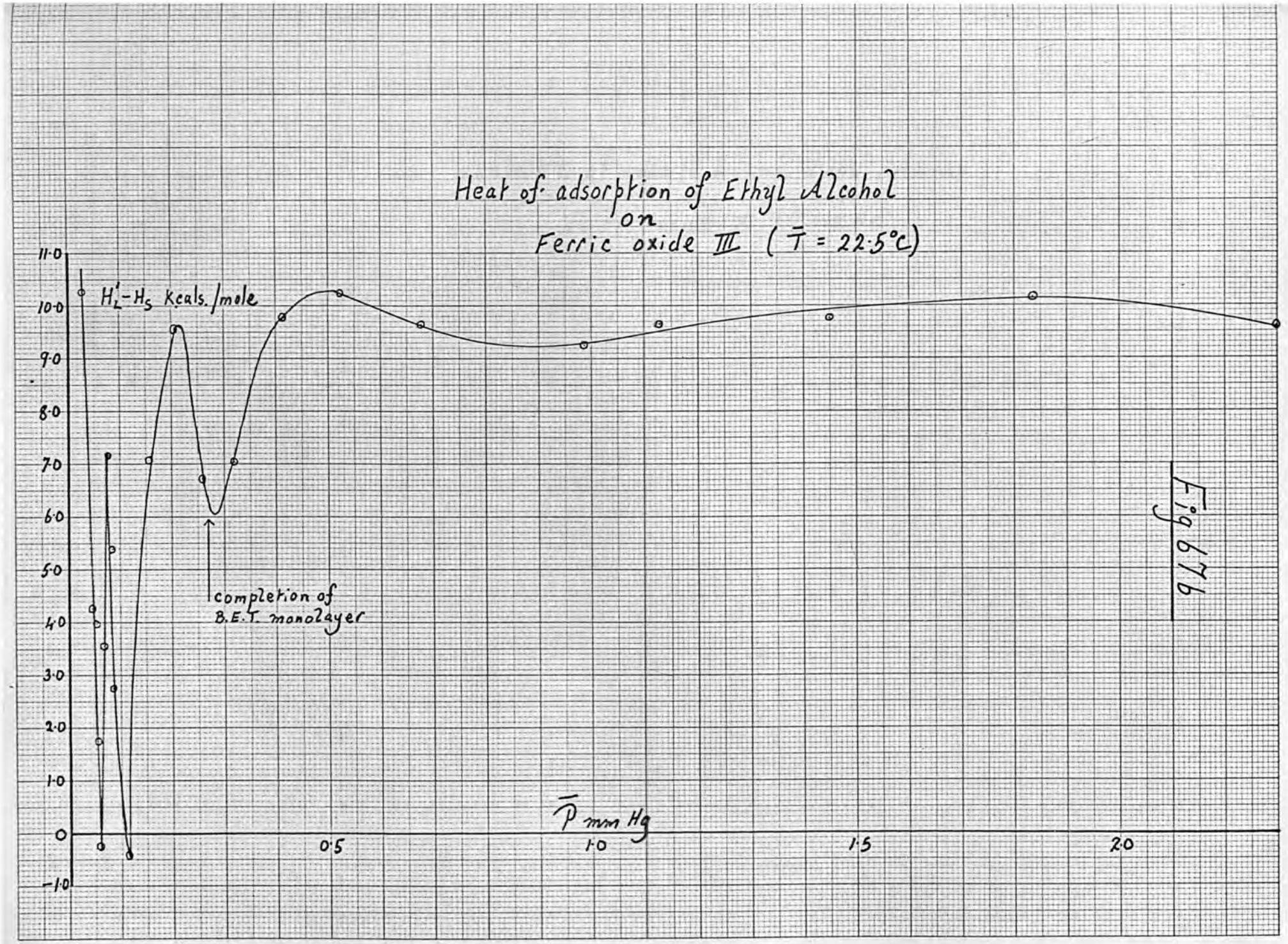
Heat of adsorption of Ethyl Alcohol
on
Ferric oxide III ($\bar{T}$ = 22·5°C)
$H'_L - H_S$ Kcals./mole
11·0
10·0
9·0
8·0
7·0
6·0
5·0
4·0
3·0
2·0
1·0
0
-1·0
completion of
B.E.T. monolayer
$\bar{P}$ mm Hg
0·5
1·0
1·5
2·0
Fig 6176

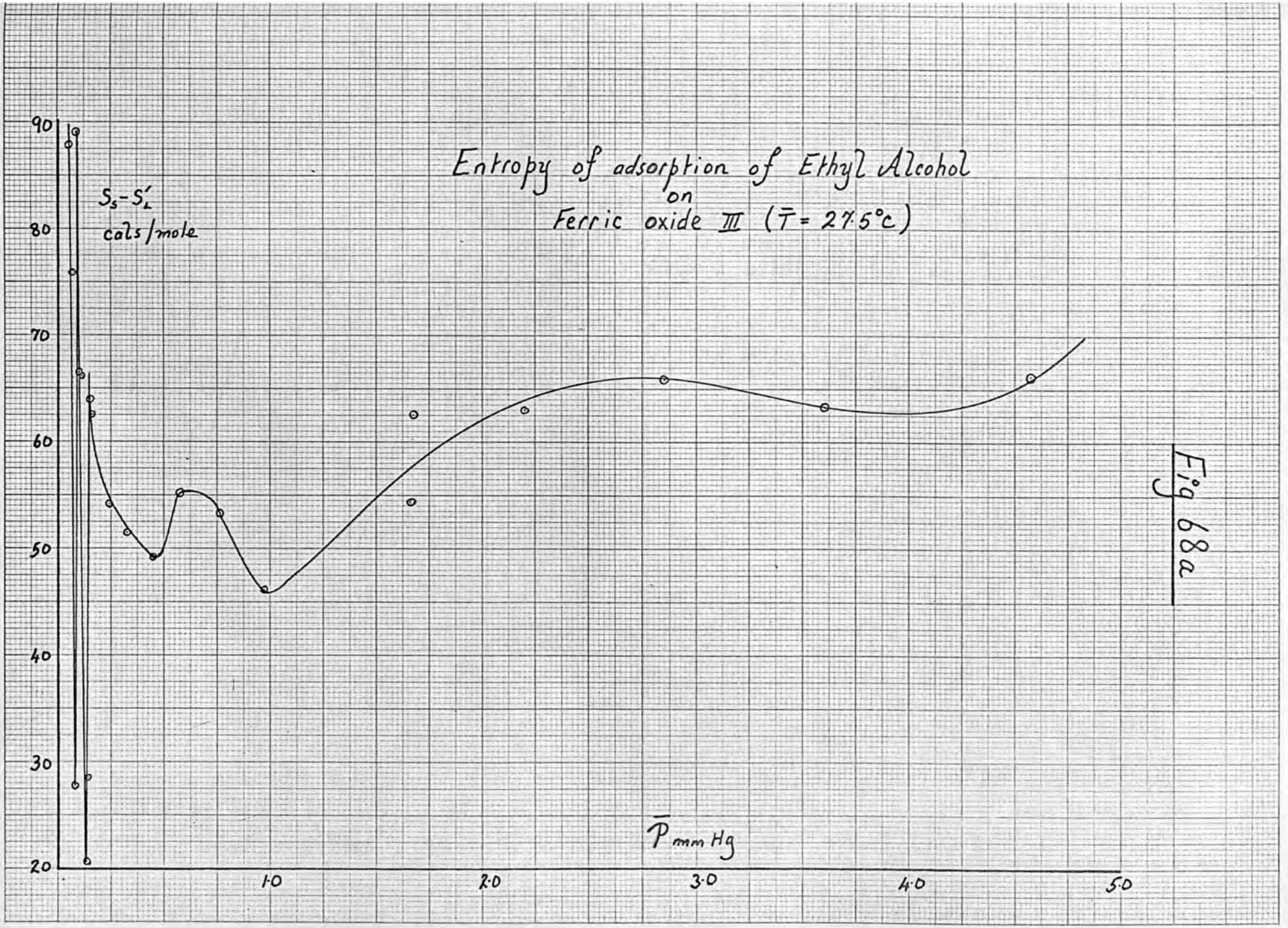
Entropy of adsorption of Ethyl Alcohol
on
Ferric oxide III ($\bar{T}$ = 27.5°C)
$S_s - S'_L$
cals/mole
90
80
70
60
50
40
30
20
1·0
2·0
3·0
4·0
5·0
$\bar{P}$ mm Hg

Fig 68a

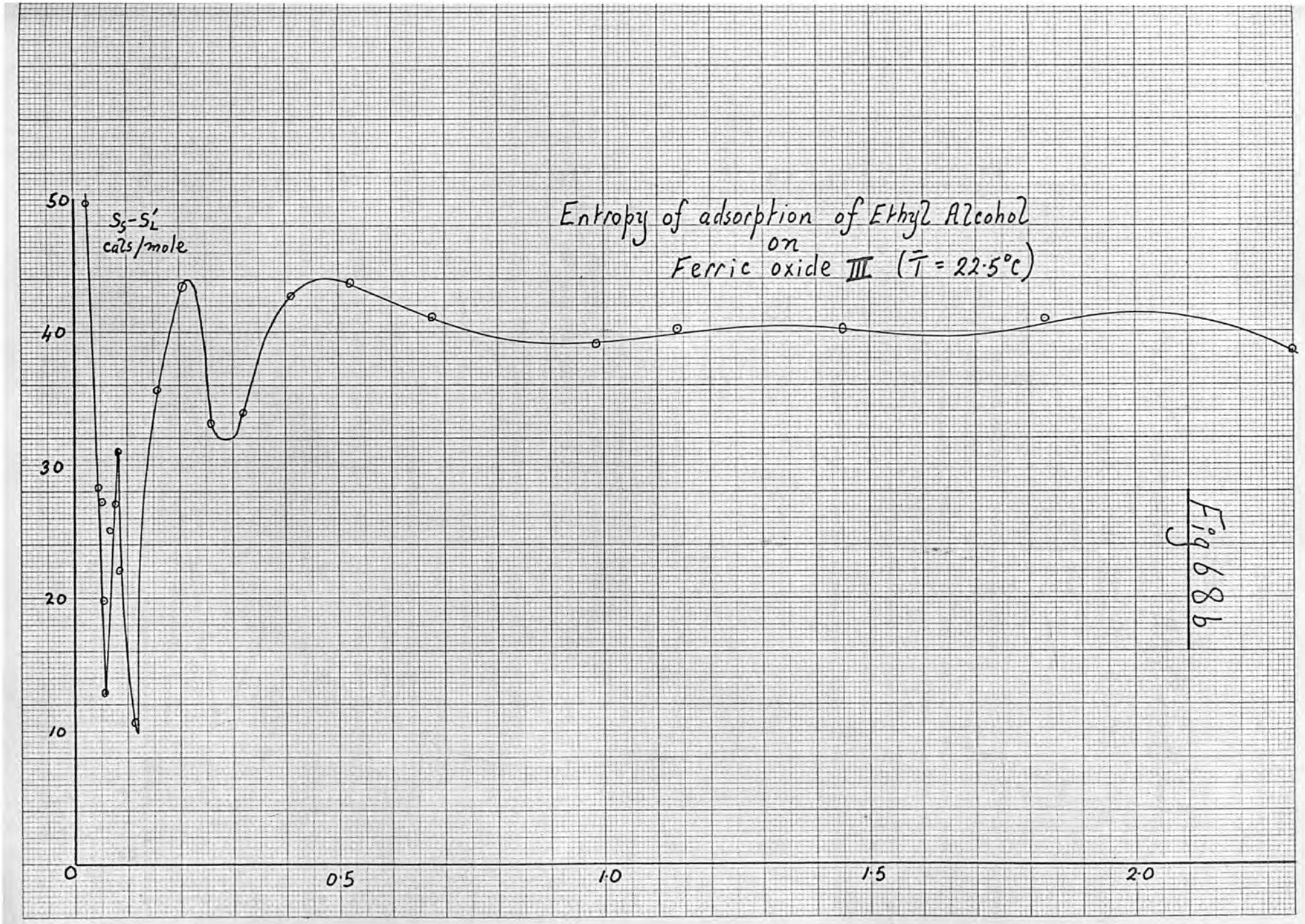
Entropy of adsorption of Ethyl Alcohol
on
Ferric oxide III ($\bar{T}$ = 22·5°C)
$S_S - S'_L$
cals/mole
50
40
30
20
10
0
0·5
1·0
1·5
2·0

Fig 68b

Fig 69a

Heat of adsorption of β trifluoroethanol on Ferric oxide III ($\bar{T}$ = 27.5°C)

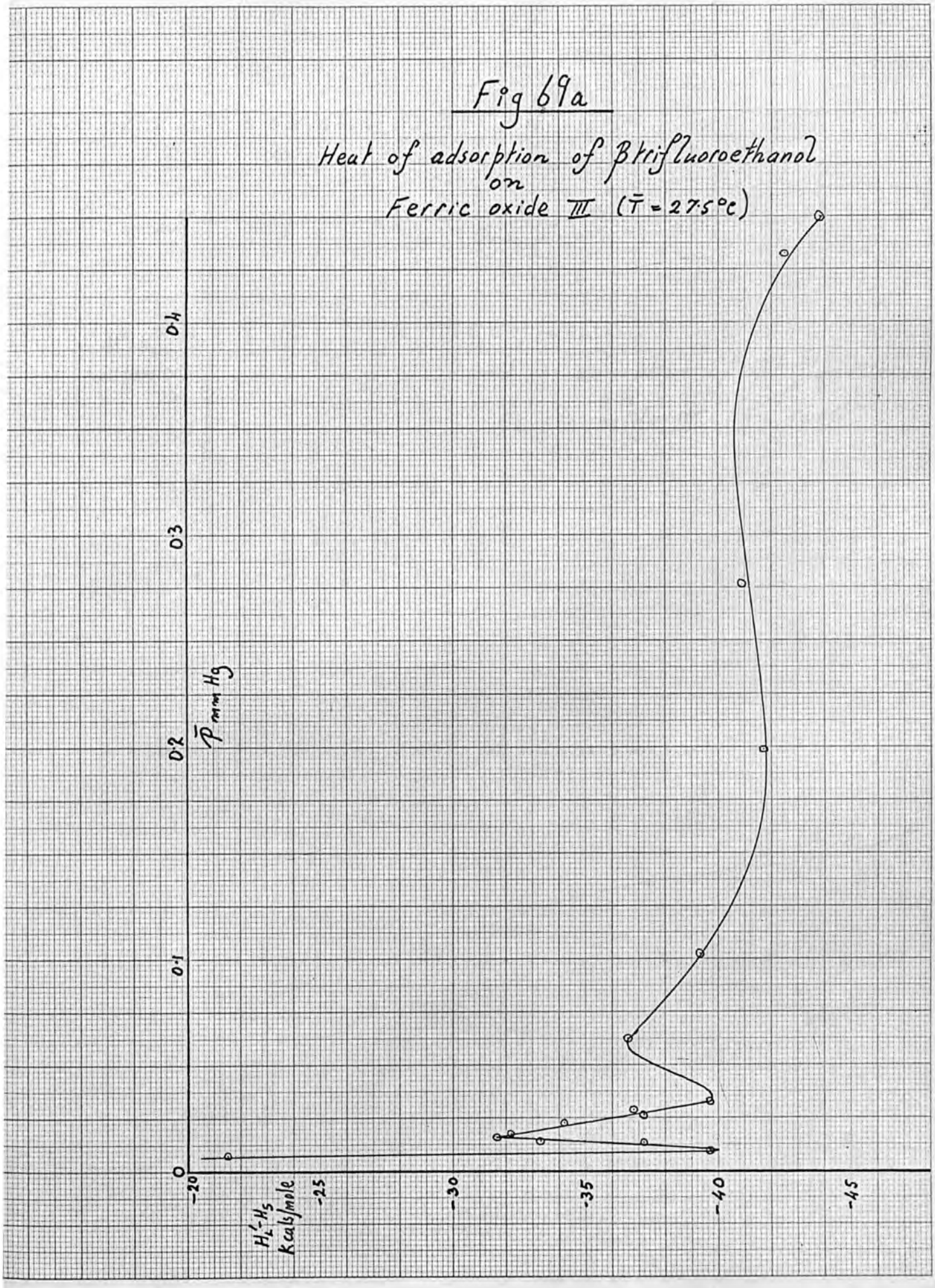

Fig 69b

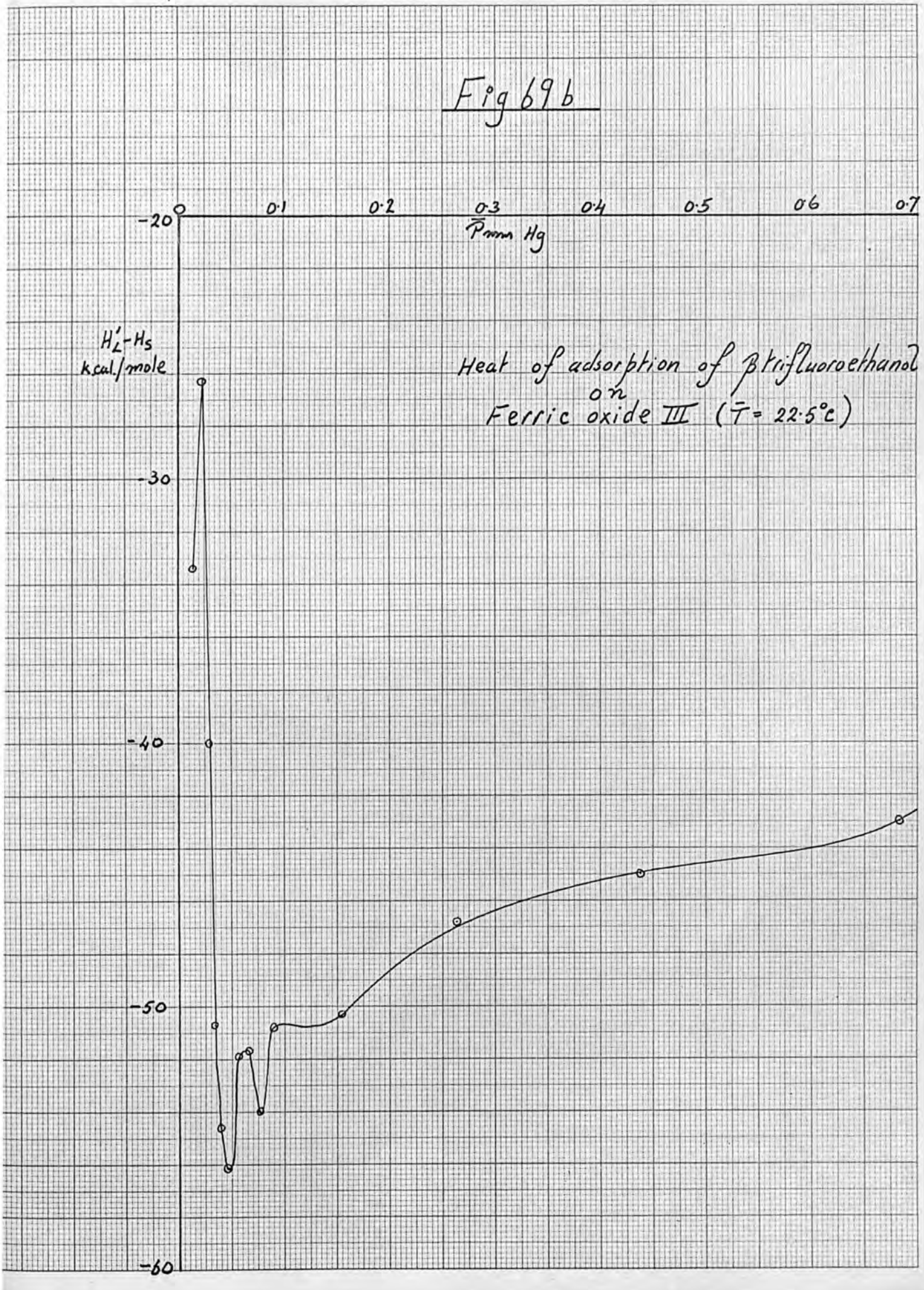
0·1
0·2
0·3
0·4
0·5
0·6
0·7
$\bar{P}$ mm Hg
-20
-30
-40
-50
-60
$H'_L - H_S$
k.cal./mole
Heat of adsorption of β trifluoroethanol
on
Ferric oxide III ($\bar{T}$ = 22·5°C)

Fig 70a

Entropy of adsorption of β trifluoroethanol on Ferric oxide III ($\bar{T}$ = 27.5°c)

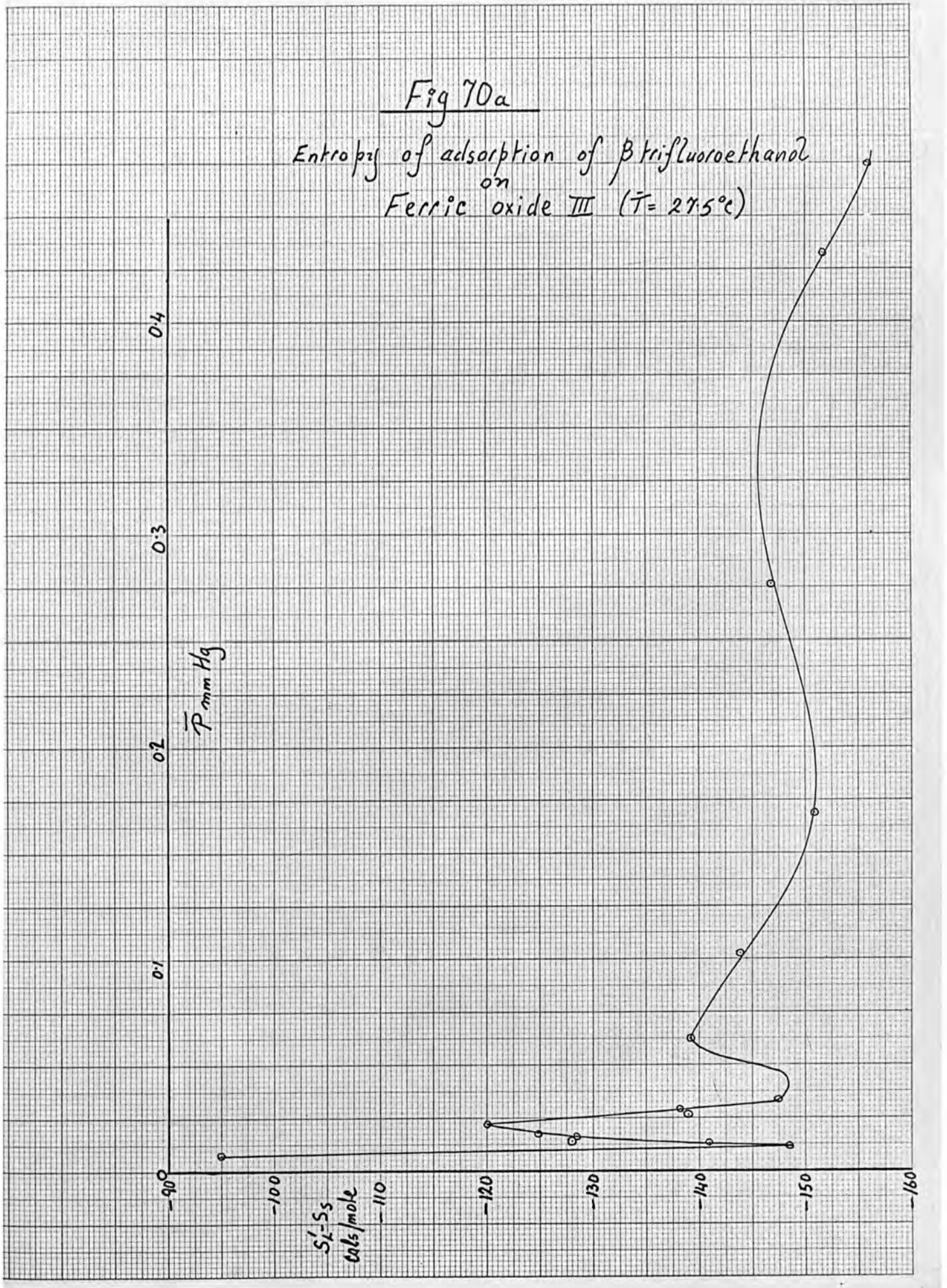

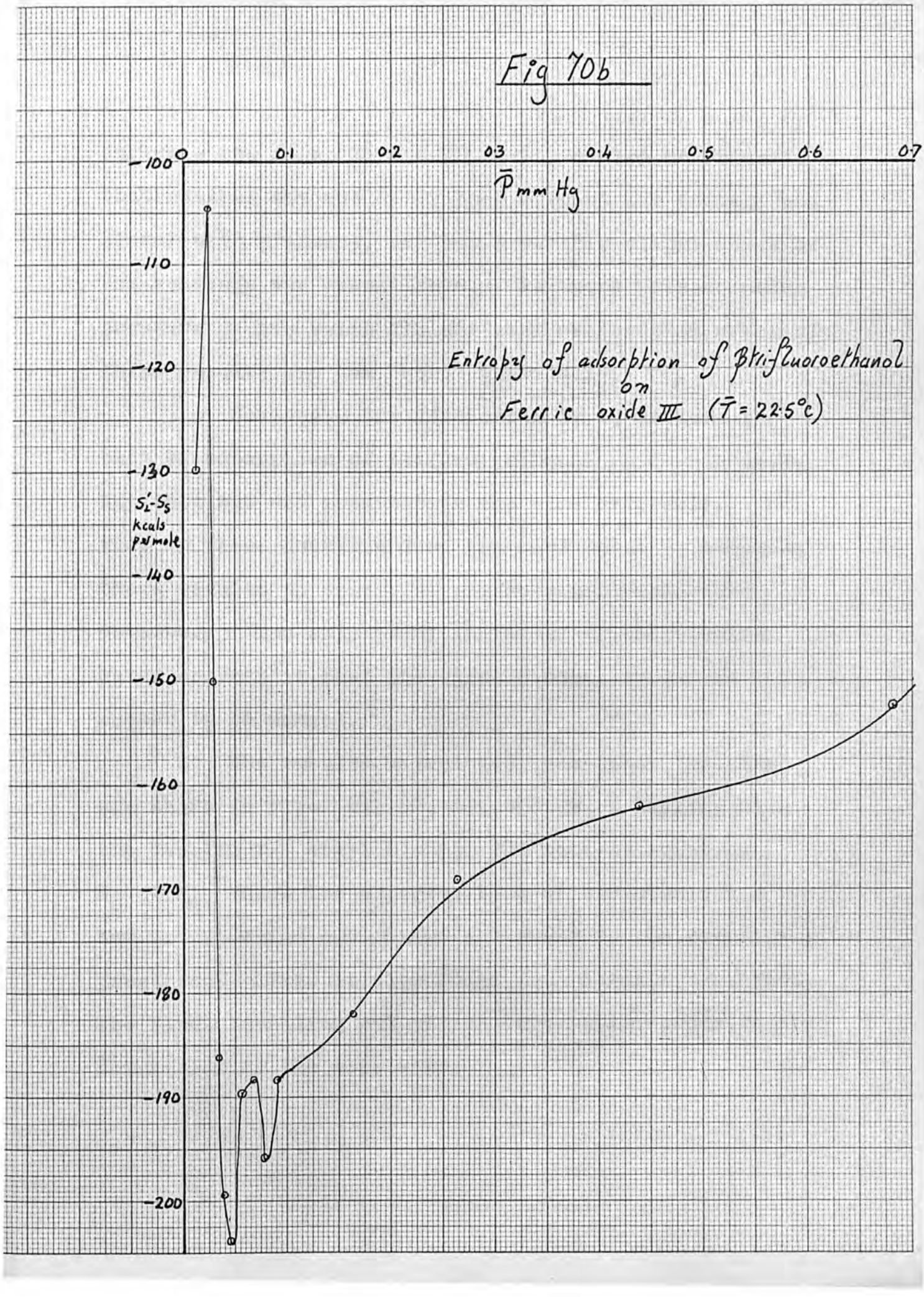
Fig 70b
0
0·1
0·2
0·3
0·4
0·5
0·6
0·7
$\bar{P}$ mm Hg
-100
-110
-120
-130
-140
-150
-160
-170
-180
-190
-200
$S_L' - S_S$
kcals
per mole
Entropy of adsorption of β tri-fluoroethanol
on
Ferric oxide III ($\bar{T}$ = 22·5°C)

curves - see figs. 74 and 75. It is also unfortunate that neither the out of balance current nor voltage was linear with pressure, so that even this slight check on the readings was unavailable. As there were no other pressure gauges which did not need calibration available these results are the "best" obtainable.

Obviously the best check is to measure the heat of adsorption of trifluoroethanol on ferric oxide but this was not possible in the time available. In view of these doubts and of the time spent in checking these results no other low pressure isotherms were obtained. The only point in favour of the results being correct is that the ethyl alcohol isotherms appear to be normal.

The results calculated from these isotherms are shown in figs. 67, 68, 69, and 70. Dealing with the results for ethyl alcohol the heat of sorption $H_L' - H_S$ shows the expected type of curve except a number of maxima and minima are found at the very lowest pressures. This is also found for β trifluoroethanol. The final levelling out of the curve corresponds to the completion of the monolayer.

Fig 78

β' vs ϕ for Ethyl Alcohol on Ferric oxide III at 25°C

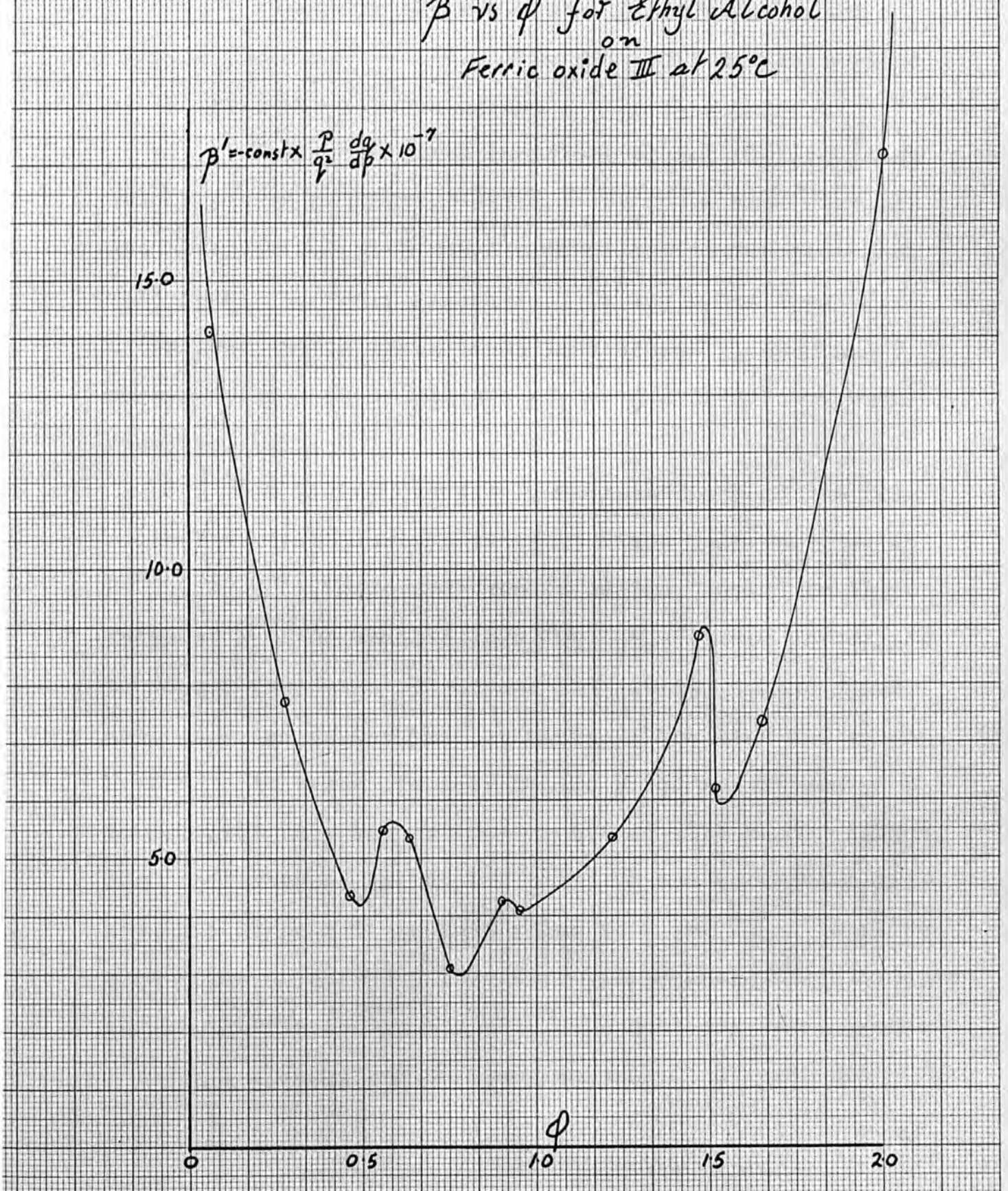

Naturally the same form is mirrored in the entropy, $S_S - S_L'$, curve. The same effects are noticed in the trifluoroethanol curves.

Again the question arises of how much reliance can be placed on these results. That the same features are observed for both ethyl alcohol and trifluoroethanol cast doubts on their validity. On the other hand inflexions and/or small peaks in the heat or entropy curves before the completion of the monolayer have been observed, (65).

If a graph showing compressability of the film against surface pressure is plotted for ethyl alcohol at 25°C (fig. 78) there are seen to be two "bumps" in the graph at φ = ·58 and 1·3 ergs./sq. cm. These correspond to vapour pressures of ·09 mm. and ·16 mm., which agree well with the values for the peaks in the heat and entropy curves. As these are only finite peaks and do not go to infinity they can not be identified with phase changes such as liquid to solid, but could be due to changes like expanded gaseous to gaseous films that are found in fatty acid films on water. This type of reasoning would explain the similarity in the shapes of the heat and entropy curves for ethyl alcohol and trifluoroethanol. At such low

Fig 71

Equilibrium function for ethyl alcohol
on
Ferric oxide III at 25°C

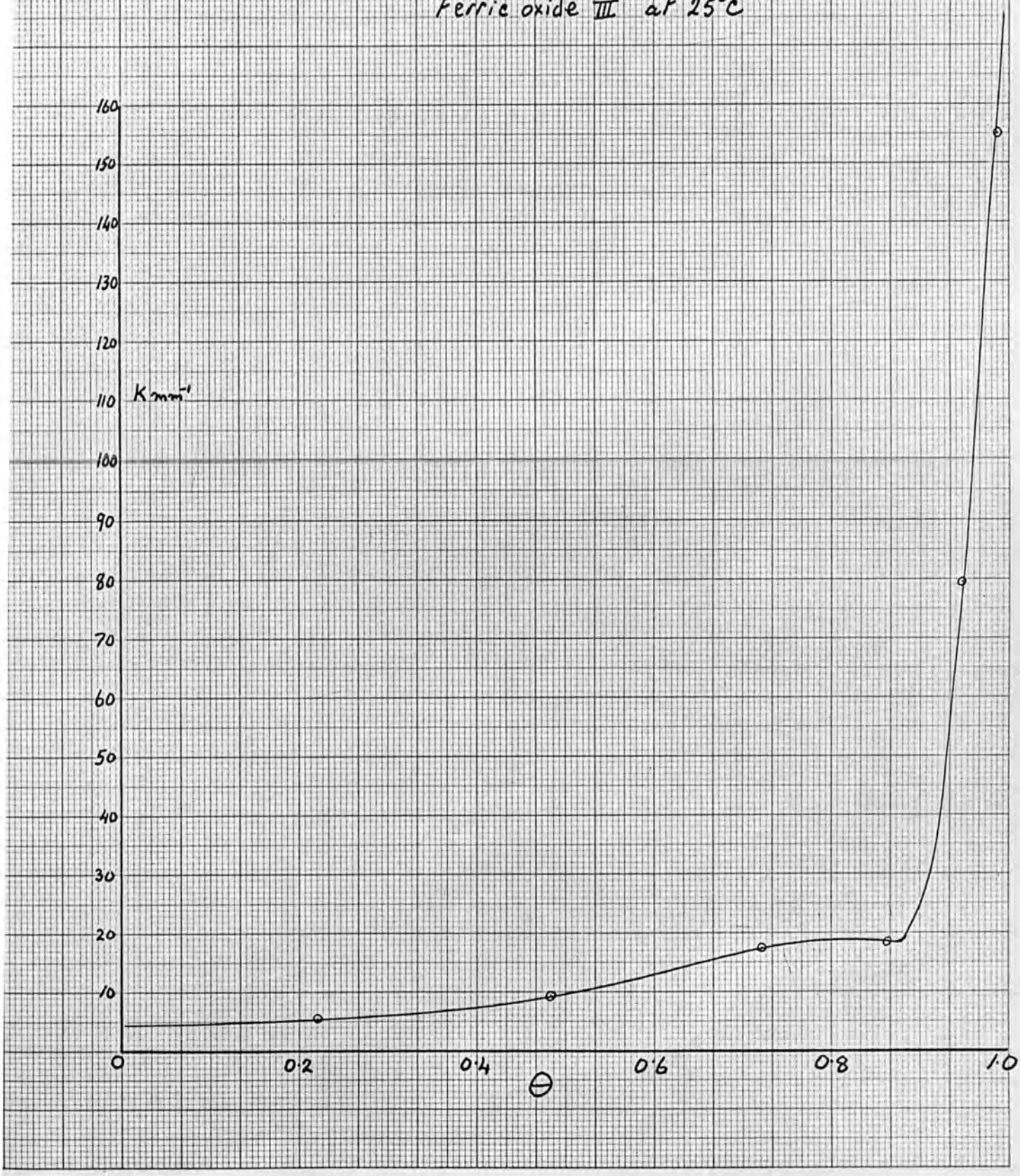

Fig 72

Equilibrium function for β trifluoroethanol on Ferric oxide III at 25°C

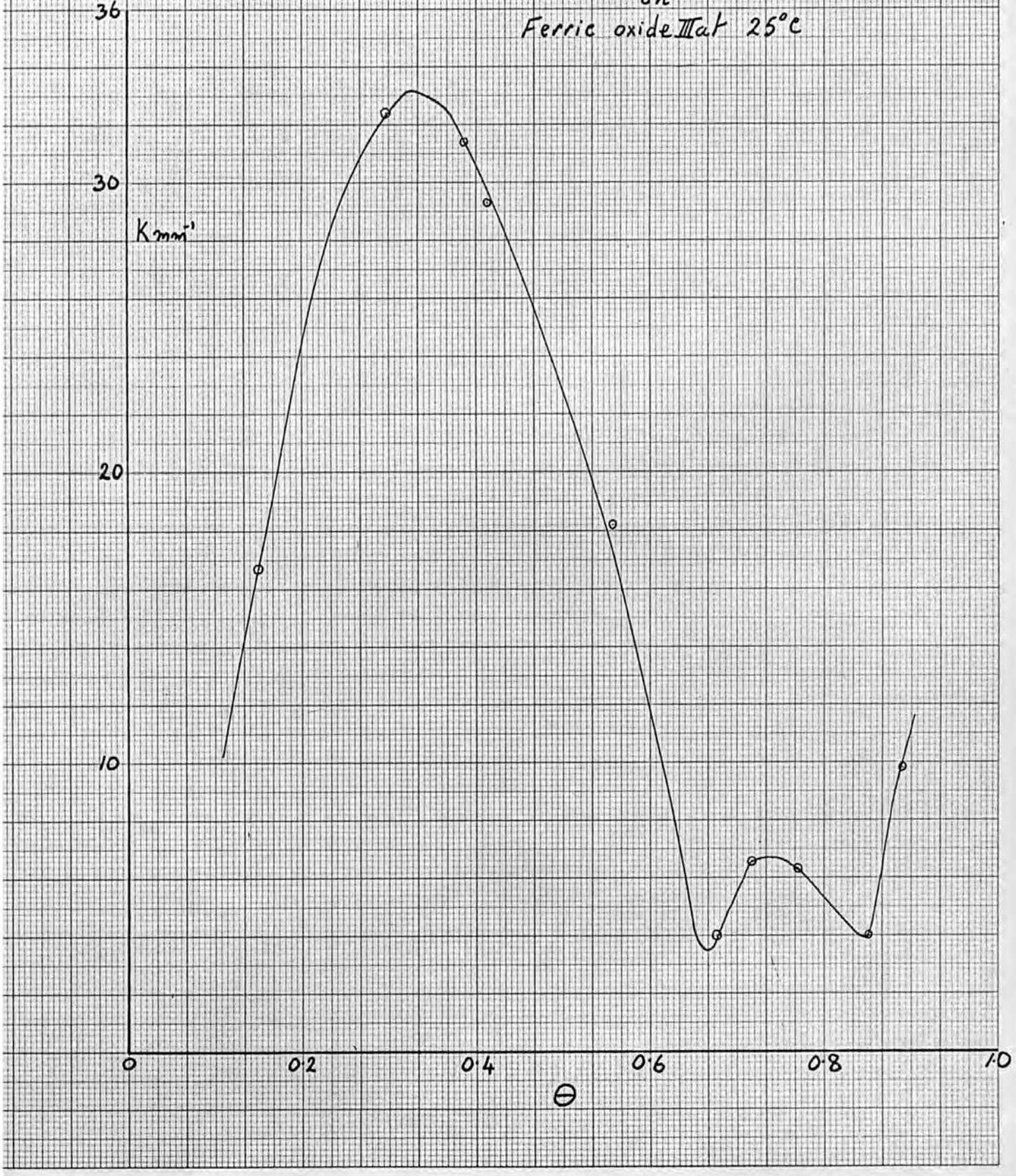

Fig 73

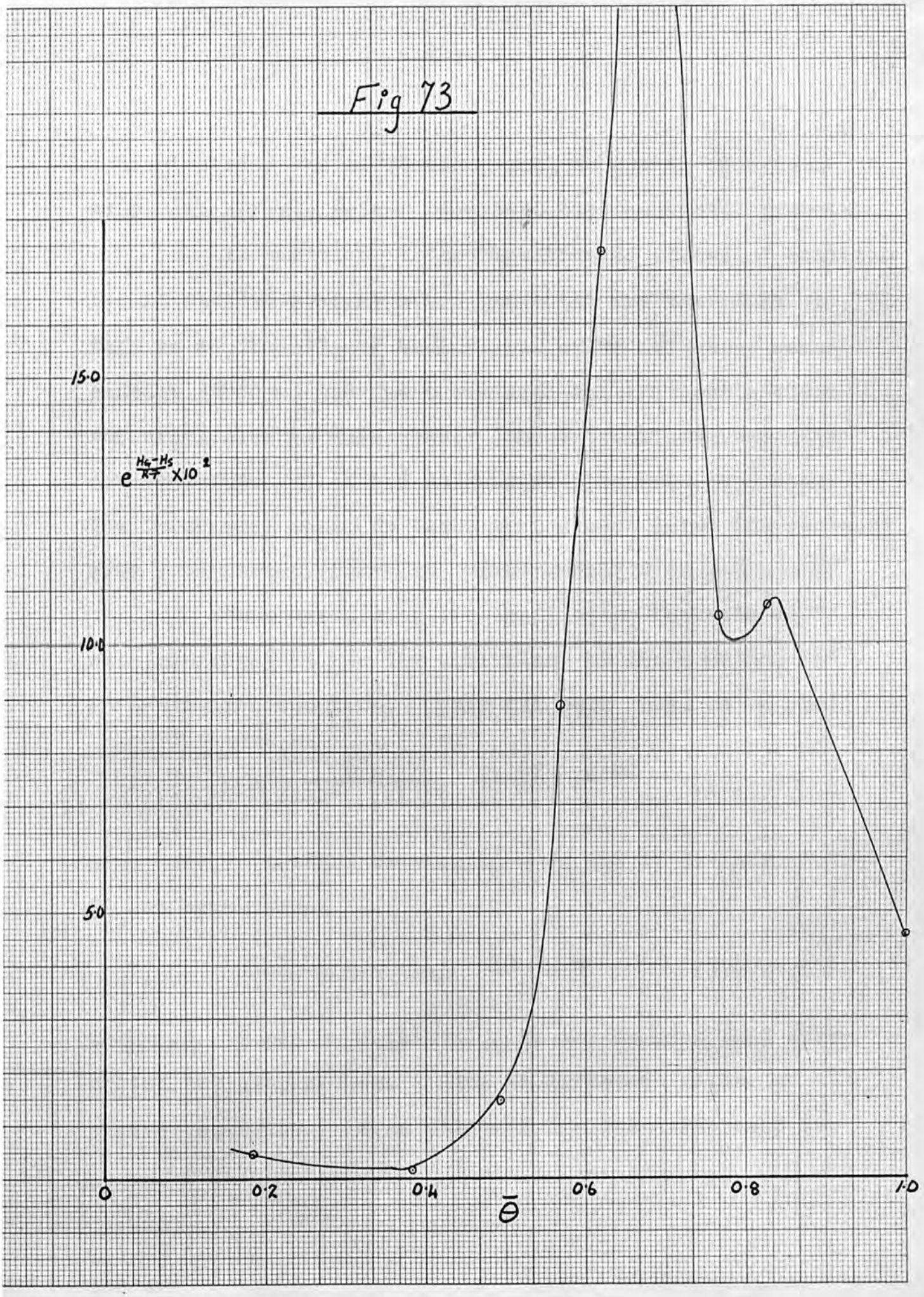

concentrations any differences will be due to adsorbate/adsorbent effects rather than adsorbate/adsorbate effects.

In addition if the "equilibrium function", equation 34, is plotted against θ for these two systems (figs. 71, 72) then it would indicate that ferric oxide III has a homogeneous surface, and there are some interactions between the ethyl alcohol molecules. The trifluoroethanol does not fall into any of the categories discussed by Graham. The large peak could be taken to indicate large interactions over a surface coverage of approximately 0 to 0.6.

When discussing the equilibrium function it was shown that it was the equivalent of the constant 'b' in Langmuir's equation. This has been shown to be (44)

$$b = \frac{h^3}{(2\pi m)^{3/2} (kT)^{5/2}} \frac{fa\,(T)}{fg\,(T)} e^{q/kT} \qquad (35)$$

if q here is identified with $H_S - H_G$ and it is assumed that 35 can be written

$$b = \text{const. exp.} \frac{H_S - H_G}{R\bar{T}} \qquad (37)$$

then fig. 73 can be obtained. It can be seen that each of the two graphs shows a peak at different values of surface coverage. Even allowing for the difference in

temperature and the various approximations in the calculation it is obvious that $H_S - H_G$ cannot be identified with q in equation 35.

This suggests that as the partition function for the vapour should remain constant, then the partition function of the adsorbed molecules must vary with increasing adsorption. This should provide an explanation for the negative heats of sorption found, whilst still showing a type IV isotherm. One could imagine the molecules adsorbing on the surface and then interacting in some way that would affect the partition function, this interaction being possible by drawing heat from the thermostat.

It is pointless to speculate any further until the low pressure results can be checked, preferably by calorimetry. If, then, they were shown correct, perhaps spectroscopy could be used to gain further information on the state of the adsorbed molecules which would either contradict or confirm the above reasoning.

Final Summary

The isotherms of twenty-two adsorbates have been examined on ferric oxide, twenty-four on silica gel. In the main they all resemble type IV isotherms and most

of them have hysteresis loops. It is noted that in a number of cases the isotherm moves on repeated adsorption and desorption and two causes are suggested, viz. 1) progressive chemisorption takes place during the experiment; 2) the gel structure is broken down by solvent action.

The isotherms of benzene and perfluorobenzene show a very low point 'A' value from which it is suggested that they lie parallel to the surface and cover more than one site.

But taken all together the isotherms of the hydrocarbons seem to be strictly comparable to those of the corresponding fluorocarbons. This is rather a disappointing observation as it had been hoped that the substitution of fluorine for hydrogen would affect the mode of adsorption, whereas the main effect would seem to be to activate or depress the chemical activity of the functional group in the molecule.

The main exception to this is n-3:3:2:2 tetrafluoropropanol on ferric oxide, but no reason can be given for the large adsorption obtained. It may be tentatively suggested, if the low pressure work of β trifluoroethanol is found to be valid, that there is a similar co-operative effect among the tetrafluoropropanol molecules, but now it extends further than the first layer

of adsorbed molecules, and is far stronger.

However these low pressure results need checking, preferably by an independent method. Adsorption, where the net effect is to take up heat from the surroundings is rare and no previous case has been reported where this has been associated with a type I or IV isotherm. One also notes that the heats of adsorption for ethyl alcohol determined by this method are rather higher than would have been expected.

If these results are valid then the peaks in the heat curves at very low pressures can be explained as phase changes of the type that are observed with surface films on liquids e.g. expanded gaseous to gaseous. That they appear in both the ethyl alcohol and trifluoroethanol curves would argue the importance - and incidentally the homogenaity - of the ferric oxide surface. Some support for the validity of these results comes from Graham's method of plotting the equilibrium function against the surface coverage.

The internal consistency of using Point 'A' to represent the completion of the statistical monolayer was noted, and these results are presented, together with those for the saturation volumes, graphically for ease of comparison.

APPENDIX

Table I

Adsorbate	T°C	Density D_4^T	Surface Tension γT	Effective Molecular Area $A^{\circ 2}$
Ethylalcohol	25	•7852	21•9	23•0
βTrifluoroethanol	25	1•381+	21•2+	26•6
βmonofluoroethanol	25	1•171+	32•3+	22•0
n propanol	25	•7998	23•4	27•2
3:3:3:2:2:pentafluoro-propan-1-ol	25	1•341+	$17•2_5$+	35•5
3:3:2:2 tetrafluoro-propan-1-ol	25	1•477	14•1	30•6
n butanol	25	•8057	24•2	31•2
4:4:4:3:3:2:2 hepta-fluorobutan-1-ol	25	1•533+	14•7+	39•4
Ethylacetate	25	•8945	23•1	32•6
Ethyltrifluoroacetate	25	1•180+	11•6+	37•3
Ethyl propionate	25	•8845	23•5	36•3
Ethyl pentafluoro-propionate	25	1•186+	20•7+	45•4
n-propylamine	0	•7117	21•4+	29•5
n-3:3:3:2:2 pentafluoro-popylamine	0	1•431+	18•6+	33•9
n-butylamine	25	•7369	23•7	26•0
n-4:4:4:3:3:2:2 hepta-fluorobutylamine	25	1•487+	16•0	40•0
Benzene	25	•8738	28•3	30•6
Perfluorobenzene	25	1•606+	23•3	21•2
Acetone	0	•8125	26•1	25•5
1:1:1 trifluoroacetone	0	1•207+	-	31•4
Acetic acid	25	1•043	27•3	22•8
Trifluoroacetic acid	25	1•478+	16•3+	27•7

+ Personal measurements. Other constants are the averages of the best literature values.

Table II
Data for silica gel

Adsorbate	Pt. 'A' mg/gm	Saturation Value mg/gm	Saturation Volume mm^3/gm	Surface Area $cm^2/gm. \times 10^6$	p_i/p_o	r_k Å	r_w Å
Ethanol	125	550	700	3·76	·635	23·3	36·4
βTrifluoroethanol	237	955	692	3·80	·639	28·6	35·4
βmonofluoroethanol	190	755	645	3·94	·519	23·6	33·4
n-propanol	153	555	694	4·17	·536	21·3	36·0
3:3:3:2:2 pentafluoropropan-1-ol	272	865	645	3·88	·678	31·0	33·4
3:3:2:2: tetrafluoropropanol	212	966	654	2·96	·473	22·8	34·0
n-butanol	165	530	658	4·18	·594	37·6	34·2
4:4:4:3:3:2:2 heptafluorobutan-1-ol	330	995	649	3·92	·541	27·45	33·6
Ethyl acetate	152	640	715	3·39	·402	20·2	39·2
Ethyl trifluoroacetate	213	818	693	3·80	·507	16·5	35·4
Ethyl propionate	138	536	606	2·96	·412	27·0	31·4
Ethyl pentafluoropropionate	261	868	732	3·71	·466	34·1	38·0
n-propylamine	173	520	731	5·11	·501	25	38·0
n-3:3:3:2:2 pentafluoropropylamine	364	835	584	4·98	·487	25·2	30·2
n-butylamine	190	575	780	4·07	·522	31·9	40·4
n-4:4:4:3:3:2:2 heptafluorobutylamine	432	1030	693	5·25	·509	28·1	36·0
Acetone	121	566	697	3·24	·479	20·4	36·2
1:1:1 trifluoroacetone	390	-	-	6·58	-	-	-
Acetic acid	175	720	690	4·00	·344	11·9	35·8
trifluoroacetic acid	238	918	621	3·48	·348	9·6	32·2
Benzene	34	585	670	·80	·453	28·3	34·8
Perfluorobenzene	39	1160	722	·33	·430	22·7	37·4

Fig 61

Surface area plot for Silica gel

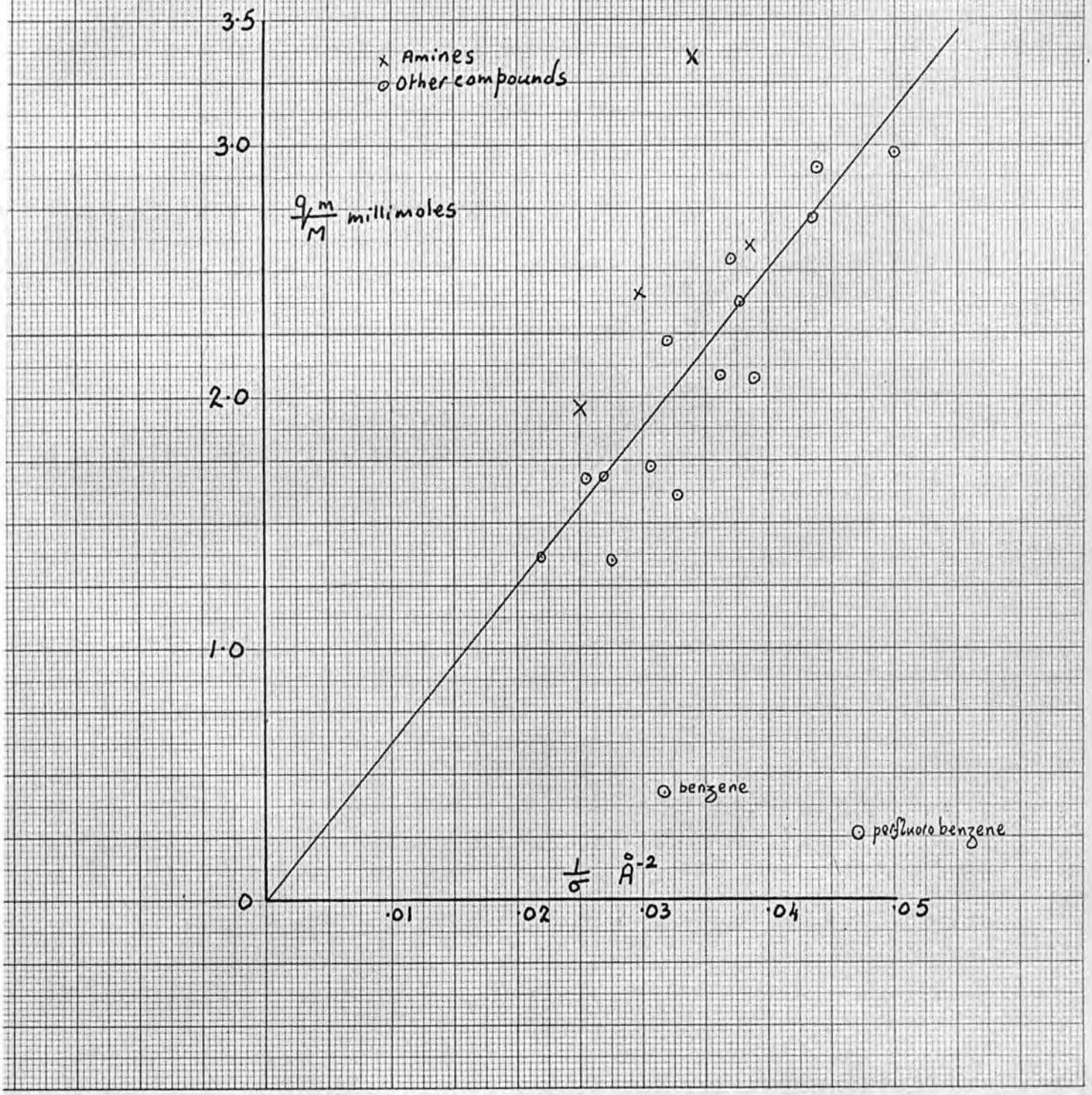

Fig 62

Saturation value plot for Silica gel

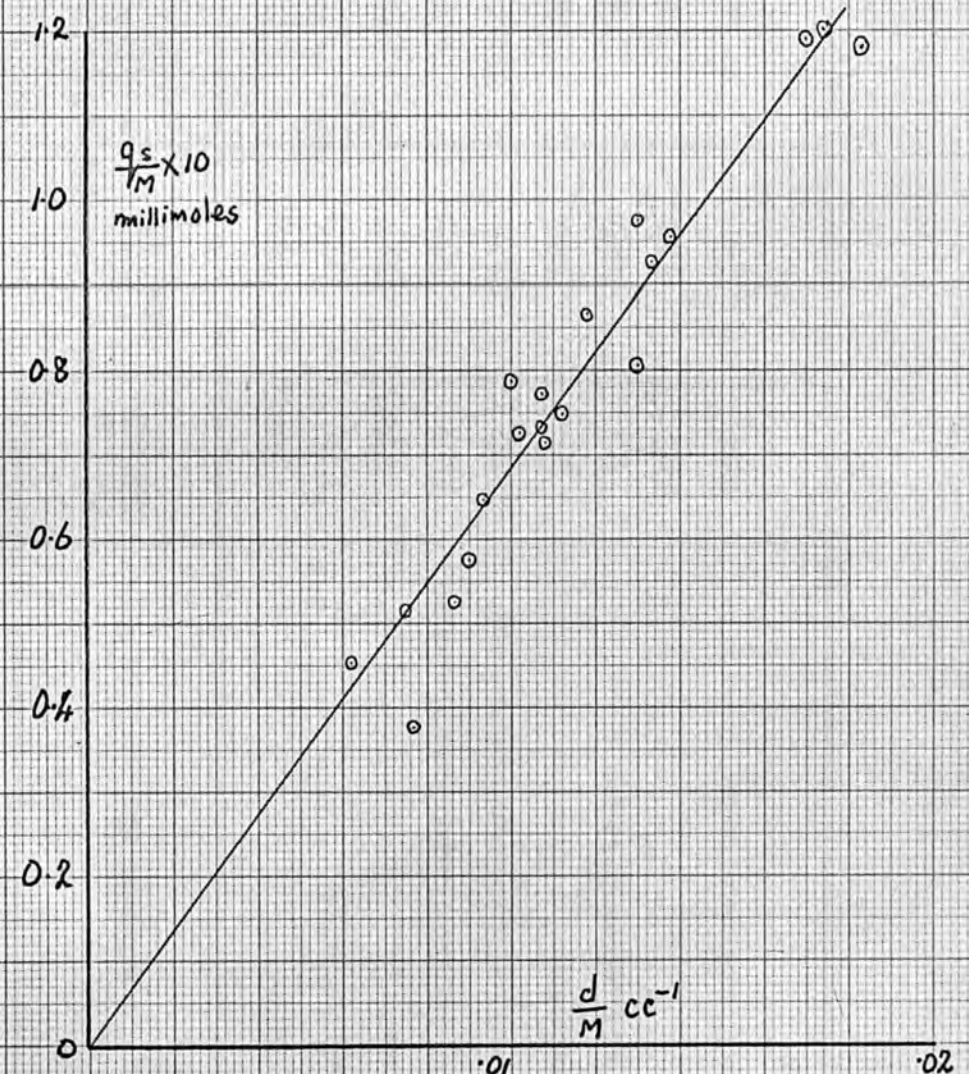

Table III

Data for ferric oxide I

Adsorbate	Pt. 'A' mg/gm	Saturation Value mg/gm	Saturation Volume mm^3/gm	Surface Area $cm^2/gm \times 10^5$	p_i/p_o	r_k Å	r_w Å
Ethyl alcohol	50.5	304	387	15.2	.732	34.0	50.6
βtrifluoroethanol	116	520	377	18.6	.833	35.3	51.8
n-propanol	77.5	317	396	15.4	.625	28.2	51.8
3:3:3:2:2 pentafluoropropan-1-ol	143	555	413	20.4	.651	31.0	54.0
3:3:2:2 tetrafluoropropan-1-ol	1110	1526	1033	155	.548	28.9	135
Ethyl acetate	69	340	380	15.4	.560	31.9	49.6
Ethyl trifluoroacetate	95	465	394	15.0	.569	17.7	51.4
Acetone	140	320	394	37.3	.337	10.2	51.4
1:1:1 trifluoroacetone	630	-	-	106.4	-	-	-

Fig 63

Surface area plot for Ferric oxide I

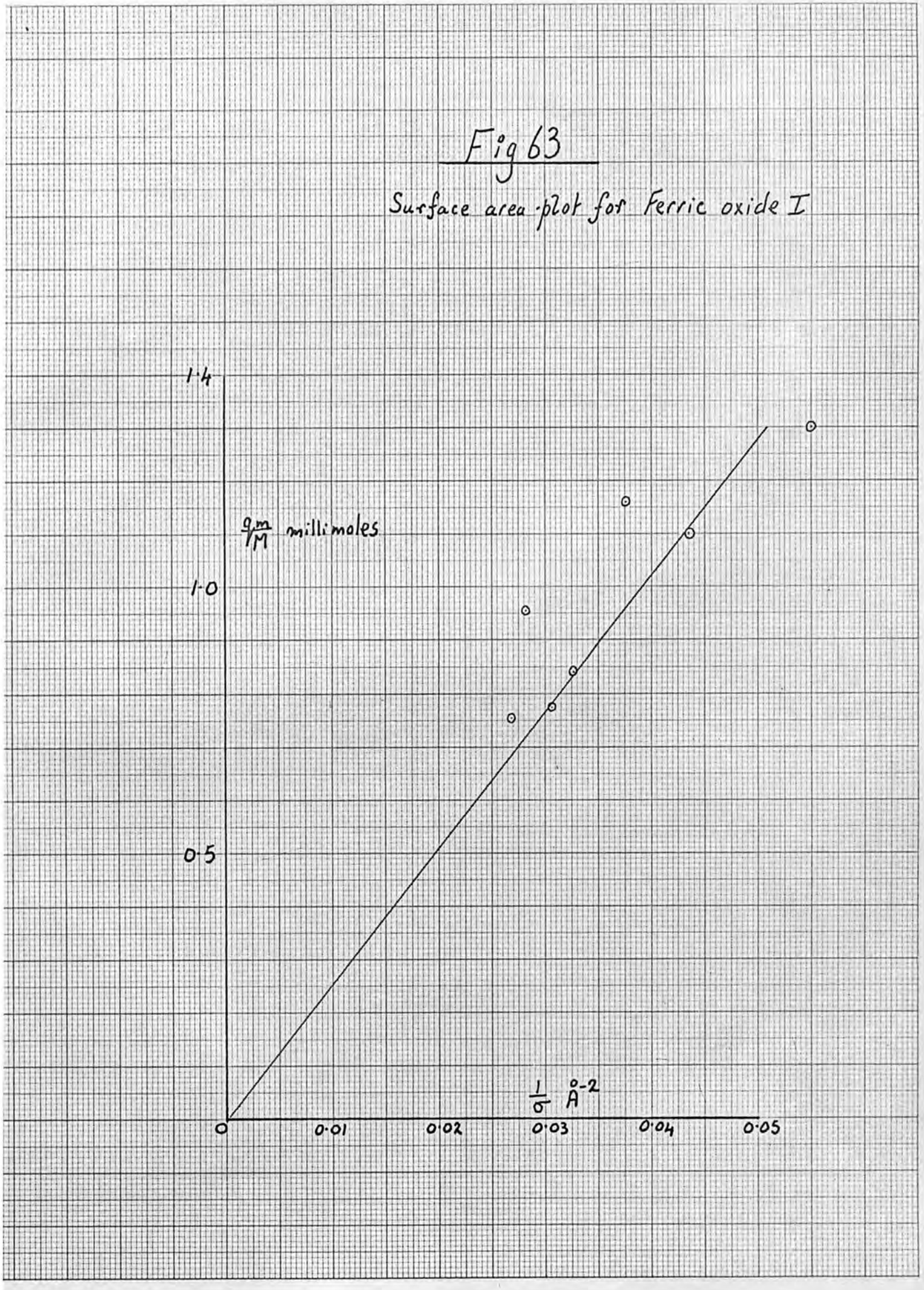

Fig 64

Saturation value plot for Ferric oxide I

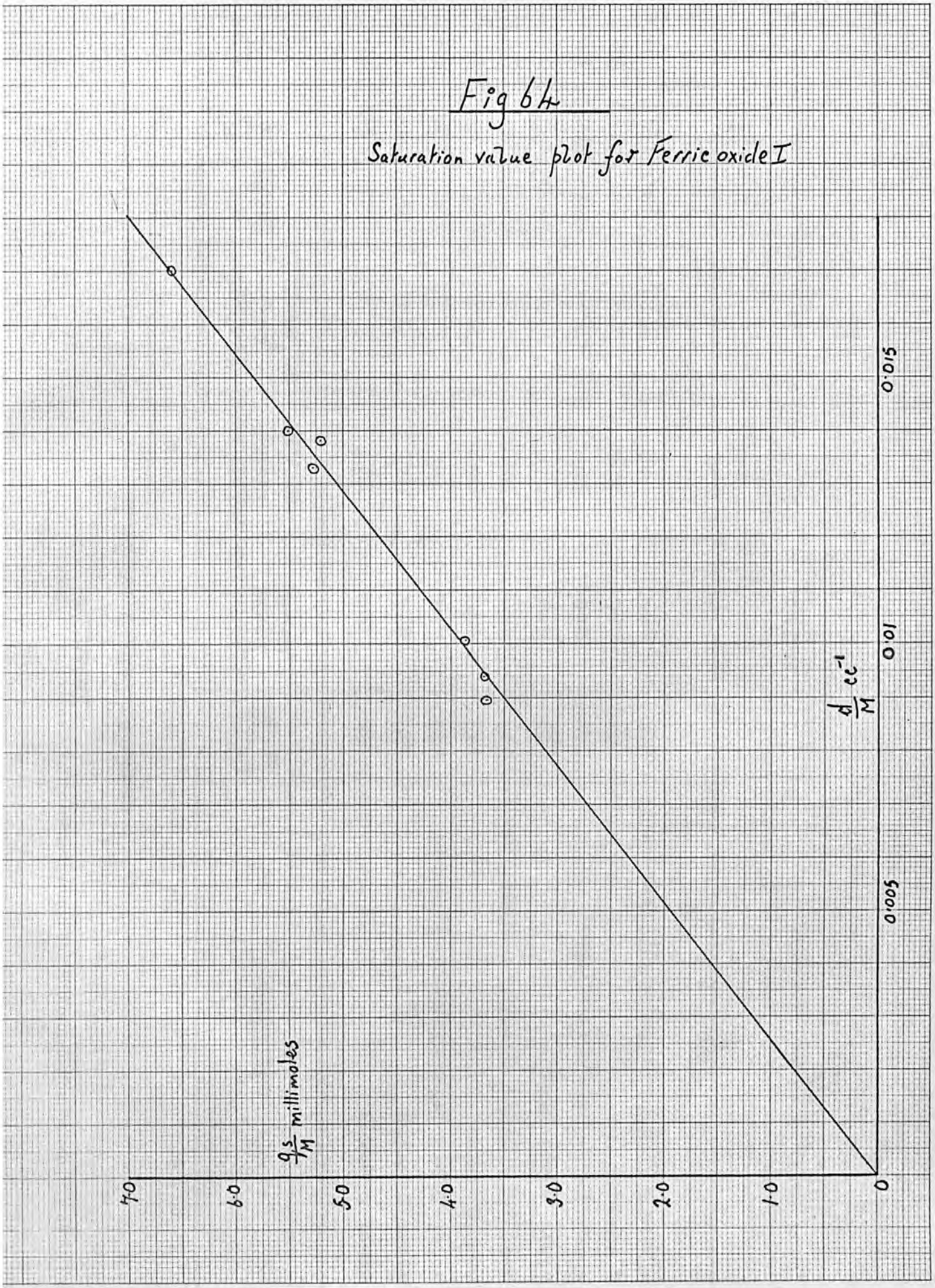

Table IV

Data for ferric oxide II

Adsorbate	Pt. 'A' mg/gm	Saturation Value mg/gm	Saturation Volume mm^3/gm	Surface Area $cm^2/gm, x10^6$	p_i/p_o	r_k Å	r_w Å
Ethyl alcohol	42	175	223	1·26	·513	15·2	37·8
n-propylamine	129	231	325	3·81	·225	10·1	51·6
n-3:3:3:2:2 pentafluoropropylamine	236	415	290	3·22	·243	12·1	46·0
n-butylamine	123	195	265	3·32	·131	9·3	42·0
n-4:4:4:3:3:2:2 heptafluorobutylamine	235	430	289	2·84	·356	16·8	46·0
Ethyl propionate	50	176	199	1·07	·229	15·0	31·6
Ethyl pentafluoropropionate	79	268	226	1·13	·284	20·0	35·8
n butanol	80	166	206	2·03	·344	16·9	32·6
4:4:4:3:3:2:2 heptafluorobutan-1-ol	148	257	233	1·76	·330	15·3	37·0

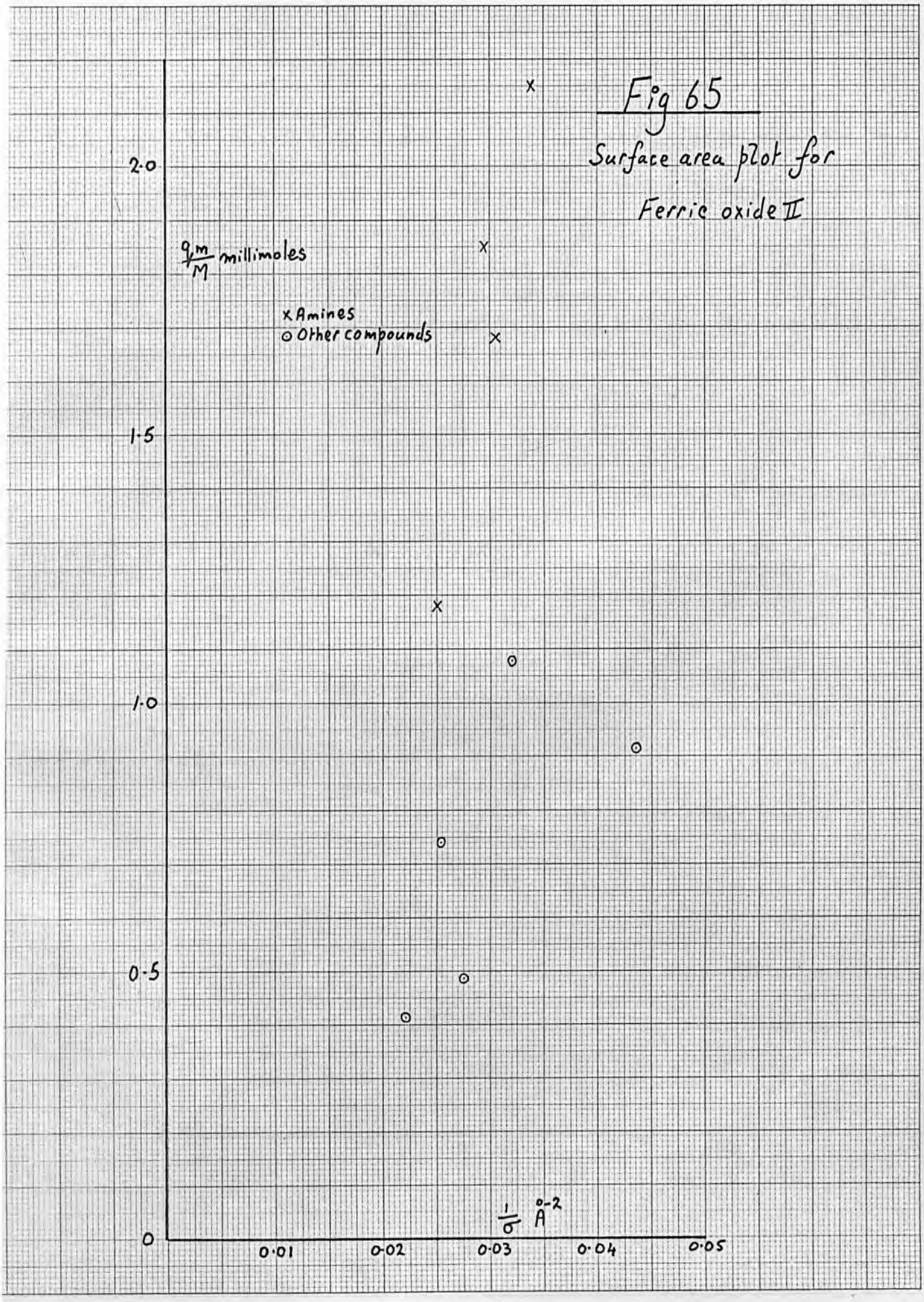
Fig 65
Surface area plot for
Ferric oxide II
2·0
1·5
1·0
0·5
0
$\frac{g_m}{M}$ millimoles
x Amines
⊙ Other compounds
$\frac{1}{\sigma}$ A^{0-2}
0·01
0·02
0·03
0·04
0·05

Fig 66

Saturation value plot for Ferric oxide II

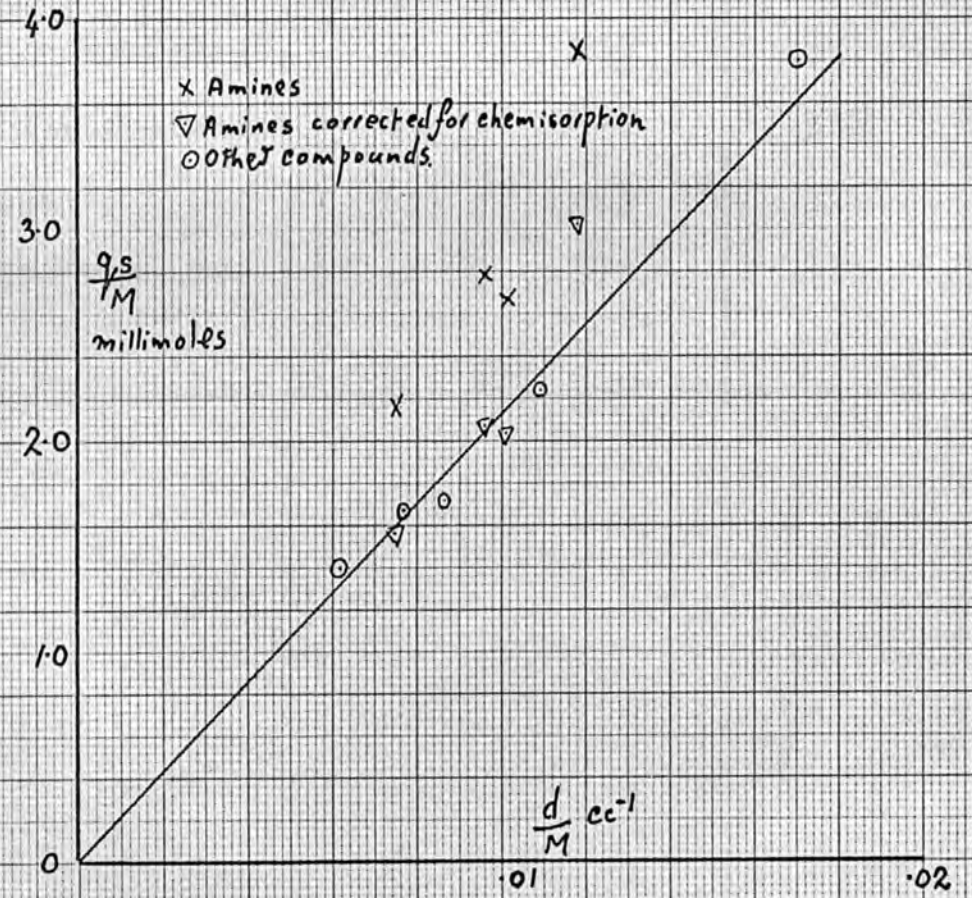

Table V

Data for ferric oxide III

Adsorbate	Pt. 'A' mg/gm	Saturation Value mg/gm	Saturation Volume mm^3/gm	Surface Area $cm^2/gm. x10^5$
Ethyl alcohol	50	283	361	15•1
βTrifluoroethanol	97	480	347	15•5
βmonofluoroethanol	64	392	335	13•3
Benzene	33	283	324	7•8
perfluorobenzene	71	570	355	4•9

Table VI

Boiling Points of compounds XR

R \ X	CF_3-	HCF_2-	H_2CF-	H_3C-
-CH_2OH	74°C	96°C	103°C	78°C
-$CH_2.CH_2OH$	100-1	28°/12 mm.	127	98
-CF_2CH_2OH	81	106	-	-
-COOH	72	134	132	108
-CF_3	- 79-8	-48°	-26	-47
=CF_2	-	$CF=CF_2$ -76	$HCF=CF_2$ -51	$H_2C=CF_2$ -82

Fig 74

Low pressure calibration curve
for
Ethyl Alcohol

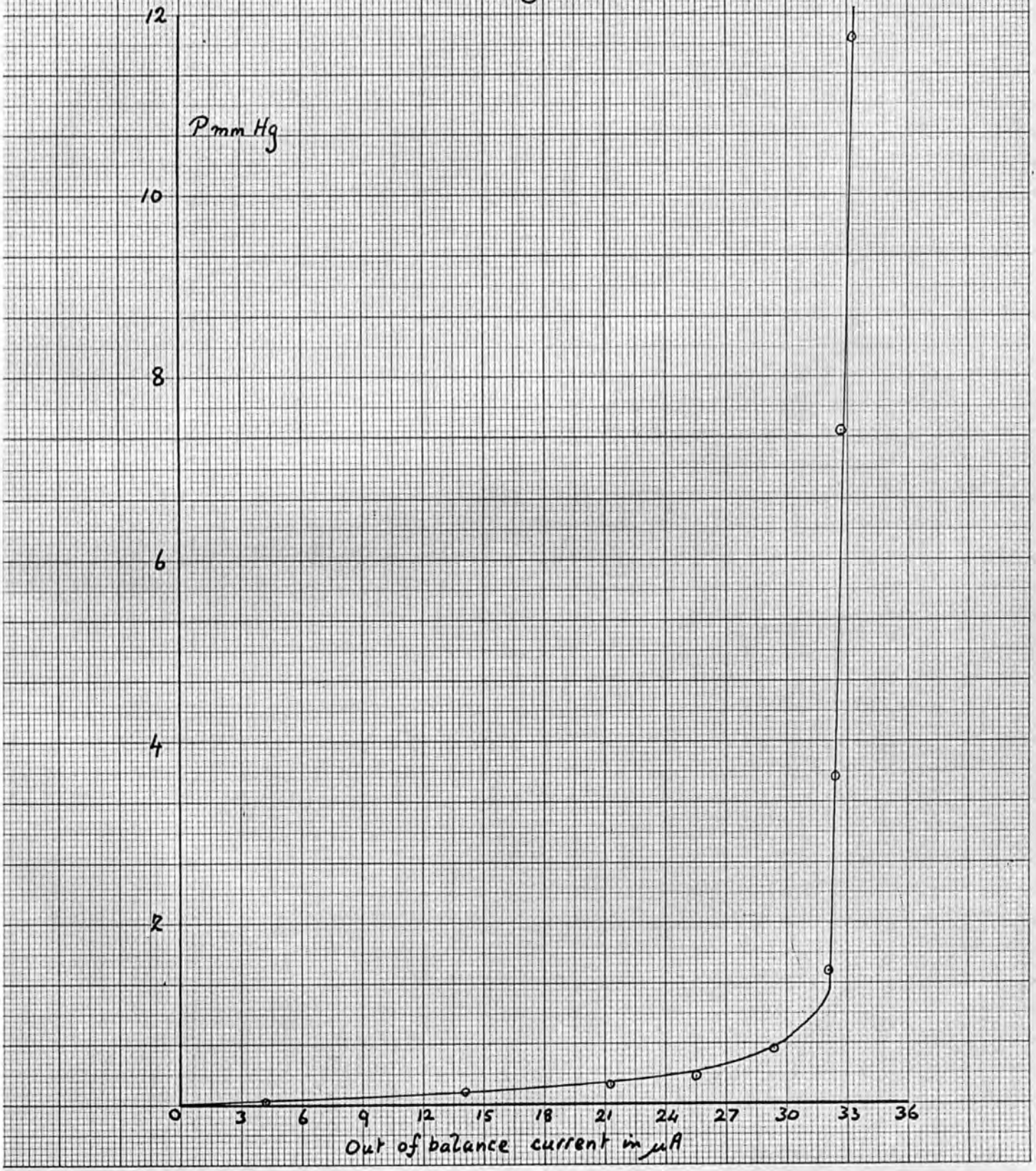

Fig 75

Low pressure calibration curve
for
β trifluoroethanol

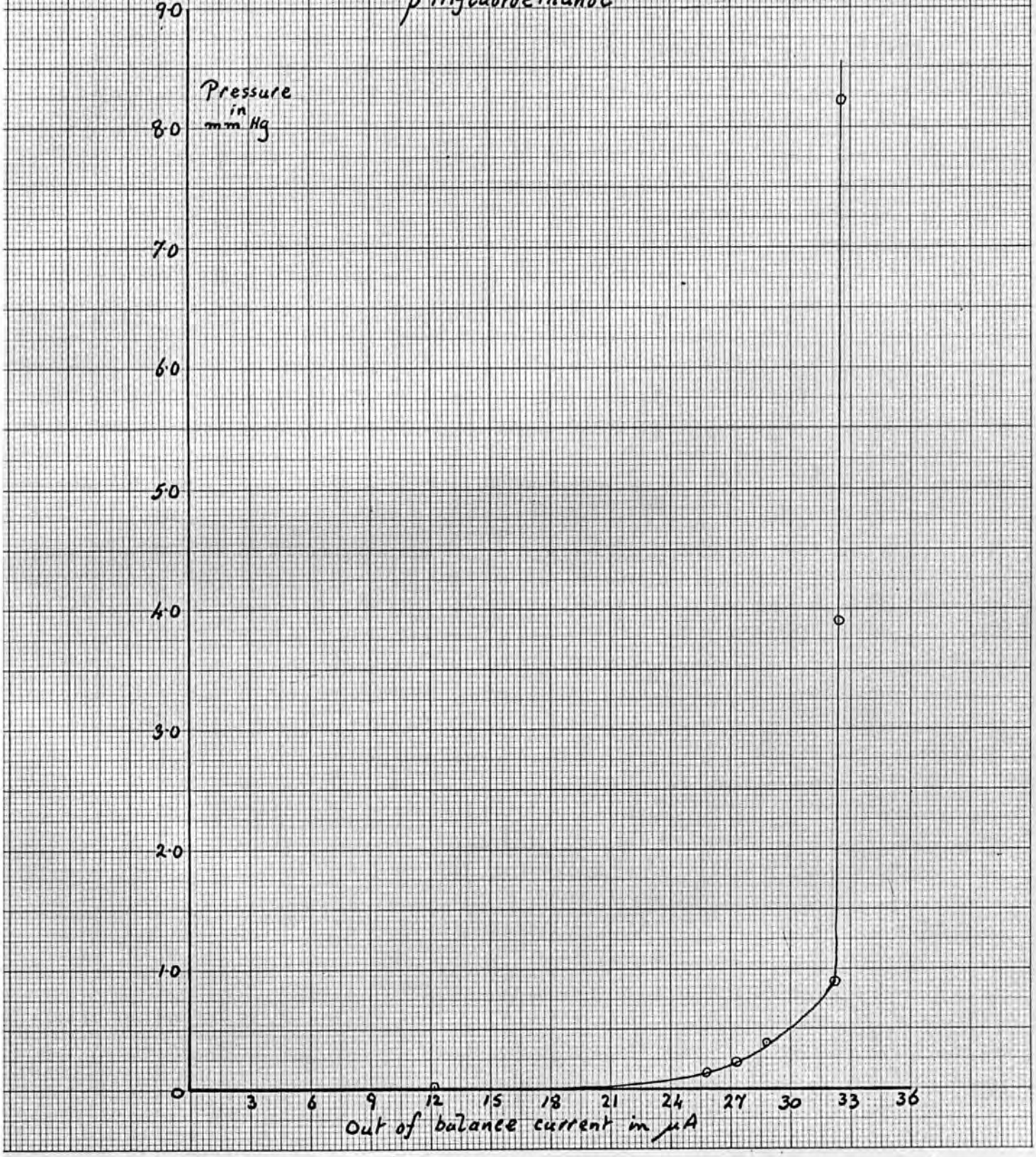

Fig 76

Vapour pressure curve for β trifluorobethanol.

Equation of 'best' straight line (from a least squares calculation) :-

$$\log p_{mm} = -2{\cdot}4045 \times 10^{3} \frac{1}{T^{\circ}A} + 9{\cdot}9128$$

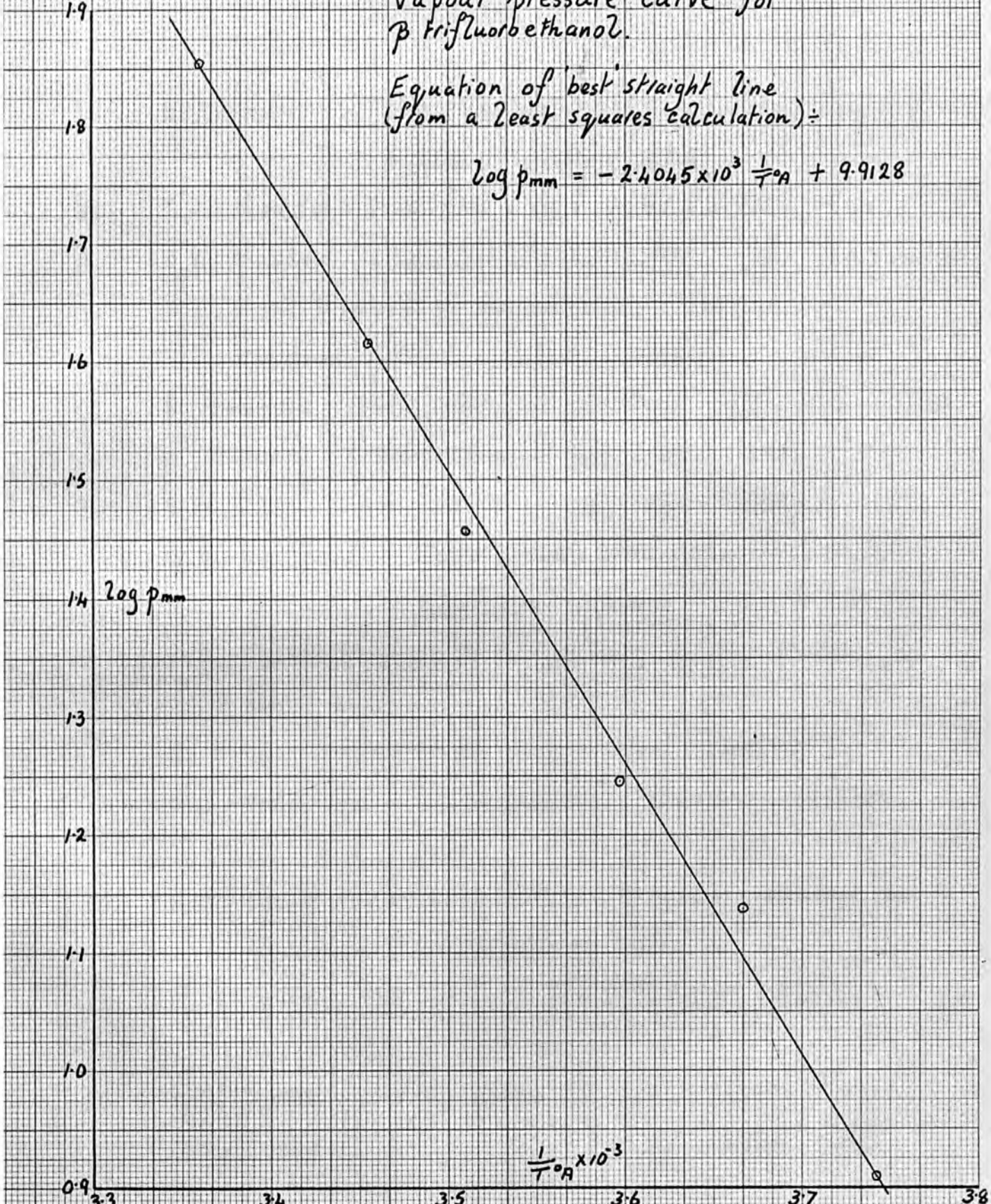

REFERENCES

1. S. Brunauer "Physical Adsorption of Gases and Vapours" P.150 O.U.P. 1944
2. I. Langmuir J.A.C.S. 40 1361 1918
3. R.H. Fowler Proc.Camb.Phil.Society 32 144 1936
4. R.H. Fowler and E.A. Gaggenheim "Statistical Thermodynamics" C.U.P. 1949
5. R. Peierls Proc.Camb.Phil.Society 32 471 1936
6. M. Volmer Z.Phys.Chem. 115 253 1925
7. T.L. Hill Advances Cat. 4 211 1952
8. S.Z. Roginskii Compt.Rendu Acad.Sci. U.R.S.S. 45 194 1944
9. G.D. Halsey Jr. and H.S. Taylor J.Chem.Phys. 15 624 1947

   R. Sips J.Chem.Phys. 16 490 1948

   O.M. Todes and A.K. Bondareva Zhur.Priklad.Khim. 21 693 1948
10. D.M. Young and A.D. Crowell "Physical Adsorption of Gases" Butterworths 1962
11. S. Brunauer, P.H. Emmett and E. Teller J.A.C.S. 60 309 1938
12. D.C. Jones and E.W. Birks J.C.S. 1127 1951

    D.C. Jones J.C.S. 1464 1951

13. C. Orretal J. Metals (N.Y.) 4 657 1954
H.E. Riesetal J.Chem.Phys. 14 465 1946
P.C. Carman A.S.T.M. Symposium on New Methods of Partical Size Determination in the Subsieve Range P.24 1941
T.W. Rhodin J.A.C.S. 72 4343 1950
R.K. Schonfield Trans.Brit.Ceram.Society 48 207 1949
14. G.L. Kington and J.G. Ashton J.A.C.S. 73 1934 1951
15. C.J. Gorter and H.P.R. Frederikse Physica 15 891 1949
16. S. Brunauer and P.H. Emmett J.A.C.S. 57 1754 1935
17. S. Brunauer and P.H.Emmett J.A.C.S. 59 1553 1937
R.A. Beebe and D.M. Young J.Phys.Chem. 57 469 1953
18. G.D. Halsey J.A.C.S. 73 2693 1951
19. H.K. Livingstone J.A.C.S. 66 569 1944
20. M. Brown and A.G. Foster J.C.S. 1139 1952
21. J. Frenkel "Kinetic Theory of Liquids" Clarendon Press 1946
22. G.D. Halsey J.Chem.Phys. 16 931 1948
23. T.L. Hill J.Phys.Chem. 54 1186 1950
24. R.M. Barrer and A.B. Robins Trans.Farad.Society 47 773 1951

25. T.L. Hill J.Chem.Phys. 19 261, 1203 1951
20 141 1952

26. B. Lambert and A.G. Foster Proc.Roy.Society A 134 246 1931

27. K.S. Rao J.Phys.Chem. 45 513 1941

28. R.Z. Zsigmondy Anorg.Chem. 71 356 1911

29. W. Thompson Phil.Mag. 42 448 1871

30. M. Thomä Z.Physik. 64 224 1930

31. V.K. de la Mer and R. Gruen Trans.Farad.Society 48 410 1952

32. M.B. Coelingh Kolloid Z. 87 251 1939

33. A.G. Foster Trans.Farad.Society 28 645 1932

34. J.H. de Boer "The Structure and Properties of Porous Materials" Coulson Research Papers P.68 Butterworths 1958

35. H.L. Watson, R.R. Cardell and W. Heller J.Phys.Chem. 66 1757 1962

36. L.S. Dent Glasser, F.D. Glasser and H.W.F. Taylor Quart.Revs. 16 343 1962

37. A.V. Kiselev "The Structure and Properties of Porous Materials" Coulson Research Papers P.195 Butterworths 1958

38. L. Gurvich J.Russ.Phys.Chem.Soc.(Chem.Part.) 47 805 1915

39. W. Bachmann Z.Anorg.Chem. 79 202 1912

40. D.H. Everett Proc.Chem.Soc. 1957 1938

41. L.E. Drain Sci.Prog. 42 608 1954

42. T.L. Hill J.Chem.Phys. 17 520 1949

43. T.L. Hill J.Chem.Phys. 18 246 1950

44. D. Graham J. Phys.Chem. 57 665 1953

45. R.H. Fowler Proc.Camb.Phil.Soc. 31 260 1935

46. J.M. Thorp Thesis Lond.Univ. 1951

47. B. Lambert and A.M. Clark Proc.Roy.Soc. A 122 497 1929

48. R.N. Hazeldine and K. Leedham J.C.S. 1548 1953

49. F.W. Hoffmann J.A.C.S. 70 2596 1948

50. K.N. Campbell, J.O. Knoblock and K.B. Campbell J.A.C.S. 72 4380 1950

51. D.R. Husted and A.H, Ahlbrecht J.A.C.S. 75 1605 1953

52. M. Polley and G.Cabot Anal.Chem. 23 545 1951

53. M.W. Travers and A. Jaquerod Phil.Trans.Roy.Soc. A 200 111 1903

54. S. Dushman "The Scientific Foundations of Vacuum Techniques" John Wiley 1949

55. B.J. Fontana and M. Calvin Ind.Eng.Chem.(Anal.Ed.) 14 185 1942

56. A. Ferguson Endeavour 2 34 1943

57. A.G. Foster Proc.Roy.Soc. A 147 128 1936

58. S.C. Liang J.Appl.Phys. 22 148 1951
J.Phys.Chem. 56 660 1952
J.Phys.Chem. 57 910 1953
Canad.J.Chem. 33 279 1955

59. D.H. Everett Trans.Farad.Soc. 46 453 1950

60. T.L. Hill J.A.C.S. 73 5012 1951

61. Yule and Kendal "An Introduction to the Theory of Statistics" 1944

62. Yung-fang Yu Yao J.Phys.Chem. 67 2055 1963

63. E. Herington and E.Rideal Trans.Farad.Soc. 40 505 1944

64. Techniques of Organic Chemistry Vol. VII Ed.Weisberger John Wiley 1955

65. L.E. Drain and J.A. Morrison Trans.Farad.Soc. 49 654 1953

66. S.J.Gregg and F.A.P. Maggs Trans.Farad.Soc. 44 123 1948